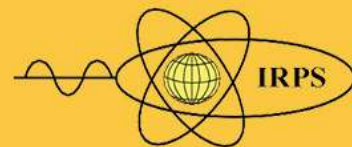


**SUNWAY**  
UNIVERSITY

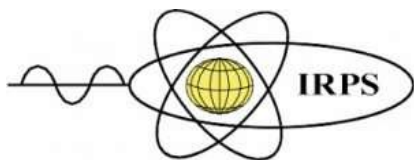


**BOOK OF ABSTRACTS**

# THE 15<sup>TH</sup> INTERNATIONAL SYMPOSIUM ON RADIATION PHYSICS (ISRP-15)

**KUALA LUMPUR, MALAYSIA**  
**6<sup>TH</sup> - 10<sup>TH</sup> DEC 2021**





**ISRP 2021**  
**International Symposium on Radiation Physics**  
**Kuala Lumpur – Malaysia**  
**6 – 10 December 2021**

## **DISCLAIMER**

All content of the abstracts were published based on those submitted by the authors. Accuracy of the content is the sole responsibility of the authors.

The content of this document was updated as on 5 December 2021.

## **ABSTRACT REVIEWERS**

We thank the following people for their time and effort in reviewing the abstracts for the symposium.

Professor David Bradley	Sunway University
Professor Suhairul Hashim	Universiti Teknologi Malaysia
Associate Professor Chai Hong Yeong	Taylor's University
Associate Professor Faizal Mohamed	Universiti Kebangsaan Malaysia
Associate Professor Jeannie Wong	Universiti Malaya
Associate Professor Ung Ngie Min	Universiti Malaya
Associate Professor Noramaliza Mohd Noor	Universiti Putra Malaysia
Associate Professor Rafidah Zainon	Universiti Sains Malaysia
Dr Hafiz Zin	Universiti Sains Malaysia
Dr Izyan Hazwani binti Hashim	Universiti Teknologi Malaysia
Dr Julia Abdul Karim	Malaysian Nuclear Agency
Dr Siok Ee Lam	Sunway University
Dr Meng Hock Koh	Universiti Teknologi Malaysia
Dr Ming Tsuey Chew	Sunway University
Dr Mohamad Syazwan Mohd Sanusi	Universiti Teknologi Malaysia
Dr Muhammad Khalis	Universiti Putra Malaysia
Dr Muhammad Safwan Bin Ahmad Fadzil	Universiti Kebangsaan Malaysia
Dr Nur Nabihah binti Yusof	Universiti Teknologi Malaysia
Dr Nurul Hashikin Ab. Aziz	Universiti Sains Malaysia
Dr Suffian Mohamad Tajudin	Universiti Sultan Zainal Abidin

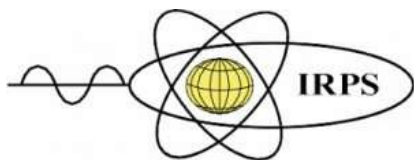
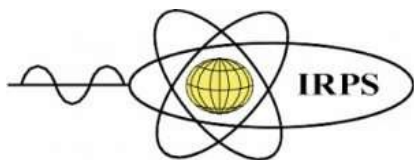


**TABLE OF CONTENTS**

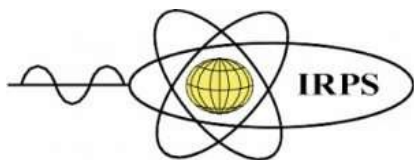
**1 Contents**

DISCLAIMER .....	i
ABSTRACT REVIEWERS .....	i
TABLE OF CONTENTS .....	ii
<b>2 ISRP-15 STATISTICS .....</b>	<b>1</b>
<b>3 SCIENTIFIC PROGRAMME SCHEDULE .....</b>	<b>4</b>
<b>4 ABSTRACTS .....</b>	<b>1</b>
Pre-conference (5 December 2021) .....	1
Workshop - Radiation and Radiobiology in Extreme Circumstances .....	1
B003 - Radiation Hormesis.....	1
A285 - Uncertainties in Radiation Biology and Implications for Research .....	2
A283 - Quantification of Chemotherapy Contributions to Chemoradiotherapy .....	3
A204 - An Overall Framework for Neutron RBEs, Ultra-High Dose/Flash Effects And RBE/OER Changes in Photon, Proton and Ion Beams.....	4
A198 – Radiation Track Structure: How Does Their Spatial and Temporal Properties Drive the Radiobiological Response.....	5
A282 - Radiotherapy Treatment Delays in The UK During The Covid-19 Pandemic.....	6
Monday (6 December 2021) .....	7
Keynote address .....	7
A202 - Building a Nuclear Technology Infrastructure: Malaysian Experience .....	7
Plenary Talk .....	8
B004 - Th-229m And The Quantum Clock .....	8
A197 - Isomers As A Bridge Between Nuclear And Atomic Physics.....	9
Invited Talks .....	10
A219 - Recent Development Of Neutron Detectors For Spectrum And Dose Estimation..	10
A196 - The Life and Times of Lise Meitner: Beta-Decay and Non-Radiative Electromagnetic Transitions.....	11
B005 - Direct Measurements of Carbon Burning at Astrophysical Energies .....	12
Tuesday (7 December 2021).....	14
Plenary Talk .....	14
B001 - Radiation Studies of Items of Cultural Heritage.....	14
Invited Talks .....	15
A110 - The Measure of All Things.....	15



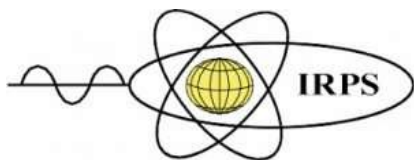
**ISRP 2021**  
**International Symposium on Radiation Physics**  
**Kuala Lumpur – Malaysia**  
**6 – 10 December 2021**

A189 - The Status of the NIST Radiation Interaction Databases .....	16
A200 - Advances in Atomic and Molecular Physics [Theoretical Investigations and Quantitative Analytical Techniques in Radiation Physics] .....	17
A075 - State-of-The-Art of Radiation Protection and Dosimetry in the Medical Applications of Radiation - Hot Topics and Emerging Issues .....	18
A289 - Radiation Processing – Applications and Dosimetry .....	19
Wednesday (8 December 2021).....	20
Plenary Talk .....	20
A213 - The Application Of INAA For Agricultural And Health Related Studies In Jamaica .....	20
Invited Talks .....	21
A215 - Rescue Effect: A Non-Targeted Biological Effect Of Ionizing Radiation .....	21
A212 - Physical Studies of The Epithelial Mesenchymal Transition In Breast Tissues .....	22
A275 - X-Ray Spectrometry: Theoretical and Experimental Determinations.....	23
Forum Forum on Women in Nuclear Science and Technology .....	24
Thursday (9 December 2021) .....	25
Invited Talks .....	25
A103 - The Significance of Nuclear Data For Accelerator-Based Production of Novel Radionuclides For Theranostic Applications.....	25
A201 - Distributed Optical Fiber Radiation Dosimetry.....	26
A269 - The Singapore Synchrotron Light Source (SSLS).....	27
B002 - Compact and Very High Dose-Rate Plasma Radiation Sources for Medical Applications .....	28
A222 - Capillary Guiding for Beams and Radiations .....	29
A226 - Advances in Silica Bead Dosimetry .....	31
Friday (10 December 2021).....	32
Invited Talks .....	32
A199 - Geoneutrons.....	32
A214 - Mineral Wealth and NORM. Standing Up a New Rare Earths Industry in the United States.....	33
A288 - Medical Physics Education: The Way Forward .....	34
ORAL PRESENTATIONS.....	35
A003 - Assessment of natural radioactivity and radiological risks from groundwater and vegetation samples collected from farms in Qatar.....	35
A006 - Radiation Dose Estimation Study for Sparse-View CT: Monte-Carlo Simulation. 36	



**ISRP 2021**  
**International Symposium on Radiation Physics**  
**Kuala Lumpur – Malaysia**  
**6 – 10 December 2021**

A007 - Investigation Flexible Nanocomposite Membranes of ZnO-CuO-PVA For X-Ray Detectors .....	37
A008 - Radiological Dispersion of I-131, I-133 and I-135 Isotopes Due to Hypothetical Accidental Release from Nigerian Research Reactor-1.....	38
A009 - A Novel Glass System Based on Iraqi White Sand and Lead Oxide For Gamma Ray Shielding Purposes.....	39
A010 - New Glass Based on Iraqi Sand and Modified By Lead Oxide To Protect Against Gamma-Ray: Fabrication, Mechanical And Shielding Properties Examination .....	40
A012 - The Potential Use Oo Silica-Based Commercial Float Glass For Protection Of Gamma-Radiation .....	41
A016 - Network-Modifying Role of Er <sup>3+</sup> ions on the Structural, Optical, Mechanical, and Radiation Shielding Properties of ZnF <sub>2</sub> -BaO-Al <sub>2</sub> O <sub>3</sub> -Li <sub>2</sub> O-B <sub>2</sub> O <sub>3</sub> Glass .....	42
A021 - Investigation of The Photon Shielding Capability Of Kaolin Clay Added With Micro And Nanoparticles Of Bi <sub>2</sub> O <sub>3</sub> .....	43
A023 - Removal of Uranium From Nuclear Effluent Using Regenerated Bleaching Earth Steeped In β-Naphthol.....	44
A026 - Peculiarities of Rare Earth Elements Removal From Chloride Solution Using Cetylpyridinium Bromide/Polyvinyl Chloride .....	45
A028 - The effect of CNTs on The Radiation Attenuation Properties Of The Composite Of BaTiO <sub>3</sub> Doped With Spinnel Ferrite .....	46
A033 - Lithium aluminate borate glass mixed with tin slag for radioactive immobilization .....	47
A038 - Characterization of thermoluminescence properties for Al <sub>2</sub> O <sub>3</sub> :Ge,Sr prepared by combustion synthesis method .....	48
A039 - Radiation shielding features for a new glass system based on tellurite oxide.....	49
A040 - Characterization and gamma rays shielding performance of calcinated bentonite nanoparticles .....	50
A041 - Solution optical spectra of anticancer drug vandetanib using robust quantum mechanical calculations .....	51
A042 - Intramolecular hydrogen bonding of hydroxybenzoic acid isomers revealed using XPS: theory and experiment* .....	52
A044 - Ta <sub>2</sub> O <sub>5</sub> -doped bismuth zinc tellurite glass: fabrication, optical, and radiation shielding evaluation.....	53
A046 - Solving self-absorption in fluorescence.....	54
A047 - Developing a novel technique of radon detection for all three naturally occurring radon ( <sup>222</sup> Rn , <sup>220</sup> Rn and <sup>219</sup> Rn).....	55
A049 - On the study for TeO <sub>2</sub> -WO <sub>3</sub> -TiO <sub>2</sub> -ZnO -Na <sub>2</sub> O glass containing Pr <sub>2</sub> O <sub>3</sub> in radiation shielding applications: Theoretical computations via EPICS2017 .....	56



**ISRP 2021**  
**International Symposium on Radiation Physics**  
**Kuala Lumpur – Malaysia**  
**6 – 10 December 2021**

A050 - Assessment of Radiation attenuation properties for novel alloys: An experimental approach .....57

A051 - Assessment of geogenic impact on thoron activity concentration in soil gas of Perak state, Malaysia.....58

A052 - High accuracy determination of photoelectric cross sections, X-ray Absorption Fine Structure and nanostructure analysis of zinc selenide using the X-ray Extended Range Technique.....59

A053 - Computation of Gamma Buildup factors and Heavy Ions Penetrating Depths in Clay Composite Material using Phy-X/PSD, EXABCal and SRIM Codes ..... 60

A058 - Luminescence Studies of Fabricated Gd:Mg-Doped Silica Glass Exposed to Neutron Radiation ..... 62

A059 - Radiation response of marble-glass media in medical radiation applications ..... 63

A060 - Activity Concentration and Radiological Impact Assessment of  $^{226}\text{Ra}$ ,  $^{232}\text{Th}$  and  $^{40}\text{K}$  in Beach Sands and Sediments Samples Around Badagry Coastal Areas of Lagos..... 64

A062 - New methodology for solving nanostructures within dilute and amorphous systems: a trend study of Nickel-doped borate glass by the X-ray Extended Range Technique (XERT) and eFEFFIT fitting software for XAFS..... 65

A063 - Radon concentration in groundwater sources for public consumption in Bosso community, north central Nigeria and consequent annual effective dose estimation..... 66

A064 - Review of borosilicate glass for radiation dosimetry ..... 67

A066 - Review of the effect of reduced background radiation on living organisms..... 68

A067 - Gamma Ray Attenuation Studies of Brass Alloy as Tissue Equivalent Material for Radiotherapy Applications..... 69

A069 - Analysis of radiation dose distribution in paediatric exams ..... 70

A070 - Fluoroscopy time influence on DAP values of interventional cardiac procedures .71

A072 - Monte Carlo simulation of HDR Brachytherapy dosimetric parameters in a different medium ..... 72

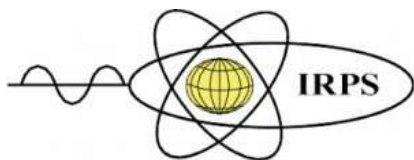
A077 - Determination of  $^{40}\text{K}$  and  $^{238}\text{U}$  radionuclides concentration in some granite rocks by gamma spectroscopy and Energy Dispersive X-ray analysis. .... 73

A079 - The impact of various instances of solar wind speed on the fluctuations of cosmic radiation in the solar minimum (23, 24, and 25)..... 74

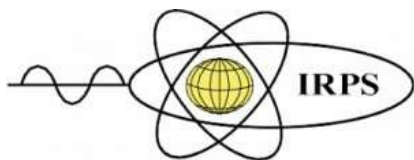
A081 - Simulation and computational improvements of the mutual optical intensity function in two dimensions ..... 76

A084 - Exploring of Monte Carlo Simulation from Case Study of Particle Transport in Gamma Knife Machine..... 77

A085 - Miniature  $4\pi\beta(\text{LS})-\gamma(\text{LaBr}_3)$  coincidence system at KRISS ..... 78

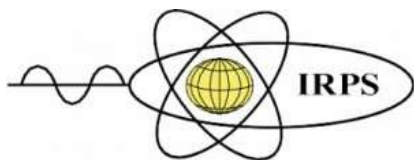


A086 - Synthesis physical and photoluminescence investigation of Eu <sup>3+</sup> doped gadolinium borate scintillating glass.....	79
A088 - Radiation hazard assessments of natural radioactivity in cosmetic products .....	80
A089 - Variability of estimated organ dose based on different Monte Carlo radiation transport codes for NORM-added consumer product radiation exposures.....	81
A091 - Effect of mixed glass former on structural, elastic and gamma radiation shielding properties of 70[xTeO <sub>2</sub> -(1-x)B <sub>2</sub> O <sub>3</sub> ]-20Bi <sub>2</sub> O <sub>3</sub> -10Li <sub>2</sub> O glasses .....	82
A093 - Novel efficient alloys for radiation shielding applications: A theoretical investigation .....	83
A095 - A setup for integral measurements of multiple scattering by 10- to 100-keV electrons .....	84
A096 - Incidental finding of hepatocellular carcinoma using Ga68-PSMA PET-CT: future use for detection and theranostics? .....	85
A097 - Investigation of polyvinyl alcohol (PVAL) composites and the effect of variation in breast densities on image quality and dose in full-field digital mammography: A phantom study.....	86
A100 - Characterization of Target Transfer Function (TTF) performances for detection of pulmonary nodule in lung from current protocol.....	87
A102 - Rapid separation of thorium via electrosorption with carbon electrode towards efficiently managing rare-earth extraction residue .....	88
A109 - MRI-LINAC dosimetry approach by Monte Carlo methods coupling charged particle radiation transport with strong magnetic fields .....	89
A113 - Feasibility of mean glandular dose determination of digital breast tomosynthesis unit using LuSy dosimeter .....	90
A114 - 2D vs 3D dose analysis of PRESAGE® Dosimeters using 3DMicroHD-OCT System: an in-house Optical CT system for radiotherapy dosimetry .....	91
A115 - High accurate mass attenuation coefficients and nanostructure of Zinc from X-ray absorption Spectroscopy at room temperature.....	92
A117 - Synthesis, luminescence and scintillation properties of LaCl <sub>3</sub> :Tm <sup>3+</sup> crystal.....	93
A118 - Estimate of Effective Dose for Adults' Patients from Nuclear Medicine Examinations in Sudan .....	94
A119 - Precision measurement of the phase fine structure across the iron K-edge. ....	95
A120 - Applications of MOSkin as a real-time detector for <i>in vivo</i> dosimetry during high-dose rate Cobalt-60 brachytherapy .....	96
A121 - Structural fitting using the measured complex atomic fine structure spectra across the copper K-edge .....	97
A122 - A New Compact Octagonal Split Ring Resonator based Tuning Fork-Hammer Shape Perfect Metamaterial Absorber for C-Band Applications .....	98



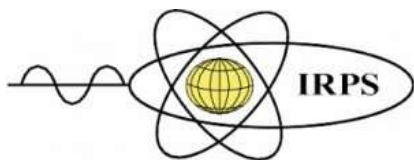
**ISRP 2021**  
**International Symposium on Radiation Physics**  
**Kuala Lumpur – Malaysia**  
**6 – 10 December 2021**

A123 - Complex atomic fine structure across the copper K-edge: new results and opportunities .....	99
A126 - Development of FPGA-based Coincidence Module for TDCR Counting System	100
A130 - Proton radioactivity of Dysprosium.....	101
A136 - Dose Assessment in CT Examination of Pelvis and Establishment of Provincial Diagnostic Reference Levels in Taif, Saudi Arabia.....	102
A139 - Development of flexible radiation shielding materials from natural rubber/ Sb <sub>2</sub> O <sub>3</sub> composites.....	103
A141 - Simultaneous X-ray Scattering and Spectroscopy Computed Tomography – Monte Carlo Simulation and Experiment.....	104
A142 - Barium Sulfate and Concrete Mixture as High Energy X-ray Radiation Shielding .....	105
A143 - Fourier Transform Holography with Extended Reference: a step toward the use of photons of higher energy .....	106
A145 - Relation between energy dependence and dosimeter size: An experimental study on glass TLDs .....	107
A147 - Dosimetry audit of megavoltage photon beams under non-reference conditions: Comparison of fabricated Ge-doped optical fibres and TLD-100 systems .....	108
A148 - X ray spectrometry methodologies for sustainable cancer tissue analysis – recent advances and limitations .....	109
A154 - COMBAT algorithm for the coordination of delineation of multiple radiologists of nodule boundaries in lung computed tomography images .....	110
A155 - Overview of methods for determining the depth distribution of elements in X-ray fluorescence analysis .....	111
A156 - New analysis method for neutron dosimetry with Fluorescent Nuclear Track Detectors .....	112
A159 - Sonologist occupational exposure and ambient dose resulted from patients underwent nuclear medicine procedure .....	113
A163 - Aluminum oxide crystals for high spatial resolution dosimetry of photon beams	115
A164 - Effective dose and radiogenic risk during certain computed tomography examinations .....	116
A166 - Carbon isotope composition ( <sup>14</sup> C and <sup>13</sup> C) of the atmospheric CO <sub>2</sub> at several locations in Croatia.....	117
A168 - A Markov Random Field Approach for CT Image Lung Classification using Image Processing .....	118
A175 - Pediatric radiation dosimetry and radiogenic risk estimation from computed tomography examinations.....	119



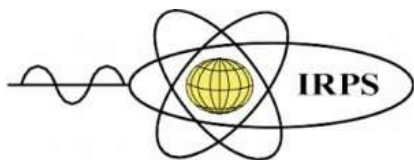
**ISRP 2021**  
**International Symposium on Radiation Physics**  
**Kuala Lumpur – Malaysia**  
**6 – 10 December 2021**

A179 - Primary scintillation in gaseous xenon for x-rays and alpha-particles .....	120
A181 - Contribution to the economic heavy minerals of East El- Arish coastal sediments, North Sinai, Egypt. ....	121
A182 - Radiological Hazards associated to a raw material of Um Bogma area, southwestern Sinai, Egypt.....	122
A185 - New studies on Neutral Bremsstrahlung in Xenon optical TPCs.....	123
A190 - Development of a KRISS Rn-mini radon detector at KRISS.....	124
A192 - Time-resolved radiation dosimetry using a Cerium and Terbium co-doped YAG crystal scintillator.....	125
A193 - Enhancing Information Learned from Auger Processes.....	127
A194 - Thermoluminescence characteristics of customised Ge-doped optical fibres (CusOF) under Am-Be neutron source as a potential to be used for space radiation detector .....	128
A195 - The Impact of Tube Current and Iterative Reconstruction Algorithm on Dose and Image Quality of Infant CT Head Examination : A Phantom Study .....	129
A205 - Dosimetric characteristics of fabricated Germanium doped optical fibres for electron beam therapy audit.....	130
A206 - Radiological and Environmental studies on granitic rocks of Abu Furad area used in construction purposes and ceramic industry .....	131
A207 - Effect of different source-to-image distance on radiation dose and the quality of image in posteroanterior hand X-ray examination.....	132
A208 - The Auger Effect and its Applications .....	133
A211 - Performance of Ge-doped silica optical fiber radioluminescence scintillators for radiotherapy dosimetry .....	134
A223 - Tomographic gamma-ray imaging of industrial processes and equipment.....	135
A225 - Flattening filter design for intraoperative radiotherapy with 12 MeV electron beam with large applicators using Monte-Carlo simulations .....	136
A227 - Development of a unique neutron irradiation facility for medical radionuclides and advanced nuclear technologies .....	137
A228 - Medical radionuclide prioritisation and the development of the Production Rate Assessment Tool.....	138
A230 - Wavefield Characterisation of MHz XFEL Pulses.....	139
A231 - Glass microspheres as a novel targeting vector for proton-boron therapy .....	140
A234 - Radiation treatment in ensuring traceability and biosafety of aquatic food and its environment .....	141
A239 - Determination of the radon diffusion coefficient of thin polyethylene and aluminium foils .....	142
A243 - First results from FATIMA within the DESPEC collaboration at FAIR-0.....	143



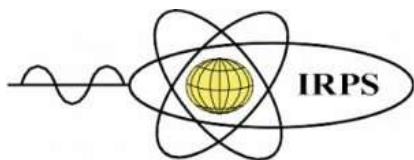
**ISRP 2021**  
**International Symposium on Radiation Physics**  
**Kuala Lumpur – Malaysia**  
**6 – 10 December 2021**

A245 - Gamma-gamma coincidence method for determination of Fe and Tb in Montana II Soil and Coal Fly Ash sample.....	144
A258 - Characterisation of Cadmium Telluride Zinc photon counting detector for soft tissue imaging .....	145
A259 - Simulation of $K\alpha$ X-ray emission lines in metallic Cu from first principles.....	146
A260 - X-ray phase contrast imaging with a simple prototype system: polyenergetic beam and a dental imaging detector. ....	147
A261 - Proton therapy monitoring with orthogonal prompt-gamma imaging: the case of prostate irradiation .....	148
A262 - Polycapillary X-ray techniques for archeological studies: the Peltuinum excavation site.....	149
A263 - High Resolution CT@XlabF: Future Tomographic Studies .....	150
A270 - Assessment Of Environmental Radioactivity In The Spacial Area Of Titanium Mining At Ha Tinh Province (Vietnam).....	151
A276 - Resolution of ferrocene and deuterated ferrocene conformations using dynamic vibrational IR spectroscopy .....	152
A278 - Calculating Characteristic Spectral Profiles: Copper $K\alpha$ and $K\beta$ .....	153
POSTER PRESENTATIONS.....	154
A004 - A Study of the Neutron Induced Event Rate during Solar Eclipse Using Superheated Emulsion Detector .....	154
A005 - Stability measurement of R-134a superheated emulsion detector.....	155
A011 - Tomographic Voxel Deformable Phantom, Full Body Model for Radiation Protection Assessment.....	156
A013 - Synthetic heavyweight concrete for low and mid-gamma ray energy protection applications .....	157
A014 - Study the radiation attenuation properties of ball clay-cement- slag iron composites by experimental and theoretical methods .....	158
A015 - New recommended containers as a protection method against the intermediate level of radioactive wastes.....	159
A017 - An experimental technique for measuring the photon attenuation features of the glass system $P_2O_5$ -CaO- $K_2O$ - $N_2O$ -PbO.....	160
A018 - Comparison of radiation shielding ability of bulk and nanoparticle $Bi_2O_3$ radiation shields .....	161
A019 - Determination of 3D distribution of toxic chemical elements in historical plaster with surface and confocal X-ray fluorescence mapping.....	162
A020 - From counting-rate profile to $^{137}Cs$ profile.....	163



**ISRP 2021**  
**International Symposium on Radiation Physics**  
**Kuala Lumpur – Malaysia**  
**6 – 10 December 2021**

A022 - Assessment of radioactivity in the granite of granitoids at Nikeiba, south Eastern Desert, Egypt; radionuclides concentrations and radiological hazard parameters. ....	164
A024 - The efficacy of WCu composites in shielding of ionizing radiation; experimental and theoretical studies.....	165
A025 - Effect Of Bi <sub>2</sub> O <sub>3</sub> Addition On Radiation Shielding And Elastic Properties Of Mixed Ionic-Electronic 98[20Li <sub>2</sub> O-XBi <sub>2</sub> O <sub>3</sub> -(80-X)TeO <sub>2</sub> ]-2Ag Glass System .....	166
A027 - Modified irradiation technique for transfusable blood using a clinical linear accelerator .....	167
A029- The amplitude and phase distributions of cosmic ray anisotropy at different conditions of Forbush decrease .....	168
A030 - Dose Assessment Level in Industrial Betatron Electron Beam .....	169
A031 - Evaluation of Organ Dose Mapping in 128-Slice Multi-Detector Computed Tomography .....	170
A034 - Dose Assessment with NORM added Consumer Products Using Geant4 Monte Carlo Simulations .....	171
A035 - The Naturally Occurring Radioactivity of Tourmaline-based Healthcare Products and Associated Radiation Risk .....	172
A036 - A study of proton small field collimator-scattering function into the Geant4 (PTSim) simulation.....	173
A037 - Temporal (spatial) resolution of a neutron probe for C/O nuclear well logging ...	174
A043 - Absorption and fluorescence spectra of an EGFR inhibitor AG-1478 using TD-DFT methods.....	175
A045 - Optimization of Tumour Segmentation Threshold in Gallium-68 PET/CT Neuroendocrine Imaging .....	176
A048 - Least square optimization for modelling ridge filters in the proton wobbling nozzle .....	177
A054 - Identify Malaysian residential buildings with high Radon concentration and their possibility for remedy .....	178
A055 - Structural and Defect Changes in Black Carbon Charcoal Irradiated with Gamma .....	179
A056 - Evaluation of Perturbation Effects in Small Field Dosimeter using Monte Carlo Simulation.....	180
A057 - Optical Characterisation of Borosilicate Microscope Glass Slides .....	181
A061 - Evaluation of Dose-Area Product in pediatric interventional cardiology .....	182
A065 - Bismuth tellurite glasses doped with CeO <sub>2</sub> for gamma radiation shielding and dosimetry application.....	183



**ISRP 2021**  
**International Symposium on Radiation Physics**  
**Kuala Lumpur – Malaysia**  
**6 – 10 December 2021**

A068 - Evaluation of radiation shielding characteristics of B<sub>2</sub>O<sub>3</sub>-K<sub>2</sub>O- Li<sub>2</sub>O - HMO (HMO = TeO<sub>2</sub>/ SrO /PbO/Bi<sub>2</sub>O<sub>3</sub>) glass system: A simulation study using Geant4 code..... 184

A071 - Structural and Optical Properties of graphite-rich media under low level neutron doses for radiation dosimetry ..... 185

A073 - Time-division multiplexing in real-time radioluminescent dosimetry system for high energy photon..... 186

A074 - Formation of a clavicle phantom for radiography using hydrated lime for the purposes of education and quality assurance ..... 187

A078 - An annual effective dose due to <sup>222</sup>Rn in spring and some surface waters of Johor state, Malaysia..... 188

A080 - Effects of Inorganic Salts and Maltose on the Dose-Response of HEMA Polymer Gel Dosimeters at the Diagnostic Range ..... 189

A082 - Scattering radiation exposure to eye lenses in the fluoroscopy-guided interventional procedures ..... 190

A083 - The functionality assessment of fabricated automated radiopharmaceutical dispenser system ..... 191

A087 - Doped Plastic Scintillator Properties for Soft Tissue Dosimetry ..... 192

A090 - The impact of gamma rays on the structural, optical and electrical properties of copper iodide (CuI) thin films prepared by SILAR technique ..... 193

A092 - Computerized glow curve deconvolution of proton-irradiated Ge-doped optical fibres ..... 194

A094 - Photo and X-ray induced luminescences behaviors of Dy<sup>3+</sup> ions doped alkaline borophosphate glasses..... 195

A098 - Potential of amino acid based vesicle as hydrogen peroxide radiosensitizer carrier ..... 196

A099 - Radiation induced alterations in carbon rich media ..... 197

A104 - Extraction and Purification of high-purity ThO<sub>2</sub> from monazite ores for thorium fuel-based reactor ..... 198

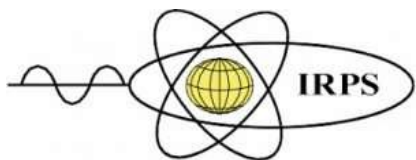
A105 - Industrial Contamination Assessment of Natural Radionuclides and Heavy Metals to the Environment: Case Study of Unregulated Industry in Malaysia ..... 199

A106 - Radiation hazard indices of sediment and water samples in Amang processing plant in Perak state ..... 200

A107 - Radiological Dose Assessment of internal exposure due to Radon in Groundwater affected by Tin Mining in Doguwa, Kano State, Nigeria ..... 201

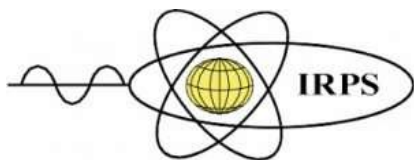
A108 - Occupational dose and technical parameters in pediatric upper gastrointestinal series ..... 202

A111 - Screening in bremsstrahlung at high-energies ..... 203



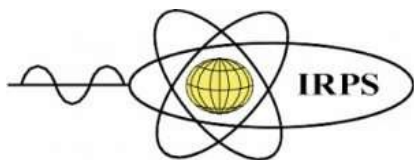
**ISRP 2021**  
**International Symposium on Radiation Physics**  
**Kuala Lumpur – Malaysia**  
**6 – 10 December 2021**

A112 - Dosimetric Comparison in Adjuvant Radiotherapy for Early Stage and Advance Stage for Left-Side Breast Cancer using Volumetric Modulated Arc Therapy.....	204
A116 - Influence of Bi <sub>2</sub> O <sub>3</sub> content on structural, optical and radiation shielding properties of transparent Bi <sub>2</sub> O <sub>3</sub> -Na <sub>2</sub> O-TiO <sub>2</sub> -ZnO-TeO <sub>2</sub> glass ceramics .....	205
A124 - The effect of BaO on the luminescence and radiation shielding properties of borosilicate glass system.....	206
A125 - Evaluation of radiation-exposed graphite sheets for passive dosimetry and damage studies .....	207
A128 - Raman and FTIR spectroscopy of synovial fluid after gamma irradiation .....	208
A129 - Radioactivity and hazard risk analysis of soil samples taken from former mining area in Klang Valley .....	209
A131 - A study on Competition between proton and beta decay for some β-therapeutic nuclides .....	210
A132 - Synthesis and characterisation of CuFe <sub>2</sub> O <sub>4</sub> for X-ray/gamma radiation shielding.....	211
A133 - X-ray/gamma radiation absorption studies in transition metal doped ZnO.....	212
A134 - Radioactivity of Radon .....	213
A138 - Gamma and X-ray shielding properties of Gallium alloys.....	214
A140 - Simulated Technique to Calculate the Coincidence Summing Factor for a voluminous γ-ray Sources.....	215
A144 - Enhancement of <sup>18</sup> F-FDG PET phantoms imaging accuracy using MCNP5 .....	216
A146 - Effect of gamma irradiation on lubricin concentration in synovial fluid .....	217
A149 - The Rhisotope Project; Using radioisotopes to devalue rhinoceros horn.....	218
A150 - Gamma rays induced effects on the properties of CsPbBr <sub>3</sub> perovskite thin film ..	220
A151 - Determination of the Fetal Radiation Dose during Various-Row Multi-Detector Computed Tomography Imaging: Phantom Study .....	221
A152 - Supressing Moiré artefacts in grating-based X-ray phase-contrast imaging .....	222
A153 - Dosimetric comparison of renewable product-based composite phantoms .....	223
A157 - Development and characterization of a portable CT system for wooden sculptures analysis.....	224
A158 - XRF analysis of amorphous silicate slags in cremation remains from the Roman period .....	225
A160 - Evaluation of internal structure of concrete after gamma irradiation.....	226
A161 - Pediatric organ and effective doses and radiogenic risk during chest contrast enhanced computed tomography procedure .....	227
A165 - Study of digital filters to 3D position-sensitive pixelated CdZnTe detector .....	228



**ISRP 2021**  
**International Symposium on Radiation Physics**  
**Kuala Lumpur – Malaysia**  
**6 – 10 December 2021**

A167 - Patients radiation dose reduction during contrast enhanced computed tomography urography examination .....	229
A169 - Estimation of Breast radiation dose and radiogenic risk during PET/CT imaging procedures .....	230
A170 - Estimation of Effective dose and radiogenic risk during certain computed tomography examinations .....	231
A171 - Patients' tissues and organs radiation equivalent doses in interventional orthopedic procedures .....	232
A172 - Prompt Gamma Spectroscopy of Metallic Implants in Proton Therapy: A Phantom Study .....	234
A174 - Dosimetric evaluation of an epitaxial silicon diode as an online dosimeter for orthovoltage photon beam radiotherapy .....	235
A176 - Dose rate mapping in an industrial <sup>60</sup> Co irradiator using an online photodiode-based dosimetry system .....	236
A177 - Model to Estimate of cumulative dose in real-time.....	237
A178 - Cyclotron-based p(27)+Be neutron source for activation experiments.....	238
A180 - Assessment of the effective radiation dose and cancer induction probability in urographic imaging procedures.....	239
A183 - Evaluation of doses in dental radiographic units using 3d printed pediatric phantom .....	240
A184 - Staff occupational exposure in the south region, Saudi Arabia.....	241
A186 - Natural radioactivity in Sediments from Nile River and its tributaries in Khartoum State, Sudan.....	242
A187 - Survey on radon activity in the air of dwellings, water and soil of Carambeí rural region (Paraná State, Brazil) .....	243
A188 - Characterization of digital systems used in x-ray imaging.....	244
A191 - Evaluation of computed tomography imaging Protocol and pediatric doses to the sensitive organs.....	245
A203 - Proton radiography using Discrete Range Modulation method – A Monte Carlo study .....	246
A209 - Accelerator selection for industry and medical applications.....	247
A210 - Natural radioactivity analysis and radiological impact assessment of coal, bottom, and fly ash from a coal power plant.....	248
A216 - Assessment of $\gamma$ -radiation shielding behavior of some mixed nature clays .....	249
A217 - Full energy peak efficiency of a rectangular NaI (Tl) detector using standard non axial point sources.....	250



**ISRP 2021**  
**International Symposium on Radiation Physics**  
**Kuala Lumpur – Malaysia**  
**6 – 10 December 2021**

A218 - The effect of FerroSilicon materials to enhance the radiation shielding ability of some clay .....251

A220 - Estimation of Average Annual Committed Effective Dose Due to Intake of Medicinal Plants Collected from Chattogram, Bangladesh. ....252

A221 - Studies on the radiation absorption characteristics of different commercial granites collected from Saudi Arabia .....253

A224 - The effect of gamma and electron beam irradiation on the properties of bioactive glass-polymer composite film patch for soft tissue healing.....254

A127 - Development and establishment of medical Radiation Protection Officer certification program in Malaysia .....255

A229 - Geant4 track structure simulation of electron beam interaction with a gold nanoparticle.....256

A232 - Evaluation of level of compliance of patients’ doses and exposure parameters at a University Hospital (UNIMEDTH) in Nigeria during routine diagnostic imaging.....257

A233 - Dosimetric characterization for experimental mouse irradiation using novel add-on collimator system combined with a standard cell irradiator .....258

A235 - Tungsten carbide and tungsten carbide cobalt based epoxy resin composites for lead-free gamma ray radiation shielding in nuclear medicine .....259

A236 - Towards real-time analysis of liquid jet alignment in SFX.....260

A237 - Establishing diagnostic reference levels based on clinical indications for enhanced computed tomography abdomen and pelvis examinations .....261

A240 - Effective and Organ equivalent doses in Neck Computed Tomography Imaging 262

A242 - Modelization of radon emanation generated by natural and artificial sources as a laboratory scale .....264

A244 - Initial application of radiomics and deep learning in lung cancer diagnosis.....265

A246 - Chemical evaluation of vitrified spent resin with steel slag as a binder.....266

A248 - Benchmarking of Monte Carlo codes in Phantom Dose Distribution Simulation.267

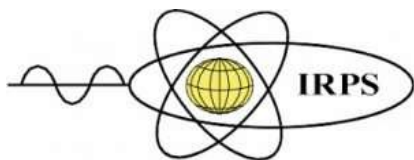
A249 - Evaluation of impact of image reconstruction on 18F-FDG-PET/CT imaging radiomics features in head and neck cancer .....268

A250 - Investigation of the different nanoparticles effects on the mass attenuation coefficient in diagnostic radiology: A Monte Carlo study.....269

A251 - Literacy challenges for nuclear science and technology in Thailand .....270

A252 - Development of a methodology for dose optimization in abdominal exams using two Computerized Radiology (CR) systems.....272

A254 - Monte Carlo simulation of the experimental beamline of the Particle Physics and Beam Delivery Core Laboratory at the Chang Gung Memorial Hospital .....273



A255 - Correlation between the different mammography dose quantities, breast thickness and scan parameters using regression models .....	274
A256 - Natural radioactivity and associated radiation hazard indicators from granite rocks in Gabal-Qash-Amir area, south Eastern Desert, Egypt .....	275
A257 - Evaluation Of Patient-Specific VMAT QA Dosimetry Systems for Linac Mechanical Errors and Investigation of Correlations with Dose Volume Histogram in SBRT Treatment .....	276
A264 - Study on trace elements concentration and electron density variation in canine mammary tissues using a synchrotron-based micro X-ray fluorescence system.....	277
A265 - Electrons and positrons collision cross sections with DNA and water in the low and intermediate energy regime.....	278
A266 - Monte Carlo simulation of electron energy deposited and backscattered fractions in dry and hydrated DNA.....	279
A267 - Study of contrast, SNR and CNR of digital images from biomaterial applied in odontology .....	280
A268 - The establishment of radioactive radon measurement technology in hot spring water .....	281
A273 - Correlation Between Radiation Damage And Electrical Characteristics Of The Proton-Irradiated Silicon PN Diode.....	282
A274 - Application Of Migrad Optimization Subroutine In Root Framework To Precisely Calculating U-235 And Ra-226 Photopeak Intensities In NORM.....	283
A277 - A Study of Linear Attenuation Coefficients of Materials from X-ray Radiography Using Fluorescent Screen and Digital Camera .....	284
A280 - Measurement of Reactive Oxygen Species Generation By Iridium Nanoparticles in External Beam Radiotherapy .....	285
A281 - Conceptual framework of effective dose evaluation in NORM-added products using Monte Carlo simulations and ICRP computational human phantom .....	286
A284 - Humidity dependence of radon equilibrium factor measurement using an alpha beta filter detector.....	287
A286 - Low-dose radiation effects on wound healing – a review .....	288
A287 - Characterization of a cost-efficient OPT101 photodiode as relative dosimeter in low-energy radiation dosimetry: An IoT application .....	289
A290 - Monte Carlo modelling of PMTs System for optical detection of alpha sources..	290
A291 - Ab Initio $K\alpha$ and $K\beta$ Energy Calculations in 3d Transition Metals .....	291
A292 - The use of fabricated optical fibres for dose mapping of Cs-137 gamma rays in blood irradiator machine .....	292

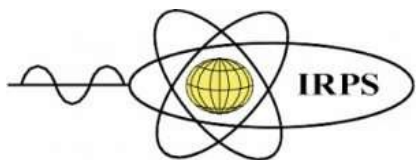
## 2 ISRP-15 STATISTICS

These data were updated on 3 December 2021.

- 324 registrations
- 297 abstracts submitted
- 121 students submitted
- 43 countries (Figure 1)
- Publicity outreach via ISRP-15 website (<https://isrp15.com/>) reached 84 countries. (Figure 2)

The scientific programme comprised of :-

- 1 keynote speech
- 4 plenary talks & 20 invited speakers from 16 countries
- 1 pre- conference workshop (6 speakers)
- 1 forum
- 12 themes (Figure 3)
- 19 parallel oral presentation sessions
- 114 oral presentations
- 104 poster presentations



**ISRP 2021**  
**International Symposium on Radiation Physics**  
**Kuala Lumpur – Malaysia**  
**6 – 10 December 2021**

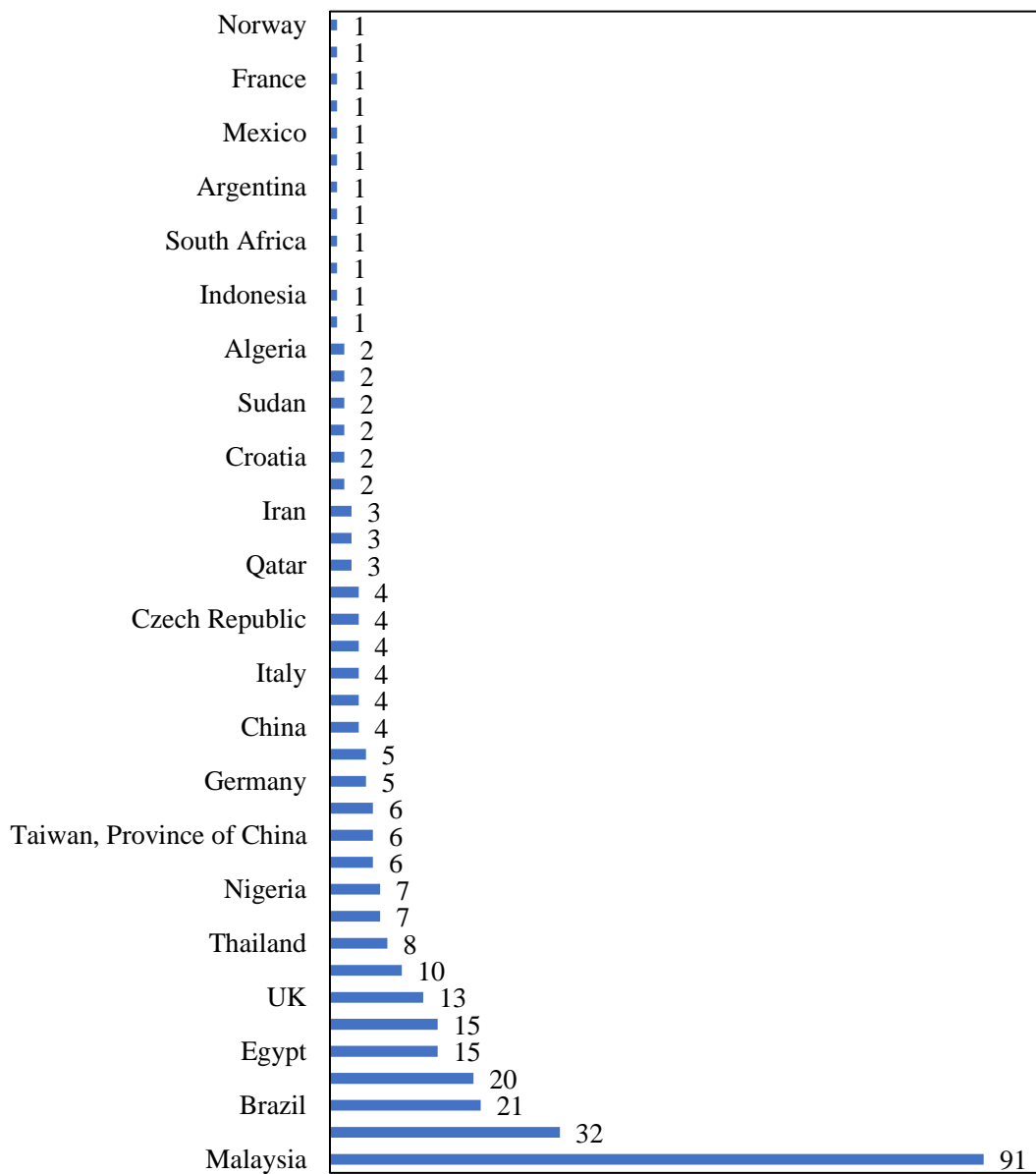
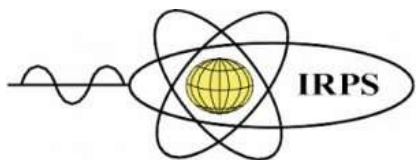


Figure 1: Countries that registered for the symposium



**ISRP 2021**  
**International Symposium on Radiation Physics**  
**Kuala Lumpur – Malaysia**  
**6 – 10 December 2021**

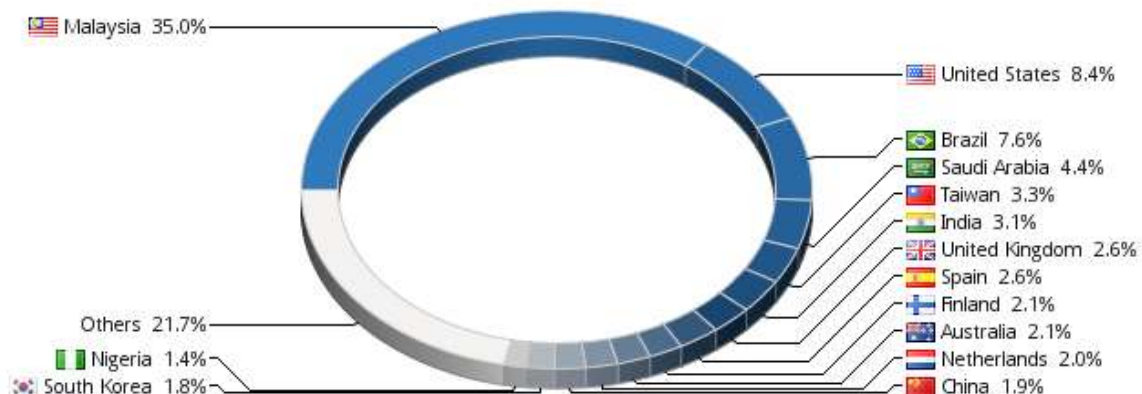


Figure 2: Website visited by 6,239 from 83 countries (<https://s11.flagcounter.com/more30/9GCq>)

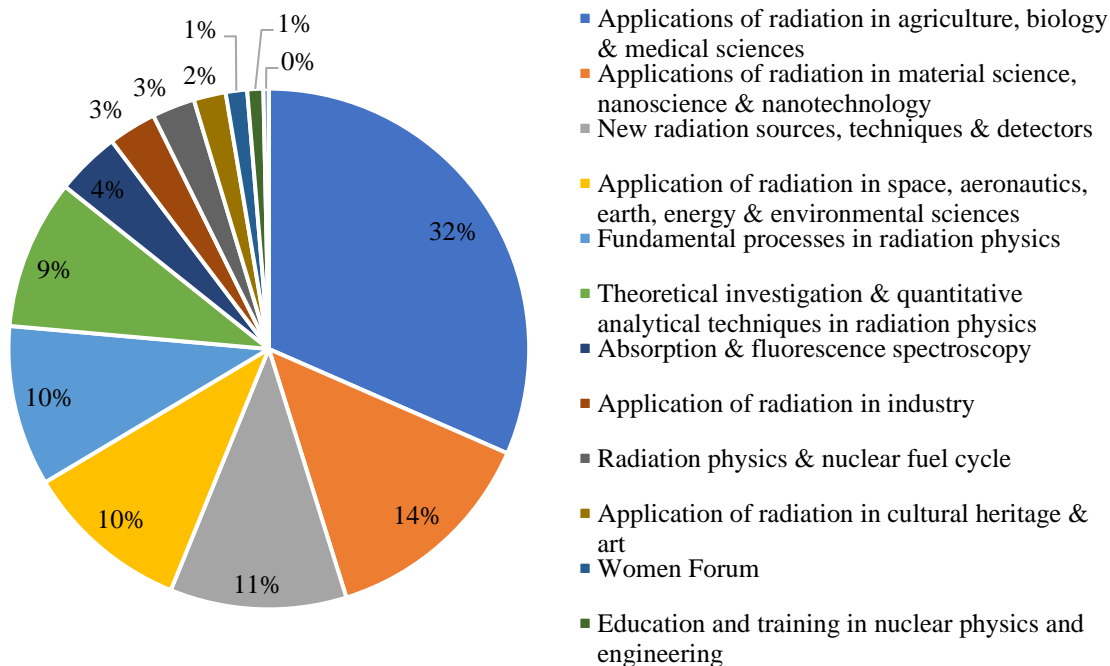
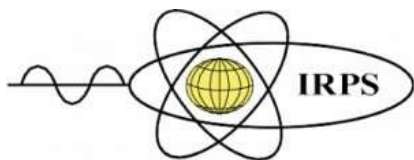


Figure 3: Pie chart showing the distribution of the article contribution for each of the themes.



### 3 SCIENTIFIC PROGRAMME SCHEDULE

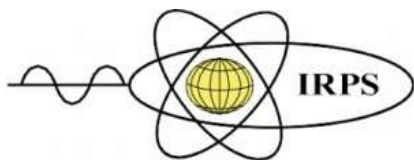
Updated as per 5 December 2021

#### 05 December 2021

<b>02:00 PM – 6:00 PM</b>		
<b>WORKSHOP</b>		
02:00 PM	Radiation hormesis	Ming Tsuey Chew
02:40 PM	Uncertainties in Radiation Biology and Implications for Research	Andrew Nisbet
03:20 PM	Quantification of chemotherapy contributions to chemoradiotherapy	Roger Dale
04:00 PM	An overall framework for neutron RBEs, ultra-high dose/Flash effects and RBE/OER changes in photon, proton and ion beams	Bleddyn Jones
04:40 PM	Radiation track structure: how does their spatial and temporal properties drive the radiobiological response	Mark Hill
05:20 PM	Radiotherapy treatment delays in the UK during the Covid-19 pandemic	Roger Dale; Bleddyn Jones

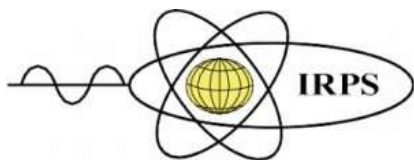
#### 06 December 2021

8:30 AM	Registration	
09:00 AM	Plenary : Th-229m and the quantum clock	Koji Yoshimura
09:30 AM	Keynote Address: Building a nuclear technology infrastructure: Malaysian experience	Siti A'iasah Hashim
10:00 AM	OPENING CEREMONY	
11:00 AM	Invited Speaker : Recent development of neutron detectors for spectrum and dose estimation	Pradip Kumar Sarkar
<b>Morning A: Radiation Physics And Applications</b>		
11:30 AM	A023 - Removal of Uranium from nuclear effluent using regenerated bleaching earth steeped in $\beta$ -naphthol	Ibrahim F. Al-Hamarneh
11:45 AM	A044 - Ta <sub>2</sub> O <sub>5</sub> -doped bismuth zinc tellurite glass: fabrications, optical, and radiation shielding characterization	Asmaa Mansour Abuelsoad
12:00 PM	A091 - Effect of mixed glass former on structural, elastic and gamma radiation shielding properties of $70[x\text{TeO}_2-(1-x)\text{B}_2\text{O}_3]-20\text{Bi}_2\text{O}_3-10\text{Li}_2\text{O}$ glasses	Mohd Ashmir Yahya
12:15 PM	A041 - Solution optical spectra of anticancer drug vandetanib using robust quantum mechanical calculations	Lewis McArthur



**ISRP 2021**  
**International Symposium on Radiation Physics**  
**Kuala Lumpur – Malaysia**  
**6 – 10 December 2021**

12:30 PM	A064 - Review of borosilicate glass for radiation dosimetry	Ying Cheah	Ying
12:45 PM	A143 - Fourier Transform Holography with Extended Reference: a step toward the use of photons of higher energy	Minh Dao	Hong
<b>Morning B: Fundamental Processes In Radiation Physics</b>			
11:30 AM	A016 - Network-Modifying Role of Er <sup>3+</sup> ions on the Structural, Optical, Mechanical, and Radiation Shielding Properties of ZnF <sub>2</sub> -BaO-Al <sub>2</sub> O <sub>3</sub> -Li <sub>2</sub> O-B <sub>2</sub> O <sub>3</sub> Glass	Nimitha Prabhu	S.
11:45 AM	A026 - Peculiarities of rare earth elements removal from chloride solution using cetylpyridinium bromide/polyvinyl chloride	Eman Allam	M.
12:00 PM	A038 - Characterization of thermoluminescence properties for Al <sub>2</sub> O <sub>3</sub> :Ge,Sr prepared by combustion synthesis method	Abdul Rahman Tamuri	
12:15 PM	A051 - Assessment of geogenic impact on thoron activity concentration in soil gas of Perak state Malaysia	Habila Nuhu	
12:30 PM	A193 - Enhancing Information Learned from Auger Processes	Eric L. Shirley	
12:45 PM	A243 - First results from FATIMA within the DESPEC collaboration at FAIR-0	Shaheen Jazrawi	
<b>Morning C: Theoretical Investigation &amp; Quantitative Analytical Techniques In Radiation Physics</b>			
11:30 AM	A021 - Investigation of the photon shielding capability of kaolin clay added with micro and nanoparticles of Bi <sub>2</sub> O <sub>3</sub>	M. Elsafi	
11:45 AM	A042 - Intramolecular hydrogen bonding of hydroxybenzoic acid isomers revealed using XPS: theory and experiment	Alexander Hill	
12:00 PM	A052 - High accuracy determination of photoelectric cross sections, X-ray Absorption Fine Structure and nanostructure analysis of zinc selenide using the X-ray Extended Range Technique	Daniel Sier	
12:15 PM	A053 - Computation of Gamma Buildup factors and Heavy Ions Penetrating Depths in Clay Composite Material using Phy-X/PSD, EXABCAL and SRIM Codes	Aamir Raza	
12:30 PM	A088 - Radiation hazard assessments of natural radioactivity in cosmetic products	Noor Zati Hani Abu Hanifah	

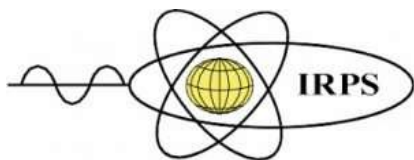


**ISRP 2021**  
**International Symposium on Radiation Physics**  
**Kuala Lumpur – Malaysia**  
**6 – 10 December 2021**

12:45 PM	A208 - The Auger Effect and its Applications	Jonathan W Dean
01:00 PM	Lunch/Vendor Talk	
<b>Afternoon: Applications of Radiation In Industry</b>		
02:30 PM	A223 - Tomographic gamma-ray imaging of industrial processes and equipment	Geir Anton Johansen
02:45 PM	A100 - Characterization of Target Transfer Function (TTF) performances for detection of pulmonary nodule in lung from current protocol	Hanif Bin Haspi Harun
03:00 PM	Invited Speaker : The Life and Times of Lise Meitner: beta-decay and non-radiative electromagnetic transitions	Heinz-Eberhard Mahnke
03:30 PM	Coffee Break/Exhibitor Video	
04:00 PM	Invited Speaker : Direct Measurements of Carbon Burning at Astrophysical Energies	Sandrine Courtin
04:30 PM	Plenary : Isomers as a bridge between nuclear and atomic physics	Philip Walker

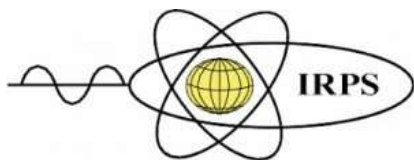
**07 December 2021**

09:00 AM	Invited Speaker : The Measure of All Things	Larry Hudson
09:30 AM	Invited Speaker : The status of the NIST radiation interaction databases	Paul Bergstrom
10:00 AM	Coffee Break/Exhibitor Video	
10:30 AM	Invited Speaker : Advances in Atomic and Molecular Physics	Christopher Chantler
<b>Morning A: Theoretical Investigation &amp; Quantitative Analytical Techniques In Radiation Physics</b>		
11:00 AM	A276 - Resolution of ferrocene and deuterated ferrocene conformations using dynamic vibrational spectroscopy: Experiment and theory	Nicholas Thien Tam Tran
11:15 AM	A278 - Calculating Characteristic Spectral Profiles: Copper Ka and Kb	Hamish A Melia
11:30 AM	A072 - Monte Carlo simulation of HDR Brachytherapy dosimetric parameters in a different medium	Nor Shazleen Ab Shukor
11:45 AM	A130 - Proton radioactivity of Dysprosium	HC Manjunatha
12:00 PM	A081 - Simulation and computational improvements of the mutual optical intensity function in two dimensions	Jake John Rogers
12:15 PM	A259 - Simulation of $K\alpha$ X-ray emission lines in metallic Cu from first principles	Mauro Guerra



**ISRP 2021**  
**International Symposium on Radiation Physics**  
**Kuala Lumpur – Malaysia**  
**6 – 10 December 2021**

12:30 PM	A102 - Rapid separation of thorium via electrosorption with carbon electrode towards efficiently managing rare-earth extraction residue	Aznan Fazli Ismail
12:45 PM	A192 - Time-resolved radiation dosimetry using a Cerium and Terbium co-doped YAG crystal scintillator	Azmi Abdullah Basaif
<b>Morning B: Applications of Radiation In Agriculture, Biology &amp; Medical Sciences</b>		
11:00 AM	A142 - Barium Sulfate and Concrete Mixture as High Energy X-ray Radiation Shielding	Izyan Hazwani Hashim
11:15 AM	A145 - Relation between energy dependence and dosimeter size: An experimental study on glass TLDs	Farhad Moradi
11:30 AM	A095 - A setup for integral measurements of multiple scattering by 10- to 100-keV electrons	Marcos N Martins
11:45 AM	A063 - Radon concentration in groundwater sources for public consumption in Bosso community, north central Nigeria and consequent annual effective dose estimation	Matthew Tikpangi Kolo
12:00 PM	A211 - Performance of Ge-doped silica optical fiber radioluminescence scintillators for radiotherapy dosimetry	Adebiyi Oresegun
12:15 PM	A136 - Dose Assessment in CT Examination of Pelvis and Establishment of Provincial Diagnostic Reference Levels in Taif, Saudi Arabia	Hamid O Osman
12:30 PM	A207 - Effect of different source-to-image distance on radiation dose and the quality of image in posteroanterior hand X-ray examination	Inayatullah Shah Sayed
12:45 PM	A114 - 2D vs 3D dose analysis of PRESAGE® Dosimeters using 3DMicroHD-OCT System: an in-house Optical CT system for radiotherapy dosimetry	Muhammad Zamir Mohyedin
<b>Morning C: Absorption &amp; Fluorescence Spectroscopy</b>		
11:00 AM	A046 - Solving self-absorption in fluorescence	Ryan M Trevorah
11:15 AM	A077 - Determination of 40K and 238U radionuclides concentration in some granite rocks by gamma spectroscopy and Energy Dispersive X-ray analysis.	M. A.El-Nahal
11:30 AM	A086 - Synthesis physical and photoluminescence investigation of Eu <sup>3+</sup> -doped gadolinium borate scintillating glass	Benchaphorn Damdee
11:45 AM	A115 - High accurate mass attenuation coefficients and nanostructure of Zinc from X-ray absorption Spectroscopy at room temperature	Ruwini S K Ekanayake

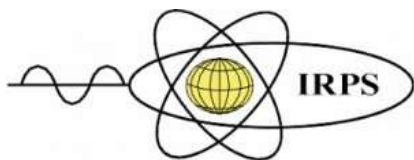


**ISRP 2021**  
**International Symposium on Radiation Physics**  
**Kuala Lumpur – Malaysia**  
**6 – 10 December 2021**

12:00 PM	A117 - Synthesis, luminescence and scintillation properties of LaCl <sub>3</sub> :Tm <sup>3+</sup> crystal	Yaowaluk Tariwong
12:15 PM	A119 - Precision measurement of the phase fine structure across the iron K-edge	Tony Kirk
12:30 PM	A121 - Structural fitting using the measured complex atomic fine structure spectra across the copper K-edge	Paul Di Pasquale
12:45 PM	A263 - High Resolution $\mu$ CT@XlabF: Future Tomographic Studies	Dariusz Hampai
01:00 PM	Sponsored Lunch Talk - A123 - Complex atomic fine structure across the copper K-edge: new results and opportunities	Chanh Quoc Tran
01:30 PM	Lunch Break	
<b>Afternoon: Application of Radiation In Cultural Heritage &amp; Art</b>		
02:30 PM	A155 - Overview of methods for determining the depth distribution of elements in X-ray fluorescence analysis	Ladislav Musílek
02:45 PM	A262 - Polycapillary X-ray techniques for archeological studies: the Peluvinum excavation site	Valeria Guglielmotti
03:00 PM	Invited Speaker : State-of-the-art of the medical applications of radiation - hot topics and emerging issues	Pedro Vaz
03:30 PM	Coffee Break/Exhibitor Video	
04:00 PM	Invited speaker :Radiation Processing – Applications and Dosimetry	Arne Miller
04:30 PM	Plenary :Radiation studies of items of cultural heritage	Heinz-Eberhard Mahnke

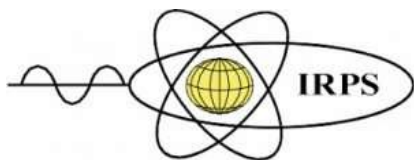
**08 December 2021**

09:00 AM	Plenary : The Application of INAA for agricultural and health related studies in Jamaica	Charles Grant
09:30 AM	Invited Speaker :Rescue effect: a non-targeted biological effect of ionizing radiation	Peter K.N. Yu
10:00 AM	Coffee Break/Exhibitor Video	
10:30 AM	Invited Speaker :Physical studies of the Epithelial Mesenchymal Transition in Breast Tissues	Siti Fairus Abdul Sani
<b>Morning A: Applications of Radiation In Agriculture, Biology &amp; Medical Sciences</b>		
11:00 AM	A109 - MRI-LINAC dosimetry approach by Monte Carlo methods coupling charged particle radiation transport with strong magnetic fields	Amiel Rocio Gayol



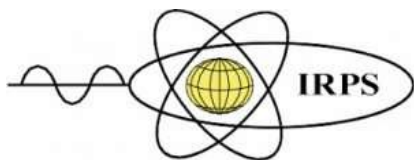
**ISRP 2021**  
**International Symposium on Radiation Physics**  
**Kuala Lumpur – Malaysia**  
**6 – 10 December 2021**

11:15 AM	A113 - Feasibility of mean glandular dose determination of digital breast tomosynthesis unit using LuSy dosimeter	Janatul Madinah Wahabi
11:30 AM	A156 - New analysis method for neutron dosimetry with Fluorescent Nuclear Track Detectors	Anna Becker
11:45 AM	A163 - Aluminum oxide crystals for high spatial resolution dosimetry of photon beams	José Vedelago
12:00 PM	A181 - Contribution to the economic heavy minerals of East El- Arish coastal sediments, North Sinai, Egypt	Mahmoud Awad
12:15 PM	A182 - Radiological Hazards associated to a raw material of Um Bogma area, southwestern Sinai, Egypt	El Saeed R. Lasheen
12:30 PM	A205 - Dosimetric characteristics of fabricated Germanium doped optical fibres for electron beam therapy audit	Norhayati Abdullah
12:45 PM	A231 - Glass microspheres as a novel targeting vector for proton-boron therapy	Fiona J Pearce
<b>Morning B: Applications of Radiation In Agriculture, Biology &amp; Medical Sciences</b>		
11:00 AM	A260 - X-ray phase contrast imaging with a simple prototype system: polyenergetic beam and a dental imaging detector.	Michel Stephani da Silva Gobo
11:15 AM	A261 - Proton therapy monitoring with orthogonal prompt-gamma imaging: the case of prostate irradiation	José Teodoro
11:30 AM	A006 - Radiation Dose Estimation Study for Sparse-View CT: Monte-Carlo Simulation	Vicent Vidal
11:45 AM	A012 - The potential use of silica-based commercial float glass for protection of gamma-radiation	Sabina Yasmin
12:00 PM	A066 - Review of the effect of reduced background radiation on living organisms	Ming Tsuey Chew
12:15 PM	A069 - Analysis of radiation dose distribution in paediatric exams	Paula Vosiak
12:30 PM	A070 - Fluoroscopy time influence on DAP values of interventional cardiac procedures	Akemi Yagui
12:45 PM	A084 - Exploring of Monte Carlo Simulation from Case Study of Particle Transport in Gamma Knife Machine	Freddy Haryanto
<b>Morning C: Applications of Radiation In Agriculture, Biology &amp; Medical Sciences</b>		
11:00 AM	A089 - Variability of estimated organ dose based on different Monte Carlo radiation transport codes for NORM-added consumer product radiation exposures	Mohamad Syazwan Mohd Sanusi



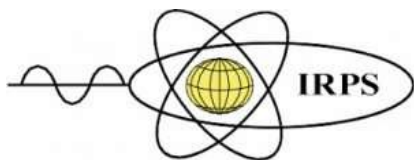
**ISRP 2021**  
**International Symposium on Radiation Physics**  
**Kuala Lumpur – Malaysia**  
**6 – 10 December 2021**

11:15 AM	A096 - Incidental finding of hepatocellular carcinoma using Ga68-PSMA PET-CT: future use for detection and theranostics?	Ew-Jun Chen
11:30 AM	A097 - Investigation of polyvinyl alcohol (PVAL) composites and the effect of variation in breast densities on image quality and dose in full-field digital mammography: A phantom study	Franca Oyiwoja Okoh
11:45 AM	A118 - Estimate of Effective Dose for Adults' Patients from Nuclear Medicine Examinations in Sudan	Mohamed Ahmed Ali
12:00 PM	A147 - Dosimetry audit of megavoltage photon beams under non-reference conditions: Comparison of fabricated Ge-doped optical fibres and TLD-100 systems	Muhammad Safwan Bin Ahmad Fadzil
12:15 PM	A195 - The Impact Of Tube Current And Iterative Reconstruction Algorithm On Dose And Image Quality Of Infant Ct Head Examination: A Phantom Study	Nor Azura Muhammad
12:30 PM	A154 - COMBAT algorithm for the coordination of delineation of Multiple radiologists of nodule boundaries in lung computed tomography images	Xiaolei Zhang
12:45 PM	A159 - Sonologist occupational exposure and ambient dose resulted from patients underwent nuclear medicine procedure	Ghada Ahmed Khouqeer
01:00 PM	Lunch/Vendor Talk	
<b>Afternoon A: Forum on "Women in Nuclear Science and Technology"</b>		<b>Jeannie Wong; Siti A'iasah Hashim; Kholoud Almugren; Isabel Lopes; Shakardokht Jafari</b>
<b>Afternoon B: Applications of Radiation In Agriculture, Biology &amp; Medical Sciences</b>		
02:30 PM	A164 - Establishment of diagnostic reference for specific computed tomography procedures	Abdelmoneim Sulieman
02:45 PM	A168 - A Markov Random Field Approach for CT Image Lung Classification using Image Processing	Khairul Azha A Aziz
03:00 PM	A175 - Pediatric radiation dosimetry and radiogenic risk estimation from computed tomography examinations	Nissren Tamam
3:15 PM	A148 - X ray spectrometry methodologies for sustainable cancer tissue analysis – recent advances and limitations	Sofia Pessanha



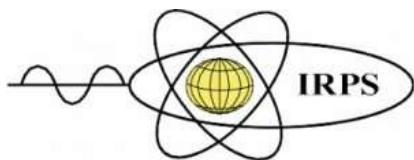
**ISRP 2021**  
**International Symposium on Radiation Physics**  
**Kuala Lumpur – Malaysia**  
**6 – 10 December 2021**

3:30 PM	A225 - Flattening filter design for intraoperative radiotherapy with 12 MeV electron beam with large applicators using Monte-Carlo simulations	Belen Jeanne Juste Vidal
3:45 PM	A234 - Radiation treatment in ensuring traceability and biosafety of aquatic food and its environment	Subha Bhassu
4:00 PM	A003 - Assessment of natural radioactivity and radiological risks from groundwater and vegetation samples collected from farms in Qatar	Yehia Manawi
4:15 PM	A228 - Medical radionuclide prioritisation and the development of the Production Rate Assessment Tool	Bethany Slingsby
<b>Afternoon C: Applications of Radiation In Material Science, Nanoscience &amp; Nanotechnology</b>		
02:30 PM	A062 - New methodology for solving nanostructures within dilute and amorphous systems: a trend study of Nickel-doped borate glass by the X-ray Extended Range Technique (XERT) and eFEFFIT fitting software for XAFS.	Geoffrey P. Cousland
2:45 PM	A067 - Gamma Ray Attenuation Studies of Brass Alloy as Tissue Equivalent Material for Radiotherapy Applications	Sakinah Buang
03:00 PM	A093 - Novel efficient alloys for radiation shielding applications: A theoretical investigation	Raghad Alsharhan
3:15 PM	A139 - Development of flexible radiation shielding materials from natural rubber/ Sb <sub>2</sub> O <sub>3</sub> composites	Supakit Yonphan
3:30 PM	A141 - Simultaneous X-ray Scattering and Spectroscopy Computed Tomography “ Monte Carlo Simulation and Experiment	Andre L.C. Conceicao
3:45 PM	A007 - Investigation flexible nanocomposite membranes of ZnO-CuO-PVA for x-ray detectors	Ahmad I. Ayesh
4:00 PM	A059 - Radiation response of marble-glass media in medical radiation applications	Amjad Rashed Alyahyawi
4:15 PM	A245 - Gamma-gamma coincidence method for determination of Fe and Tb in Montana II Soil and Coal Fly Ash sample	Truong Van Minh
04:30 PM	Invited speaker: X-ray spectrometry: theoretical and experimental determinations	José Paulo Santos
05:00 PM	Break Time	
08:00 PM	Conference dinner	



**09 December 2021**

09:00 AM	Invited Speaker : The significance of nuclear data for accelerator-based production of novel radionuclides for theranostic applications	Mayeen Khandaker
09:30 AM	Invited Speaker : Distributed Optical Fiber Radiation Dosimetry	Hairul Azhar
10:00 AM	Coffee Break/Exhibitor Video	
10:30 AM	Invited speaker : The Singapore Synchrotron Light Source (SSLS)	Mark Breese
<b>Morning A: New Radiation Sources, Techniques and Detectors</b>		
11:00 AM	A047 - Developing a novel technique of radon detection for all three naturally occurring radon (Rn-222 , Rn-220 and Rn-219)	Amos Vincent Ntarisa
11:15 AM	A085 - Miniature $4\pi\beta$ (LS)- $\gamma$ (LaBr3) coincidence system at KRISS	Minji Han
11:30 AM	A120 - Applications of MOSkin as a real-time detector for in vivo dosimetry during high-dose rate Cobalt-60 brachytherapy	Ngie Min Ung
11:45 AM	A126 - Development of FPGA-based Coincidence Module for TDCR Counting System	Agung Agusbudiman
12:00 PM	A179 - Absolute primary scintillation yield in Xe for electrons and alpha particles	Carlos Alberto de Oliveira Henriques
12:15 PM	A185 - New studies on Neutral Bremsstrahlung in Xenon optical TPCs	Cristina M B Monteiro
12:30 PM	A190 - Development of a KRISS Rn-mini radon detector at KRISS	Sanghoon Hwang
12:45 PM	A230 - Wavefield Characterisation of MHz XFEL Pulses	Trey W Guest
<b>Morning B: Applications of Radiation In Material Science, Nanoscience &amp; Nanotechnology</b>		
11:00 AM	A009 - A novel glass system based on Iraqi white sand and lead oxide for gamma ray shielding purposes	Haneen M Alsafi
11:15 AM	A010 - New glass based on Iraqi sand and modified by lead oxide to protect against gamma-ray: Fabrication, mechanical and shielding properties examination	H. F. El-Saeedi
11:30 AM	A028 - The effect of CNTs on the radiation attenuation properties of the composite of BaTiO <sub>3</sub> doped with spinnel ferrite	E. Hannachi
11:45 AM	A039 - Radiation shielding features for a new glass system based on tellurite oxide	Shadin Alhugail

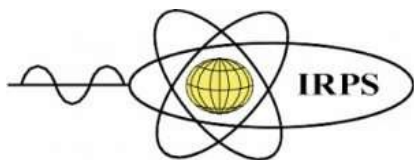


**ISRP 2021**  
**International Symposium on Radiation Physics**  
**Kuala Lumpur – Malaysia**  
**6 – 10 December 2021**

12:00 PM	A040 - Characterization and gamma rays shielding performance of calcinated bentonite nanoparticles	Eloic Lacomme
12:15 PM	A049 - On the study for TeO <sub>2</sub> -WO <sub>3</sub> -TiO <sub>2</sub> -ZnO -Na <sub>2</sub> O glass containing Pr <sub>2</sub> O <sub>3</sub> in radiation shielding applications: Theoretical computations via EPICS2017	Recep Kurtulus
12:30 PM	A050 - Assessment of Radiation attenuation properties for novel alloys: An experimental approach	Marwa Aldikhel
12:45 PM	A058 - Luminescence Studies of Fabricated Gd:Mg-Doped Silica Glass Exposed to Neutron Radiation	Nidal Taha Abahre
01:00 PM	Lunch/Vendor Talk	
<b>Afternoon A: New Radiation Sources, Techniques and Detectors</b>		
02:30 PM	A239 - Determination of the radon diffusion coefficient of thin polyethylene and aluminium foils	Beatriz Ruvira Quintana
02:45 PM	A258 - Characterisation of Cadmium Telluride Zinc photon counting detector for soft tissue imaging	Kamran Hameed
<b>Afternoon B: Mixed Theme</b>		
02:30 PM	A227 - Development of a unique neutron irradiation facility for medical radionuclides and advanced nuclear technologies	Allan Simpson
02:45 PM	A122 - A New Compact Octagonal Split Ring Resonator based Tuning Fork-Hammer Shape Perfect Metamaterial Absorber for C-Band Applications	Md. Salah Uddin Afsar
03:00 PM	Invited Speaker :Compact and very High Dose-rate Plasma Radiation Sources for Medical Applications	Marco Sumini
03:30 PM	Coffee Break/Exhibitor Video	
04:00 PM	Invited Speaker : Capillary Guiding for Beams and Radiations	Sultan Dabagov
04:30 PM	Invited Speaker : Advances in silica bead dosimetry	Shakardokht Jafari

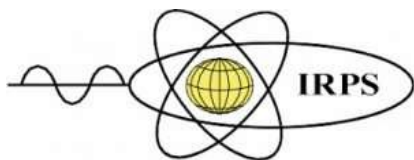
**10 December 2021**

09:00 AM	Invited Speaker : Geoneutrons	Hector Rene Vega-Carrillo
09:30 AM	Invited Speaker : Mineral Wealth and NORM. Standing Up a New Rare Earths Industry in the United States	Phil Egidi



**ISRP 2021**  
**International Symposium on Radiation Physics**  
**Kuala Lumpur – Malaysia**  
**6 – 10 December 2021**

10:00 AM	Coffee Break/Exhibitor Video	
10:30 AM	Invited Speaker : Medical Physics professional developments	Ng Kwan Hoong
<b>Morning A: Application of Radiation In Space, Aeronautics, Earth, Energy &amp; Environmental Sciences</b>		
11:00 AM	A033 - Lithium aluminate borate glass mixed with tin slag for radioactive immobilization	Syaza Amira Zulkeplee
11:15 AM	A079 - The impact of various instances of solar wind speed on the fluctuations of cosmic radiation in the solar minimum (23, 24, and 25)	N M Wateed
11:30 AM	A194 - Thermoluminescence characteristics of customised Ge-doped optical fibres (CusOF) under Am-Be neutron source as a potential to be used for space radiation detector	Farid bin Bajuri
11:45 AM	A206 - Radiological and Environmental studies on granitic rocks of Abu Furad area used in construction purposes and ceramic industry	S. A. Taalab
<b>Morning B: Application of Radiation In Space, Aeronautics, Earth, Energy &amp; Environmental Sciences</b>		
11:00 AM	A060 - Activity Concentration and Radiological Impact Assessment of <sup>226</sup> Ra, <sup>232</sup> Th and <sup>40</sup> K in Beach Sands and Sediments Samples Around Badagry Coastal Areas of Lagos	Michael Adekunle Olatunji
11:15 AM	A166 - Carbon isotope composition ( <sup>14</sup> C and <sup>13</sup> C) of the atmospheric CO <sub>2</sub> at several locations in Croatia	Ines Krajcar Bronić
11:30 AM	A270 - Assessment Of Environmental Radioactivity In The Spacial Area Of Titanium Mining At Ha Tinh Province (Vietnam)	Sy Minh Tuan Hoang
11:45 AM	A008 - Radiological Dispersion of I-131, I-133 and I-135 Isotopes Due to Hypothetical Accidental Release from Nigerian Research Reactor-1	Mayeen Khandaker
12:00 PM	CLOSING CEREMONY	



**ISRP 2021**  
**International Symposium on Radiation Physics**  
**Kuala Lumpur – Malaysia**  
**6 – 10 December 2021**

## **4 ABSTRACTS**

**Pre-conference (5 December 2021)**

**Workshop - Radiation and Radiobiology in Extreme Circumstances**

### **B003 - Radiation Hormesis**

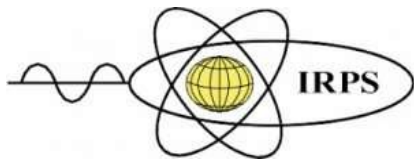
Ming Tsuey Chew<sup>1</sup>, David Bradley<sup>1,2</sup>

<sup>1</sup>Centre for Applied Physics and Radiation Technologies, Sunway University, Malaysia

<sup>2</sup>Department of Physics, University of Surrey, United Kingdom.

Corresponding author: mtchew@sunway.edu.my

Throughout life, organisms are continuously exposed to ionizing radiation, from sources of cosmic, solar, and terrestrial origin. With living organisms having the ability to develop powerful defence mechanisms against radiation, also with current understanding of the mechanisms of radiation damage and repair, radiation induced gene expression and other genotoxic agents, the beneficial effects of radiation could be exploited, especially at low doses. Radiation hormesis is the phenomena whereby low doses of ionizing radiation provoke stimulatory or beneficial effects in otherwise unstressed cells, while increasingly larger doses are harmful. In some circumstances, beneficial low dose irradiation effects have been observed at levels  $\leq 100$  mGy. Some of the potential benefits of radiation hormesis, such as protective (stimulate antioxidant production), anti-inflammatory, activated DNA reparative processes and protective apoptosis, prevent harm from elevated doses. These, together with selective removal of precancerous growth, stimulated anti-cancer effects, other immunity, slowing down of aging, and prolonged life will be factors that will be discussed/presented.



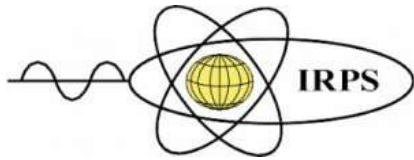
**ISRP 2021**  
**International Symposium on Radiation Physics**  
**Kuala Lumpur – Malaysia**  
**6 – 10 December 2021**

### **A285 - Uncertainties in Radiation Biology and Implications for Research**

Andrew Nisbet

Department of Medical Physics and Biomedical Engineering, University College London

It is well known that successful radiotherapy outcomes rely upon the accurate delivery of radiation dose to the clinical target volume, whilst sparing the surrounding organs at risk. The achievable accuracy in radiotherapy from a dosimetric perspective have been extensively considered. Furthermore, the delivered dose should be traceable to a primary standards laboratory. The quantification of uncertainty within the dosimetry chain from the primary standard to the calibration of a cancer centre's treatment unit has also been determined and the implications of such uncertainty on the tumour control and normal tissue complication probabilities assessed. However, the determination of uncertainties in radiation biology have been less well addressed in the literature. This presentation seeks to review the sources and magnitude of uncertainties in radiation biology and the implications of such uncertainties on clinical translation of radiobiological studies, considering in particular the implications for future research.



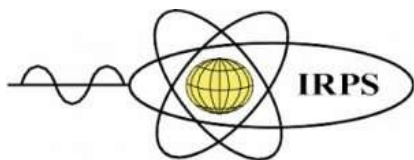
**ISRP 2021**  
**International Symposium on Radiation Physics**  
**Kuala Lumpur – Malaysia**  
**6 – 10 December 2021**

### **A283 - Quantification of Chemotherapy Contributions to Chemoradiotherapy**

Roger Graham Dale

Imperial College

Chemoradiotherapy treatments are those which use chemotherapy drugs to improve the tumour control obtainable from radiotherapy schedules. Chemotherapy is known to be beneficial and is widely prescribed but the methodologies employed for defining chemotherapy and radiation doses are entirely different, meaning that quantitative elucidation of the chemotherapy contribution to a chemoradiotherapy schedule remains difficult. One solution is to express the chemotherapy effect in terms of its radiation-equivalent and several authors have examined ways of doing this. The usual approach is to express the chemotherapy contribution as the additional biologically effective dose (BED) which it adds to the basic radiation schedule. Unfortunately, the BED-equivalents derived this way are dependent on the clinical end-point at which the assessment is undertaken, i.e. such determinations do not yield an absolute measure of drug effect. This article outlines an approach which, by consideration of the general underlying shape of dose-response curves, suggests a way in which absolute measures of drug improvement can be derived.



**ISRP 2021**  
**International Symposium on Radiation Physics**  
**Kuala Lumpur – Malaysia**  
**6 – 10 December 2021**

### **A204 - An Overall Framework for Neutron RBEs, Ultra-High Dose/Flash Effects And RBE/OER Changes in Photon, Proton and Ion Beams**

Bleddyn Jones

Gray Laboratory, Department of Oncology, Old Road Campus, University of Oxford, OX3 7DQ, United Kingdom

Corresponding author: [Bleddyn.Jones@oncology.ox.ac.uk](mailto:Bleddyn.Jones@oncology.ox.ac.uk)

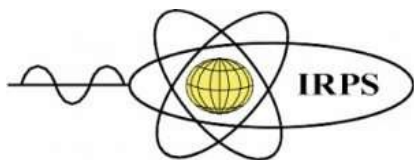
The talk will cover recent work where neutron RBEs for beams in the range 0.2-30 MeV including those with maximum energy of 62 MeV are estimated from consideration of recoil proton energies. The data of Hall et al (Radiation Res. 64, 245-255, 1975) and others are used to verify the model. It also appears that:

The single neutron energy value for a spectrum can represent the entire beam in terms of overall RBE: this is approximately 0.087 of the maximum energy.

The most reasonable linear energy transfer (LET) for maximal proton recoil RBE is found to be around  $63 \text{ keV} \cdot \mu\text{m}^{-1}$  rather than the value around 30 previously identified by Belli and colleagues. The discrepancy is probably due to the severe range limitations for a proton beam of decreasing energy to cover a cell whereas a neutron beam produces recoil protons throughout its length so is not so restricted.

If the maximal or peak RBE is obtained at  $\text{LET}_U$ , and lower RBE's at higher LET values due to overkill effects, further studies of these LET-RBE 'turnover points' show that  $\text{LET}_U$  is higher in the case of hypoxic cells than for oxic cells irradiated in neon, carbon and helium beams, from which it is possible to estimate the oxygen enhancement ratios (OER) as they change with increasing LET. By applying a volumetric form of LET (by multiplying LET with fluence) and considering instantaneous fluence rates, it is inevitable that the  $\text{LET}_U$  position will occur at much lower values of LET if dose rate (and instantaneous fluence) is increased, since the energy released per unit micro-volume will rise more rapidly until the energy level required for overkill occurs. The OER is around 1.25 at  $\text{LET}_U$ , so that shifting  $\text{LET}_U$  to lower values will probably cause the fall of OER with LET to become more efficient.

By applying time factors as ratios of times at different dose rates, the phenomena found at ultra-high dose rates and in FLASH radiotherapy with protons can be simulated. These will be shown graphically. Equations that link dose rates and dose to achieve iso-effective FLASH effects are derived. These all form a testable basis to guide further experiments and provide an overall working framework for further research.



**A198 – Radiation Track Structure: How Does Their Spatial and Temporal Properties Drive the Radiobiological Response**

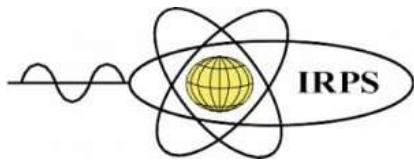
Mark A. Hill

MRC Oxford Institute for Radiation Oncology, University of Oxford, ORCRB Roosevelt Drive, Oxford OX3 7DQ, United Kingdom

Ionising radiation is far more effective at producing a wide range of biological effects than might be expected from the limited amount of energy deposited or the comparatively small amount of DNA damage induced, compared to the vast amount of endogenous damage arising from normal metabolism of the cell. This is due to the unique way energy is deposited along highly structured tracks of ionisation and excitation events, which results in the correlation of DNA damage sites from the nanometre to the micrometre scale. Correlation of these events along the track on the nanometre scale results in clustered damage, which not only result in the formation of DNA double-strand breaks (DSB) and the more difficult to repair complex DSB (which includes additional damage within a few base pairs) but also non-DSB clusters. The track structure varies significantly with radiation quality and the increase in RBE observed with increasing LET in part corresponds to an increase in the probability and complexity of clustered DNA damage produced. Likewise, with increasing LET there is an increase probability of correlation over larger scales, associated with packing of DNA and associated chromosomes within the cell nucleus. This can also have a major impact on biological response, with difference becoming more pronounced with low doses associated with radiation protection exposures. The proximity of the correlated damage along the track increases the probability of miss-repair through pairwise interactions resulting in an increase in probability and complexity of DNA fragments/deletions, mutations and chromosomal rearrangements. The temporal properties radiation exposure may also have a major impact on the resulting biological effectiveness. While this is well known for low dose rate and fractionated exposures, there is now extensive interest in the variation in biological effectiveness at ultra-high 'FLASH' dose rates ( $> 40$  Gy/s) which has been observed to result in a reduction in normal tissue toxicity without compromising the anti-tumour response.

Understanding the mechanisms underlying the biological effectiveness of ionising radiation can provide an important insight into the resulting radiation biology, improving the efficacy of radiotherapy, as well as the risks associated with exposure. This requires a multi-scale approach for modeling, considering the physics of the track structure from millimetre scale down to the nanometre scale, temporal aspects of exposure, the structural packing of the DNA within the nucleus, the resulting chemistry in the context of the highly reactive environment of the nucleus, along with the subsequent biological response. In addition to an overview of the link between physical interactions, associated chemistry and biological response, the presentation will also highlight some of the common misconceptions.

ABSTRACTS| Workshop - Radiation and Radiobiology in Extreme Circumstances



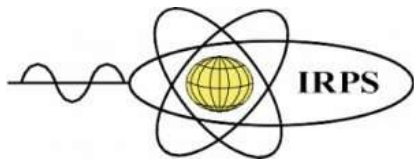
**ISRP 2021**  
**International Symposium on Radiation Physics**  
**Kuala Lumpur – Malaysia**  
**6 – 10 December 2021**

**A282 - Radiotherapy Treatment Delays in The UK During The Covid-19 Pandemic.**

Roger Graham Dale

Imperial College

There is a wealth of clinical evidence which confirms that unscheduled interruptions (treatment gaps) during radiotherapy can allow increased tumour repopulation and, as a consequence, decreased tumour control. The radiobiology of the repopulation effect has been widely investigated and, within the UK, national recommendations have been developed to provide guidance on ways of modifying interrupted schedules in order to fully or partially offset the deleterious effects of treatment gaps. During 2020/21 the rapid spread of Covid-19 has meant that many patients undergoing radiotherapy have had their treatments compromised as a consequence of either illness or enforced self-isolation and considerable effort has been devoted to providing guidance on how best to implement the available guidelines. This talk will outline the radiobiological considerations which are involved and will discuss the UK experience.



**ISRP 2021**  
**International Symposium on Radiation Physics**  
**Kuala Lumpur – Malaysia**  
**6 – 10 December 2021**

**Monday (6 December 2021)**

**Keynote address**

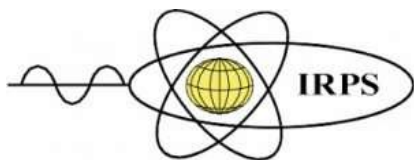
**A202 - Building a Nuclear Technology Infrastructure: Malaysian Experience**

Siti A'iasah Bt. Hashim

Malaysian Nuclear Agency

Corresponding author: [aiasah@nm.gov.my](mailto:aiasah@nm.gov.my)

Not many people knew that Malaysia was one of the earliest users of an x-ray machine in the world when Taiping Hospital received one in 1897, two years after its invention by Wilhelm Conrad Roentgen. However, only in 1972 nuclear research was initiated when the Cabinet officially approved the establishment of the Tun Ismail Atomic Research Centre (PUSPATI). On June 28<sup>th</sup> 1982, the Reaktor TRIGA Puspati reached its first criticality that marked the beginning of Malaysia's research in nuclear technology. Since then the country's nuclear infrastructure had expanded significantly but limited mostly within the research institution which is now known as Malaysian Nuclear Agency. All the major facilities in the agency are being utilised for R&D as well as servicing the industrial needs.



**ISRP 2021**  
**International Symposium on Radiation Physics**  
**Kuala Lumpur – Malaysia**  
**6 – 10 December 2021**

## **Plenary Talk**

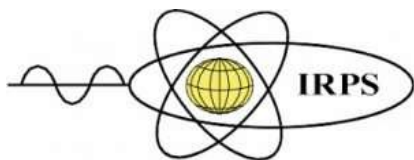
### **B004 - Th-229m And The Quantum Clock**

Koji Yoshimura<sup>1</sup>

<sup>1</sup>Research Institute for Interdisciplinary Science, Okayama University, Japan

Corresponding author: yosimura@okayama-u.ac.jp

Among thousands of nuclei, Thorium-229 is the only nucleus which has nuclear state with level of a few electronvolts. The state, if it really exists low-lying and long-lived, could be manipulated with coherent laser optics, which are commonly used in atomic physics. One promising application is the "nuclear clock". Since nuclei are shielded with core electrons, "nuclear clock" is less sensitive to external field and could potentially outperform atomic clock. The transition could also be utilized for many applications, including test of temporal variation of fundamental physics constant, dark matter search, geodesy, and so on. To utilize the isomeric transition, we should first observe it and determine its energy level precisely enough for laser excitation. Despite many experimental attempts for more than forty years, no successful laser excitation nor observation of optical transition has been achieved so far. This is because of the large uncertainties in energy and lifetime and the lack of method to artificially generate the isomer state. However, the situation has changed significantly in the last few years. Starting with the first observation of the transition of emitting internally converted electrons from the isomer state in 2016, several experimental results have been reported, and the energy accuracy has greatly improved. And our group, for the first time, succeeded in artificially generating an isomer state via 2nd excited state. Mysterious veil is now being removed and many groups are competing to make a first detection of the optical isomeric transition. In this talk, I will introduce the recent progress in the Thorium-229 projects and its future prospect.



**ISRP 2021**  
**International Symposium on Radiation Physics**  
**Kuala Lumpur – Malaysia**  
**6 – 10 December 2021**

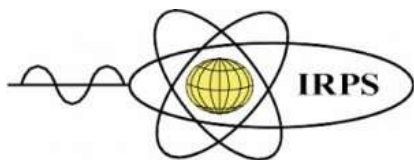
**A197 - Isomers As A Bridge Between Nuclear And Atomic Physics**

Philip M. Walker

Department of Physics, University of Surrey, Guildford GU2 7XH, UK

Corresponding author: p.walker@surrey.ac.uk

The year 2021 marks exactly 100 years since Otto Hahn discovered the first example of nuclear isomerism. The existence of long-lived nuclear excited states opens a window on nuclear structure and applications. From isomers, the availability of an electromagnetic decay pathway enables coupling to the atomic electrons, such that nuclear and atomic transitions become interdependent. The nuclear decay process of internal electron conversion is the most well known. However, observation of its inverse, nuclear excitation by electron capture, is controversial and requires further research. In this presentation, the relationship between nuclear and atomic transitions is outlined, together with applications. Some of these applications are well established, while others await basic advances.



**ISRP 2021**  
**International Symposium on Radiation Physics**  
**Kuala Lumpur – Malaysia**  
**6 – 10 December 2021**

### **Invited Talks**

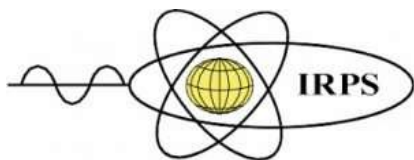
#### **A219 - Recent Development Of Neutron Detectors For Spectrum And Dose Estimation**

Pradip Kumar Sarkar

MCNS, Manipal Academy for Higher Education, Karnataka, India

Corresponding author: pksarkar02@gmail.com

Detection, measurement and analysis of neutron energy distributions (spectrum) for estimation of radiation dose and other related quantities constitute important research activities in radiation physics. Neutrons are not directly ionising radiations (particles) and hence energies and intensities of secondary particles like protons, alphas or gamma rays emitted from neutron induced nuclear reactions are measured to estimate the incident neutron spectrum and the dose. Measured energy distributions of protons (in proton recoil scintillators) or alpha particles (in He-3 detectors or in BF<sub>3</sub> detectors with different moderator sizes) are used to estimate the neutron related quantities (spectrum, dose etc.). These measured distributions of secondary particles are required to be deconvoluted using matrix inversion and other techniques like the genetic algorithm-based unfolding with the help of the estimated response matrix of the detection system. These response matrices are mostly generated using theoretical simulations (Monte Carlo). When the neutron spectrum is estimated from the proton recoil distributions, the unfolding techniques based on matrix inversions are generally used. On the other hand, the data used from prompt gammas (recent development), delayed gammas or the moderated BF<sub>3</sub> detectors (Bonner spheres), special techniques for solving underdetermined inverse problems are used. This is because in these cases the measured data are less in number compared to the number of energy bins at which the solution is sought. Several techniques are available to solve such ill-posed inverse problems, however, a genetic algorithm-based search embedded in Monte Carlo loops seems to work satisfactorily. For dose estimation two different methods can be utilised, One, is to estimate the neutron spectrum and then multiplying it with the fluence to dose conversion coefficients. The other method is to apply multivariate linear regression to fit the detector responses with the energy differential fluence to dose conversion coefficients and then using the fitting coefficients to estimate the dose from the measured gamma intensities. A recent development of neutron dose estimation from delayed or prompt gammas utilises such technique.



**ISRP 2021**  
**International Symposium on Radiation Physics**  
**Kuala Lumpur – Malaysia**  
**6 – 10 December 2021**

### **A196 - The Life and Times of Lise Meitner: Beta-Decay and Non-Radiative Electromagnetic Transitions**

Heinz-Eberhard Mahnke<sup>1,2,3</sup>

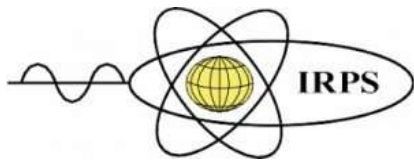
<sup>1</sup>Fachbereich Physik, Freie Universität Berlin, Germany

<sup>2</sup>Helmholtz-Zentrum Berlin für Materialien und Energie GmbH, Germany

<sup>3</sup>Ägyptisches Museum und Papyrussammlung, Staatliche Museen zu Berlin, Germany

Corresponding author: mahnke@helmholtz-berlin.de

The current activities in neutrino physics prompts us to look back onto the research activities a century ago which had led to the discovery of these weakly interacting particles. One of the leading researchers was Lise Meitner, who observed electrons with well-defined energy besides the continuous energy spectrum emitted in beta decay. While she tried almost desperately to understand the reason for the continuous energy spectrum - the puzzle was finally resolved when Wolfgang Pauli proposed a new particle, the "neutrino" - the origin of the electron lines was well explained by Lise Meitner. These electron lines are understood as radiationless nuclear transitions competing with  $\gamma$  ray emission, the so-called *internal conversion* process. In the case of transition energies of around 100 keV or higher, the origin of these electrons clearly lies within the nucleus; in the energy regime below 100 keV, however, such electrons may originate from transitions in the electronic shells as a non-radiative alternative to X-ray emission, the process known as *Auger effect*. In the case of Auger electrons, Lise Meitner certainly described such a process within the electronic shells of the atom when she presented her results on the decay of UX1, nowadays known as  $^{234}\text{Th}$ , but in fact, she did not observe such electrons experimentally. In the case of  $^{234}\text{Th}$ , she was misled by an unfortunate coincidence ("bad luck"). Following the beta decay, two nuclear transitions between the excited levels in the daughter nucleus  $^{234}\text{Pa}$  have almost exactly the same transition energy as compared to the characteristic X-ray energies of Th or Pa. While her "competitor" in Cambridge, Charles D. Ellis, already questioned her interpretation, it took more than 50 years to clarify that these electrons result from non-radiative **nuclear** rather than atomic transitions, i.e. *internal conversion*, a result overlooked for more than 40 years.



**B005 - Direct Measurements of Carbon Burning at Astrophysical Energies**

G. Fruet,<sup>1</sup> S. Courtin,<sup>1,2,1</sup> M. Heine,<sup>1</sup> D.G. Jenkins,<sup>3</sup> P. Adsley,<sup>4</sup> A. Brown,<sup>3</sup> R. Canavan,<sup>5,6</sup> W.N. Catford,<sup>5</sup> E. Charon,<sup>7</sup> D. Curien,<sup>1</sup> S. Della Negra,<sup>4</sup> J. Duprat,<sup>8</sup> F. Hammache,<sup>4</sup> J. Lesrel,<sup>4</sup> G. Lotay,<sup>5</sup> A. Meyer,<sup>4</sup> E. Monpriat,<sup>1</sup> D. Montanari,<sup>1,2</sup> Morris,<sup>3</sup> M. Moukaddam,<sup>1</sup> J. Nippert,<sup>1</sup> Zs. Podolyák,<sup>5</sup> P.H. Regan,<sup>5,6</sup> I. Ribaud,<sup>4</sup> Richer,<sup>1</sup> M. Rudigier,<sup>5</sup> R. Shearman,<sup>5,6</sup> N. de Séréville,<sup>4</sup> and C. Stodel<sup>9</sup>

<sup>1</sup>Université de Strasbourg, CNRS, IPHC UMR 7178, F-67000 Strasbourg, France

<sup>2</sup>USIAS/Université de Strasbourg, Strasbourg, F-67083, France

<sup>3</sup>University of York, York, YO10 5DD, UK

<sup>4</sup>Institut de Physique Nucléaire, CNRS/IN2P3, Université Paris-Sud, Université Paris-Saclay, F-91406 Orsay Cedex, France

<sup>5</sup>Department of Physics, University of Surrey, Guildford, GU2 7XH, UK

<sup>6</sup>National Physical Laboratory, Teddington, Middlesex, TW110 LW, UK

<sup>7</sup>NIMBE, CEA, CNRS, Université Paris-Saclay, CEA Saclay F-91191 Gif sur Yvette, France

<sup>8</sup>Centre de Sciences Nucléaires et de Sciences de la Matière (CSNSM), Université Paris Sud, UMR 8609-CNRS/IN2P3, F-91405 Orsay, France

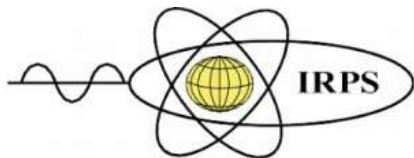
<sup>9</sup>GANIL, CEA/DSM-CNRS/IN2P3, Caen, F-14076, France

Fusion reactions play an essential role in the energy production, the nucleosynthesis of chemical elements and the evolution of massive stars. Among these reactions, carbon burning is a crucial ingredient to understand the late stages of massive stars [1] essentially driven by the  $^{12}\text{C}+^{12}\text{C}$  reaction. It presents prominent resonances at energies ranging from a few MeV/nucleon down to sub-Coulomb barrier energies, possibly due to molecular  $^{12}\text{C}-^{12}\text{C}$  configurations of  $^{24}\text{Mg}$  [2,3]. The possible persistence of these resonances to deep sub-Coulomb barrier relative energies causes colossal uncertainties of extrapolations of  $^{12}\text{C}+^{12}\text{C}$  fusion cross section towards the experimentally challenging region of astrophysics interest with extremely small cross sections. The direct measurement of key fusion reactions at stellar energies offers an unbiased and evident experimental access, but calls for innovative measures for efficient background reduction.

This contribution will discuss recent results obtained in the  $^{12}\text{C}+^{12}\text{C}$  system at deep sub-barrier energies using the STELLA setup combined with the UK-FATIMA detectors for the exploration of fusion cross-sections of astrophysical interest [4]. Characteristic gamma-rays of the exit channels have been measured with an array of  $\text{LaBr}_3$  detectors and the protons and alpha particles associated to the major final states were identified using double-sided silicon strip detectors. A novel rotating target system employing large thin self-supporting target foils

---

<sup>1</sup> E-mail: Sandrine.Courtin@iphc.cnrs.fr



**ISRP 2021**  
**International Symposium on Radiation Physics**  
**Kuala Lumpur – Malaysia**  
**6 – 10 December 2021**

has been developed to sustain carbon beams with micro-A intensity delivered by the ANDROMEDE 4 MV Pelletron facility of the University Paris-Saclay and IJC Lab (France). The gamma-particle coincidence technique combined with the merit of nanosecond-timing measurements have been used to minimize background contributions for cross-section determination at the highest precision reached so far. This has allowed to obtain astrophysical  $S$ -factors, which will be presented and discussed in terms of sub-barrier hindrance effects as well as possible resonant features in the  $^{24}\text{Mg}$  compound system, down to the Gamow window [5]

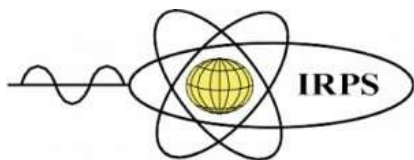
C. E. Rolfs and W.S. Rodney, *Cauldrons in the Cosmos* (Univ of Chicago Press, 1988), 1st ed.

D. Jenkins and S. Courtin *J. Phys. G: Nucl. Part. Phys.* 42, 034010 (2015).

Y. Chiba and M. Kimura, *Phys. Rev. C* 91, 061302(R) (2015)

M. Heine *et al.*, *Nucl. Inst. Methods A*, 903 1 (2018), and references therein.

G. Fruet *et al.*, *Phys. Rev. Lett.* 124, 192701 (2020).



**ISRP 2021**  
**International Symposium on Radiation Physics**  
**Kuala Lumpur – Malaysia**  
**6 – 10 December 2021**

**Tuesday (7 December 2021)**

### **Plenary Talk**

#### **B001 - Radiation Studies of Items of Cultural Heritage**

Heinz-Eberhard Mahnke<sup>1,2,3</sup>

<sup>1</sup>Ägyptisches Museum und Papyrussammlung, Staatliche Museen zu Berlin, Germany

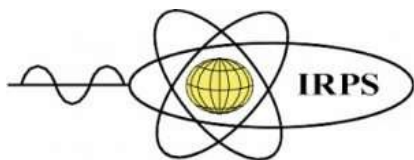
<sup>2</sup>Helmholtz-Zentrum Berlin für Materialien und Energie GmbH, Germany

<sup>3</sup>Fachbereich Physik, Freie Universität Berlin, Germany

Corresponding author: mahnke@helmholtz-berlin.de

When we see a piece of art or an archaeological object for the first time, a painting, a jewel, a sculpture or merely a simple piece of pottery on display in a museum or in an exhibition, we might be fascinated by its beauty or by its simplicity. However, many questions often arise in connection with such items on display, about its origin, its context, its provenance, its authenticity. Finding complete answers is a fully interdisciplinary task between art, humanities and natural sciences. Concerning the contribution from natural science, it often needs the application of just the best methods and techniques out of a multitude of possible options, starting from simply viewing with or without a magnifying glass up to highly sophisticated and advanced techniques developed in atomic physics, nuclear physics and chemistry, and even biophysics. Over recent decades, especially techniques using various types of radiation have been optimized for applications to objects of cultural heritage. This will be reviewed and illustrated by discussing examples, such as paintings, gemstones, or gold finds, which have recently attracted public interest. Finally, latest results of our multidisciplinary cooperation\* on revealing hidden text on ancient manuscripts such as papyri by virtual unfolding will be presented as part of the ERC Project “Localizing 4000 Years of Cultural History. Texts and Scripts from Elephantine Island”. The project is led by the PI Verena Lepper, curator for Egyptian and Oriental Papyri at the Ägyptisches Museum und Papyrussammlung, Staatliche Museen zu Berlin, which houses one of the largest papyrus collections from Elephantine.

\*in cooperation with Tzulia Angos, Tobias Arlt, Daniel Baum, Marc Etienne, Hans-Christian Hege, Felix Herter, Norbert Lindow, Ingo Manke, Eve Menei, and Verena Lepper.



**ISRP 2021**  
**International Symposium on Radiation Physics**  
**Kuala Lumpur – Malaysia**  
**6 – 10 December 2021**

### **Invited Talks**

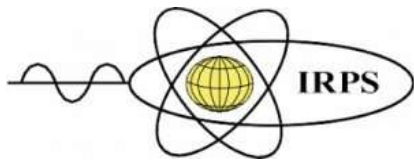
#### **A110 - The Measure of All Things**

Larry Hudson

Radiation Physics Division, National Institute of Standards & Technology, USA

Corresponding author: [larry.hudson@nist.gov](mailto:larry.hudson@nist.gov)

The Enlightenment project to define physical measures based upon nature was in a sense completed by the General Conference on Weights and Measures in 2019 with the complete elimination of measurement artifacts from the international system of units (the SI). By fixing the numerical values of key constants of the universe, the units of the SI have now all been thereby redefined and with durable stability. It is now nonsensical to measure, for example, the speed of light, the Planck constant, the elementary electric charge, the Boltzmann constant, or the Avogadro constant; they (and others) are effectively known to infinite precision. Aside from the profound conceptual shift, continuity with existing measurements was maintained. This talk will highlight advantages that now follow from this recent metrology revolution, generally, but with an emphasis on aspects related to radiation physics. For example, it now follows that a standard for a quantum of electromagnetic radiation can now be realized and transferred as a frequency ( $\nu$ ), a length ( $\lambda$ ), or an energy ( $E$ ) with formal equivalency. We shall also review the contributions of radiation physics to the redefinition of the SI, particularly that of precision x-ray metrology to the redefinition of the kg.



**ISRP 2021**  
**International Symposium on Radiation Physics**  
**Kuala Lumpur – Malaysia**  
**6 – 10 December 2021**

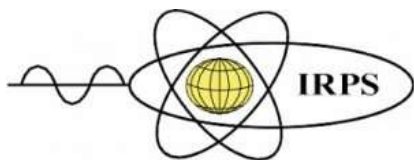
**A189 - The Status of the NIST Radiation Interaction Databases**

P. M. Bergstrom

Radiation Physics Division, National Institute of Standards and Technology, USA

Corresponding author: paul.bergstrom@nist.gov

Since the 1950's, the National Institute of Standards and Technology (then the National Bureau of Standards) has provided a series of increasingly sophisticated database for fundamental processes of radiation interacting with matter. These databases explore the interactions of photons, electrons and some heavy charged particles with isolated atoms. The uses of these data are ubiquitous, finding application in primary standards, medical applications, industrial irradiation facilities and shielding problems among others. In this talk, I discuss the provenance of these databases, pointing out approximations made and areas where improvement is possible. Several points of common confusion are also addressed. Finally, I discuss prospects for further refinement and whether or where those improvements might matter.



**ISRP 2021**  
**International Symposium on Radiation Physics**  
**Kuala Lumpur – Malaysia**  
**6 – 10 December 2021**

**A200 - Advances in Atomic and Molecular Physics [Theoretical Investigations and Quantitative Analytical Techniques in Radiation Physics]**

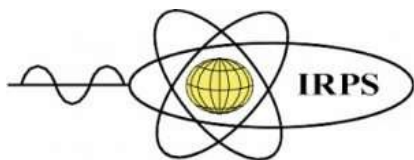
Christopher T. Chantler<sup>1</sup>

<sup>1</sup>School of Physics, University of Melbourne, Victoria, Australia

Corresponding author: chantler@unimelb.edu.au

**Abstract:**

Atomic physics is the core of calibration and understanding of radiation physics. New theory can now see the impact of Auger processes. New theory can now see the 100-1000 spectral components of characteristic X-ray radiation for X-ray spectroscopy and fundamental processes. New experiment can see these new processes for the first time. We live in an exciting world and in exciting times for Science and Understanding. Molecular physics and Condensed Matter science are also making great strides in theoretical and experimental understanding with XERT, Hybrid, and Complex form factor measurement. Yet, questions: QED and scattering disagree on the spectrum of atomic hydrogen and muonic hydrogen possibly relating to the nuclear radius... is this resolved? An anomaly in QED exists for most (X-ray) measurements of few-electron exotic atoms ... what is this due to and what does it mean? What is the status of  $g-2$  free and bound experiments? What do we learn from exotic atoms for conventional synchrotron or laboratory science? XFEL and RIXS technology are new, exciting and confusing to understand theoretically – what can they tell us about nature? I promise not to answer all questions!



**ISRP 2021**  
**International Symposium on Radiation Physics**  
**Kuala Lumpur – Malaysia**  
**6 – 10 December 2021**

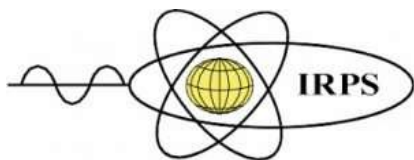
**A075 - State-of-The-Art of Radiation Protection and Dosimetry in the Medical Applications of Radiation - Hot Topics and Emerging Issues**

Pedro Vaz

Centro de Ciências e Tecnologias Nucleares, Instituto Superior Técnico, Universidade de Lisboa, Portugal

Corresponding author: pedrovaz@ctn.tecnico.ulisboa.pt

Medical applications of ionizing radiation pose significant Radiation Protection- and Radiation Safety-related challenges, due to the need to avoid unnecessary and undue exposures to ionizing radiation of medical staff, patients and members of the public. The International System of Radiation Protection is articulated around three fundamental principles – Justification of practices, Optimization of protection and Dose Limitation – and its implementation and operational aspects in clinical settings mobilizes different communities of experts, including medical doctors, medical physicists, radiographers, as well as researchers, and representatives of regulatory authorities, among others. In this paper, the state-of-the-art of Radiation Protection in the medical applications of ionizing radiation will be described, addressing different dosimetry aspects and topics in radiodiagnostic, interventional procedures, nuclear medicine and radiotherapy, including emerging and hot topics associated to, *inter alia*, the use of radionuclides and radiopharmaceuticals in molecular radiotherapy and targeted radionuclide therapy, cumulative exposure doses in radiodiagnostic and the use of monochromatic x-rays for different purposes. Progress in the implementation of the aforementioned Justification (using appropriateness criteria and referral guidelines) and Optimization (through the establishment of Diagnostic Reference Levels) principles will be discussed. The adequacy of the International System of Radiation Protection to overcome the aforementioned challenges and the need to evolve towards a more individual-risk based approach including genetic, gender, age, lifestyle and other factors will be succinctly discussed. Last but not least, Radiation Protection education and training issues will also be discussed.



**ISRP 2021**  
**International Symposium on Radiation Physics**  
**Kuala Lumpur – Malaysia**  
**6 – 10 December 2021**

### **A289 - Radiation Processing – Applications and Dosimetry**

Arne Miller

DTU, Denmark

Radiation processing covers a large range of processes, with the main ones being radiation sterilization of medical devices, polymer modification through curing and crosslinking, and irradiation of food for extending storage time, and a brief review of these and a few other radiation applications are reviewed.

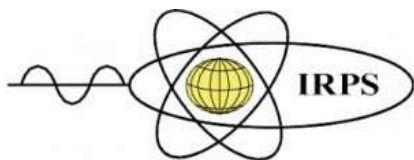
Industrial radiation sources for these applications are gamma (mainly Co-60), electron beams with energies from 80 keV to 10 MeV, and x-rays generated at 150 kV to 7.5 MV, and they are briefly discussed-

Measurement of absorbed dose is the key for documenting that the radiation process is operating within specifications. These are specified in terms of a required dose for the process to be effective and a maximum acceptable dose in order for the product properties not to be impaired.

Dose measurements must – in most cases – be traceable to national standards and the measurement uncertainty must be known. Many dosimetry systems have been developed over the years, but in practice only a few are used commercially. These are reviewed, along with calibration methods and the importance of establishing uncertainty budgets.

There is still room for improvement in dosimetry, and in international standards committees work is ongoing in support of dosimetry development, in particular with respect to interpretation and use in establishing process specifications.

Examples of specific dosimetry challenges are finally discussed.



**ISRP 2021**  
**International Symposium on Radiation Physics**  
**Kuala Lumpur – Malaysia**  
**6 – 10 December 2021**

**Wednesday (8 December 2021)**

**Plenary Talk**

**A213 - The Application Of INAA For Agricultural And Health Related Studies In Jamaica**

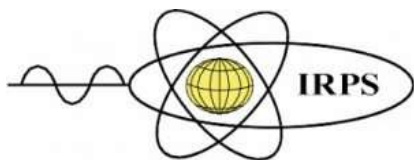
Charles Grant<sup>1</sup>

<sup>1</sup> International Centre for Environmental and Nuclear Sciences,

University of the West Indies, Jamaica

Corresponding author: [charles.grant@uwimona.edu.jm](mailto:charles.grant@uwimona.edu.jm)

The SLOWPOKE-2 research reactor at the International Centre for Environmental and Nuclear Sciences (ICENS) is a light water moderated open swimming pool type reactor with a beryllium reflector. The first criticality was achieved in March 1984. The reactor, which is the only one in the English-speaking Caribbean, has been utilized mainly for Instrumental Neutron Activation Analysis (INAA) and has played an important role in the development of research programs in the areas of agriculture, archaeology, biology, chemistry, environmental studies, forensics, geochemistry, and health. Although INAA is now a mature technique, improvements in gamma spectroscopy detectors and fast counting systems have led to incremental reductions in detection limits allowing INAA to remain competitive with newer techniques such as inductively coupled plasma-mass spectrometry ICP-MS. The ability to quantify elements in almost any matrix without dissolution and the dynamic analytical quantification range, make INAA an ideal tool for the study of the total environment, where matrices vary from geological, with percentage level concentrations, to biological, with elemental concentration levels in the parts per billion range. This presentation reports on the performance of the SLOWPOKE-2 reactor and its utilization to assess the fate of trace elements in soil-food-animal chain and their potential impact on human health. The quality control employed and detection limits for the major sample types analysed over the last twenty-eight years at ICENS are shown. The data presented here illustrates how INAA can be used to provide valuable data applicable across a wide spectrum of programmes, particularly in agricultural and health sciences. It is this type of application that may well play an important role in the future of small reactor facilities.



**ISRP 2021**  
**International Symposium on Radiation Physics**  
**Kuala Lumpur – Malaysia**  
**6 – 10 December 2021**

### **Invited Talks**

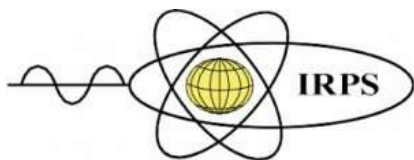
#### **A215 - Rescue Effect: A Non-Targeted Biological Effect Of Ionizing Radiation**

K.N. Yu

Department of Physics, City University of Hong Kong, Hong Kong, China

Corresponding author: peter.yu@cityu.edu.hk

Rescue effect related to ionizing-radiation or “radiation-induced rescue effect” (RIRE) was discovered in 2011, where detrimental effects in the cells irradiated with ionizing radiation (targeted cells) were reduced upon their receiving feedback signals from co-cultured non-irradiated cells (bystander cells). Specifically, in the presence of co-cultured bystander cells, the levels of p53-binding protein 1 (53BP1) and micronucleus (MN) formation in  $\alpha$ -particle-irradiated cells were lowered, while the corresponding surviving fractions and the number of annexin V-positive (FL1-H) apoptotic cells were increased and decreased, respectively. RIRE was subsequently referred to the phenomenon where detrimental effects in irradiated cells were diminished upon receiving feedback signals from bystander cells, or from the medium previously conditioning these bystander cells. Research on RIRE required an understanding of the radiation-induced bystander effect (RIBE), which was a related non-targeted effect of ionizing radiation first observed in *in vitro* experiments in 1992. RIBE referred to the phenomenon where bystander cells responded as if they had been irradiated upon receiving signals from irradiated cells, or from the medium previously conditioning these irradiated cells. The present paper reviewed the research and findings on RIRE since its discovery in 2011, but did not aim to provide a review on RIBE since there were already many excellent reviews on the latter in the literature. In particular, the present paper reviewed the potentially far-reaching influence of RIRE on standard assays for determining the effects of ionizing radiation therapy such as the colony formation assay (CFA), and on the choice of irradiation field size to provide local exposures in *in vitro* experiments (the latter known as radiation-induced field size effect or RIFSE). Priorities and directions for future RIRE research were also discussed.



**A212 - Physical Studies of The Epithelial Mesenchymal Transition In Breast Tissues**

S.F. Abdul Sani<sup>1</sup>, L.M. Looi<sup>2</sup>, D.A. Bradley<sup>3,4</sup>

<sup>1</sup>Department of Physics, Faculty of Science, University of Malaya, 50603, Kuala Lumpur, Malaysia

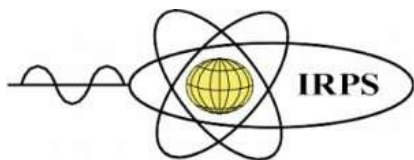
<sup>2</sup>Department of Pathology, Faculty of Medicine, University of Malaya, 50603 Kuala Lumpur, Malaysia

<sup>3</sup>Sunway University, Centre for Biomedical Physics, Jalan Universiti, 46150 PJ, Malaysia.

<sup>4</sup>Department of Physics, University of Surrey, Guildford, GU2 7XH, UK.

Corresponding author: s.fairus@um.edu.my

Breast cancer is one of the leading cancers in women worldwide. Notwithstanding the clear advances being made in treatment, early diagnosis of the disease can certainly be expected to reduce morbidity and mortality. With increasing evidence of the role of epithelial to mesenchymal transition (EMT) in tumour progression, early detection of this phenomenon is suggested to be important given that the majority of breast cancer deaths are due to tumour invasion and metastasis. Although histopathology and biomedical imaging techniques continue to be used as standard procedures in breast cancer diagnosis, these techniques have a number of disadvantages, including being time-consuming, the imaging in particular having attendant limited resolution, sensitivity, and specificity, leading to results that are prone to errors in human interpretation. Study of metabolic changes during the EMT process is important in seeking to understand the biochemical changes associated with cancer progression, not least in scoping for therapeutic strategies aimed at targeting EMT. Due to its rapidity and high specificity, Raman spectroscopy has emerged as a diagnostic tool for breast cancer, useful in identifying malignancy of breast cells, correlated with the EMT phenotype, expressed at the molecular level. Tissue from 23 patients were collected, comprising non-lesional, EMT and non-EMT formalin-fixed and paraffin embedded breast cancer samples. Analysis was made in the fingerprint Raman spectra region ( $600\text{--}1800\text{ cm}^{-1}$ ) best associated with cancer progression biochemical changes in lipid, protein, and nucleic acids. The ANOVA test followed by the Tukey's multiple comparisons test were conducted, revealing significant differences in the intensity between the non-lesional and EMT samples, as well as the EMT and non-EMT samples. This study demonstrated the capability of Raman spectroscopy supported by multivariate analysis in analysing metabolic changes in EMT breast cancer tissue.



**ISRP 2021**  
**International Symposium on Radiation Physics**  
**Kuala Lumpur – Malaysia**  
**6 – 10 December 2021**

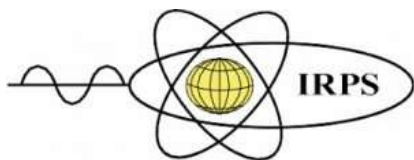
**A275 - X-Ray Spectrometry: Theoretical and Experimental Determinations**

José Paulo Santos<sup>1</sup>

<sup>1</sup>Laboratory of Instrumentation, Biomedical Engineering and Radiation Physics (LIBPhys), Department of Physics, NOVA School of Science and Technology, NOVA University Lisbon, 2829-516 Caparica, Portugal.

Corresponding author: [jps@fct.unl.pt](mailto:jps@fct.unl.pt)

Accurate critical data related to the interactions of X-rays with matter are required for the whole range of applications, and the lack of recent reliable values with low associated uncertainties was pointed out by the scientific and industrial communities. Such accurate data are needed in several fields, such as laboratorial and astrophysical plasma, medical technology, environmental control, and materials analysis. It will be presented the theoretical and experimental methods used in the determination of several atomic parameters like transition energies, line widths, and fluorescence yields.

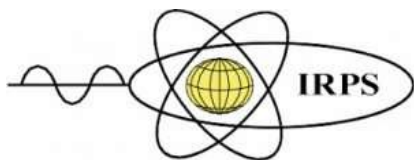


**ISRP 2021**  
**International Symposium on Radiation Physics**  
**Kuala Lumpur – Malaysia**  
**6 – 10 December 2021**

**Forum Forum on Women in Nuclear Science and Technology**

Moderator: Associate Professor Dr Jeannie Wong

<b>Time (pm)</b>	<b>Talk title</b>	<b>Speaker/Moderator</b>
<b>2.30 -2.40</b>	Welcome and introduction of the speakers	Dr Jeannie Wong
<b>2.40 -3.00</b>	“Participation of Malaysian Women in Nuclear Science and Technology”	Ts Dr Siti Ai’asah Hashim Director General, Malaysian Nuclear Agency, Malaysia
<b>3.00-3.20 (10 am Riyadh)</b>	“Women in nuclear science, challenges and achievements”	Dr Khuloud Saad Almogren Professor of Nuclear Science Princess Nourah Bint Abdulrahman University, Riyadh, Saudi Arabia.
<b>3.20-3.40 (7.20 am – Lisbon)</b>	“A case study on Women Nuclear Science and Technology: the Manhattan Project”	Dr Isabel Lopes Professor, Department of Physics, University of Coimbra, Portugal.
<b>3.40-4.00 (7.40 am – London)</b>	“What it took me to become a nuclear scientist?”	Dr Shakardokht Jafari TrueInvivo & Portsmouth Hospital, United Kingdom
<b>4.00-4.30</b>	Panel discussion & wrap up	All panel



**ISRP 2021**  
**International Symposium on Radiation Physics**  
**Kuala Lumpur – Malaysia**  
**6 – 10 December 2021**

**Thursday (9 December 2021)**

### **Invited Talks**

#### **A103 - The Significance of Nuclear Data For Accelerator-Based Production of Novel Radionuclides For Theranostic Applications**

Mayeen Uddin Khandaker<sup>1,\*</sup>, D.A. Bradley<sup>1</sup>, Hamid Osman<sup>2</sup>, M. I. Sayyed<sup>3,4</sup>, A. Sulieman<sup>5</sup>

<sup>1</sup>Centre for Applied Physics and Radiation Technologies, School of Engineering and Technology, Sunway University, 47500, Bandar Sunway, Selangor, Malaysia

<sup>2</sup>Department of Radiology, College of Applied Medical Sciences, Taif University, 21944, Taif, Saudi Arabia

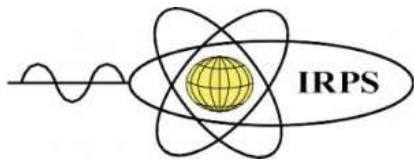
<sup>3</sup>Department of physics, Faculty of Science, Isra University, Amman, Jordan

<sup>4</sup>Department of Nuclear Medicine Research, Institute for Research and Medical Consultations, Imam Abdulrahman bin Faisal University, Dammam, 31441, Saudi Arabia

<sup>5</sup>Department of Radiology and Medical Imaging, College of Applied Medical Sciences, Prince Sattam Bin Abdulaziz University, P.O. Box 422, Alkharj 11942, Saudi Arabia

Corresponding author: mayeenk@sunway.edu.my (MUK)

Accurate knowledge of nuclear reaction cross sections and/or nuclear data are important for production of a radionuclide via charged particle-induced reactions. This study outlined the availability and scarcity of standardized nuclear data for production of promising medical radionuclides via accelerator-route. The data are considered for the radionuclides that have potentials to be used in theranostic applications, dual-mode imaging, and targeted radionuclide therapy. The current trends in nuclear data production and evaluation activities using accelerators are discussed in detail. This work is expected to provide a direction on the accelerator based production of promising radionuclides in no carrier added form for various medical applications.



**ISRP 2021**  
**International Symposium on Radiation Physics**  
**Kuala Lumpur – Malaysia**  
**6 – 10 December 2021**

## **A201 - Distributed Optical Fiber Radiation Dosimetry**

Zubair H. Tarif<sup>1,4</sup>, K. Y. Choo<sup>1</sup>, S. A. Ibrahim<sup>1</sup>, H. A. Abdul-Rashid<sup>1</sup>, D. A. Bradley<sup>2,3</sup>

<sup>1</sup>Fibre Optics Research Centre, Faculty of Engineering, Multimedia University, Jalan Multimedia 63100, Cyberjaya, Malaysia.

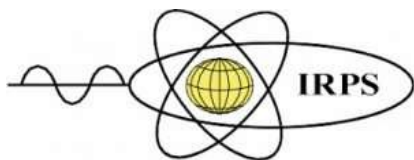
<sup>2</sup>Centre for Applied Physics and Radiation Technologies, Sunway University, 46150 PJ, Malaysia.

<sup>3</sup>Department of Physics, University of Surrey, Guildford, GU2 7XH, UK.

<sup>4</sup>Lumisysns Technology Sdn Bhd, Cyberjaya 63100, Selangor, Malaysia

Corresponding author: hairul@mmu.edu.my

Ionizing radiation in medical, industrial, reactors and high energy accelerator facilities have adverse effects on installed electronics. Such effects will eventually limit equipment lifetimes. Monitoring radiation levels across a facility requires an accurate radiation dosimetry which is distributed in nature. Specialty optical fiber has demonstrated its potential as both passive and active radiation dosimetry in such facilities. The coupled ability of specialty optical fiber as a sensor and as a waveguide opens a new dimension of distributed radiation sensing that is both in-situ, real-time and high-resolution. In this work, a review is presented on suitable materials used in a specialty optical fiber that would provide suitable means to sense radiation ranging from Thermoluminescence (TL), Radioluminescence (RL), Optically Stimulated Luminescence (OSL) and Radiation Induced Attenuation (RIA). Moving on, a review is provided on distributed measurement techniques such as Optical Time Domain Reflectometer (OTDR), Phase-sensitive Optical Time Domain Reflectometer and Optically Optical Frequency Domain Reflectometer (OFDR). The discussion will pose challenges that face distributed radiation sensing systems such as the ability to measure distributed radiation dynamically over time. Preliminary results based on a P-doped specialty optical fiber dosimeter coupled with an OFDR system are presented to demonstrate such a concept.



**ISRP 2021**  
**International Symposium on Radiation Physics**  
**Kuala Lumpur – Malaysia**  
**6 – 10 December 2021**

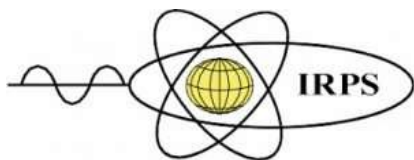
**A269 - The Singapore Synchrotron Light Source (SSLS)**

Mark Breese

5 Research Link, National University of Singapore, Singapore 117603

**Abstract**

Synchrotron radiation is a powerful tool for analytical purposes and for advanced fabrication, which has become indispensable in many disciplines such as the life sciences, materials science, environmental analysis, and micro/nano fabrication. Synchrotron radiation enables us to look into living organisms, man-made materials and advanced engineering components, in vivo, almost non-destructively, in situ, and with spatial and time resolution, revealing detailed structural, chemical, electronic, and magnetic properties. Our, superconducting storage ring uses a 700 MeV electron energy and 4.5 Tesla magnetic field to produce synchrotron radiation with a characteristic photon energy of 1.47 keV and characteristic wavelength of 0.845 nm. We have seven Synchrotron beam lines covering the full spectrum of radiated photon energies, from infrared to X-rays of about 10 keV. This presentation will give an overview of SSLS, covering the accelerator, beam lines and range of applications.



**ISRP 2021**  
**International Symposium on Radiation Physics**  
**Kuala Lumpur – Malaysia**  
**6 – 10 December 2021**

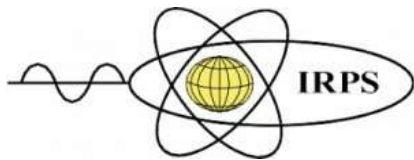
## **B002 - Compact and Very High Dose-Rate Plasma Radiation Sources for Medical Applications**

Marco Sumini<sup>1</sup>, Lorenzo Isolan<sup>1</sup>

<sup>1</sup>Industrial Engineering Department, University of Bologna, Italy

Corresponding author: marco.sumini@unibo.it

As it is well known, a Dense Plasma Focus (DPF) is a pulsed device able to produce a hot and dense short-lived plasma that could become a flash radiation source both for diagnosis and radiotherapy. The plasma is generated through a discharge of a capacitors bank with consequent low pressure gas ionization and confined thanks to a concatenated electromagnetic field. The plasma confinement phase, identified as “pinch”, lasts few tens of nanoseconds, during which thermonuclear temperatures and densities could be reached. The DPF versatility in terms of product types, emission yield and scalability, allows different applications in industry, research, and medicine. The DPF characteristics make it suitable to be used as compact sources for diagnostic applications, external radiotherapy, or intra-operative radiation therapy: when the plasma vacuum chamber is filled with gases such as nitrogen or argon, the only significant output are self-collimated charged particle beams (electrons and ions in opposite direction) produced in some tens of nanoseconds. Using as source that electron beam, it is possible to devise an ultra-high dose-rate source, with possible uses for direct irradiation of a tumour bed or for photon conversion after the interaction with a suitable target. The ultrahigh dose rate could have potential benefits in mitigating the intrinsic or acquired radioresistance of malignant cells, which can be considered the main obstacle to the long-term survival of a patient, also sparing healthy tissues. This is due because the faster is the dose deposition, the more relevant is the radiobiological effect, as the tumour cells do not have the time to activate the sub-lethal damage repair mechanisms responsible of the radio-resistance. A review of the operating mechanisms, technological background, applications and potential break-through within the medical field is proposed.



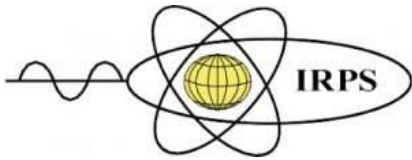
## **A222 - Capillary Guiding for Beams and Radiations**

S.B. Dabagov

INFN Laboratori Nazionali di Frascati, Frascati (RM), Italy

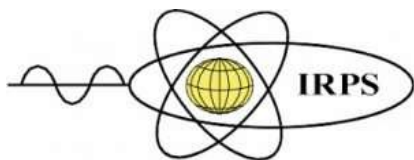
Handling the beams of charged (electrons, protons, ions, muons) particles and radiations (soft and hard x-rays, thermal neutrons) had occupied the minds of physicists and engineers throughout the last century. Till now, research in this area remains relevant directing us to basic research on interaction of beams and radiations in external electromagnetic fields of various origins. Typically, electromagnetic fields for beam optics are generated by special devices known as dipoles, quadrupoles, solenoids, etc., which are characterised by a rather complex design. Most often, solids are used as simple collimators, scatterers, and absorbers. However, strong electromagnetic interactions also take place in solids (any dense medium) as well as in the immediate vicinity of a solid surface, sometimes offering field gradients far beyond our technical capabilities, implemented in specialized scientific instruments. Strong fields generated by solid samples of a certain geometry make it possible to manipulate beams and radiations, giving them the required characteristics for use in many fundamental and applied research. And it should be noted that the advances in materials science presently allow creating various solid samples of complex microgeometry. Since recently, capillaries or capillary structures of various configurations have been considered as one of the most promising techniques for the formation either particle beams or radiations. Despite the difference in the physics of the processes, a clear example is capillary x-ray optics, which has grown from a beautiful idea into a widely used x-ray radiation control tool. In fact, even before the development of capillary/polycapillary x-ray optics, in the early 1980s, the possibility of using curved reflecting surfaces as an alternative method to shape ion beams was discussed in a number of experimental works with theoretical estimates based on the physics of charged particle channeling in crystals. The interaction of an incident ion with a reflecting surface was described in the approximation of a continuous surface atomic potential, confirming very small angles of ion reflection from a smooth surface regardless of the change in the beam charge characteristics. In order to increase the angles of deflection of the beams, to use curved surfaces, in particular, dielectric capillaries, was proposed. However, these studies were not properly continued, while the further use of capillaries (capillary bundles) in relation to x-rays and thermal neutrons has been resulted in developing a new optical tool, nowadays known as capillary/polycapillary optics. The gap in the use of capillary structures for controlling beams and radiations can be explained by the complexity of the phenomena to be evaluated in the case of interaction of charged beams at the interface, in comparison with the phenomena for radiations. The undoubted interest in the development of capillary optics for particle beams has given rise to a wide range of experimental work devoted to this phenomenon, with disproportionately less activity in theoretical studies, which were mainly based on Monte Carlo simulations. Within this talk I'm going to present a newly proposed and developed common general analytical theory for the capillary guiding of beams. This phenomenology is based on main principles of channeling theory and allows predicting very fine features in particle beams redistribution, spatial and angular, behind capillaries/capillary structures. And a better

ABSTRACTS| Thursday (9 December 2021) 29



**ISRP 2021**  
**International Symposium on Radiation Physics**  
**Kuala Lumpur – Malaysia**  
**6 – 10 December 2021**

understanding of the nature of the interaction of beams and radiation with a reflecting surface will serve as another impetus for new technological solutions to important applied problems.



**ISRP 2021**  
**International Symposium on Radiation Physics**  
**Kuala Lumpur – Malaysia**  
**6 – 10 December 2021**

### **A226 - Advances in Silica Bead Dosimetry**

Shakardokht Jafari<sup>1,2,3</sup>

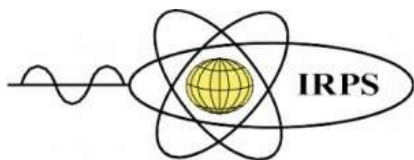
<sup>1</sup> Medical Physics Department, Queen Alexandra Hospital, Portsmouth Hospitals NHS Trust, Portsmouth, UK

<sup>2</sup> Department of Physics, Faculty of Engineering and Physical Science, University of Surrey, UK

<sup>3</sup> TrueInvivo LTD, Research Park, Guildford, UK

Corresponding author: shakardokht.jafari@porthosp.nhs.uk

**Purpose:** an overview of taking a PhD research in developing a novel radiation detector for radiotherapy, to receiving awards, research grants and financial investment to develop a company and products that will facilitate improved radiation dosimetry for radiotherapy. **Method:** an inexpensive, high performance, low maintenance thermoluminescent dosimetry (TLD) system developed using micro size jewellery silica beads for in vivo dosimetry that would comply with the requirements of modern radiotherapy technology. Characterization measurements have been performed utilizing a range of modalities and energies of clinical beams; photons, electrons, proton, carbon ions and HDR brachytherapy sources of <sup>60</sup>Co and <sup>192</sup>Ir. The results were promising, offering in many cases a better performance in comparison with other commonly available in vivo dosimeters; a better batch homogeneity, a linear response over a large dynamic range from mGy to more than 100 Gy, a response independent from dose rate and angle of incident beam, lower fading and an almost flat energy response over the megavoltage energy beams. These results encouraged investigation into their different clinical dosimetric applications including small field dosimetry, patient specific treatment plan dosimetry verification, a postal dosimetry audit programme of lung SABR techniques within 20 radiotherapy departments in UK, and high resolution in-body in vivo dosimetry for patients treated with HDR Brachytherapy and kV X-ray beams. The physical shape of silica beads, their low cost and inert nature, in addition to favourable dosimetric properties, has led to the production of flexible 1D, 2D and 3D in-vivo TL dosimetry systems (DOSEmappers™). A fully automated TLD-reader and data processor were developed to speed up the readout process with a factor of 10. TRUEinvivo Ltd spinout company from The University of Surrey were formed to commercialize the products. This innovative idea has won a *UKTI SIRIUS programme* grant, *ICURE Award*, Various *InnovateUK* grants including a “Women in Innovation” award.



**ISRP 2021**  
**International Symposium on Radiation Physics**  
**Kuala Lumpur – Malaysia**  
**6 – 10 December 2021**

**Friday (10 December 2021)**

### **Invited Talks**

#### **A199 - Geoneutrons**

Hector Rene Vega-Carrillo<sup>1</sup>, Laszlo Sajo-Bohus<sup>2</sup>, Segundo Agustin Martinez-Ovalle<sup>3</sup>, Arturo Agustin Ortiz-Hernandez<sup>4</sup>

<sup>1</sup>UaEN, Universidad Autonoma de Zacatecas, Mexico

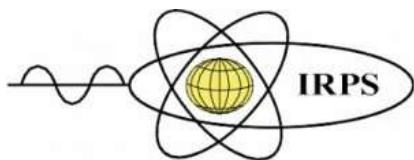
<sup>2</sup>Physics Department, Universidad Simon Bolivar, Venezuela

<sup>3</sup>Nuclear Physics and Simulation Group, UPT de Colombia, Colombia

<sup>4</sup>Research Department AOR Tech & Universidad Politecnica de Zacatecas, Mexico

Corresponding author: [fermineutron@yahoo.com](mailto:fermineutron@yahoo.com)

At any point on the surface of the planet there are naturally occurring neutrons. Neutrons on the lithosphere are originated through nuclear reactions between cosmic rays and nuclei on the atmosphere (Cosmic neutrons), in nuclear reactions induced during thunderclouds and lightning (Thunder neutrons), and those produced by the planet (Geoneutrons, Telluric neutrons or Geogenic neutrons). Geoneutrons are produced during ( $\alpha$ , n) reactions in the soil, where  $\alpha$  particles are produced along the decay of  $^{235}\text{U}$ ,  $^{238}\text{U}$  and  $^{232}\text{Th}$  in the ground. Research efforts (to study, to understand and to characterize), have been addressed mostly on cosmic neutrons mainly motivated by the radiological risks of these neutrons during air traveling and due to the amount of Thunder and Geoneutrons is small and hard to be measured. In this work a model of Geoneutron spectrum has been calculated and was used as source term in the ground to estimate the neutron fluence and absorbed dose in sensitive organs in a BOMAB phantom standing on the ground. In the aim to measure the Geoneutrons and two distinguish from Cosmic neutrons a series, still on-going, of experiments were carried out. In this work is also presented the obtained results of these experiments.



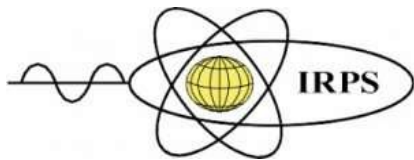
**ISRP 2021**  
**International Symposium on Radiation Physics**  
**Kuala Lumpur – Malaysia**  
**6 – 10 December 2021**

**A214 - Mineral Wealth and NORM. Standing Up a New Rare Earths Industry in the United States**

Philip Egidi,

United States Environmental Protection Agency

This talk will focus on efforts to stand up a new domestic rare earths industry in the United States (US). In the past, the US had one major mine and mill that produced many of the light rare earth minerals. That operation went bankrupt in the early 2010s and has since been sold off to various investors. Ore from the mine is currently shipped overseas for processing. Many modern technologies utilize rare earths in magnets, electronics and defense applications to name a few. However, many rare earth deposits are associated with radioactivity and may be found in residuals and products made from rare earth elements. Current efforts in the US to explore and develop domestic sources of rare earths will be discussed along with environmental challenges for residuals management and disposition.



**ISRP 2021**  
**International Symposium on Radiation Physics**  
**Kuala Lumpur – Malaysia**  
**6 – 10 December 2021**

## **A288 - Medical Physics Education: The Way Forward**

Kwan Hoong Ng, PhD, DABMP

Department of Biomedical Imaging, University of Malaya, Kuala Lumpur, Malaysia

Corresponding author: ngkh@ummc.edu.my

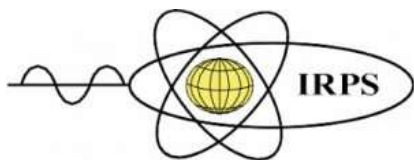
Medical physics is a branch of physics concerned with the applications of physics to medicine. Traditionally, but not exclusively, related to the use of ionizing radiation in the diagnosis and treatment of diseases. However, the field has expanded tremendously to include advanced technologies, novel modalities and big data applications.

Medical physics is unique as it is both a science and a profession. The science is very much applied, translational and multidisciplinary in nature. Conventionally, the profession includes clinical practice specializing in radiation oncology, diagnostic radiology, nuclear medicine, health physics and industry environment. However, the inclusion of artificial intelligent and big data in medicine demand the expansion of traditional medical physics curriculum to cover new fields.

The major outcome of education would include: to provide students with a thorough grounding in the physiological basis, analytical methods and fundamental aspects of medical physics and instil an attitude of integrity, professionalism, critical thinking and scientific rigor. On these broad foundations, students can focus on more advanced topics depending on their aptitude and inclination.

Good teaching is very important for the advancement of society in general. Ideally, the teacher should be a practising medical physicist with solid knowledge of the fundamental underlying physics and the subject matter and be equipped to communicate the concepts clearly and express enthusiasm.

One of the major driving forces behind technological advances in medicine is medical physics and technological development. There are no shortcuts to education. Hard work and steady work from both the student and the teacher are essential. We should explore computers and virtual web-based teaching to enhance the learning experience, but good traditional teaching still has its place.



**ISRP 2021**  
**International Symposium on Radiation Physics**  
**Kuala Lumpur – Malaysia**  
**6 – 10 December 2021**

## **ORAL PRESENTATIONS**

Ordered by abstract number

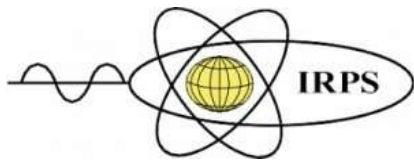
### **A003 - Assessment of natural radioactivity and radiological risks from groundwater and vegetation samples collected from farms in Qatar**

Dr. Yehia Manawi and Dr. Huda Al-Sulaiti\*

Qatar Environment and Energy Research Institute, Hamad Bin Khalifa University, Qatar Foundation, PO Box 34110, Doha, Qatar.

Corresponding author: ymanawi@hbku.edu.qa

Over the last decade, the quality of groundwater in Qatar has been observed to show substantial deterioration in their quality and quantity following the overconsumption of groundwater in agriculture at rates way higher than the natural replenishment rate. This resulted in a drop in the water table to an unprecedented level. In the present work, the radioactivity analysis of groundwater and vegetation collected from three Qatari farms was conducted. The activity concentration of  $^{226}\text{Ra}$ ,  $^{228}\text{Ra}$  and  $^{40}\text{K}$  in the collected vegetation was measured using high purity germanium detector (HPGe). Moreover, the radiological risks were evaluated by estimating the average annual effective dose due to the intake of the above-mentioned radionuclides through ingestion of vegetation samples. The average activity concentration (dry-weight) of  $^{226}\text{Ra}$ ,  $^{228}\text{Ra}$  and  $^{40}\text{K}$  in Rocca were:  $84.4 \pm 1.4$ ,  $3.05 \pm 0.32$  and  $1730 \pm 72$ , respectively. The average activity concentration (dry weight) of  $^{226}\text{Ra}$ ,  $^{228}\text{Ra}$  and  $^{40}\text{K}$  in Corchorus were:  $111 \pm 2.15$ ,  $5.1 \pm 0.53$  and  $1800 \pm 75$ , respectively. Qatar follows the Gulf Cooperation Council (GCC) Standardization Organization (GSO) limit which states that the total activity level permitted in food products (wet weight) shall not exceed 75 Bq/L (GSO-998/1998). While the activity level of these radionuclides were found to be within the acceptable level, such levels are quite high, when compared to other countries, and attract the scientists to carefully investigate the sources, fate and impacts of such levels on human and environment.



**A006 - Radiation Dose Estimation Study for Sparse-View CT: Monte-Carlo Simulation.**

Sandra Oliver <sup>1</sup>, Vicent Giménez-Alventosa <sup>2</sup>, Mónica Chillarón <sup>3</sup>, Vicent Vidal <sup>3</sup>, Gumersindo Verdú <sup>1</sup>

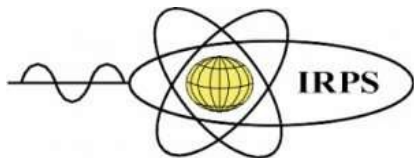
<sup>1</sup> Instituto de Seguridad Industrial, Radiofísica y Medioambiental, Universitat Politècnica de València, Spain

<sup>2</sup> Instituto de Instrumentación para Imagen Molecular - CSIC, Universitat Politècnica de València, Spain

<sup>3</sup> Depto. de Sistemas Informáticos y Computación, Universitat Politècnica de València, Spain

Corresponding author: gverdu@iqn.upv.es

Computed Tomography (CT) is still one of the most used test in clinical practice for image-guided diagnosis. However, the ionizing radiation produced by the X-ray sources poses a potential risk to patients who need to go under this medical test. One of the state-of-the-art research lines about dose reduction for CT is the proposal of a sparse-angle sampling process in order to reduce the total time needed to perform a scan. This approach is very promising towards reducing the radiation dose induced to the patients, but the reconstruction of the images becomes a challenge. When the number of views is too small, the sparsity of the data produces streak artifacts on the reconstructed images. The traditional analytical reconstruction methods based on the Filtered Back-Projection (FBP) don't perform well in this case, so new algebraic methods are used, either iterative or direct. Since this type of acquisition has not yet been adapted to commercial CT scanners, measuring how the reduction of the samples affects the total dose absorbed by the patients requires simulating this data. To obtain the simulated data needed, in this work we adapt and expanded the capabilities of the current Monte-Carlo simulation code PenRed, based on PENELOPE version 2018, adding the capability to simulate a CT scanner. With this implementation we can obtain a set of artificial sinograms with different number of projections and their corresponding dose deposition. The aim of this study is to reconstruct the CT images with algebraic methods measuring the reduction of the dose absorbed by the patient when the number of projections is reduced, without compromising the image quality. For this purpose different simulations have been carried out with a phantom and with DICOM images of real patients to reconstruct the images and calculate the absorbed dose in different elements of the geometry.



**ISRP 2021**  
**International Symposium on Radiation Physics**  
**Kuala Lumpur – Malaysia**  
**6 – 10 December 2021**

### **A007 - Investigation Flexible Nanocomposite Membranes of ZnO-CuO-PVA For X-Ray Detectors**

Ahmad I. Ayesh<sup>1,2,\*</sup>, Leena Al-Sulaiti<sup>2</sup>, Belal Salah<sup>1</sup>, Rama Nawwas<sup>3</sup>, Asmaa S. Almarri<sup>3</sup>, Aisha N. Al-Thani<sup>3</sup>; Alanoud M. Al-Ahbabi<sup>3</sup>, and Noof A. Al Haidous<sup>3</sup>

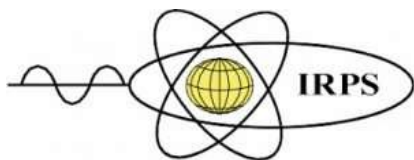
Qatar University, Doha, Qatar

Department of Math., Stat. and Physics, Qatar University, Doha, Qatar

Department of Computer Science & Engineering, Qatar University, Doha, Qatar

\* Presenting author, email: ayesh@qu.edu.qa

Organic matrixes of nanocomposite membranes of that integrate metal-oxide nanoparticles and polymer have high potential for implementation to produce flexible devices. Flexible membranes are produced for x-ray detector devices of CuO and/or ZnO nanoparticles along with poly(vinyl alcohol) (PVA) and glycerol (GL) that serves as a plasticizer. Both types of nanoparticles are generated by a solvothermal procedure and mixed with PVA + GL solution to produce the membranes. The average sizes of nanoparticles are  $8 \pm 3$  nm and  $10 \pm 4$  nm for ZnO and CuO, in order. The composition of the synthesized nanoparticles as well as the membranes are examined by energy dispersive x-ray spectroscopy along with x-ray spectroscopy. The glass transition temperature of the membranes is shifted to low temperatures and their thermal resistance is enhanced upon increasing the concentration of nanoparticles. Fourier-transform infrared spectroscopy (FTIR) illustrates the development of hydrogen bonds among nanoparticles and PVA due to intramolecular and intermolecular hydrogen bonds. Electrical impedance spectroscopy investigation demonstrates that the membranes have negative temperature coefficient of resistivity. Their activation energy decreases for high concentration of nanoparticles. The flexible membranes have a clear response to x-ray, and the response increase with the generator energy. Membranes with both CuO and ZnO nanoparticles exhibit the best xray response, due to the different bandgaps of nanoparticles that allow a wide spectrum of excitation energy to be included. The produced membranes exhibit several advantages including their semiconducting properties, flexibility, and viability of production on a large scale with rational cost. Therefore, those composite flexible membranes can be used for prototype elements in x-ray detectors for different applications.



**ISRP 2021**  
**International Symposium on Radiation Physics**  
**Kuala Lumpur – Malaysia**  
**6 – 10 December 2021**

**A008 - Radiological Dispersion of I-131, I-133 and I-135 Isotopes Due to Hypothetical Accidental Release from Nigerian Research Reactor-1**

\*J. Simon<sup>1</sup>, Y.V. Ibrahim<sup>2</sup>, M.U. Khandaker<sup>3</sup>, D.J. Adeyemo<sup>2</sup>, N.N. Garba<sup>1</sup>, A. Asuku<sup>2</sup>

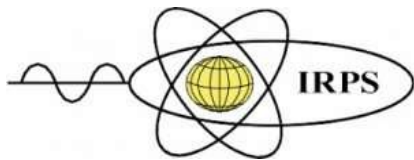
<sup>1</sup>Department of Physics, Ahmadu Bello University, Zaria, Nigeria

<sup>2</sup>Centre for Energy Research and Training, Ahmadu Bello University, Zaria, Nigeria

<sup>3</sup>Centre for Applied Physics and Radiation Technologies, School of Engineering and Technology, Sunway University, Bandar Sunway, Malaysia.

Corresponding Author: sjkahugu@yahoo.com

Nuclear accidents are known to be associated with severe radiological contamination of the environment. The severe nuclear disaster in April 1986, following the unit 4 power reactor accidents in Chernobyl nuclear power plant and the 2011 Fukushima Daiichi nuclear power plant accident left an indelible scar on the civilian applications of nuclear technology. After every nuclear accident, Iodine is known to be an immediate radionuclide to be detected in areas surrounding the nuclear reactor site owing to its fast mobility in air. Because of its radiological concern, pharmaceutical approaches have developed for immediate response to the release of iodine following a nuclear accident. Since Pharmaceutical approach to radiological response is not the best global practice, it is imperative to carry out hypothetical studies to establish safe distances around any nuclear facility vis-à-vis the release of Iodine in the event of an accident. In this study, the source terms of I-131, I-133 and I-135 isotopes from the Nigeria Research Reactor-1 were calculated using TRITON computational sequence that is coupled with ORIGEN code. The concentrations of the radionuclides at various distances from the reactor were determined using Hot-Spot computer code. The results showed that the concentration of I-131, I-133 and I-135 were greatest at 10 m from the reactor and decreases with distance as expected. However, the concentrations of the radionuclides at 100-300 m from the reactor were found to be higher than the permissible limit recommended by the United State Environmental Protection Agency and hence indicating the possibility of air contamination due to accidental released of I-131, I-133 and I-135 from Nigeria Research Reactor-1 beyond 300 m from the reactor site.



**A009 - A Novel Glass System Based on Iraqi White Sand and Lead Oxide For Gamma Ray Shielding Purposes**

H. F. Al-Saeedi<sup>1</sup>, Haneen M Alsafi<sup>1,\*</sup>, K.A. Mahmoud<sup>1,2</sup>, M.I. Sayyed<sup>3,4</sup>, Mayeen Uddin Khandaker<sup>5</sup>, O L Tahlykov<sup>1</sup>, F. L. Kapustin<sup>1</sup>

<sup>1</sup>Ural Federal University, 19 Mira St, 620002, Ekaterinburg, Russia,

<sup>2</sup>Nuclear Materials Authority, P.O. Box 530 El-Maadi, Cairo, Egypt.

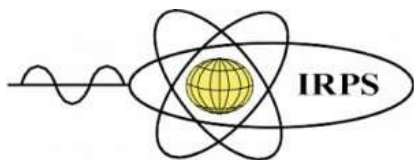
<sup>3</sup>Department of Physics, Faculty of Science, Isra University, Amman 11622, Jordan

<sup>4</sup>Department of Nuclear Medicine Research, Institute for Research and Medical Consultations, Imam Abdulrahman bin Faisal University, Dammam 31441, Saudi Arabia

<sup>5</sup>Center for Applied Physics and Radiation Technologies, School of Engineering and Technology, Sunway University, 47500 Bandar Sunway, Selangor Darul Ehsan, Malaysia

Corresponding author: haneenalsafi.1991@gmail.com

Since the beginning of the last century, a good type of glass sand is discovered in the western Iraqi desert due to the climate conditions in this region, where the Iraqi climate is hot, dry summers and cool, rainy winters that led to configure this sand. The main location that contains the purest types of glass is located in the city of Anbar (Ramadi). The Iraqi sand contains glass sand with high quality technical and economic requirements. The present study aims to produce a new gamma-ray shielding material based mainly on lead oxide and Iraqi sand. Firstly, the collected sand from Ramadi were treated physically (magnetic separation for impurities and wash using ordinary water). The sand was then saved and separated into various fractions according to the particle size. The separated part with grain size between 0.2 and 0.615 mm was mixed with the lead oxide, transferred to an aluminum crucible, and heated to 1580 °C in an electric muffle. The molten was molded, and the sample was annealed to get rid of the internal pressure and surface tension. The dispersive energy X-Ray (EDX) was used to utilize the chemical composition of the fabricated glasses. Besides, the MH-300A density meter was used to obtain an accurate measurement of the glass density. The average density obtained after five repetitions is  $3.276 \pm 0.005$  g/cm<sup>3</sup>. The Monte Carlo simulation method was used to evaluate the material shielding parameters. The simulation showed that the linear attenuation coefficient at 0.662 MeV is  $0.266$  cm<sup>-1</sup> and  $0.165$  cm<sup>-1</sup> for the gamma energy 1.25 MeV (the energy yield for Co-60 radioactive Source). Moreover, the Phy-X/PSD program was applied to calculate the geometric-progression (G-P) fitting parameters, exposure buildup factor, and energy absorption buildup factor.



**ISRP 2021**  
**International Symposium on Radiation Physics**  
**Kuala Lumpur – Malaysia**  
**6 – 10 December 2021**

**A010 - New Glass Based on Iraqi Sand and Modified By Lead Oxide To Protect Against Gamma-Ray: Fabrication, Mechanical And Shielding Properties Examination**

H. F. El-Saeedi<sup>1,\*</sup>, K.A. Mahmoud<sup>1,2</sup>, M.I. Sayyed<sup>3,4</sup>, F. L. Kapustin<sup>1</sup>, Mayeen Uddin Khandaker<sup>5</sup>

<sup>1</sup>Ural Federal University, 19 Mira St, 620002, Ekaterinburg, Russia,

<sup>2</sup>Nuclear Materials Authority, P.O. Box 530 El-Maadi, Cairo, Egypt.

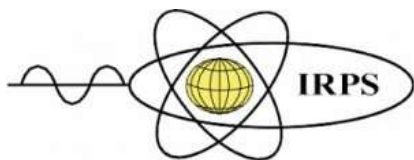
<sup>3</sup>Department of Physics, Faculty of Science, Isra University, Amman 11622, Jordan

<sup>4</sup>Department of Nuclear Medicine Research, Institute for Research and Medical Consultations, Imam Abdulrahman bin Faisal University, Dammam 31441, Saudi Arabia

<sup>5</sup>Center for Applied Physics and Radiation Technologies, School of Engineering and Technology, Sunway University, 47500 Bandar Sunway, Selangor Darul Ehsan, Malaysia

Corresponding author: Farhan\_fatimah@yahoo.com

A barium oxide-based on natural Iraqi sand was prepared. The natural Iraqi sand from Al-Arma government with a size between 0.2 and 0.615 mm after performing some purification processes (washing with water and collecting magnetic impurities), was mixed with sodium oxide (barium oxide, magnesium oxide, and aluminum oxide. The mixture was placed in an aluminum crucible and melted at a temperature of 1580 °C for 30 min. After that, the sample was easily poured into an iron mold and returned to the muffle at a temperature between 530 to 550 °C for annealing. The annealing of the sample aims to get rid of the internal pressure and surface tension. The density of the fabricated glass sample was measured experimentally using the MH-300A density meter. It is found to be  $2.642 \pm 0.0006$  g/cm<sup>3</sup>. The chemical composition is also measured for the fabricated glasses. The fabricated glass measured density, composition, compounds packing density, and compounds dissociation energy were utilized to predict the elastic module (Young, Shear, Bulk, and Longitudinal) and some important mechanical properties. Moreover, a Monte Carlo simulation code was utilized to predict the fabricated glass's protection capacity, such as linear attenuation coefficient, transmission factor, half-value layer, and radiation protection efficiency. The shielding characteristics are evaluated for gamma rays with energies varied between 0.059 and 2.506 MeV.



**ISRP 2021**  
**International Symposium on Radiation Physics**  
**Kuala Lumpur – Malaysia**  
**6 – 10 December 2021**

### **A012 - The Potential Use Of Silica-Based Commercial Float Glass For Protection Of Gamma-Radiation**

S. Yasmin<sup>1,\*</sup>, M. U. Khandaker<sup>2</sup>, D.A. Bradley<sup>2</sup>, M.I. Sayyed<sup>3</sup>

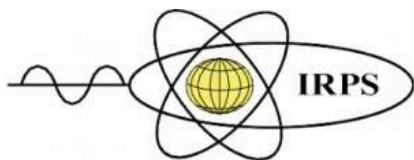
<sup>1</sup>Department of Physics, Chittagong University of Engineering and Technology, Chattogram, Bangladesh

<sup>2</sup>Centre for Applied Physics and Radiation Technologies, School of Engineering and Technology, Sunway University, 47500 Bandar Sunway, Selangor, Malaysia

<sup>3</sup>Department of physics, Faculty of Science, Isra University, Amman 11622, Jordan

Corresponding author: sabinayasmin309@gmail.com

In addition to the symbol of luxury, glass is largely used as a decorative and structural material in buildings all over the world. At present, one of the leading float glasses named Nasir glass is widely using for the mentioned purposes in Bangladesh and the rest of the world. Six different thicknesses (0.25cm, 0.32 cm, 0.5 cm, 0.59 cm, 0.79 cm and 1 cm) of Nasir float glass is studied herein for the  $\gamma$ -ray shielding properties. The  $\gamma$ -ray transmission probability for 59 keV, 661 keV, 1173 keV and 1332 keV photon energies was measured by using a well shielded HPGe  $\gamma$ -ray spectrometer associated with necessary electronics. The measured transmission data was then used to calculate numerous radiations shielding parameters namely linear attenuation co-efficient, mass attenuation co-efficient, half value layer, radiation protection efficiency for the studied glass samples. The effective atomic number of the studied glass ( $Z_{\text{eff}} = 13.6$ ) was obtained by EDX technique, which is very close to the TLD-200 ( $Z_{\text{eff}} = 16.3$ ). To apprehend the shielding ability of the studied material, the experimental data were compared with the literature data of standard materials, for instance lead. Moreover, MCNP simulation was performed for the studied material, and the obtained data were compared with the experimental findings. Properties and facets of same material considering the numerous thicknesses have not previously been studied.



**ISRP 2021**  
**International Symposium on Radiation Physics**  
**Kuala Lumpur – Malaysia**  
**6 – 10 December 2021**

**A016 - Network-Modifying Role of Er<sup>3+</sup> ions on the Structural, Optical, Mechanical, and Radiation Shielding Properties of ZnF<sub>2</sub>-BaO-Al<sub>2</sub>O<sub>3</sub>-Li<sub>2</sub>O-B<sub>2</sub>O<sub>3</sub> Glass**

Nimitha S. Prabhu<sup>1</sup>, M. I. Sayyed<sup>2,3</sup>, Aljawhara H. Almuqrin<sup>4</sup>, Mayeen Uddin Khandaker<sup>5</sup>, Sudha D. Kamath\*<sup>1</sup>

<sup>1</sup>Department of Physics, Manipal Institute of Technology, Manipal Academy of Higher Education, Manipal, Karnataka, India.

<sup>2</sup>Department of Physics, Faculty of Science, Isra University, Amman, Jordan.

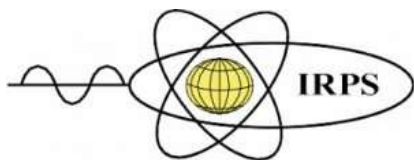
<sup>3</sup>Department of Nuclear Medicine Research, Institute for Research and Medical Consultations (IRMC), Imam Abdulrahman bin Faisal University (IAU), Dammam, Saudi Arabia.

<sup>4</sup>Department of Physics, College of science, Princess Nourah bint Abdulrahman University, Riyadh, Saudi Arabia.

<sup>5</sup>Center for Applied Physics and Radiation Technologies, School of Engineering and Technology, Sunway University, 47500 Bandar Sunway, Selangor Darul Ehsan, Malaysia

Corresponding author: sudha.kamath@manipal.edu

This work evaluates the role of Er<sup>3+</sup> ions on the structural, optical, mechanical, and radiation shielding properties of the 15ZnF<sub>2</sub>-10BaO-8Al<sub>2</sub>O<sub>3</sub>-12Li<sub>2</sub>O-(55-x) B<sub>2</sub>O<sub>3</sub>-xEr<sub>2</sub>O<sub>3</sub> (x = 0.5-1.5 mol %) glass system. Fourier Transform Infrared spectroscopy established the presence of the different vibrational groups in the glass network and a diminution in the network rigidity due to the change of [BO<sub>4</sub>] into [BO<sub>3</sub>] units and Non-Bridging Oxygens (NBOs) with continuous Er<sup>3+</sup> doping. This was consistent with the ionicity increase and decrease in the average coordination number of the glass. The decreasing bandgap of the glass with Er<sup>3+</sup> doping was correlated to the upsurge in the number of NBOs known to produce localized states within the energy gap. The reduction in the Vicker's microhardness and elastic constants of the glasses with Er<sup>3+</sup> doping was interpreted by the fall in the network rigidity. The radiation shielding parameters like Mass Attenuation Coefficient, Linear Attenuation Coefficient, Half Value Layer, and Mean Free Path were determined as function of gamma photon energy through MCNP5 and WinXCom codes. The scope of the glasses can be extended for shielding as their features were on par with some commercial shielding glasses.



**ISRP 2021**  
**International Symposium on Radiation Physics**  
**Kuala Lumpur – Malaysia**  
**6 – 10 December 2021**

**A021 - Investigation of The Photon Shielding Capability Of Kaolin Clay Added With Micro And Nanoparticles Of Bi<sub>2</sub>O<sub>3</sub>**

M. Almatari<sup>1</sup>, Yousry.Koraim<sup>2</sup>, I.H.Saleh<sup>2</sup>, M.I.Sayyed<sup>3,4</sup>, Mayeen Uddin Khandaker<sup>5</sup>, M.Elsafi<sup>2,\*</sup>

<sup>1</sup>Department of Physics, Faculty of Sciences, Al-Balqa Applied University, Al-Salt 19117, Jordan

<sup>2</sup>Physics Department, Faculty of Science, Alexandria University, 21511 Alexandria, Egypt.

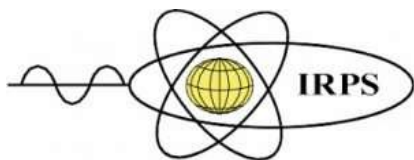
<sup>3</sup>Department of Physics, Faculty of Science, Isra University, Amman – Jordan

<sup>4</sup>Department of Nuclear Medicine Research, Institute for Research and Medical Consultations (IRMC), Imam Abdulrahman bin Faisal University (IAU), PO Box 1982, Dammam, 31441, Saudi Arabia

<sup>5</sup>Center for Applied Physics and Radiation Technologies, School of Engineering and Technology, Sunway University, 47500 Bandar Sunway, Selangor Darul Ehsan, Malaysia

Corresponding author: mohamedelsafi68@gmail.com

Improving the clay for shielding photons become very important at this time, especially in developing countries. In this work, kaolin clay was improved by adding micro and nano bismuth oxide in gradual percentages from 5 to 20% of the proportion of kaolin. The samples were visualized with a Scanning Electron Microscope (SEM) to investigate the presence, size and percentage of Bi<sub>2</sub>O<sub>3</sub> particles inside the sample. The linear attenuation coefficient, or LAC of all samples was measured experimentally using a HPGe detector and different radioactive sources were used to obtain a wide range of energy. To verify the validity of the experimental results, the micro samples were compared with the results obtained from the XCOM program, and it was found that there is a great agreement, which indicates the validity of the results also for the experimental measurements in the case of adding nanoparticles to kaolin. The LAC calculations showed that improving kaolin with bismuth oxide nanoparticles is better for shielding photons than microparticles, especially at low and medium energies. Other attenuator parameters were calculated. In all cases, the samples to which the nano-oxide was added had a higher shielding efficiency of photons than the samples to which the micro-oxide was added.



**ISRP 2021**  
**International Symposium on Radiation Physics**  
**Kuala Lumpur – Malaysia**  
**6 – 10 December 2021**

**A023 - Removal of Uranium From Nuclear Effluent Using Regenerated Bleaching Earth Steeped In  $\beta$ -Naphthol**

Ahmed K. Sakr<sup>1\*</sup>, Ibrahim F. Al-Hamarneh<sup>2</sup>, Hassanien Gomaa<sup>3</sup>, Mostafa M. Abdel Aal<sup>1</sup>, Mohamed F. Cheira<sup>1</sup>, M. Y. Hanfi<sup>1,4</sup>, M. I. Sayyed<sup>5,6</sup> Mayeen Uddin Khandaker<sup>7</sup>

<sup>1</sup>Nuclear Materials Authority, P.O. Box 530, Maadi, Cairo, Egypt

<sup>2</sup>Department of Physics, Faculty of Science, Al-Balqa Applied University, Al-Salt 19117, Jordan

<sup>3</sup>Chemistry Department, Faculty of Science, Al-Azhar University, 71524 Assiut, Egypt

<sup>4</sup>Institute of Physics and Technology, Ural Federal University, Ekaterinburg, Russia

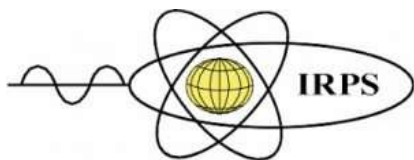
<sup>5</sup>Department of Nuclear Medicine Research, Institute for Research and Medical Consultations (IRMC), Imam Abdulrahman bin Faisal University (IAU), P.O. Box 1982, Dammam, 31441, Saudi Arabia

<sup>6</sup>Department of physics, Faculty of Science, Isra University, Amman – Jordan

<sup>7</sup>Center for Applied Physics and Radiation Technologies, School of Engineering and Technology, Sunway University, 47500 Bandar Sunway, Selangor Darul Ehsan, Malaysia

Corresponding Author: akhchemist@gmail.com

The pre-concentration and separation of uranium on different adsorbents are effective alternative methods for its recovery from liquid waste solutions. Many sophisticated synthetic adsorbent materials have recently been developed for the adsorption of uranium from aqueous solutions. In recent times, clay has become a vital mineral to be considered in uranium recovery due to the proposed utilization of bentonite or clay minerals as adsorbent materials in wastewater. In this study, a spent bleaching earth from an edible oil refinery was treated and impregnation in order to remove the edible oil remnants and impregnated by  $\beta$ -naphthol to enhance its adsorption properties. The clay is characterised by Fourier Transform Infrared Spectrometer (FTIR), surface area analyser, Environmental Scanning Electron Microscope (ESEM), Energy-dispersive X-ray spectroscopy (EDX), and X-ray diffraction (XRD). The experiments have been conducted upon uranium adsorption efficiency to optimise the influence of pH value, contact time, adsorbent dose, initial uranium ions concentration, and temperature. The adsorption capacity of the adsorbent is calculated as 175.1 mg.g<sup>-1</sup>. The kinetics and isotherm of adsorption process were evaluated and the data followed pseudo second order kinetic model as well as Langmuir isotherm model. The thermodynamic study reveals that the adsorption process of uranium ions is spontaneous. The adsorption process is exothermic and the negative value of  $\Delta S^\circ$  indicates the feasibility of adsorption and the decreased randomness for the new adsorbent clay.



**A026 - Peculiarities of Rare Earth Elements Removal From Chloride Solution Using Cetylpyridinium Bromide/Polyvinyl Chloride**

Eman M. Allam<sup>1,\*</sup>, Taysser A. Lashen<sup>1</sup>, Saeyda A. Mohamed<sup>2</sup>, Mohamed A. Hassanin<sup>1</sup>, Ahmed K. Sakr<sup>1</sup>, Mohamed F. Cheira<sup>1,\*</sup>, M. Y. Hanfi<sup>1,3</sup>, M. I. Sayyed<sup>4,5</sup> Mayeen Uddin Khandaker<sup>6</sup>

<sup>1</sup>Nuclear Materials Authority, P.O. Box 530, El Maadi, Cairo, Egypt.

<sup>2</sup>Chemistry Department, Faculty of Science, Menoufiya University, Egypt.

<sup>3</sup>Institute of Physics and Technology, Ural Federal University, Ekaterinburg, Russia

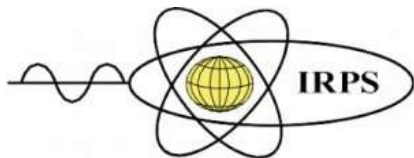
<sup>4</sup>Department of physics, Faculty of Science, Isra University, Amman – Jordan

<sup>5</sup>Department of Nuclear Medicine Research, Institute for Research and Medical Consultations (IRMC), Imam Abdulrahman bin Faisal University (IAU), P.O. Box 1982, Dammam, 31441, Saudi Arabia

<sup>6</sup>Center for Applied Physics and Radiation Technologies, School of Engineering and Technology, Sunway University, 47500 Bandar Sunway, Selangor Darul Ehsan, Malaysia

Corresponding author: dr\_e.allam@yahoo.com, mf.farid2008@yahoo.com

A novel cetylpyridinium bromide/polyvinyl chloride (CPB/PVC) adsorbent was synthesized and applied to study the removal characterization of rare earth elements from its solution. Cetylpyridinium bromide/polyvinyl chloride adsorbent is characterized by FTIR, XRD, TGA, and SEM. To scrutinize the effect of CPB/PVC removal efficiency, adsorption of rare earth ions were studied from the mixture solutions by CPB/PVC adsorbent. The effect of varied factors containing pH value, contact time, initial rare earth ions concentration, and CPB/PVC dosage on the adsorption procedure were deliberated. The best pH was 6.0 and adsorption equilibrium was realized at 45 min at room temperature. The removal efficiency of rare-earth ions on CPB/PVC was 182.6 mg/g. The kinetic and equilibrium adsorption of rare earth ions onto CPB/PVC adsorbent fitted well both pseudo-second-order kinetic and Langmuir isotherm model proposing that RE ions were adsorbed via a chemical reaction. Furthermore, the adsorption thermodynamic process of rare-earth ions was spontaneous and exothermic for CPB/PVC adsorbent. In addition, the desorption of rare-earth ions from their loaded CPB/PVC was examined. The best desorption conditions were 1 M HCl, and 1:60 S:L phase ratio, for 60 min contact time at room temperature. Consequently, the prepared CPB/PVC adsorbent was documented as a prospective candidate for rare earth adsorption applications.



**ISRP 2021**  
**International Symposium on Radiation Physics**  
**Kuala Lumpur – Malaysia**  
**6 – 10 December 2021**

**A028 - The effect of CNTs on The Radiation Attenuation Properties Of The Composite Of BaTiO<sub>3</sub> Doped With Spinnel Ferrite**

M.Elsafi<sup>1</sup>, E. Hannachi<sup>2,\*</sup>, M.I. Sayyed<sup>2,3</sup>, Mayeen Uddin Khandaker<sup>4</sup>

<sup>1</sup>Physics Department, Faculty of Science, Alexandria University, 21511 Alexandria, Egypt.

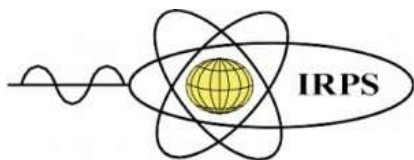
<sup>2</sup> Department of Nuclear Medicine Research, Institute for Research and Medical Consultations (IRMC), Imam Abdulrahman bin Faisal University (IAU), PO Box 1982, Dammam, 31441, Saudi Arabia

<sup>3</sup>Department of Physics, Faculty of Science, Isra University, Amman – Jordan

<sup>4</sup>Center for Applied Physics and Radiation Technologies, School of Engineering and Technology, Sunway University, 47500 Bandar Sunway, Selangor Darul Ehsan, Malaysia

Corresponding author: [annechi.essia@gmail.com](mailto:annechi.essia@gmail.com)

This work studies the effect of carbon nanotubes (CNTs) on some characteristics of Barium Titanate (BaTiO<sub>3</sub>) including the structure and the radiation attenuation performances. The discussed samples were represented by: 100% BaTiO<sub>3</sub>(S1), BaTiO<sub>3</sub>+10% Co<sub>0.3</sub>Ni<sub>0.5</sub>Mn<sub>0.2</sub>Eu<sub>0.08</sub>Fe<sub>1.92</sub>O<sub>4</sub> (S2) and BaTiO<sub>3</sub>+10% Co<sub>0.3</sub>Ni<sub>0.5</sub>Mn<sub>0.2</sub>Eu<sub>0.08</sub>Fe<sub>1.92</sub>O<sub>4</sub>+ 10% CNTs (S3). The samples were prepared by the sol-gel method and characterized by the XRD technique. To measure the attenuation properties of the studied samples, the important coefficient called linear attenuation (LAC) coefficient was measured experimentally using the collimated technique measurement. The Sodium Iodide Scintillation detector (NaI) and different point sources such as Ba-133 (81 and 356 keV), Cs-137 (662 keV), Co-66 (1173 and 1333 keV), and Eu-152 (121, 244, 780, 964, 1111 and 1408 keV) were used to calculate the LAC with a broad range of energies. The LAC for the first sample (S1) was evaluated theoretically by the XCOM software to ensure the validity of the experimental results and the comparison was in agreement between the two results. The results indicated that the LAC of S3>S2>S1, and that's mean the effect of CNTs increases the LAC of the sample, and the shielding characteristic in the present CNTs is better.



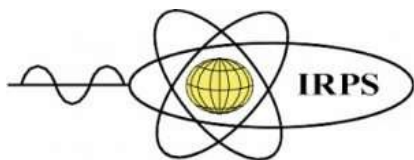
**A033 - Lithium aluminate borate glass mixed with tin slag for radioactive immobilization**

S.A Zulkeplee<sup>1</sup>, N.E Ahmad<sup>1</sup>, M.S.M Sanusi<sup>1</sup>, S. Hashim<sup>1</sup>, F.M Nor<sup>1</sup>

<sup>1</sup>Department of Physics, Faculty of Science, Universiti Teknologi Malaysia, Malaysia

Corresponding author: syazaamira@graduate.utm.my

In this study, lithium aluminate borate glass with the composition of  $(50-0.5x) \text{Li}_2\text{O}-x\text{Al}_2\text{O}_3-(50-0.5x) \text{B}_2\text{O}_3$  ( $0.0 \leq x \leq 4.0 \text{ mol}\%$ ) was fabricated and mixed with 5 wt.% and 30 wt.% of tin slag to understand the compatibility of the glass as a host for radioactive waste. The glasses were synthesized by conventional melt quenching technique and their durability was studied in vitro using immersion test in distilled water up to 14 days at 90 °C in a drying oven. Characterizations using pH meter, Fourier Transform Infrared (FTIR) spectrometer and High Purity Germanium (HPGe) Gamma Ray Spectroscopy detector were made after 3, 7 and 14 days of leaching tests. Once the samples were in contact with water, process of ion exchange or interdiffusion occurred. The increasing pH values of the leachates from 7.00 up to 10.93 with increasing immersion time (day 0 to day 14) were due to the addition of alkali metal (lithium) in the glass composition. For the appearance of FTIR analysis, it can be found that 5 obvious peaks that are Al-O bonding,  $\text{BO}_4$  bonding,  $\text{BO}_3$  bonding, the relaxation mode for B-O  $\text{BO}_3$  and O-H stretching were found. After 3 days of leaching tests, O-H peaks were observed at range up to  $3200 \text{ cm}^{-1}$  which indicates the occurrence of hydrolysis process. The total activity concentration of radionuclide (Bq/g) of all samples were obtained using HPGe spectroscopy detector i.e., reference sample (initial tin slag) contained 207 Bq/g, 59 Bq/g and 94 Bq/g while sample 4 after 14 days leaching tests have recorded 62 Bq/g, 8 Bq/g and 74 Bq/g of  $^{238}\text{U}$ ,  $^{232}\text{Th}$  and  $^{40}\text{K}$  respectively. From these two results, it can be observed that the radioactivity level had reduced to approximately 70% from its initial value, even though most of the samples have exceeded the limit of IAEA Safety Standard i.e., 10 Bq/g for  $^{238}\text{U}$  and  $^{232}\text{Th}$  and 1Bq/g for  $^{40}\text{K}$ . From all the characterization works done, it is concluded that radioactive waste glass containing 30 wt.% of tin slag with 4 mol% of  $\text{Al}_2\text{O}_3$  is durable among the samples since the addition of aluminium oxides could enhanced the mechanical features of lithium borate such as hydrolytic resistant which contribute to the ideal composition for the radioactive immobilised materials.



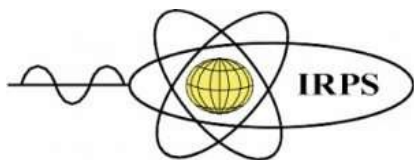
**A038 - Characterization of thermoluminescence properties for Al<sub>2</sub>O<sub>3</sub>:Ge,Sr prepared by combustion synthesis method**

Nurul Syazlin Shahrin<sup>1</sup>,\*Abd Rahman Tamuri<sup>1</sup>, Nor Ezzaty Ahmad<sup>1</sup>

<sup>1</sup>Physics Department, Faculty of Science, Universiti Teknologi Malaysia, Johor Bharu, Johor, Malaysia.

Corresponding author: rahmantamuri@utm.my

The thermoluminescence (TL) properties of Al<sub>2</sub>O<sub>3</sub>:Ge and Al<sub>2</sub>O<sub>3</sub>:Ge;Sr in powder forms irradiated by Cobalt-60 gamma rays were studied. Samples were prepared using combustion synthesis technique. The annealing was determined at 400 °C for 1 h, followed by 80 °C for 16 h, with the heating rate of 3 °C s<sup>-1</sup> and minimum detectable dose was 0.0065 mGy. Analysis of its kinetic parameters revealed that the sample possess second order kinetic supported by the whole glow peak technique. The calculated activation energy is  $E = 1.00 \pm 0.007$  eV and frequency factor,  $s = 4.36 \pm 1.67 \times 10^{10}$  s<sup>-1</sup>. The samples exhibited good linearity and sensitivity at 52.72 nC mg<sup>-1</sup>Gy<sup>-1</sup> with correlation coefficient, R<sup>2</sup> of 0.9961 at high dose range 10 Gy – 80 Gy and 43.40 nC mg<sup>-1</sup>Gy<sup>-1</sup> of 0.9681 at low dose range 0.5 Gy - 4.0 Gy respectively. The sample also shows low fading with the percentage loss of 33% at low dose of 4Gy and 34 % at high dose of 50 Gy after 60 days. The sample possessed good reproducibility with the percentage of standard deviation of 2.4% at 4 Gy and 6.5% at 50 Gy. The existence of several peaks in XRD clarified the sample was in polycrystalline state. TEM micrographs confirmed this sample was nanocrystalline with 9.36 nm in size. In conclusion, Al<sub>2</sub>O<sub>3</sub>: Ge 3.0 mol %, Sr 0.3 mol% was found to be a potential material to be used as a TL dosimeter which satisfies most of the desirable TL characteristics.



**A039 - Radiation shielding features for a new glass system based on tellurite oxide**

Mohammad Abu Mhareb<sup>1,2\*</sup>; M. I. Sayyed<sup>3,4</sup>; S. Hashim<sup>5,6</sup>; Maha Alshammari<sup>1</sup>; Shadin Alhugail<sup>1</sup>; Houra Aldoukhi<sup>1</sup>; M. Kh. Hamad<sup>7</sup>; Y. S. Alajerami<sup>8</sup>, Mayeen Uddin Khandaker<sup>9</sup>

<sup>1</sup>Department of Physics, College of Science, Imam Abdulrahman Bin Faisal University, P.O. Box 1982, 31441 Dammam, Saudi Arabia

<sup>2</sup>Basic and Applied Scientific Research Center, Imam Abdulrahman Bin Faisal University, PO Box 1982, 31441 Dammam, Saudi Arabia

<sup>3</sup>Department of Physics, Faculty of Science, Isra University, Amman, Jordan

<sup>4</sup>Department of Nuclear Medicine Research, Institute for Research and Medical Consultations (IRMC), Imam Abdulrahman Bin Faisal University (IAU), P.O. Box 1982, 31441 Dammam, Saudi Arabia

<sup>5</sup>Department of Physics, Faculty of Science, Universiti Teknologi Malaysia, Johor, 81310 UTM, Skudai, Malaysia

<sup>6</sup>Ibnu Sina Institute for Scientific and Industrial Research (ISISIR), Universiti Teknologi Malaysia, Johor, 81310 UTM, Skudai, Malaysia

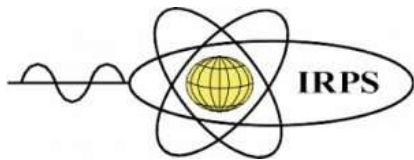
<sup>7</sup>Department of Basic Sciences, School of Social and Basics Sciences, Al Hussein Technical University, Amman, Jordan

<sup>8</sup>Medical Imaging Department, Applied Medical Sciences Faculty, Al Azhar University-Gaza, P.O. Box 1277, Gaza, Palestine

<sup>9</sup>Center for Applied Physics and Radiation Technologies, School of Engineering and Technology, Sunway University, 47500 Bandar Sunway, Selangor Darul Ehsan, Malaysia

Corresponding author: mhsabumhareb@iau.edu.sa

Recently, the demand for shielding materials increased with the increasing use of ionizing radiation in our lives. In this work, we fabricated five tellurite glass samples with a composition  $20\text{BaO}-10\text{SrO}-(70-x)\text{TeO}_2-x\text{MoO}_3$  (where  $x = 0, 5, 10, 15,$  and  $20$  mol%) by conventional melt-quench method for exploring gamma radiation shielding features. The amorphous nature was defined by using X-ray diffraction, and all samples affirmed this behavior. Various physical properties were calculated based on density values for glass samples. The density values show a gradual increment with the addition of  $\text{MoO}_3$  instead of  $\text{TeO}_2$ . Different gamma radiation shielding properties such as linear attenuation coefficient (LAC), half-value layer (HVL), mean free path (MFP), tenth value layer (TVL), transmission factor (TF), radiation protection efficiency (RPE), and effective atomic number ( $Z_{\text{eff}}$ ) were determined based on XCOM and Phy-X programs. All shielding properties showed improvement with the addition of  $\text{MoO}_3$  to the glass system, and STBM20 shows superior shielding properties compared with other samples. It can be concluded the possibility to use current samples in the radiation shielding field.



**A040 - Characterization and gamma rays shielding performance of calcinated bentonite nanoparticles**

Fawzy H. Sallam<sup>1</sup>, K.A. Mahmoud<sup>1,2</sup>, M.I. Sayyed<sup>3,4</sup>, Eloic Lacomme<sup>5,\*</sup>, Mayeen Uddin Khandaker<sup>6</sup>

<sup>1</sup>Nuclear Materials Authority, P.O. Box 530 El-Maadi, Cairo, Egypt.

<sup>2</sup>Ural Federal University, 19 Mira St, 620002, Ekaterinburg, Russia

<sup>3</sup>Department of Physics, Faculty of Science, Isra University, Amman 11622, Jordan

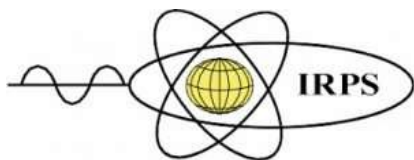
<sup>4</sup>Department of Nuclear Medicine Research, Institute for Research and Medical Consultations, Imam Abdulrahman bin Faisal University, Dammam 31441, Saudi Arabia

<sup>5</sup>Advance Science Research, Junior, Eastchester High School, Eastchester, NY, United States

<sup>6</sup>Center for Applied Physics and Radiation Technologies, School of Engineering and Technology, Sunway University, 47500 Bandar Sunway, Selangor Darul Ehsan, Malaysia

Corresponding author: e.lacommeeastchester@gmail.com

Calcinated bentonite is a promising material for gamma-ray shielding as it has a variety of mineral content. Bentonite clay is volcanic ash transformed during the deposition in the presence of water. It has a high cation exchange capacity which allows minerals to bind with organic and inorganic cations. These organic cations and water can be eliminated by calcination at 700 °C also keeps mineralogy and pore structure undestroyed. Calcinated bentonite was ball milled in high-energy mortar to refine particle size into a nanometer scale. Both calcinated and ball-milled calcinated bentonite are pressed into cylindrical samples at different thicknesses and different pressing pressure of 50, 100, and 150 bar. Calcinated and ball-milled bentonite structure is characterized by chemical analysis, density, weight fraction, XRD diffraction analysis, particle size measurements in addition to morphological studies using TEM and SCAN. Shielding performance of bentonite samples against gamma rays was investigated and determined in the energy range from 0.015 MeV to 15 MeV using the MCNPX program. Mass attenuation coefficients of calcinated and ball-milled bentonite samples pressed at 150 bar varies from 12.5442 cm<sup>2</sup>/g at 0.015 MeV to 0.02258 cm<sup>2</sup>/g at 15 MeV while linear attention coefficients varies from 23.332 cm<sup>-1</sup> at 0.015 MeV to 0.042 cm<sup>-1</sup> for calcinated bentonite and from 26.0294 cm<sup>-1</sup> at 0.015 MeV to 0.04687 cm<sup>-1</sup> at 15 MeV for ball-milled bentonite. Similarly, HVL, TVL, and mfp were calculated for all samples. Mass attenuation coefficients values obtained from simulation were set in comparison with available experimental and theoretical data.



**ISRP 2021**  
**International Symposium on Radiation Physics**  
**Kuala Lumpur – Malaysia**  
**6 – 10 December 2021**

**A041 - Solution optical spectra of anticancer drug vandetanib using robust quantum mechanical calculations**

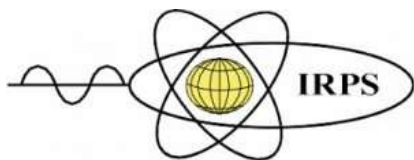
Lewis McArthur<sup>1</sup>, Sallam Alaghawani<sup>1</sup>, Vladislav Vasilyev<sup>2</sup> and Feng Wang<sup>1\*</sup>

<sup>1</sup>Department of Chemistry and Biotechnology, Swinburne University of Technology, Melbourne, Victoria 3122, Australia

<sup>2</sup>National Computational Infrastructure, Australian National University, Canberra, ACT 0200, Australia

Corresponding author: fwang@swin.edu.au

Tyrosine kinase inhibitors (TKIs) based on the quinazoline-aniline scaffold represent a significant class of small molecule medicine under development and in clinical practice for disease states such as cancer. Recent research revealed that this class of inhibitors designed for the epidermal growth factor receptor (EGFR) family are located in the ATP binding site of their cognate tyrosine kinase in twisted conformations, rather than the global minimum structure in isolation. In a recent solvent benchmarking study of a number of important density functional theory (DFT) functionals, it is discovered that B3WP91/6-311++G(d,p) predicts the most accurate maximum absorption and emission spectral transitions of AG-1478, a TKIs with the same scaffold. The present study quantum mechanically calculates the absorption UV-vis spectrum and the fluorescence spectrum of vandetanib (ZD6474) in methanol solvent using time-dependent-DFT methods. The results are compared with the measured UV-vis spectra in the same solvent in literature.



**ISRP 2021**  
**International Symposium on Radiation Physics**  
**Kuala Lumpur – Malaysia**  
**6 – 10 December 2021**

**A042 - Intramolecular hydrogen bonding of hydroxybenzoic acid isomers revealed using XPS: theory and experiment\***

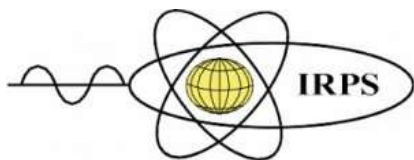
Alexander Hill,<sup>1</sup> Kevin C. Prince<sup>1,2</sup> and Feng Wang<sup>1\*</sup>

<sup>1</sup>Department of Chemistry and Biotechnology, Swinburne University of Technology, Melbourne, Australia

<sup>2</sup>Elettra Sincrotrone Trieste, in Area Science Park, 34149 Basovizza, Trieste, Italy

Corresponding author: fwang@swin.edu.au

Hydrogen bonding in molecules is a valence event as well as a core event. Oxygen is an important hydrogen acceptor, and its oxygen core electron ionization binding energy in a molecule will respond to through space and through bond intramolecular interactions in organic isomers such as hydroxybenzoic acid isomers. The present study investigates the impact of intramolecular hydrogen bonding of three hydroxybenzoic acid (HBA) position isomers using density functional theory (DFT) based calculations and synchrotron sourced measurement. The obtained oxygen 1s (O1s) and carbon 1s (C1s) x-ray photoemission spectra (XPS) are compared in order to understand their structure-property relationships and intramolecular hydrogen bonding. It is found that the O1s XPS spectra of the HBAs are strongly influenced by the existence of intramolecular hydrogen bonding of the isomers, depending on the relative position and distance of O···H, which is most significant in 2-HBA due to through space interaction. Such interactions are less apparent in 3-HBA and 4-HBA as they lack such intramolecular hydrogen bonding.



**A044 - Ta<sub>2</sub>O<sub>5</sub>-doped bismuth zinc tellurite glass: fabrication, optical, and radiation shielding evaluation**

F.I. El-Agawany<sup>1</sup>, Gokhan Kilic<sup>2\*</sup>, Buse Ozen Ilik<sup>3</sup>, A.M. Abu El-Soad<sup>4,5\*</sup>, Erkan Ilik<sup>2</sup>, E. Yousef<sup>6,7</sup>, Y.S. Rammah<sup>1</sup>

<sup>1</sup>Department of Physics, Faculty of Science, Menoufia University, Shebin El-Koom 32511, Menoufia, Egypt.

<sup>2</sup>Eskisehir Osmangazi University, Faculty of Science and Letters, Department of Physics, TR-26040 Eskisehir, Turkey

<sup>3</sup>General Directorate of Mineral Research and Exploration, Ankara, Turkey

<sup>4</sup>Ural Federal University, 19 Mira St, 620002, Yekaterinburg, Russia.

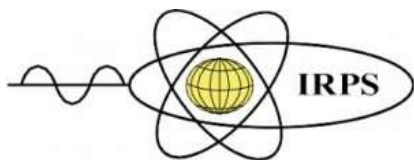
<sup>5</sup>Nuclear Materials Authority, P. O. Box 530, El Maadi, Cairo, Egypt.

<sup>6</sup>Research Center for Advanced Materials Science (RCAMS), King Khalid University, P. O. Box 9004, Abha 61413, Saudi Arabia.

<sup>7</sup>Physics Dep., Faculty of Science, King Khalid University, P. O. Box 9004, Abha 61413, Saudi Arabia

Corresponding author: chemistasmaa60@yahoo.com, Gokhan Kilic (gkilic@ogu.edu.tr)

A glass system consisting of Bi<sub>2</sub>O<sub>3</sub>-TeO<sub>2</sub>- ZnO- Ta<sub>2</sub>O<sub>5</sub> was fabricated. The Analytik Jena Specord 210 plus was used to estimate photons' absorbance and transmission with wavelengths ranging between 190-1100 nm. The optical energy-gap ( $E_g$ ) and Urbach energy ( $\Delta E$ ) were calculated for the fabricated glass samples. Moreover, the Monte Carlo simulation (MCNP-5 code) and XCOM software program were used to estimate the fabricated glass samples' mass attenuation coefficient (MAC). The achieved results showed that the highest MAC values achieved for the highest ratio of Ta<sub>2</sub>O<sub>5</sub> (BTZT6) decreased from 64.684 to 0.042 cm<sup>2</sup> g<sup>-1</sup>. In contrast, the lowest MAC values achieved for (BTZT0) without Ta<sub>2</sub>O<sub>5</sub> content varied between 57.816 to 0.0414 cm<sup>2</sup> g<sup>-1</sup>, when the gamma photon energy increased from 0.015 to 15 MeV, respectively. The software program BXCCom was used to estimate the equivalent atomic number ( $Z_{eq}$ ), effective atomic number ( $Z_{eff}$ ), exposure build-up factors (energy absorption build-up factor (EABF), and exposure build-up factor (EBF)). The values of the EBF and EABF were increased with increasing the Ta<sub>2</sub>O<sub>5</sub> insertion ratio. The fast neutron effective removal cross-section was also calculated using a theoretical method; the BTZT0 glass sample poses the highest removal cross-section  $\sum_R = 0.0176$  cm<sup>2</sup> g<sup>-1</sup>, while the BTZT6 glass sample contains the lowest cross section  $\sum_R = 0.0173$  cm<sup>2</sup> g<sup>-1</sup>.



**ISRP 2021**  
**International Symposium on Radiation Physics**  
**Kuala Lumpur – Malaysia**  
**6 – 10 December 2021**

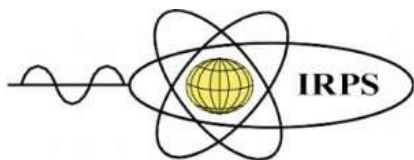
#### **A046 - Solving self-absorption in fluorescence**

Ryan Trevorah<sup>1</sup>, Christopher T. Chantler<sup>1</sup>

<sup>1</sup>School of Physics, University of Melbourne, Australia

Corresponding author: ryanmt@student.unimelb.edu.au

95% of XAS research uses measurement of secondary fluorescence photons, which suffers from uncalibrated detector efficiencies and a dominant systematic of self-absorption of the fluorescence photon, which compromises accuracy, analysis and insight. We have developed, coded and implemented a novel self-consistent method to correct for self-absorption seen in high-energy fluorescence X-ray measurements. This method and the resulting software package can be applied to any fluorescence data set. The complexes considered here, n-pr and i-pr, have been shown to have local metal environments with approximate tetrahedral and square planar coordination geometries using transmission mode XAS. This provides an excellent test of fluorescent multi pixel data, and demonstrates the merit of using complimentary techniques to confirm molecular geometries. A dramatic discrepancy is seen between the spectra from the two measurements. This is due to the self-absorption systematic and also to uncalibrated detector efficiencies in the fluorescence measurement. While the detector efficiency can be corrected for, there is currently no self-consistent method for removing the effect of self-absorption from the spectra. In this work, we predict to high accuracy the magnitude of dispersion and energy functional due to self-absorption. As a result, the dispersion is greatly reduced, and the spectral shape follows the classic XAS trend. The results presented here demonstrate a dramatic improvement over any previous work in the literature. Our modern theory is of the best quality, allowing our self-absorption correction to be applied to any fluorescence XAS data set and opening up an entire class of experimental investigation.



**ISRP 2021**  
**International Symposium on Radiation Physics**  
**Kuala Lumpur – Malaysia**  
**6 – 10 December 2021**

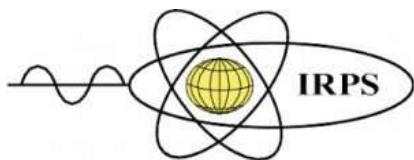
**A047 - Developing a novel technique of radon detection for all three naturally occurring radon ( $^{222}\text{Rn}$ ,  $^{220}\text{Rn}$  and  $^{219}\text{Rn}$ )**

Amos Vincent Ntarisa, H.J. Kim\*, Pabitra Aryal, Nguyen Duy Quang,

Department of Physics, Kyungpook National University, Daegu, 41566,

Corresponding Author, Email: hongjoo@knu.ac.kr

Radon is the largest contributor to the population exposures from natural radiation sources and is the second causes of lung cancer after smoking. There are three naturally occurring radon isotopes which are  $^{222}\text{Rn}$ (radon),  $^{220}\text{Rn}$ (thoron) and  $^{219}\text{Rn}$ (actinon) which are members of natural decay series of  $^{238}\text{U}$ ,  $^{232}\text{Th}$  and  $^{235}\text{U}$ , respectively. We report a novel technique to detect these isotopes of radon with liquid scintillator and photomultiplier tube using delayed coincidence technique (DCT) and pulse shape discrimination (PSD) method implemented by digital charge comparison. We use Ultima Gold AB (UG-AB) liquid scintillation cocktail which are designed for alpha/beta discrimination in liquid scintillation counting. We fed radon source from air for 48 hours in 700 mL of UG-AB in the sample container of 1- liter of Stainless Steel (SUS) with teflon coating inside and 2 mm SUS outside of 5 mm glass window. The sample was kept in a glove box for 48 hours and was stirred time to time to allow radon source to enter in the container. Neutron Tagging Module (NGT400) tags neutron signal from a liquid scintillation detector and accepts an input pulse with width from 20 to 1270 ns. In these ways isotopes having a relatively short half-life can be selected out by their characteristic energy and decay-time distributions. This technique can be used to estimate radon level by DCT with  $\alpha$  and  $\beta$  requirements, where PSD is used to identify  $\alpha$  and  $\beta$ . This technique can be used to detect all three naturally occurring radon ( $^{222}\text{Rn}$ ,  $^{220}\text{Rn}$  and  $^{219}\text{Rn}$ ) compared to many other developed techniques which are based only on the detection of  $^{222}\text{Rn}$ . The gamma response functions of UG-AB organic liquid scintillation detector with standard  $^{22}\text{Na}$ ,  $^{137}\text{Cs}$  and  $^{60}\text{Co}$  gamma sources are under studying with Monte Carlo Neutron Particle Simulation (MCNP).



**ISRP 2021**  
**International Symposium on Radiation Physics**  
**Kuala Lumpur – Malaysia**  
**6 – 10 December 2021**

**A049 - On the study for TeO<sub>2</sub>-WO<sub>3</sub>-TiO<sub>2</sub> -ZnO -Na<sub>2</sub>O glass containing Pr<sub>2</sub>O<sub>3</sub> in radiation shielding applications: Theoretical computations via EPICS2017**

M.I. Sayyed<sup>1,2</sup>, C.V. Balderas<sup>3</sup>, Recep Kurtulus<sup>4</sup>, Taner Kavas<sup>4</sup>, Mayeen Uddin Khandaker<sup>5</sup>

<sup>1</sup>Department of physics, Faculty of Science, Isra University, Amman – Jordan

<sup>2</sup>Department of Nuclear Medicine Research, Institute for Research and Medical Consultations (IRMC), Imam Abdulrahman bin Faisal University (IAU), P.O. Box 1982, Dammam, 31441, Saudi Arabia

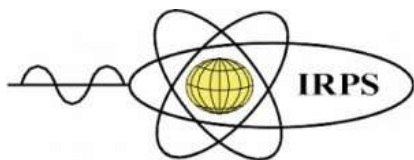
<sup>3</sup>Department of Science and Technology – Philippine Nuclear Research Institute (DOST-PNRI), Commonwealth Avenue, Diliman, Quezon City 1101, Philippines

<sup>4</sup> Afyon Kocatepe University, Faculty of Engineering, Department of Materials Science and Engineering, Afyonkarahisar, Turkey

<sup>5</sup> Center for Applied Physics and Radiation Technologies, School of Engineering and Technology, Sunway University, 47500 Bandar Sunway, Selangor Darul Ehsan, Malaysia

Corresponding author: rkurtulus@aku.edu.tr

In this work, we aimed to study the role of the Pr<sub>2</sub>O<sub>3</sub> on the radiation shielding features of the glass systems with general composition TeO<sub>2</sub>-WO<sub>3</sub>-TiO<sub>2</sub> -ZnO -Na<sub>2</sub>O-Pr<sub>2</sub>O<sub>3</sub>. For this aim, we used EPICS2017 for the calculations of the mass attenuation coefficient of the TePrX-glasses between 81 and 1333 keV. The comparison between the EPICS2017 and Phy-X data showed strong agreement with an overall average relative difference of 0.18%. With respect to the energy, the average relative difference per sample ranged from 0.18%-0.19% while the average relative difference per energy ranged from 0.02%-0.26%. The Linear attenuation coefficient (LAC) value is enhanced from 0.420 to 0.428 cm<sup>-1</sup> by inserting Pr<sub>2</sub>O<sub>3</sub> from 0 to 5 mol% at 662 keV. At all the investigated energies, an increase in LAC values is clearly achieved with increasing the amount of Pr<sub>2</sub>O<sub>3</sub>, which in turn improving radiation shielding properties for the examined glasses. The half value layer (HVL) values ascend to the higher values (greater than 2.5 cm) for the photon energy of 1333 keV. Tenth-value layer (TVL) for the selected glasses is also determined. The calculated TVL thicknesses vary between 0.148 and 8.467 cm, and the lowest thickness was achievable by TePr5 sample. The TVL values change in the order of TePr4<TePr3<TePr2<TePr1<TePr0 for the remaining samples. The electron density ( $N_{\text{eff}}$ ) varies in the range of  $6.35 \times 10^{23}$  and  $2.69 \times 10^{23}$  electrons/g for the measured photon energies.



**ISRP 2021**  
**International Symposium on Radiation Physics**  
**Kuala Lumpur – Malaysia**  
**6 – 10 December 2021**

**A050 -Assessment of Radiation attenuation properties for novel alloys: An experimental approach**

M. I. Sayyed<sup>1,2</sup>, M. Kh. Hamad<sup>3</sup>, Mohammad Abu Mhareb<sup>4,5</sup>, Y. S. Alajerami<sup>6</sup>, Marwa Aldikhel<sup>4</sup>, Mayeen Uddin Khandaker<sup>7</sup>, D. A. Bradley<sup>7,8</sup>

<sup>1</sup>Department of Physics, Faculty of Science, Isra University, Amman, Jordan

<sup>2</sup>Department of Nuclear Medicine Research, Institute for Research and Medical Consultations (IRMC), Imam Abdulrahman Bin Faisal University (IAU), P.O. Box 1982, 31441 Dammam, Saudi Arabia

<sup>3</sup>Department of Basic Sciences, School of Social and Basics Sciences, Al Hussein Technical University, Amman, Jordan

<sup>4</sup>Department of Physics, College of Science, Imam Abdulrahman Bin Faisal University, P.O. Box 1982, 31441 Dammam, Saudi Arabia

<sup>5</sup>Basic and Applied Scientific Research Center, Imam Abdulrahman Bin Faisal University, PO Box 1982, 31441 Dammam, Saudi Arabia

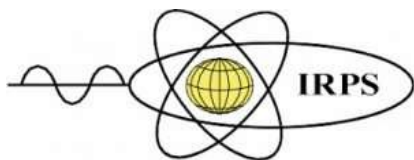
<sup>6</sup>Medical Imaging Department, Applied Medical Sciences Faculty, Al Azhar University-Gaza, P.O. Box 1277, Gaza, Palestine

<sup>7</sup>Center for Applied Physics and Radiation Technologies, School of Engineering and Technology, Sunway University, 47500 Bandar Sunway, Selangor Darul Ehsan, Malaysia

<sup>8</sup>Department of Physics, University of Surrey, Guildford, Surrey GU2 7XH, UK

Corresponding author: 2180500171@iau.edu.sa

Radiations are widely utilized in medicinal fields and many other fields. Ionizing radiation has sufficient energy to detach electrons from atoms on the human body, which can cause great damage if not properly attenuated. In order to avoid these unwanted effects, radiation shielding materials are used to absorb incoming photons. In this work, we used the conventional solid-state reaction to fabricate four Cr-based alloys ( $\text{CrTe}$ ,  $\text{CrTe}_{0.95}\text{Sb}_{0.05}$ ,  $\text{CrTe}_{0.90}\text{Sb}_{0.10}$  and  $\text{CrTe}_{0.80}\text{Sb}_{0.20}$ ) and we explored their gamma radiation shielding features. Gamma radiation attenuation for the four prepared alloys were performed using “transmission method” with photons emitting source from ( $\text{Ho-166}$  and  $\text{Cs-137}$ ). The experimental results were compared with the theoretical data generated from Phy-X software and a good agreement between both methods was reported. Moreover, the radiation protection efficiency for the prepared alloys was reported between 0.184 and 0.81 MeV. The half value layer (HVL) value for the four prepared alloys was also computed and we discussed the variation of the HVL with the chemical composition for these alloys. Finally, we compared the radiation shielding features for the prepared alloys with other shielding materials to examine the possibility of using these alloys in different radiation shielding applications.



**A051 - Assessment of geogenic impact on thoron activity concentration in soil gas of Perak state, Malaysia**

Habila Nuhu<sup>1,3</sup>, Suhairul Hashim<sup>1,2</sup>, Mohamad Syazwan Sanusi<sup>1</sup>

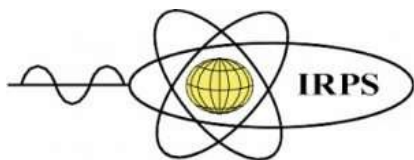
<sup>1</sup>Department of Physics, Universiti Teknologi Malaysia, Skudai, Johor, Malaysia.

<sup>2</sup> Ibnu Sina Institute for Scientific and Industrial Research (ISISIR), Universiti Teknologi Malaysia, Skudai, Johor, Malaysia.

<sup>3</sup> Department of Science, Plateau State Polytechnic Barkin Ladi, Jos Plateau State, Nigeria.

Corresponding author: nuhabila@gmail.com

The contribution of thoron ( $^{220}\text{Rn}$ ) to ionizing radiation exposure is frequently overlooked, owing to its short half-life (55.6 s). A thorium ( $^{232}\text{Th}$ )-rich environment, on the other hand, can be a source of  $^{220}\text{Rn}$  radiation hazards. Long-term exposure to high concentrations of  $^{220}\text{Rn}$  and its short-lived progeny [Polonium ( $^{216}\text{Po}$ )], an alpha particle emitter, can be hazardous to one's health. Thus, this study aims to establish fundamental  $^{220}\text{Rn}$  activity concentration data based on the geological formations and major soil types of Perak state, Malaysia. The activity concentration of  $^{220}\text{Rn}$  in the study area's soil gas was determined using a RAD7 detector. The in-situ measurement procedure involved setting the RAD7 to the THORON protocol and connecting it to a soil probe which was driven to a depth of 0.8m in the ground. The concentration of  $^{220}\text{Rn}$  in soil gas ranged from 0 to 562.58 kBq m<sup>-3</sup>, with a mean of  $37.69 \pm 11.14$  kBq m<sup>-3</sup>. High  $^{220}\text{Rn}$  activity was detected in the study area's Granite and Triassic-Jurassic geological formations. Low  $^{220}\text{Rn}$  activity was found in the Quaternary and Silurian geological formations of the study area. The  $^{220}\text{Rn}$  activity concentrations were found to be elevated in peat, riverine, and granite source soils. The concentration of  $^{220}\text{Rn}$  activity in soil gas in marine soils and miscellaneous soils was both low. A primary map of  $^{220}\text{Rn}$  activity in soil gas was produced, indicating that high  $^{220}\text{Rn}$  activity is concentrated in the central part of Perak state, Malaysia.



**ISRP 2021**  
**International Symposium on Radiation Physics**  
**Kuala Lumpur – Malaysia**  
**6 – 10 December 2021**

**A052 - High accuracy determination of photoelectric cross sections, X-ray Absorption Fine Structure and nanostructure analysis of zinc selenide using the X-ray Extended Range Technique**

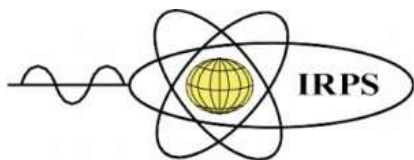
Daniel Sier<sup>1</sup>, Geoffrey P Cousland<sup>1</sup>, Ryan M Trevorah<sup>1</sup>, Ruwini S K Ekanayake<sup>1</sup>, Chanh Q Tran<sup>2</sup>, James R Hester<sup>3</sup> and Christopher T. Chantler<sup>1</sup>

<sup>1</sup>The University of Melbourne, Australia

<sup>2</sup>La Trobe University, Australia,

<sup>3</sup>Australian Nuclear Science and Technology Organisation, Menai Australia

Measurements of mass attenuation coefficients and X-ray absorption fine structure (XAFS) of zinc selenide (ZnSe) are reported to accuracies typically better than 0.13%. The high accuracy of the results presented here is due to our successful implementation of the X-ray Extended Range Technique (XERT), a relatively new methodology, which can be set up on most synchrotron X-ray beamlines. 561 attenuation coefficients were recorded in the energy range of 6.8 keV to 15 keV with measurements concentrated at the zinc and selenium pre-edge, near edge and fine structure absorption edge regions. This accuracy yielded detailed nanostructural analysis of room temperature ZnSe with full uncertainty propagation. Bond lengths, accurate to 0.003 Å to 0.009 Å, or 0.1% to 0.3%, are plausible and physical. Small variation from a crystalline structure suggests local dynamic motion beyond that of a standard crystal lattice, noting that XAFS is sensitive to dynamic correlated motion. The results obtained in this work are the most accurate to date with comparisons to theoretically determined values of the attenuation showing discrepancies from literature theory of up to 4%, motivating further investigation into the origin of such discrepancies.



**ISRP 2021**  
**International Symposium on Radiation Physics**  
**Kuala Lumpur – Malaysia**  
**6 – 10 December 2021**

**A053 - Computation of Gamma Buildup factors and Heavy Ions Penetrating Depths in Clay Composite Material using Phy-X/PSD, EXABCal and SRIM Codes**

S. F. Olukotun<sup>\*1</sup>, M. I. Sayyed<sup>2,3</sup>, O. F. Oladejo<sup>4</sup>, S. T. Gbenu<sup>5</sup>, S. A. Adejo<sup>1</sup>, Aamir Raza Bashir<sup>6</sup>, M. K. Fasasi<sup>5</sup>, Mayeen Uddin Khandaker<sup>7</sup>

<sup>1</sup>Department of Physics and Engineering Physics, Obafemi Awolowo University, Ile-Ife, Nigeria

<sup>2</sup>Department of physics, Faculty of Science, Isra University, Amman – Jordan

<sup>3</sup>Department of Nuclear Medicine Research, Institute for Research and Medical Consultations (IRMC), Imam Abdulrahman bin Faisal University (IAU), P.O. Box 1982, Dammam, 31441, Saudi Arabia

<sup>4</sup>Department of Physics, Osun State University, Osogbo, Nigeria

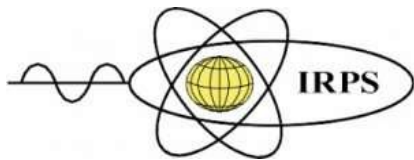
<sup>5</sup>Centre for Energy Research and Development (CERD), Obafemi Awolowo University, Ile-Ife, Nigeria

<sup>6</sup>Department of physics, Faculty of Science, Bahauddin Zakarya University-60800 Multan Pakistan.

<sup>7</sup>Center for Applied Physics and Radiation Technologies, School of Engineering and Technology, Sunway University, 47500 Bandar Sunway, Selangor Darul Ehsan, Malaysia

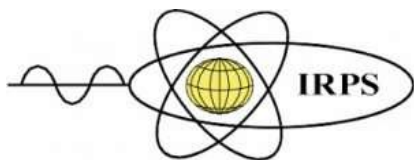
Corresponding Author: olukotunsf@oauife.edu.ng (S. F. Olukotun), Phone Number: +234 8033955996.

Recent studies on the radiation shielding capabilities of clay, an abundant eco-friendly refractory material have shown the suitability of possible application of clay materials for radiation shielding. However, these studies were based on Lambert-Beer law ( $I = I_0 e^{-\mu x}$ ) which assumes monochromatic rays, thin absorbing material, and narrow beam geometry. Any deviation from the mentioned assumptions requires the Lambert-Beer law to be modified. The modified equation is usually written as ( $I = BI_0 e^{-\mu x}$ ) where B is the buildup factors – Exposure Buildup Factor (EBF) and Energy Absorption Buildup Factor (EABF). More also, the knowledge of energy transfer from energetic heavy ions to a material predicts the performance of the material when subjected to high irradiation environments. The interactions of the ions are with both electrons and atomic nuclei of the material. Displacement of atoms from their original sites, creating atomic-scale defects in the material structure can result from nuclear energy loss due to elastic energy transfer to target atoms. Likewise, production of electron-hole pairs that can cause localized electronic excitations, rupture of chemical bonds, charging of pre-existing defects, and enhancing defect and atomic diffusions can be caused by inelastic energy transfer to the electrons (either bound or free), termed as electronic energy loss. In this study, the gamma buildup factors of clay composite material would be computed using



**ISRP 2021**  
**International Symposium on Radiation Physics**  
**Kuala Lumpur – Malaysia**  
**6 – 10 December 2021**

Phy-X/PSD and EXABCal software. While the stopping power and range of ions such as  $^{137}\text{Cs}$  and  $^{90}\text{Sr}$  (being some principal fission products from nuclear waste) would be estimated using the stopping and range of ions in matter (SRIM) code. These computations are aim to provide more information about the gamma radiation shielding capability (GRSC) and to initiate investigation of possibility application of the material in the nuclear waste management.



**A058 - Luminescence Studies of Fabricated Gd:Mg-Doped Silica Glass Exposed to Neutron Radiation**

N.T. Abahre<sup>1</sup>, S.F. Abdul Sani<sup>1</sup>, Laura Elizabeth Fernando<sup>1</sup>, S.S. Ismail<sup>2</sup>, Julia A. Karim<sup>3</sup>, K.S. Almugren<sup>4</sup>, F.H. Alkallas<sup>4</sup>, D.A. Bradley<sup>2,5</sup>

<sup>1</sup>Department of Physics, Faculty of Science, University of Malaya, 50603, Kuala Lumpur, Malaysia

<sup>2</sup>Sunway University, Centre for Biomedical Physics, Jalan Universiti, 46150 PJ, Malaysia.

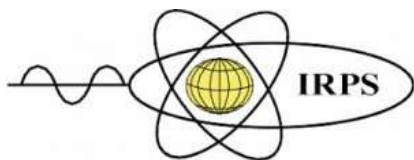
<sup>3</sup>Nuclear and Reactor Physics Section, Nuclear Technology Center, Technical Support Division, Malaysian Nuclear Agency Kajang, Malaysia.

<sup>4</sup>Department of Physics, Princess Nourah Bint Abdulrahman University, Riyadh, Saudi Arabia.

<sup>5</sup>Department of Physics, University of Surrey, Guildford, GU2 7XH, UK.

Corresponding author: s.fairus@um.edu.my

Silicate glasses are known as excellent host materials for many technological applications due to its outstanding performance, in particular thermal and high irradiation power stability. The latter leads to a promising candidate as scintillators in medical, industry and radiation sensor. By applying a sol gel technique, present work has succeeded in producing silica glass composing of silicon and oxygen, extrinsically doped with gadolinium (Gd) and magnesium (Mg) of different dopant concentrations for which direct characterization by thermoluminescence (TL) upon exposure to ionizing radiation is possible. The latter gives rise to appreciable TL due to the rich presence of intrinsic defects in Gd:Mg-doped SiO<sub>2</sub>. This phenomenon can be explained by the electron/hole pairs generated and trapped during irradiation which can be thermally stimulated, leading to release of the stored energy as light. The light intensity is recorded as a function of sample temperature, producing one or more TL peaks where the electron release at greater temperature equating to deeper trapping levels. Present TLD work examines Gd:Mg doped SiO<sub>2</sub> of 1-10 mol% dopant concentration, including dose response linearity and glow curve subjected to 750 kW neutron (<sup>241</sup>AmBe source) flux thermal power. The structural and optical properties of Gd:Mg-doped silica glass with neutron irradiation have been investigated by Raman spectroscopy, photoluminescence, and X-ray diffraction. In condition of irradiation, the formation of point defect and microstructural change with regards to different dopant concentrations have been identified. The goal of this research is to obtain a broad understanding of the magnitude of the TL signal for a variety of Gd:Mg concentration for the need in radiation dosimetry.



**ISRP 2021**  
**International Symposium on Radiation Physics**  
**Kuala Lumpur – Malaysia**  
**6 – 10 December 2021**

**A059 - Radiation response of marble-glass media in medical radiation applications**

Amjad Alyahyawi<sup>1,2</sup>, D.A. Bradley<sup>2,3</sup>

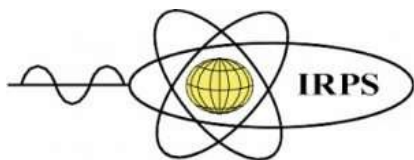
<sup>1</sup>Department of Diagnostic Radiology, College of Applied Medical Sciences, University of Ha'il, Ha'il, Saudi Arabia

<sup>2</sup>Centre for Nuclear and Radiation Physics, Department of Physics, University of Surrey, Guildford, Surrey GU2 7XH, UK

<sup>3</sup>Sunway University, Centre for Applied Physics and Radiation Technologies, Jalan Universiti, 47500 Subang Jaya, Malaysia.

Email: a.alyahyawi@uoh.edu.sa

Thermoluminescent dosimeters (TLD) have proven themselves particularly effective in radiation assessments, TLDs offering several advantages over other dosimetric forms, including typically being of small size and in certain phosphor-based cases soft tissue equivalent. Glass-based TLDs offer features that promise to extend the utility of TLD, including offering a relatively large dynamic range over which sensitivity to differing levels of radiation exposure is provided, also a water impervious nature. Several studies have demonstrated the potential of doped as well as undoped silica-glass fibres as effective dosimeters in diagnostic and radiotherapy applications. In present study, in seeking a low-cost alternative to fibres we investigate commercially available marble-glass over a range of colour and size, comparing their response over a range of radiation doses. Several characteristics have been investigated including dose response, energy response, and fading, showing good linearity and excellent response. While as expected, the dose sensitivity of marble glass is less than that of much more expensive doped Photonic Crystal Fibres (PCFs), Germanium Flat Fibres (Ge-FF) and co-doped Germanium Boron Flat Fibres (GeB-FF), they nevertheless continue to provide sufficient sensitivity for radiotherapy applications.



**ISRP 2021**  
**International Symposium on Radiation Physics**  
**Kuala Lumpur – Malaysia**  
**6 – 10 December 2021**

**A060 - Activity Concentration and Radiological Impact Assessment of  $^{226}\text{Ra}$ ,  $^{232}\text{Th}$  and  $^{40}\text{K}$  in Beach Sands and Sediments Samples Around Badagry Coastal Areas of Lagos**

Michael Olatunji<sup>1</sup>, Oluwaseun Ifetayo<sup>1</sup>, Mayeen Khandaker<sup>2</sup>, Akinmoladun Boluwatife<sup>1</sup>, Christopher Olowookere<sup>1</sup>

<sup>1</sup>Department of Physics, University of Medical Sciences, Ondo, Nigeria

<sup>2</sup>Centre for Biomedical Physics, Sunway University, Selangor, Malaysia

Corresponding author: olakunlemike@yahoo.com

Beach sands and sediments from seashore are homes to the minerals which may be enriched with radionuclides such as  $^{238}\text{U}$  and  $^{232}\text{Th}$  and their decay series. The presence of such natural radioactivity in these environmental samples may serve as an important pathway to human exposure, particularly the tourists who spend their holidays in the beach and those working or living in the coastal areas. In the present study, the levels of natural radioactivity in beach sands and sediments samples collected from coastlines around Badagry area of Lagos were investigated by gamma-ray spectrometry using NaI(Tl) detector. The mean activity concentration in  $\text{Bqkg}^{-1}$  for  $^{40}\text{K}$ ,  $^{226}\text{Ra}$  and  $^{232}\text{Th}$  radionuclides was estimated to be in the range of  $114.9 \pm 79.60$  to  $161.3 \pm 6.10$ ,  $43.02 \pm 8.52$  to  $44.52 \pm 9.42$  and  $7.01 \pm 5.77$  to  $12.85 \pm 16.26$ , respectively for the sediment samples, and from  $18.68 \pm 22.14$  to  $95.53 \pm 57.03$ ,  $32.31 \pm 23.44$  to  $51.86 \pm 27.18$  and BDL to  $8.50 \pm 1.46$ , respectively for the beach sand samples. The estimated radiological indices such as radium equivalent activity, absorbed dose rate, annual outdoor effective dose equivalent, external and internal hazard indices, gamma and alpha activity indices and annual gonadal dose equivalent showed that the values fall within the international standard recommendations. This implies that sediments and beach sand from Badagry coastal areas of Lagos are safe and could be used for construction purposes without posing any undue radiological health concern to the general public.



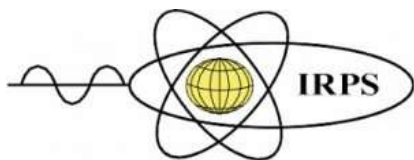
**ISRP 2021**  
**International Symposium on Radiation Physics**  
**Kuala Lumpur – Malaysia**  
**6 – 10 December 2021**

**A062 - New methodology for solving nanostructures within dilute and amorphous systems: a trend study of Nickel-doped borate glass by the X-ray Extended Range Technique (XERT) and eFEFFIT fitting software for XAFS.**

Geoffrey P. Cousland, Redi Pringak, C T Chantler

School of Physics, University of Melbourne, 3010, Victoria, Australia

X-ray Absorption Spectroscopy (XAS) is a powerful tool for investigating nanostructure, including the local order and disordered of amorphous materials. X-ray extended range technique (XERT) has yielded some of the highest accuracy XAFS results available. Our investigation of nickel-doped borate glass  $x\text{Li}_2\text{O} \cdot (1-x-y)\text{B}_2\text{O}_3 \cdot y\text{NiO}$  where  $x = 0.33$  and  $y = 0.05$  is the first study for a dilute disordered system and a critical test of XERT methodology. A clear XAFS was obtained across for k-range  $2.5 < k < 13.0 \text{ \AA}^{-1}$  with the modest flux provided by a bending magnet. Given the accuracy of our experiment results the critical question is how to best exploit this for investigation of our structure. We have developed a new fitting approach using eFEFFIT and will demonstrate a new methodology for solving small dilute and amorphous structures. We see that contributions due to the second NiO shell are clearly isolated. Borate and lithium motifs are progressively added to the structural network in a trend study. We then develop four candidate structures. The best fit for our most promising structure has  $\chi^2_r = 1.18$ , which agrees with constraints derived from the chemical properties for borate glasses. I conclude by discussing the effectiveness of our new approach for fitting and consider future improvements to this methodology.



**A063 - Radon concentration in groundwater sources for public consumption in Bosso community, north central Nigeria and consequent annual effective dose estimation**

Matthew Kolo<sup>1</sup>, Oyeleke Olarinoye<sup>1</sup>, Matthew Isinkaye<sup>2</sup>, Mayeen Khandaker<sup>3</sup>, Anayo Ugwuanyi<sup>1</sup>, Paul Onuche<sup>1</sup>, Opeyemi Falade<sup>1</sup>, Nwachukwu Chibueze<sup>1</sup>

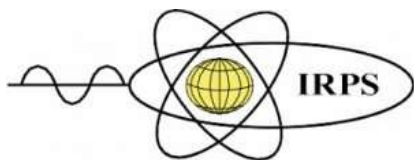
<sup>1</sup>Department of Physics, Federal University of Technology, Minna, Niger state, Nigeria

<sup>2</sup>Health and Environmental Physics Research Group, Department of Physics, Ekiti State University, Ado Ekiti, Nigeria

<sup>3</sup>Centre for Biomedical Physics, School of Healthcare and Medical Sciences, Sunway University, 47500, Bandar Sunway, Selangor, Malaysia

Corresponding author: matthewkolo@futminna.edu.ng

Radon concentrations in portable water from hand-dug wells and bore-holes in Bosso community, Minna, north central Nigeria were determined using RAD7 radon detector with RAD-H<sub>2</sub>O accessories. Annual effective doses from inhalation and ingestion of the water samples were also computed. Radon concentration in hand-dug well water varied from  $1.5 \pm 0.6$  to  $27.9 \pm 2.5$  BqL<sup>-1</sup> with average value of  $10.04 \pm 1.7$  BqL<sup>-1</sup>. Similarly, radon concentration in bore-hole water investigated ranged between  $2.8 \pm 1.1$  and  $42.5 \pm 3.1$  BqL<sup>-1</sup> with mean of  $19.53 \pm 2.1$  BqL<sup>-1</sup>. Although radon concentrations in 36% of water samples from hand-dug wells and 70% from bore-holes were higher than the USEPA maximum contaminant level of 11.1 BqL<sup>-1</sup>, the values were all below the safety limit of 100 BqL<sup>-1</sup> set by the European Union and World Health Organization. Mean annual committed effective dose due to consumption of hand-dug well water for the age groups considered were  $10.04 \mu\text{Sv y}^{-1}$  (3 months old),  $13.05 \mu\text{Sv y}^{-1}$  (1 year old),  $15.05 \mu\text{Sv y}^{-1}$  (5 years old),  $17.56 \mu\text{Sv y}^{-1}$  (10 years old),  $30.11 \mu\text{Sv y}^{-1}$  (15 years old) and  $36.63 \mu\text{Sv y}^{-1}$  (adult). Likewise, average annual committed effective dose from bore-hole water for all the age groups were 19.53, 25.39, 29.30, 34.18, 58.59 and 71.28  $\mu\text{Sv y}^{-1}$  in sequence. Although the results showed dose increase with increase in age, the values are appreciably lower than the precautionary limit of 1 mSv y<sup>-1</sup> documented in the United Nations Scientific Committee on the Effect of Atomic Radiation and World Health Organization reports. About 93.5% of the whole body dose comes from inhalation of waterborne radon, while the dose received by the walls of the stomach via ingestion pathway accounts for about 6%. Computed mean ELCR for hand-dug well and bore-hole water samples are  $0.09 \times 10^{-3}$  and  $0.18 \times 10^{-3}$  respectively, which are below the world average value of  $0.29 \times 10^{-3}$



**ISRP 2021**  
**International Symposium on Radiation Physics**  
**Kuala Lumpur – Malaysia**  
**6 – 10 December 2021**

#### **A064 - Review of borosilicate glass for radiation dosimetry**

Ying Ying Cheah<sup>1,2,3</sup>, Ming Tsuey Chew<sup>2</sup>, Ngie Min Ung<sup>4</sup>, Suhairul Hashim<sup>5</sup>, David Andrew Bradley<sup>2,6</sup>

<sup>1</sup>Department of Medical Sciences, School of Medical and Life Sciences, Sunway University, Malaysia

<sup>2</sup>Research Centre for Applied Physics and Radiation Technologies, Sunway University, Malaysia

<sup>3</sup>Centre for Stereotactic Radiosurgery, Asian Alliance Radiation & Oncology, Singapore

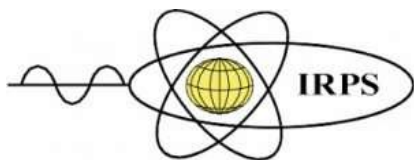
<sup>4</sup>Clinical Oncology Unit, Faculty of Medicine, University of Malaya, Malaysia

<sup>5</sup>Centre for Sustainable Nanomaterials (CSNano), Ibnu Sina Institute for Scientific and Industrial Research (ISI-SIR), Universiti Teknologi Malaysia, Malaysia

<sup>6</sup>Department of Physics, University of Surrey, United Kingdom

Corresponding author: mtchew@sunway.edu.my

Ionising radiation induces biological effects wherein the degree of damage depends on the type of radiations and dosage used. Ionising radiations are used in various sectors, such as, non-destructive testing, gauging in industry, in agriculture, and in therapeutic and diagnostic imaging. Radiation dosimetry is vital to ensure safe use of ionising radiation in all sectors, not least in accurate dosage for therapeutic purposes to ensure the best possible outcome. Passive dosimeters made from crystalline media and glass are commonly used for medical in-vivo dosimetry, personal dosimetry, and environmental dosimetry due in part to their relative cost effectiveness compared to active dosimeters. Among the glass-based radiation dosimeters, commercially available forms include silver-activated phosphate glass (Chiyoda Techno Corporation and Asahi Techno Glass Co.) which is widely used for medical, personal, environmental, and high dose dosimetry; silicate glass beads (TrueInvivo) for clinical in-vivo dosimetry and optical fibres (Lumisyns Sdn Bhd) for real-time radiotherapy dosimetry. Recent research trends have shifted from silicate glass to borate glass and borosilicate glass as potential radiation dosimeters. Borosilicate glass are found to be more resistant towards radiation damage, chemical and thermal changes. Non-doped borosilicate glass that is commercially available such as used in kitchenware, laboratory glassware, window glass, etc. are being investigated for passive dosimetry and retrospective radiation dosimetry. They exhibit good sensitivity for dosimetric applications. Some studies investigate modified borosilicate glass using rare earth and alkaline materials as dopant and it has been found that this improves dosimetric performance. Such borosilicate glass forms enjoy radiation sensitivity, dose linearity and a simple thermoluminescence glow curve.



**ISRP 2021**  
**International Symposium on Radiation Physics**  
**Kuala Lumpur – Malaysia**  
**6 – 10 December 2021**

**A066 - Review of the effect of reduced background radiation on living organisms**

Ming Tsuey Chew<sup>1</sup>, Bleddyn Jones<sup>2</sup>, Andrew Nisbet<sup>3</sup>, Mark Hill<sup>2</sup>, David A Bradley<sup>1,4</sup>

<sup>1</sup>Centre for Applied Physics and Radiation Technologies, Sunway University, Malaysia

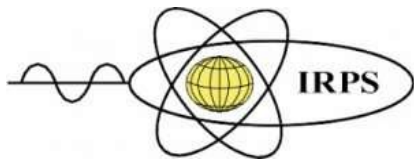
<sup>2</sup>CRUK/MRC Gray Institute for Radiation Oncology & Biology, University of Oxford, United Kingdom

<sup>3</sup>Department of Medical Physics and Biomedical Engineering, University College London, United Kingdom

<sup>4</sup>Department of Physics, University of Surrey, United Kingdom.

Corresponding author: mtchew@sunway.edu.my

It is well understood that all life is subject to continuous low levels of ionizing radiation, most prominently from the natural background of the biosphere, differing appreciably in particular situations across the surface of the globe. Added to this, albeit in much more isolated situations inclusive of particular workplaces and different environments, are exposures from ionizing radiations traced to human activities. Accordingly, studies of the effects of background-level radiations are subject to complex multifactorial influences. The present study precludes discussion of medium- and high-level radiation risks, being generally well established at doses of 100 mSv and more, based on studies (epidemiological and otherwise) that include groups exposed to different doses from nuclear device testing, nuclear fuel cycle incidents and accidents, medical irradiations, naturally occurring sources (such as radon exposures in mining situations), and workplace situations. The radiation safety regulations and limits for lower levels of exposure are based on extrapolation from more elevated doses and dose rates, embodied in the linear no-threshold (LNT) model. The LNT model predicts the relationship between biological effects and radiation dose to be linear, all doses in excess of background carrying risk. Substantiated for high dose exposures, the validity of the model is unknown for low doses, the elucidation of possible beneficial hormetic and adaptive effects remaining a challenge. Herein, an overview of the effect on organisms of reduced low-levels of radiations is presented using available evidence and discussion of theoretical possibilities.



**A067 - Gamma Ray Attenuation Studies of Brass Alloy as Tissue Equivalent Material for Radiotherapy Applications**

Sakinah Buang<sup>1</sup>, Nik Noor Ashikin Nik Ab Razak<sup>1</sup>, Mohd Zahri Abdul Aziz<sup>2</sup>, Nurul Hashikin Aziz<sup>1</sup>, Nor Zakiah Binti Yahaya<sup>3</sup>, Noriza Isa<sup>4</sup>, Ahmad Bazlie Abdul Kadir<sup>5</sup>

<sup>1</sup> School of Physics, Universiti Sains Malaysia, Malaysia

<sup>2</sup> Advanced Medical Dental Institute (IPPT), Malaysia

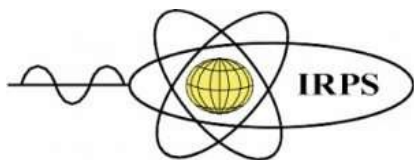
<sup>3</sup> School of Distance Learning, Universiti Sains Malaysia, Malaysia

<sup>4</sup> Makmal Fizik Perubatan, Agensi Nuklear Malaysia, Malaysia

<sup>5</sup> Makmal Dosimetri Peribadi OSL&TLD, Agensi Nuklear Malaysia, Malaysia

Corresponding author: sakinahbuang@student.usm.my , nnashikin@usm.my

Tissue equivalent material studies have been one of the high interests in radiotherapy clinical studies. This is due to the ability to represent a variety of human tissues and organs. The brass mesh has been applied clinically as a bolus, beam spoilers & compensators, contouring for skin cancer, and post-mastectomy radiotherapy (PMRT). The need for a superior bolus material has become more conspicuous with the increasing demand. However, sufficient data related to brass, especially the dosimetry quantities remain unreciprocated. This work sets out to measure attenuation coefficient value of brass alloy acquired from experimental, XCOM table, and simulation methodology. Ludlum with gamma-ray scintillator and Nanodot dosimetry system was used to run the experiment set-up. Later, the data from the experiment set-up will be applied to GEANT 4, a simulation software to run a thorough test and analysis of brass. The measured attenuation coefficient value of brass obtained by experimental was found to be in good agreement with the provided value from XCOM for breast tissue, with modest margins of error. Simulation results provided by GEANT4 were expected to validate the attenuation coefficient model. For postmastectomy chest wall radiation therapy, brass mesh is an effective alternative to tissue-equivalent bolus. Therefore, it is crucial to collect as much experimental data with verification by simulation method to better understand brass's characteristics as tissue-equivalent material and its wide potential in radiotherapy applications.



**ISRP 2021**  
**International Symposium on Radiation Physics**  
**Kuala Lumpur – Malaysia**  
**6 – 10 December 2021**

**A069 - Analysis of radiation dose distribution in paediatric exams**

Paula Vosiak<sup>1</sup>, Hugo Schelin<sup>1</sup>, Akemi Yagui<sup>1</sup>, Luiza Costa<sup>1</sup>, Rosiane Mello<sup>1</sup>, Valeriy Denyak<sup>2,3</sup>, Sergei Paschuk<sup>3</sup>, Ana Paula Bunick<sup>3</sup>, Helen Khoury<sup>4</sup>, Adriane Schelin<sup>5</sup>

<sup>1</sup>Pelé Pequeno Principe Research Institute, Pequeno Principe Faculty, Brazil

<sup>2</sup>National Science Center ‘Kharkov Institute of Physics and Technology’, Ukraine

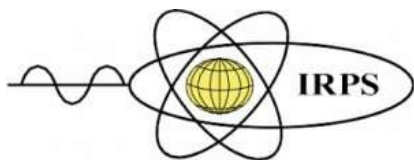
<sup>3</sup>Federal University of Technology - Paraná, Brazil

<sup>4</sup>Federal University of Pernambuco, Brazil

<sup>5</sup>University of Brasilia, Brazil

Corresponding author: paula.vosiak@gmail.com

The purpose of this study is to analyze the distribution of doses in paediatric patients who undergo conventional radiological examinations of the chest, skull, pelvis, abdomen, and sinuses. The level of doses in paediatric patients in situations of medical exposure is an important topic of research due to the need to reduce the risks of future biological effects. In contrast to adults, paediatric patients have specific features that lead to greater radiosensitivity of tissues and organs, such as high anatomical and physiological development. In this work, we estimate the doses through the output of the X-ray tube, with data from radiographic examination techniques. 743 exams were collected, being 1394 projections. Data analysis showed a heterogeneous population within the same age group, resulting in the use of different radiographic techniques in the exams. Our projections show higher doses than expected for the age groups and classification by weight as compared to international standards. In particular, we found that the most divergent factor was the product of current by exposure time, especially for the skull exam, being the average dose (3rd quartile) for the age group 1-5 years equal to  $1.09 \pm 0.35$  mGy for anteroposterior projection. The dose reference levels for this projection are in the range from 0.5 to 0.7 mGy. In the routine of the service, the grid was used in all exams. To obtain lower dose values while maintaining the same image quality, more optimization studies are required, with the creation of a local dose reference level.



**ISRP 2021**  
**International Symposium on Radiation Physics**  
**Kuala Lumpur – Malaysia**  
**6 – 10 December 2021**

**A070 - Fluoroscopy time influence on DAP values of interventional cardiac procedures**

Akemi Yagui<sup>1</sup>, Hugo Schelin<sup>1</sup>, Paula Vosiak<sup>1</sup>, Luiza Costa<sup>1</sup>, Rosiane Mello<sup>1</sup>, Valeriy Denyak<sup>2,3</sup>, Sergei Paschuk<sup>3</sup>, Danielle Filipov<sup>3</sup>, Helen Khoury<sup>4</sup>

<sup>1</sup>Pelé Pequeno Principe Research Institute, Pequeno Principe Faculty, Brazil

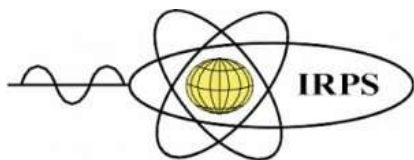
<sup>2</sup>National Science Center ‘Kharkov Institute of Physics and Technology’, Ukraine

<sup>3</sup>Federal University of Technology - Paraná, Brazil

<sup>4</sup>Federal University of Pernambuco, Brazil

Corresponding author: kemiyagui@gmail.com

In pediatrics, the cardiac catheterization procedures are performed to diagnose or treat congenital heart disease and their main advantage is that they are less invasive when compared to surgery. However, such procedures provide high doses of radiation to patients. The radiological protection in this type of radiology is essential, because children are more sensitive to radiation. The objective of this study is to estimate the dose-area product (DAP) and fluoroscopy time (FT) in pediatric patients of different age and weight groups in cardiac catheterization procedures in a pediatric hospital. The data were obtained through the report provided by the equipment, which has a dose meter attached to the output of the X-ray tube and provides the DAP values, FT, in addition to sex, age and weight of the evaluated patients. Weight or age values did not significantly influence DAP rate values. The mean age and weight of patients undergoing cardiac catheterization procedures was higher when compared to similar studies. The mean DAP and FT values estimated in the age groups were as follows:  $0.91 \pm 0.09$  Gy.cm<sup>2</sup> and 18.5 min for <1 year;  $2.3 \pm 0.2$  Gy.cm<sup>2</sup> and 18.2 min for 1–5 years;  $2.4 \pm 0.4$  Gy.cm<sup>2</sup> and 16.0 min for 5–10 years; and  $5.6 \pm 2.4$  Gy.cm<sup>2</sup> and 18.5 min for 10–15 years, respectively. The correlation between weight and age is linearly dependent, so the implementation of protocols according to the patient's age and weight range could result in DAP optimization. The DAP values were lower than those reported in other studies, and the FT values obtained were higher than those reported in similar studies.



**A072 - Monte Carlo simulation of HDR Brachytherapy dosimetric parameters in a different medium**

Nor Shazleen Ab Shukor<sup>1</sup>, Marianie Musarudin<sup>1</sup>, Reduan Abdullah<sup>2</sup>, Mohd Zahri Abd Aziz<sup>3</sup>

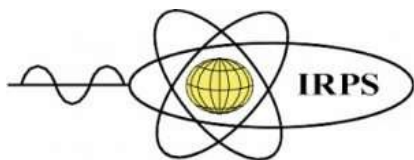
<sup>1</sup>School of Health Sciences, Universiti Sains Malaysia, Health Campus, 16150 Kubang Kerian, Kelantan, Malaysia,

<sup>2</sup>Hospital Universiti Sains Malaysia, 16150 Kubang Kerian, Kelantan, Malaysia,

<sup>3</sup>Advance Medical and Dental Institute, Universiti Sains Malaysia, Kepala Batas, Penang, Malaysia

Corresponding author: marianie@usm.my

The TG-43 dose calculation of TPS in brachytherapy (BT) is made with the assumption of homogeneous water as a reference medium. It does not account for the effects of other materials that may present in the patient's body. The present study investigates the influence of different materials on the dosimetric parameters of <sup>192</sup>Ir microSelectron HDR source using MCNP5 code. As a preliminary, verification of MCNP5 code with the published data and the relative differences were employed. Homogeneous phantoms filled with lung, bone, air, and common steels materials for a hip prosthesis, i.e., titanium alloy (Ti), stainless steel, and cobalt-chromium-molybdenum (Co-Cr-Mo), are modeled in this study. Using MCNP5 code, we construct a database for <sup>192</sup>Ir HDR-BT in a standard water phantom and other materials as described above. Then, the data obtained from the simulation was used to calculate the radial dose function  $g(r)$ , and anisotropy function  $F(r, \theta)$ . From the finding,  $g(r)$  for bone, lung, and air are water equivalent at a radial distance,  $r < 6$  cm. At  $r > 6$  cm, the TPS overestimate from 7.7%- 35.9 % for bone, and underestimate the lung dose (2.94%-33.0%) and air (2.81%-46.4%). For steels, a large relative difference of up to 62.2% is calculated due to the higher density than the water. Meanwhile, a greater relative difference for  $F(r, \theta)$  is observed at the angle parallel to the Nucletron <sup>192</sup>Ir microSelectron HDR source. An increase in the density of the medium leads to inconsistencies in the flatness of the  $F(r, \theta)$ . Great attention should be given to the region greater than 6 cm from the source. The presence of any material other than water at the respective distance could lead to significant underestimation or overestimation of the dosimetric parameters.



**ISRP 2021**  
**International Symposium on Radiation Physics**  
**Kuala Lumpur – Malaysia**  
**6 – 10 December 2021**

**A077 - Determination of  $^{40}\text{K}$  and  $^{238}\text{U}$  radionuclides concentration in some granite rocks by gamma spectroscopy and Energy Dispersive X-ray analysis.**

M.I.Sayed<sup>1,2,\*</sup>, M.Elsafi<sup>3</sup>, M.A.El-Nahal<sup>3,\*</sup>, Mayeen Uddin Khandaker<sup>4</sup>

<sup>1</sup>Department of Physics, Faculty of Science, Isra University, Amman – Jordan

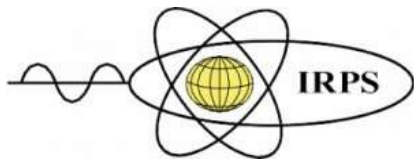
<sup>2</sup>Department of Nuclear Medicine Research, Institute for Research and Medical Consultations (IRMC), Imam Abdulrahman bin Faisal University (IAU), PO Box 1982, Dammam, 31441, Saudi Arabia

<sup>3</sup>Physics Department, Faculty of Science, Alexandria University, 21511 Alexandria, Egypt.

<sup>4</sup>Center for Applied Physics and Radiation Technologies, School of Engineering and Technology, Sunway University, 47500 Bandar Sunway, Selangor Darul Ehsan, Malaysia

Corresponding author: Igsr.nahalmoh@alexu.edu.eg

The  $^{40}\text{K}$  and  $^{238}\text{U}$  content are important naturally occurring radionuclides so that accurate determination of  $^{40}\text{K}$  and  $^{238}\text{U}$  is very essential in order to investigate the radiological hazard indices of the granite rocks. The gamma spectroscopy is a direct nondestructive method to determine the radionuclides concentration, but this method suffers from the interference of gamma lines and using secular equilibrium principle in case of  $^{238}\text{U}$ . With respect to  $^{40}\text{K}$  gamma spectroscopy affected by the interference with a background which leads to reduction in minimum detectable activity. The energy dispersive X-ray analytical technique is a reliable technique with no interference problems or background effect, but it is indirect method and the concentration of isotopes will be calculated and deduced. In the present study, the results of  $^{238}\text{U}$  and  $^{40}\text{K}$  are measured by well calibrated gamma spectroscopy and energy dispersive X-ray techniques are compared and show good agreement between the methods but with higher uncertainty in gamma spectroscopy results. The detection limits of methods are accurately determined.



**A079 - The impact of various instances of solar wind speed on the fluctuations of cosmic radiation in the solar minimum (23, 24, and 25)**

A Sh M Elshoukrofy<sup>1</sup>, N M Wateed<sup>1</sup>, H A Motaweh<sup>1,\*</sup>, M. Y. Hanfi<sup>2,3</sup>, M.I. Sayyed<sup>4,5</sup>, Mayeen Uddin Khandaker<sup>6</sup>, A A Darwish<sup>7</sup>

<sup>1</sup> Faculty of Science, Damanhur University, Damanhur, El Behera, Egypt

<sup>2</sup>Ural Federal University, Mira St., 19, 62002, Yekaterinburg, Russia

<sup>3</sup>Nuclear Materials Authority, El Maadi, Cairo, Egypt

<sup>4</sup>Department of Physics, Faculty of Science, Isra University, Amman 11622, Jordan

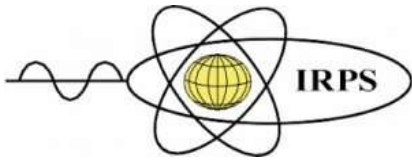
<sup>5</sup>Department of Nuclear Medicine Research, Institute for Research and Medical Consultations, Imam Abdulrahman bin Faisal University, Dammam 31441, Saudi Arabia

<sup>6</sup>Center for Applied Physics and Radiation Technologies, School of Engineering and Technology, Sunway University, 47500 Bandar Sunway, Selangor Darul Ehsan, Malaysia

<sup>7</sup> Faculty of Science, Alexandria University, Alexandria, Egypt

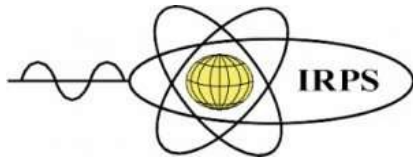
Corresponding auhtor: nohawateed.nw@gmail.com

The importance of solar wind study is determined by its key role in space weather. It has long been known that solar wind is not permanent but consists of separate plasma streams with different hydrodynamic and magnetic characteristics. The difference between the types of flows is conditional, not absolute, therefore, there is still no generally accepted nomenclature, which turns out to be different for different authors. Both the number of these types and the approach to classification are different. In this study, we had analyzed the data of solar wind speed and cosmic ray intensity from 1998 until 2020 of three solar cycles (23, 24, and 25) for four stations Apatity, Fort Smith, Hermanus, and Sanae obtained respectively from the National oceanic and atmospheric organization, and neutron monitors. Solar wind (SW) is divided into three main types - slow and fast wind, as well as disturbed streams. Slow SW has characteristic speeds of 300–500 km / s (this is about 1000 times higher than the speed of sound in air and by the same amount less than the speed of light in vacuum) and is emitted mainly from the equatorial regions of the Sun with a closed and semi-closed geometry of the magnetic field in the form coronal loops at the bottom and helmet-like structures (streamers) at high altitudes, respectively. Fast SW is emitted at speeds of 700–800 km / s from regions of the Sun with an "open" magnetic field geometry - from polar coronal holes, as well as coronal holes at low latitudes. The disturbed SW flows. They are observed not constantly, but sporadically - in total, less than half of the total observation time. These include coronal mass ejections (CMEs are large-scale plasma clouds with a magnetic field), as well as disturbances in front of them and front of fast SW streams from coronal holes. Such disturbances and the associated magnetic structures, reaching the Earth (as well as other planets), can lead to global disturbances of the magnetic field of our planet, causing magnetic storms and substorms. It is found that the solar wind is permanent during the whole period of study and the number of occurrences of the low



**ISRP 2021**  
**International Symposium on Radiation Physics**  
**Kuala Lumpur – Malaysia**  
**6 – 10 December 2021**

SW is more frequent than the rest of the species. The amplitude and phase of daily fluctuation on selected stations have been examined in all scenarios of solar wind speed.



**ISRP 2021**  
**International Symposium on Radiation Physics**  
**Kuala Lumpur – Malaysia**  
**6 – 10 December 2021**

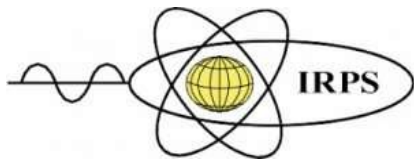
**A081 - Simulation and computational improvements of the mutual optical intensity function in two dimensions**

Jake J. Rogers<sup>1</sup>, Chanh Q. Tran<sup>1</sup>, Paul Di Pasquale<sup>1</sup>, Tony Kirk<sup>1</sup>, Hong Minh Dao<sup>1</sup>

<sup>1</sup>Department of Chemistry and Physics, La Trobe University, Australia

Corresponding author: JakeJohnRogers@Gmail.com

Understanding the coherence properties of optical wave fields is critically important in most phase based scientific applications. Full description of the coherence properties in the spatial domain of a wave field is described by the four dimensional mutual optical intensity function which makes it possible to analytically propagate the wave field in three dimensional space. We present a simulation study of how to best visualise the information embedded in the four dimensional mutual optical intensity function. The results shed light on the graphical connection between the three dimensional wave field and its four dimensional mutual optical intensity function.



**A084 - Exploring of Monte Carlo Simulation from Case Study of Particle Transport in Gamma Knife Machine**

Freddy Haryanto<sup>1</sup>, Junios<sup>2</sup>

<sup>1</sup>Department of Physics, Fakultas Matematika dan Ilmu Pengetahuan Alam,  
Institut Teknologi Bandung, Indonesia

<sup>2</sup>Department of Nursing, Institut Kesehatan Prima Nusantara Bukittinggi, Indonesia

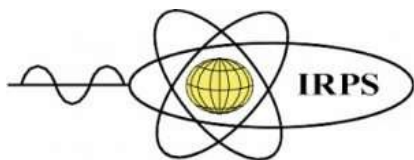
Corresponding author: [freddy@fi.itb.ac.id](mailto:freddy@fi.itb.ac.id)

Monte Carlo simulation is the golden technique to investigate particle transport in a medium. This study explores the advantages of Monte Carlo simulation for understanding the characterizations of the beam generated by the Gamma Knife machine.

For this study, the EGSnrc code is implemented to simulate the particle transport in Gamma Knife Perfexion. To know the beams characterization, Gamma Knife Perfexion is divided into three parts. The first part is to investigate the quality of beams that are emitted from encapsulated Co-60. The energy spectrum is observed in this part. The second part is focused on the forming of beams using three different collimators. From the second part, the comparison of beam profiles is taken into account. Then the last part is to learn the distributed dose in Phantom. The measured dose distribution is also made using Gafchromic EBT3 film.

The energy spectrum from encapsulated Co-60 has more low energy than the energy spectrum from the encapsulated source. It is due to the material from the capsule having reduced the energy of Co-60. From the second part, fluence and energy fluence depends on the size of the collimator. The full width of half maximum of fluence is 1.87 mm for collimator size of 4 mm, 3.80 mm for 8 mm, and 7.80 mm for 16 mm. The decreasing of energy fluence of about 18.5 keV is found for collimator size of 16 mm. From the last part, the comparison between the measured and simulated dose distribution has a good agreement. The gamma passing rates for all collimator sizes are more than 97%.

This study concludes that the Monte Carlo simulation is a comprehensive tool to analyze the beam characterization from the Gamma Knife machine. The Monte Carlo simulation helps to understand each aspect of physical phenomena which occurred in the machine.



**ISRP 2021**  
**International Symposium on Radiation Physics**  
**Kuala Lumpur – Malaysia**  
**6 – 10 December 2021**

### **A085 - Miniature $4\pi\beta$ (LS)- $\gamma$ (LaBr<sub>3</sub>) coincidence system at KRISS**

M.J. Han<sup>1,2</sup>, S.H. Hwang<sup>1,2\*</sup>, Agung Agusbudiman<sup>1,2,3</sup>, D.H. Heo<sup>1</sup>, J.M. Lee<sup>1,2</sup>, K.B. Lee<sup>1,2</sup>

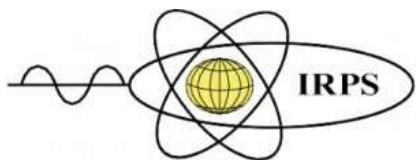
<sup>1</sup>Radioactivity Metrology Team, Korea Research Institute of Standards and Science, Republic of Korea

<sup>2</sup>Science of Measurement, University of Science and Technology, Republic of Korea

<sup>3</sup>Radiation Metrology Division, National Nuclear Energy Agency, Indonesia

Corresponding author: shhwang@kriss.re.kr

A  $4\pi\beta$ - $\gamma$  coincidence counting system has been developed for an absolute measurement of radioactivity nuclei, when nuclei decays to beta and gamma rays. KRISS has developed the  $4\pi\beta$ - $\gamma$  coincidence counting system with a pressurized proportional counter (PPC) and a liquid scintillation counter (LS) in  $4\pi\beta$  detector coupled with two 3-inch NaI(Tl) gamma detectors. The existing systems were participated in the several key comparisons organized by BIPM and APMP. However, the NaI(Tl) detectors show a poor resolution and a long decay time and it could not be operated in the high counting rate and multi-gamma emission case. We are developing new miniature  $4\pi\beta$ - $\gamma$  coincidence counting system with a LaBr<sub>3</sub> gamma detector and a Flash-ADC(FADC). The miniature system has been improved with an ultra-fast digital data taking instead of the analog signal processing. The <sup>60</sup>Co solution spiked in the Hionic Flour (HF) liquid scintillator was used. The LS cocktail was mounted in the middle of the detection system. The beta efficiency is estimated to be 87 % with liquid scintillation counter. The difference of disintegration rate is consistent with the reference ion chamber at KRISS.



**ISRP 2021**  
**International Symposium on Radiation Physics**  
**Kuala Lumpur – Malaysia**  
**6 – 10 December 2021**

**A086 - Synthesis physical and photoluminescence investigation of Eu<sup>3+</sup>-doped gadolinium borate scintillating glass**

B. Damdee<sup>1</sup>, K. Kirdsiri<sup>1,2</sup>, H.J. Kim<sup>3</sup>, K. YAMANOI<sup>4</sup>, J. Kaewkhao<sup>1,2,\*</sup>

<sup>1</sup>Physics program, Faculty of Science and Technology, Nakhon Pathom Rajabhat University, Nakhon Pathom, 73000, Thailand

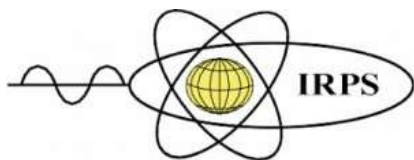
<sup>2</sup>Center of Excellence in Glass Technology and Materials Science (CEGM), Nakhon Pathom Rajabhat University, Nakhon Pathom, 73000, Thailand

<sup>3</sup>Department of Physics, Kyungpook National University, Deagu 702-701, Republic of Korea

<sup>4</sup>Institute of Laser Engineering, Osaka University, 2-6 Yamadaoka, Suita, Osaka 565-0871, Japan

Corresponding author: thangmtmt10@gmail.com, \*Email: mink110@hotmail.com

The intense reddish orange emitting Eu<sup>3+</sup>-doped gadolinium borate glasses with compositions of 25Gd<sub>2</sub>O<sub>3</sub>-(75-x) B<sub>2</sub>O<sub>3</sub>-xEu<sub>2</sub>O<sub>3</sub>; (x= 0.1, 0.3, 0.5, 1.0, 3.0, 5.0, 7.0 and 9.0 mol%) (GdBu) have been synthesized by melt-quenching method at 1400 °C for 3 h. Glass samples were prepared to study physical, photoluminescence, scintillation and lasing potential properties. Glasses absorb photons in ultraviolet, visible light and near infrared regions and the energy transfer phenomena from Gd<sup>3+</sup> → Eu<sup>3+</sup> in these glasses were observed. Ultraviolet (UV) and X-ray excitation have been indicated performance was found at 275 nm and 394 nm excitations. Luminescent properties can generate the strong red emission with 614 nm (<sup>5</sup>D<sub>0</sub> → <sup>7</sup>F<sub>2</sub>) with energy transfer from Gd<sup>3+</sup> to Eu<sup>3+</sup> content. The optimum concentration of Eu<sup>3+</sup> ion in this glass is 7.0 mol% as it results in maximum emission intensity. The radiative properties including transition probability (A), branching ratio (β<sub>R</sub>), stimulated emission cross-section (σ<sub>e</sub>) and decay time (τ<sub>R</sub>) for different excited states have been evaluated by using Judd-Ofelt parameters determined from the emission spectra. The stimulated CIE chromaticity coordinates were also calculated. The decay time of the <sup>5</sup>D<sub>0</sub> level decreases from 1.824 ms to 1.585 ms when concentration increased from 0.1 to 9.0 mol %. From RL measurement, glass samples perform the integral scintillation efficiency as 18% when compared with BGO.



**ISRP 2021**  
**International Symposium on Radiation Physics**  
**Kuala Lumpur – Malaysia**  
**6 – 10 December 2021**

**A088 - Radiation hazard assessments of natural radioactivity in cosmetic products**

N. Z. H. Abu Hanifah<sup>1</sup>, S. Hashim<sup>1,2</sup>, Halmat J. Hassan<sup>1,3</sup>, M.R. Fahmi<sup>4</sup>, M.S.M. Sanusi<sup>1</sup>

<sup>1</sup>Department of Physics Faculty of Science, Universiti Teknologi Malaysia, Malaysia

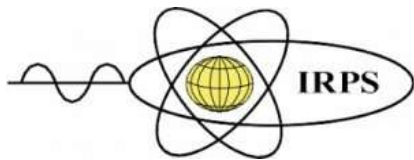
<sup>2</sup>Ibnu Sina Institute for Scientific and Industrial Research (ISISIR), Universiti Teknologi Malaysia, Malaysia

<sup>3</sup>Department of Physics, College of Education, University of Sulaimani, Kurdistan-Iraq

<sup>4</sup>School of Physics, Universiti Sains Malaysia, Malaysia

Corresponding author: noorzatihani@graduate.utm.my

Natural sources such as clays, plant extracts, and raw materials containing naturally occurring radioactive material have been used as ingredients for medicinal and cosmetic purposes since ancient times. Nowadays, a variety of commercially available cosmetics products contain radioactive substances that pose unknown radiation risks to the consumer. In this study, 12 samples of cosmetic products containing NORMs were used to conduct dose assessments on members of the public for various usage scenarios in order to evaluate the external exposure dose. Gamma-ray spectroscopy was utilized to determine the activity concentrations of  $^{238}\text{U}$ ,  $^{232}\text{Th}$ , and  $^{40}\text{K}$  in the sample. Gamma-ray spectroscopy was used to measure the activity concentration of  $^{238}\text{U}$ ,  $^{232}\text{Th}$ , and  $^{40}\text{K}$  in the sample. Meanwhile, doses to skin and other organs from these cosmetic products were modelled using Geant4 Monte Carlo simulations and the MIRD5 mathematical phantom, incorporating Dose Conversion Factors (DCFs). The results revealed that the activity concentration is lower than the reference provided by international regulation. Furthermore, the effective doses in the skin estimated in this study are significantly lower than the International Commission on Radiological Protection (ICRP) reference limit of 50 mSv per year for members of the general public. As a result, it is safe to conclude that the dose from these products poses no radiological risk to the user. The addition of NORMs in cosmetic products, on the other hand, should be done with caution because higher concentrations can raise the dose.



**A089 - Variability of estimated organ dose based on different Monte Carlo radiation transport codes for NORM-added consumer product radiation exposures**

Mohamad Syazwan, Mohd Sanusi<sup>1</sup>, Suhairul, Hashim<sup>1</sup>, Muhammad Fahmi Rizal, Abdul Hadi<sup>2</sup>, Halmat Jalal, Hassan<sup>3</sup>, Rafael García, Tenorio<sup>4</sup>, Rozman, Mohd Tahar<sup>5</sup>, Noor Fitriah, Bakri<sup>5</sup>

<sup>1</sup>Department of Physics, Universiti Teknologi Malaysia, Malaysia

<sup>2</sup>School of Physics, Universiti Sains Malaysia, Malaysia

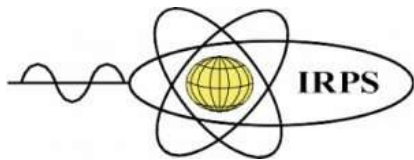
<sup>3</sup>Department of Physics, College of Education, University of Sulaimani, Sulaimani, Iraq

<sup>4</sup>Centro Nacional de Aceleradores, CNA, University of Seville-J.Andalucía-CSIC, Spain

<sup>5</sup>Atomic Energy Licensing Board, Malaysia

Corresponding author: mohamadsyazwan@utm.my

Effective dose assessment due to unavoidable radiation exposures from NORM (Naturally Occurring Radioactive Material)–added consumer products is necessary in managing public health and epidemiology studies at low-dose levels. This study was conducted to investigate the variability of organ dose estimations due to the product radiation exposures based on two different approaches of Monte Carlo radiation transport codes from MCNP5 and GEANT4. 5 products were selected based on their high prevalence of uses that is energy pendant, tourmaline socks, energy card, bracelet and thorium mantle. For MCNP5 codes, direct simulations of radiation transport were performed in human phantom; specifically, by incorporating standing computational MIRD human phantom, and using photon mode (P MODE) only with thick-target bremsstrahlung model (TTB) to take account of electron-induced photon transports. Meanwhile, GEANT4 incorporated Low Energy Electromagnetic Package EM Opt4 to simulate both photon and electron transports (PE MODE). The study found out that the discrepancies of computed organ doses based on ratios between two different codes due to short distance of product exposures (energy pendant, energy card, bracelet) were in range of 1 – 19 %. Large discrepancy over 10 % are observed for organs that located in proximity to the product of exposures. Extremely large discrepancy percentages of more than 100 % of organ dose ratios (tourmaline socks) were observed for different approaches between point sources (GEANT4) and homogeneously distributed volume source (MCNP5). For long distance of product exposures (thorium mantles), the disagreement of few to multiple tenth % of organ dose ratios were observed between the codes for both 20 and 50 cm due to different photon-electron transport approaches. The study suggests that in order to obtain high precision of organ dose estimations, the most realistic model of exposures need to be achieved for examples type of radiation mode and source geometries.



**A091 - Effect of mixed glass former on structural, elastic and gamma radiation shielding properties of  $70[x\text{TeO}_2-(1-x)\text{B}_2\text{O}_3]-20\text{Bi}_2\text{O}_3-10\text{Li}_2\text{O}$  glasses**

M.A. Yahya<sup>1,4</sup>, M.S. Sutrisno<sup>2</sup>, A.Z. Shah<sup>3</sup>, R. Hisam<sup>4,\*</sup>

<sup>1</sup>Faculty of Applied Sciences, Universiti Teknologi MARA, Perak Branch, Tapah Campus, 35400 Tapah Road, Perak, Malaysia

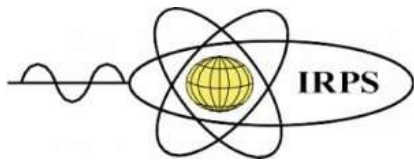
<sup>2</sup>University of Cyberjaya (UoC), Persiaran Bestari, Cyber 11, 63000 Cyberjaya, Selangor Darul Ehsan, Malaysia

<sup>3</sup>Centre of Foundation Studies, Universiti Teknologi MARA Cawangan Selangor, Dengkil Campus, 43800 Dengkil Selangor, Malaysia

<sup>4</sup>Faculty of Applied Sciences, Universiti Teknologi MARA, 40450 Shah Alam, Selangor, Malaysia

Corresponding author: [rosdiyana@uitm.edu.my](mailto:rosdiyana@uitm.edu.my)

The lead-free  $70[x\text{TeO}_2-(1-x)\text{B}_2\text{O}_3]-20\text{Bi}_2\text{O}_3-10\text{Li}_2\text{O}$  glasses were prepared by melt-quenching method to determine the effect of mixing  $\text{TeO}_2$  and  $\text{B}_2\text{O}_3$  glass formers on structural, elastic and gamma radiation shielding properties of the glass system for applications in radiotherapy laboratory and nuclear power plant control rooms. Structural analysis using FTIR results revealed competition between  $\text{TeO}_2$  and  $\text{B}_2\text{O}_3$  formers, where  $\text{TO}_4$  units indicated bridging oxygen (BO) increased with increasing  $\text{TeO}_2$  content before a large dropped at  $x=30$  mol%, while  $\text{BO}_4$  units indicated BO fluctuated for  $x<30$  mol% before it reaches the maximum at  $x=30$  mol%  $\text{TeO}_2$  concentration. Interestingly, a minimum at  $x=30$  mol% was observed for elastic moduli (longitudinal,  $C_L$  and shear,  $\mu$ ) together with bulk,  $K$ , and Young's modulus,  $Y$  which due to the high formation of BO. On the other hand, gamma radiation shielding properties have been investigated using Phy-X/PSD simulation and XCOM program. The Linear Attenuation Coefficient (LAC) showed an increasing trend with increasing the  $\text{TeO}_2$  concentration. However, at  $x=30$  mol%, a slight changes were observed which may be due to the density of the glass samples. The increased in  $\text{TeO}_2$  content decreased the values of Half Value Layer (HVL) and Mean Free Path (MFP). The effective Atomic Number ( $Z_{\text{eff}}$ ) results revealed that the gamma shielding properties increases with the increase in  $\text{TeO}_2$  content. In addition, the results demonstrated that the glass sample with 50 mol% of  $\text{TeO}_2$  content had the most desired for radiation shielding applications.



**A093 - Novel efficient alloys for radiation shielding applications: A theoretical investigation**

M. Kh. Hamad<sup>1</sup>, Mohammad Abu Mhareb<sup>2,3</sup>, M. I. Sayyed<sup>4,5</sup>, Y. S. Alajerami<sup>6</sup>, Raghad Alsharhan<sup>2</sup>, Mayeen Uddin Khandaker<sup>7</sup>

<sup>1</sup>Department of Basic Sciences, School of Social and Basics Sciences, Al Hussein Technical University, Amman, Jordan

<sup>2</sup>Department of Physics, College of Science, Imam Abdulrahman Bin Faisal University, P.O. Box 1982, 31441 Dammam, Saudi Arabia

<sup>3</sup>Basic and Applied Scientific Research Center, Imam Abdulrahman Bin Faisal University, PO Box 1982, 31441 Dammam, Saudi Arabia

<sup>4</sup>Department of Physics, Faculty of Science, Isra University, Amman, Jordan

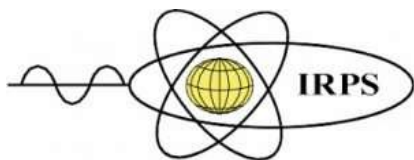
<sup>5</sup>Department of Nuclear Medicine Research, Institute for Research and Medical Consultations(IRMC), Imam Abdulrahman Bin Faisal University (IAU), P.O. Box 1982, 31441 Dammam, Saudi Arabia

<sup>6</sup>Medical Imaging Department, Applied Medical Sciences Faculty, Al Azhar University-Gaza, P.O. Box 1277, Gaza, Palestine

<sup>7</sup>Center for Applied Physics and Radiation Technologies, School of Engineering and Technology, Sunway University, 47500 Bandar Sunway, Selangor Darul Ehsan, Malaysia

\*Corresponding author: alsharhanraghad@gmail.com

In the current investigation, different types of alloys were fabricated through the solid-state reaction process. The structural properties of the prepared alloys were reported by XRD, and the density of the prepared alloys was measured experimentally to explore the radiation shielding properties. Phy-X software was generated to calculate different radiation attenuation factors for the prepared alloys between 0.01 and 15 MeV. We investigated the influence of the chemical composition of the prepared alloys on the attenuation capability. We also examined the influence of the energy at low, moderate, and high energy zones on the mass attenuation coefficient (MAC) for each alloy. We found that the MAC for the prepared alloys is high in the low-energy region, especially near the K-absorption edge of Sb and As. The results illustrate an increase in the alloy's half-value layer with increasing the energy of the radiation. The obtained results confirm the potentiality of using the prepared alloys for radiation protection applications.



**ISRP 2021**  
**International Symposium on Radiation Physics**  
**Kuala Lumpur – Malaysia**  
**6 – 10 December 2021**

**A095 - A setup for integral measurements of multiple scattering by 10- to 100-keV electrons**

M. N. Martins<sup>1</sup>, A. A. Malafrente<sup>1</sup>, A. Mangiarotti<sup>1</sup>, A. R. Petri<sup>2</sup>, J. M. Fernández-Varea<sup>3</sup>,  
N. L. Maidana<sup>1</sup>, S. F. Barros<sup>4</sup>, V. R. Vanin<sup>1</sup>

<sup>1</sup>Instituto de Física, Universidade de São Paulo, SP, Brazil

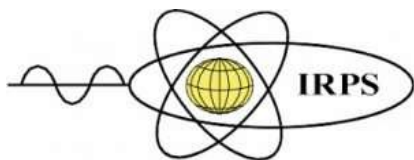
<sup>2</sup>Istituto Nazionale di Fisica Nucleare, Sezione di Milano, Italy

<sup>3</sup>Facultat de Física (FQA and ICC), Universitat de Barcelona, Catalonia, Spain

<sup>4</sup>Instituto Federal de São Paulo, Itaquaquecetuba, SP, Brazil

Corresponding author: martins@if.usp.br

Multiple scattering (MS) of charged particles is relevant in many applications of radiation physics, like the accurate simulation of energy deposition or of detector response. Electrons are important both as primary particles and as secondaries released by the interaction of photons, protons, and other ions. Despite this, data are generally old, the most recent ones published in 2008 obtained with a medical linac under poorly controlled conditions. For electrons with energies between 10 and 100 keV, the existing measurements of MS angular distributions (not to be confused with backscattering) are from 1946. A project has been started to measure MS angular distributions with the electron beams available at the São Paulo Microtron. The first step has been the study of angle-integrated distributions for 10- to 100-keV electrons impinging on targets with mass thicknesses between  $\sim 10 \mu\text{g}/\text{cm}^2$  and  $\sim 2 \text{mg}/\text{cm}^2$ , and  $Z$  ranging from 13 to 79. Electrons scattered at frontal angles have been collected with a Faraday cup covering the polar angles below  $12.0^\circ$ . To supplement this information, a ring has been installed around the entrance of the Faraday cup to cover the angles from  $12.0^\circ$  to  $23.1^\circ$ . The normalisation is provided by the current collected by the rest of the chamber, which is kept insulated from the beam line and the ground. Important construction specifications will be presented. The experience gained by operating this system will also be discussed regarding its critical aspects like: avoiding cross talk between the cup and the ring both at the physical level and during current measurements, measurement of small currents deposited on large objects (the chamber in particular), conditioning of the target surface, and correction for electron backscattering from the ring. Finally, some selected results for angle integrated MS distributions will be compared to the best available theories.



**ISRP 2021**  
**International Symposium on Radiation Physics**  
**Kuala Lumpur – Malaysia**  
**6 – 10 December 2021**

**A096 - Incidental finding of hepatocellular carcinoma using Ga68-PSMA PET-CT: future use for detection and theranostics?**

Ew-Jun Chen<sup>1</sup>, Teik Hin Tan<sup>2</sup>, Nik Muhd Aslan<sup>3</sup>

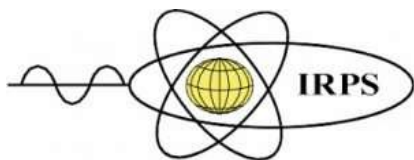
<sup>1</sup>Nuclear Medicine Centre, Sunway Medical Centre. No. 5 Jalan Lagoon Selatan, Bandar Sunway, 47500 Petaling Jaya, Selangor Darul Ehsan, Malaysia

<sup>2</sup>Centre for Biomedical Physics, School of Healthcare and Medical Sciences, Sunway University. No. 5 Jalan Universiti, Bandar Sunway, 47500 Petaling Jaya, Selangor Darul Ehsan, Malaysia

<sup>3</sup>Clinical Oncology, Sunway Medical Centre. No. 5 Jalan Lagoon Selatan, Bandar Sunway, 47500 Petaling Jaya, Selangor Darul Ehsan, Malaysia

Corresponding author: ewjunchen@gmail.com

Prostate cancer is one of the most frequent malignancy affecting men. Due to high expression of prostate-specific membrane antigen (PSMA) in the epithelial vasculature of prostatic cancer cells, radiolabelled Gallium-68-PSMA Positron Emission Tomography-Computed Tomography (Ga68-PSMA PET-CT) has now become an essential imaging modality to stage high-risk prostate cancer as well as detect biochemical relapse. However, PSMA is also over-expressed in the neovasculature epithelium of other non-prostatic high-vasculature tumours. We report a case of incidental finding of hepatocellular carcinoma (HCC) by Ga68-PSMA PET-CT. Eighty-year-old male diagnosed with prostate cancer undergoing hormonal therapy was referred for Ga68-PSMA PET-CT for further staging. PET-CT findings showed a single large irregular hepatic lesion with concordant PSMA tracer uptake, likely suggestive of primary liver malignancy. Subsequent liver biopsy confirmed HCC. Patient then received concurrent treatments for both HCC and prostate cancer. Neovascularisation is the foundation of growth, invasion and metastasis in HCC. The epithelium of neovasculatures may express PSMA, which could be a potential pitfall when staging for prostate carcinoma. Nonetheless, the expression of PSMA in HCC may suggest a possible role of Ga68-PSMA PET-CT in HCC detection and staging. Furthermore, this may allow for possible novel HCC treatments using PSMA as a potential therapeutic target in theranostics.



**A097 - Investigation of polyvinyl alcohol (PVAL) composites and the effect of variation in breast densities on image quality and dose in full-field digital mammography: A phantom study**

Franca Oyiwoja Okoh<sup>1,4</sup>, Norlaili Ahmad Kabir<sup>1</sup>, Mohd Fahmi Mohd Yusof<sup>2</sup>, Rafidah Binti Zainon<sup>3</sup>

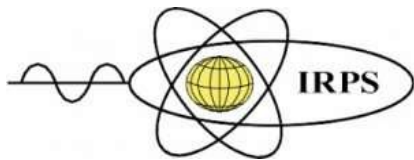
<sup>1</sup>School of Physics, Universiti Sains Malaysia, 11800 Penang, Malaysia

<sup>2</sup>School of Health Sciences, Universiti Sains Malaysia, 16150 Kelantan, Malaysia

<sup>3</sup>Advanced Medical and Dental Institute, Universiti Sains Malaysia, 13200 Penang, Malaysia

<sup>4</sup>Department of Physics, Federal University Wukari, PMB 1020 Wukari-Taraba State, Nigeria

This study focused on the image quality and dosimetry characteristics in fabricated polyvinyl alcohol (PVAL) phantoms for mammography. The densities of a number of fabricated breast equivalent phantoms made from PVAL, ethanol solution and graphite powder adhering to BIRADS (Breast Imaging Reporting and Data System) standard were investigated. An X-ray computed tomography (CT) imaging system was used to determine the mean CT numbers, relative electron densities and density distribution profiles of all PVAL composite gels. Mammograms of fabricated and standard RMI 156 mammography phantoms were acquired using full field digital mammography imaging system. The effect of breast density on contrast (Cn), contrast-to-noise ratio (CNR), signal-to-noise ratio (SNR) and mean glandular dose (MGD) were calculated. The breast phantoms made from PVAL + ethanol (E50), PVAL (P10) and PVAL + graphite (G4) showed good resemblance to water and breast tissue based on their densities, mean CT number, relative electron densities, CT density distribution profiles and percentage flatness. Higher Cn, CNR and SNR values were achieved with lower density breast equivalent phantoms. Moreover, density correlated positively with MGD and the mean values of the MGD of the different categories of phantoms produced a p-value = 0.014 (< 0.05) which implied that the dense phantoms had statistically significant higher MGD compared to the less dense ones. All MGD values recorded in this work were found to be within the acceptable limit of 3.0 mGy consistent with the ACR protocol. Therefore, these results support the suitability of E50, P10 and G4 as appropriate breast tissue-equivalent materials to mimic BIRADS category B, C and D breast.



**ISRP 2021**  
**International Symposium on Radiation Physics**  
**Kuala Lumpur – Malaysia**  
**6 – 10 December 2021**

**A100 - Characterization of Target Transfer Function (TTF) performances for detection of pulmonary nodule in lung from current protocol**

M K A Karim<sup>1,2</sup>, H H Harun<sup>1</sup>, H H Harun<sup>3</sup>

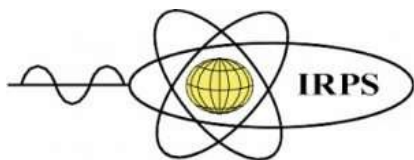
<sup>1</sup> Department of Physics, Faculty of Science, Universiti Putra Malaysia, 43400 Serdang, Selangor, Malaysia

<sup>2</sup> Center for Diagnostic Nuclear Imaging, Faculty of Medicine, Universiti Putra Malaysia, 43400 Serdang, Selangor, Malaysia

<sup>3</sup> Department of Forestry Science and Biodiversity, Faculty of Forestry and Environment, Universiti Putra Malaysia, 43400 Serdang, Selangor, Malaysia

Corresponding author: hanifhaspi@gmail.com

This prospective study was designed to evaluate the influence of different tube potential, pitch factor and iterative reconstruction (IR) algorithm on target transfer function (TTF) performance in detecting pulmonary nodule during CT thorax examination. The study utilize image quality phantom (CATPHAN 600) and was scanned under 128-slice Philips Brilliance (USA) CT scanner. We employ CT Pulmonary Angiography (CTPA) protocols with adopting different tube potential and pitch factor settings. Furthermore, the image was reconstructed using iDose<sup>4</sup> level 3 and 4 and iDose<sup>4</sup> level 2 as a current IR setup. The spatial frequency values were analyzed and TTF performance was evaluated in different settings of the tube potential, pitch factor and IR algorithm. TTF performance was relatively higher with increase of pitch factor value. However, no significant different observed on spatial frequency of TTF for various tube potential and IR settings. The suitable pitch factor setting may enhance the TTF performance for pulmonary nodule detection on the lung and improved the diagnostic performance. This study discovered a significant association between TTF performance and lung nodule detection under different data gathering settings, which can be used to improve the present CTPA protocol.



**A102 - Rapid separation of thorium via electrosorption with carbon electrode towards efficiently managing rare-earth extraction residue**

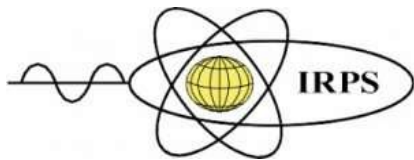
Aznan Fazli Ismail<sup>1</sup>, Eli Syafiqah Aziman<sup>2</sup>

<sup>1</sup>Nuclear Science Programme, Faculty of Science and Technology, Universiti Kebangsaan Malaysia, 43600 UKM Bangi, Selangor, Malaysia

<sup>2</sup>Water Research and Analysis Centre (ALIR), Faculty of Science and Technology, Universiti Kebangsaan Malaysia, 43600 UKM Bangi, Selangor, Malaysia

Corresponding author: [aznan@ukm.edu.my](mailto:aznan@ukm.edu.my)

Rare-earth (RE) extraction activities in Malaysia produces 64000 to 75000 tonnes of low-level radioactive residue annually which contains thorium concentration above the regulatory clearance limit. Since thorium is considered as non-economic element, large volumes of these RE processed residues are commonly disposed of without treatment. This research aims to investigate the separation capability of thorium from aqueous waste through an electrosorption technique using a carbon-based electrode. The leachate solution obtained from the digestion of RE extraction residue was treated with the electrosorption technique. Several parameters such as the applied voltage potential (0.2V - 0.8V vs Ag/AgCl), ion competition, and initial concentration were investigated. The results showed that the adsorption of thorium ion  $(\text{ThSO}_4)_3^{2-}$  was dominant at higher positive voltage with the trend of  $K_d$  value was  $\text{Th} > \text{Pr} > \text{Nd} > \text{La} > \text{Ce}$ . The specific adsorption capacity obtained in this study ranged from 1.0 to 8.4 mg-Th/g-Carbon. The adsorption of  $(\text{ThSO}_4)_3^{2-}$  conforms to the Langmuir and Freundlich adsorption isotherm models, while first and second pseudo-order kinetic models were well fitted for the separation of  $(\text{ThSO}_4)_3^{2-}$  by carbon electrodes. Characterization of the electrode carbon after treatment reveals that the migration of  $(\text{ThSO}_4)_3^{2-}$  to the surface of the carbon electrode was due to the electrostatic forces followed by diffusion into the pores and bonding with the C1s group through ion exchange and chemical non-reaction profile. This study found that the application of electrosorption technique with carbon-based electrode may reduce up to 40% volume of the radioactive residue.



**A109 - MRI-LINAC dosimetry approach by Monte Carlo methods coupling charged particle radiation transport with strong magnetic fields**

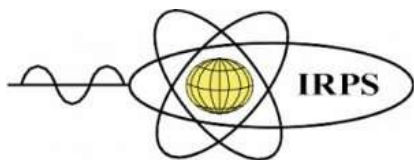
Amiel Gayol<sup>1</sup>, Mauro Valente<sup>1,2</sup>

<sup>1</sup>Instituto de Física E. Gaviola, IFEG-CONICET, & Laboratorio de Investigación e Instrumentación en Física Aplicada a la Medicina e Imágenes por Rayos X, LIIFAMIR<sup>x</sup>, Facultad de Matemática, Astronomía, Física y Computación, FAMAFA, Ciudad Universitaria, Córdoba, Argentina.

<sup>2</sup>Centro de excelencia de Física e Ingeniería en Salud, CFIS & Departamento de Ciencias Físicas, Universidad de La Frontera, Temuco, Chile.

Corresponding author: amielgayol@mi.unc.edu.ar

MRI-LINAC devices incorporate magnetic resonance imaging systems to therapeutic procedures with megavoltage photon beams produced by linear clinical accelerators. MRI-LINAC devices are considered to represent a new type of technology with great expectations for high precision radiotherapy since it allows treatment guidance by means of in-situ images of the patient. The strong magnetic fields used in these equipment influence the trajectories of secondary electrons, and charged particles in general, by means of the Lorentz force. Thus, modifying the ionizing radiation field, which may cause local variations in the absorbed dose distribution. The proper implementation of the external electromagnetic field coupling in Monte Carlo simulation codes is a key issue to confirm the feasibility of using such a tool to describe this type of complex applications along with the subsequent dosimetric effects. This work provides a framework to carefully investigate the effects of magnetic fields on charged particle tracks and on dose distributions, due to incident photon beams typically used in clinics. PENELOPE and FLUKA simulation main codes were used to study the deflection of the electron trajectories, while evaluating dosimetric effects, considering simplified arrangements to complex clinical setups. Comparisons of the numerical results achieved for the radius of curvature of the trajectories with an analytic relativistic formulation was satisfactory, and dosimetry distortions due to the presence of strong magnetic field, as required for MRI-LINAC technique, have been obtained using dedicated phantoms including interfaces and inhomogeneities as well as preliminary approaches for patient-specific clinical cases.



**A113 - Feasibility of mean glandular dose determination of digital breast tomosynthesis unit using LuSy dosimeter**

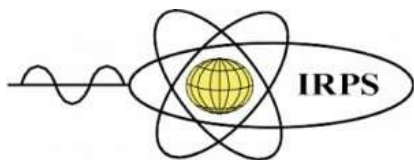
Janatul Madinah Wahabi<sup>1</sup>, Quratu' Aini Abdul Aziz<sup>1</sup>, Kwan Hoong Ng<sup>1</sup>, Kartini Rahmat<sup>1</sup>, Ngie Min Ung<sup>2</sup>, Jeannie Hsiu Ding Wong<sup>1</sup>

<sup>1</sup>Department of Biomedical Imaging, Faculty of Medicine, Universiti Malaya, Malaysia

<sup>2</sup>Clinical Oncology Unit, Faculty of Medicine, Universiti Malaya, Malaysia

Corresponding author: jeannie\_wong80@um.edu.my

Mammography is a radiological examination that utilised low-energy x-rays to detect breast cancer. The techniques available are full-field digital mammography (FFDM) and digital breast tomosynthesis (DBT), which produced 2D and 3D breast images, respectively. Mean glandular dose (MGD) can be used to monitor the dose delivered by these techniques because it estimates the photon absorption in the breast's glandular tissue. This study aimed to determine the feasibility of determining the mean glandular dose (MGD) using an in-house developed, real-time optical fibre-based dosimeter called LuSy dosimeter. LuSy was calibrated against a standard mammography dosimeter for three different target-filter combinations of W/Rh, W/Ag and W/Al. After calibration, the MGD was measured using LuSy and subsequently compared with the MGD measured by the solid-state detector and those predicted by the mammography machine. The measured calibration coefficient was  $341 \pm 8$ ,  $381 \pm 7$  and  $433 \pm 58$  counts/mGy, for W/Ag, W/Rh and W/Al target-filter combinations, respectively. For MGD, both LuSy and the mammography dosimeter measured a higher dose compared to the machine console. The mean deviation between the LuSy and the solid-state dosimeter was 3.0 %, and the mean deviation between the LuSy and the machine console was 30.3 %. Meanwhile, the mean deviation between the solid-state detector and the machine console was 32.7 %. This may be because of the slight difference in the MGD determination setup used by the mammography unit. In conclusion, the LuSy was calibrated for low-energy x-rays, and the MGD measured was comparable with a standard dosimeter.



**A114 - 2D vs 3D dose analysis of PRESAGE® Dosimeters using 3DMicroHD-OCT System: an in-house Optical CT system for radiotherapy dosimetry**

M. Z. Mohyedin<sup>1,2</sup>, Hafiz Zin<sup>3</sup>, S. Aldawood<sup>4</sup>, M. Alkhorayef<sup>5</sup>, A Sulieman<sup>6</sup>, David A. Bradley<sup>7</sup>, Suhairul Hashim<sup>8</sup>, Ahmad Taufek Abdul Rahman<sup>1,2, 4\*</sup>

<sup>1</sup>School of Physics and Material Studies, Faculty of Applied Sciences, Universiti Teknologi MARA, 40450 Shah Alam, Selangor, Malaysia.

<sup>2</sup>Centre of Astrophysics & Applied Radiation, Institute of Science, Universiti Teknologi MARA, 40450 Shah Alam, Selangor, Malaysia.

<sup>3</sup>Advanced Medical & Dental Institute, Universiti Sains Malaysia (USM), 11800 Gelugor, Penang, Malaysia.

<sup>4</sup>Department of Physics & Astronomy, College of Sciences, King Saud University, 12372 Riyadh, Saudi Arabia.

<sup>5</sup>Department of Radiological Sciences, College of Applied Medical Sciences, King Saud University, 12372 Riyadh, Saudi Arabia

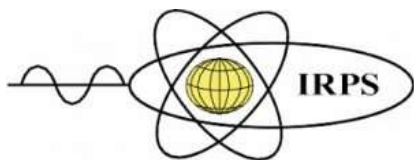
<sup>6</sup>Prince Sattam Bin Abdulaziz University, College of Applied Medical Sciences, Radiology and Medical Imaging Department, Alkharj, Saudi Arabia

<sup>7</sup>Sunway University, Institute for Health Care Development, Jalan University, 46150 Subang Jaya, Malaysia

<sup>8</sup>Department of Physics, Faculty of Science, Universiti Teknologi Malaysia, 81310 Skudai, Malaysia

Corresponding author: ahmadtaufek@uitm.edu.my

PRESAGE® dosimeter was investigated to explore the capability of the system for radiotherapy dosimetry applications when read using the in-house developed optical CT system at Universiti Teknologi MARA known as 3DMicroHD-OCT. The samples of PRESAGE® were irradiated at different field geometry and pattern to investigate the percentage depth dose, the dose linearity and dose rates dependency. It was found that the irradiated PRESAGE® accurately produces depth dose profile which shows the  $d_{max}$  at 1.5 cm for 6 MV when readout and analysed by the 3DMicroHD-OCT system in both 2D and 3D. The system also accurately measured the absorbed dose in the PRESAGE® linearly with the  $R^2$  better than 0.85. The dose linearity result is consistent with results of UV-Vis's spectrometry. It was also found that there is a dose rate effect at lowest dose rate irradiation on the dose response over the range tested. The dose rate dependency analysis was consistent with the UV-vis. This study shows that the 3DMicroHD-OCT system is capable and feasible to utilise as 3D dosimetry system.



**ISRP 2021**  
**International Symposium on Radiation Physics**  
**Kuala Lumpur – Malaysia**  
**6 – 10 December 2021**

**A115 - High accurate mass attenuation coefficients and nanostructure of Zinc from X-ray absorption Spectroscopy at room temperature.**

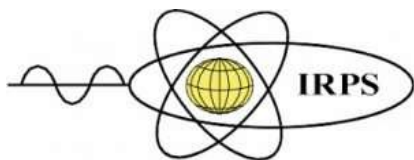
Ruwini S. K. Ekanayake<sup>1</sup>, Christopher T. Chantler<sup>1</sup>, Daniel Sier<sup>1</sup>, Martin J. Schalken<sup>1</sup>, Alexis J. Illig<sup>1</sup>, Martin D. de Jonge<sup>2</sup>, Bernt Johannessen<sup>2</sup>, Peter Kappen<sup>2</sup> and Chanh Q. Tran<sup>3</sup>.

<sup>1</sup>School of Physics, University of Melbourne, Australia

<sup>2</sup>ANSTO, Australian Synchrotron, Melbourne, Australia

<sup>3</sup>La Trobe University, Australia

High-accuracy X-ray mass attenuation coefficients were determined from the X-ray Extended Range Technique (XERT)-like experiment at the Australian Synchrotron. The accuracy of measured mass attenuation coefficients is about 0.023% to 0.036%. Experimentally measured mass attenuation coefficients deviate from the theoretical values near the zinc absorption edge, suggesting that improvements in theoretical tabulations. The zinc K-edge jump ratio, jump factor and X-ray absorption fine-structure (XAFS) are carefully determined from the high accuracy absorption data. The XAFS analysis yields bond lengths and nanostructure of zinc with uncertainties of from 0.1% to 0.3% or 0.003 Å to 0.008 Å. Thermal parameters were fitted with an accuracy of from approximately 5%, and  $S_0^2$  is determined to be  $0.904 \pm 0.037$ . A significant variation from reported crystal structures observed and it suggests local dynamic motion compared with a standard crystal lattice. XAFS is sensitive to dynamic correlated motion so that it is possible to observe any significances related to dynamic motion of materials. These results for the zinc absorption coefficient, XAFS and structure are the most accurate structural refinements of zinc at room temperature.



**ISRP 2021**  
**International Symposium on Radiation Physics**  
**Kuala Lumpur – Malaysia**  
**6 – 10 December 2021**

**A117 - Synthesis, luminescence and scintillation properties of LaCl<sub>3</sub>:Tm<sup>3+</sup> crystal**

Yaowaluk Tariwong<sup>1,2</sup>, Natthakridta Chanthima<sup>1,2</sup>, Phan Quoc Vuong<sup>3</sup>,  
Nguyen Thanh Luan<sup>3</sup>, Wuttichai Chaiphaksa<sup>1,2</sup>, Hongjoo Kim<sup>3</sup>, Jakrapong Kaewkhao<sup>1,2</sup>

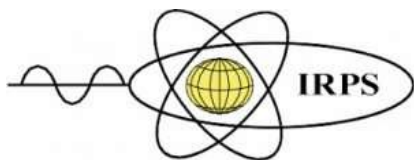
<sup>1</sup>Physics Program, Faculty of Science and Technology, Nakhon Pathom Rajabhat University,  
Nakhon Pathom 73000, Thailand

<sup>2</sup>Center of Excellence in Glass Technology and Materials Science (CEGM), Nakhon Pathom  
Rajabhat University, Nakhon Pathom 73000, Thailand

<sup>3</sup>Department of Physics, Kyungpook National University, Daegu, 702-701,  
Republic of Korea

Corresponding author: y.tariwong@gmail.com

This paper reports the luminescence and scintillation properties of LaCl<sub>3</sub>:Tm<sup>3+</sup> single crystal. Single crystal of Tm-doped LaCl<sub>3</sub> with the dimension of diameter 7 mm and length 55 mm was successfully grown from the melt by using an inhouse-developed Bridgman furnace. The luminescence property of the synthesized crystal has been analyzed under X-ray excitation, the characteristic emission of LaCl<sub>3</sub>:Tm<sup>3+</sup> crystal shows strong emission at 382 and 701 nm which comes from the STEs of LaCl<sub>3</sub> crystal and the transition of Tm<sup>3+</sup>, respectively. Pulse height spectrum under gamma excitation of the crystal coupled with a PMT was measured and compared with that of LYSO crystal. At 662 keV  $\gamma$ - rays, the light yield (LY) of 38,800 ph/MeV and energy resolution of 4.36% were studied for LaCl<sub>3</sub>:Tm<sup>3+</sup> crystal. From these results, the LaCl<sub>3</sub>:Tm<sup>3+</sup> single crystal is a promising candidate for X-rays and  $\gamma$ -rays radiation detection.



**ISRP 2021**  
**International Symposium on Radiation Physics**  
**Kuala Lumpur – Malaysia**  
**6 – 10 December 2021**

### **A118 - Estimate of Effective Dose for Adults' Patients from Nuclear Medicine Examinations in Sudan**

Suhaib Alameen<sup>1</sup>, Alaa Bashir<sup>2</sup>, Mohammed Ali<sup>1,3</sup>, Aya Ahmed<sup>1,3</sup>, Hassan Salah<sup>1,3</sup>, Nissren Tamam<sup>4</sup>, Abdelmoneim Sulieman<sup>5</sup>, D.A. Bradley<sup>6,7</sup>

<sup>1</sup>Diagnostic Radiology Department, College of Medical Radiological Science, Sudan University of Science and Technology, Khartoum, Sudan

<sup>2</sup>Sudan Academy of Sciences, P.O Box 86 Khartoum, Sudan

<sup>3</sup>Nuclear Medicine Department, INAYA Medical Collage, Riyadh, Saudi Arabia

<sup>4</sup>Physics Department, College of Sciences, Princess Nourah Bint Abdulrahman University, P.O Box 84428, Riyadh 11671, Saudi Arabia

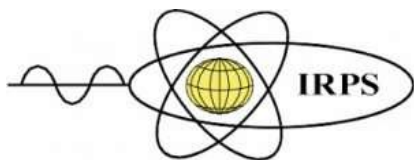
<sup>5</sup>Prince Sattam Bin Abdulaziz University, College of Applied Medical Sciences, Radiology and Medical Imaging Department, Alkharj, Saudi Arabia

<sup>6</sup>Centre for Applied Physics and Radiation Technologies, School of Engineering and Technology, 47500, Bandar Sunway, Selangor, Malaysia

<sup>7</sup>Centre for Nuclear and Radiation Physics, Department of Physics, University of Surrey, Guildford, Surrey GU2 7XH, UK

Corresponding author: hassan.salah.ibrahim1@gmail.com

Medical exposure is the primary source of radiogenic risk from artificial radiation to the general population. The contribution of artificial radiation exposure in the medical field has been growing in Sudan. This study aims to estimate effective doses for adult's patients from nuclear medicine examinations. The study involved 685 patients from five different hospitals in Sudan. In total, 300, 196, and 189 patients underwent renal, thyroid, and bone scans. All procedures were carried out using the Tc-99m radionuclide. Effective dose has been estimated using computer software depending on conductive activity. The results show that dose information for patients from thyroid, renal, and bone scan, for thyroid scan the patients age was  $42.82 \pm 16.46$  years, the patient's weight  $68.58 \pm 12.82$  kg, the activity  $4.75 \pm 0.543$  mCi and the effective dose for thyroid was  $2.28 \pm 0.26$  mSv. For renal scan, the patients' age  $45.19 \pm 16.36$  years, the weight  $65.96 \pm 13.78$  kg, the activity  $5.21 \pm 1.166$  mCi, and the effective dose  $0.94 \pm 0.211$  mSv. For a bone scan, the patients' age was  $57.59 \pm 14.92$  years, the patient's weight was  $69.48 \pm 13.71$  kg, the activity  $19.96 \pm 2.11$  mCi, and the effective dose for bone was  $4.208 \pm 0.443$  mSv. The study revealed that the administered activity is independent of patient weight. Patients received unjustified exposure due to the high amount of administered activity. Implementation of national guidelines is necessary to improve the practice and patient safety.



**ISRP 2021**  
**International Symposium on Radiation Physics**  
**Kuala Lumpur – Malaysia**  
**6 – 10 December 2021**

**A119 - Precision measurement of the phase fine structure across the iron K-edge.**

Tony Kirk<sup>1</sup>, Chanh Q. Tran<sup>1</sup>, Christopher T. Chantler<sup>2</sup>, Zwi Barnea<sup>2</sup>, Paul Di Pasquale<sup>1</sup>,  
Minh H. Dao<sup>1</sup>, Julian Ceddia<sup>3</sup>, Eugenia Balaur<sup>1</sup>, Nigel Kirby<sup>4</sup>, Stephen Mudie<sup>4</sup>

<sup>1</sup>Department of Chemistry & Physics, La Trobe University, Australia

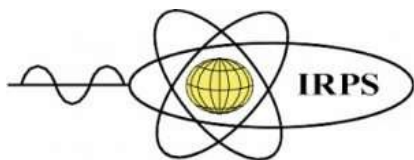
<sup>2</sup>School of Physics, University of Melbourne, Australia

<sup>3</sup>School of Physics & Astronomy, Monash University, Australia

<sup>4</sup>Australian Synchrotron, ANSTO, Australia

Corresponding author: t.kirk@latrobe.edu.au

Current applications of X-ray Absorption Fine Structure (XAFS) to low absorbing samples such as ultra-thin films in semiconductor and nano-devices have been limited. This is expected to not be the case for the phase component of the fine structure as it is generally orders of magnitude larger than the absorption component in the x-ray regime. Here, we present details of a precision measurement of both the phase and absorption components of the atomic fine structure across the K-edge of a thin iron foil. The experiment applied Fourier Transform Holography with an extended reference in spectroscopy mode and was conducted at the SAXS/WAXS beamline of the Australian Synchrotron. The results provide critical experimental benchmark for further theoretical development and has potential to delve into the phase equivalent of XAFS related techniques.



**A120 - Applications of MOSkin as a real-time detector for *in vivo* dosimetry during high-dose rate Cobalt-60 brachytherapy**

Ngie Min Ung<sup>1,3</sup>, Zulaikha Jamalludin<sup>2,3</sup>, Rozita Abdul Malik<sup>1,3</sup>, Gwo Fuang Ho<sup>1,3</sup>, Joel Poder<sup>4</sup>, Dean Cutajar<sup>4</sup>, Anatoly Rosenfeld<sup>4</sup>

<sup>1</sup>Clinical Oncology Unit, Faculty of Medicine, Universiti Malaya, Malaysia

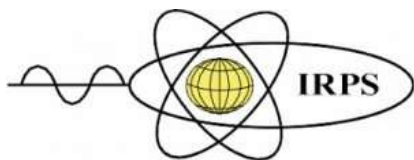
<sup>2</sup>Medical Physics Unit, University of Malaya Medical Centre, Malaysia

<sup>3</sup>Department of Clinical Oncology, University of Malaya Medical Centre, Malaysia

<sup>4</sup>Centre for Medical Radiation Physics, University of Wollongong, Australia

Corresponding author: nm\_ung@um.edu.my

Dose measurement in high dose rate (HDR) brachytherapy treatment is challenging due to the nature of steep dose gradient characteristic of brachytherapy source. MOSkin is a MOSFET-based detector which possesses the main advantages of having small active volume and water equivalent packaging as well as providing real-time measurement. It therefore has a high potential to be the detector of choice for implementation of *in vivo* dosimetry (IVD) programme in clinical brachytherapy. In this work, the aim is to evaluate the feasibility and applicability of MOSkin as an *in vivo* detector for Cobalt-60 (Co-60) brachytherapy dose measurement during brachytherapy of skin and cervical cancers. The MOSkin was first explored for a dosimetric study at lead-tissue interface to measure the dose to the targeted and normal skin regions during skin brachytherapy. Dose quantification with MOSkin performed in three different source-lead-bolus phantom setup arrangements and during treatment delivery, providing dosimetric information of tumour and normal tissue doses evaluation. There was 20% dose enhancement at the target area from source-lead-bolus (SLB) setup while > 25% dose reduction to normal skin was achieved with source-bolus-lead (SBL) setup arrangement. The suitability of the MOSkin detector for rectal dose measurement during cervical intracavitary brachytherapy (ICBT) was then investigated. Verification of classical cervical pear-shaped isodose distribution from ICBT applicator was performed in a custom-made gynaecological phantom which resulted in < 3% dose difference between the TPS planned and MOSkin measured dose. This is followed by clinical *in vivo* rectal dose measurements in 18 brachytherapy insertions with placement of single MOSkin detector, which resulted in percentage dose difference with planned doses ranging from -16.3% to 14.9%. In conclusion, the MOSkin detector has been used for IVD and the results have verified the suitability and applicability of the MOSkin as detector of choice for IVD in HDR brachytherapy using Co-60.



**ISRP 2021**  
**International Symposium on Radiation Physics**  
**Kuala Lumpur – Malaysia**  
**6 – 10 December 2021**

**A121 - Structural fitting using the measured complex atomic fine structure spectra across the copper K-edge**

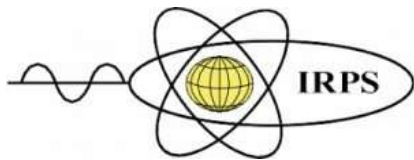
Paul Di Pasquale<sup>1</sup>, Chanh Q. Tran<sup>1</sup>, Christopher T. Chantler<sup>2</sup>, Tony Kirk<sup>1</sup>, Minh H. Dao<sup>1</sup>, Jake Rogers<sup>1</sup>

<sup>1</sup>Department of Chemistry and Physics, La Trobe University School of Molecular Sciences, Australia

<sup>2</sup>Department of Physics, Melbourne University, Australia

Corresponding author: pdipasquale@ltu.edu.au

X-ray absorption fine structure (XAFS) is widely used for investigating the properties of molecular structures that falls short when applied to weakly absorbing samples. We propose a new technique that explores the phase interactions with a sample which is known to be orders of magnitude more sensitive than absorption. The sensitivity of phase-based measurements will therefore overcome the limitations of absorption-based measurements. This new technique yields both an absorption and phase spectrum simultaneously whereas XAFS is only capable of absorption. Experimental demonstration of the new technique to achieve the complex refractive index on a relative scale shows exciting results. In this presentation, details of the structural fitting of the measured complex fine structure using the aforementioned technique will be discussed.



**ISRP 2021**  
**International Symposium on Radiation Physics**  
**Kuala Lumpur – Malaysia**  
**6 – 10 December 2021**

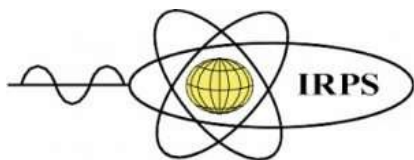
**A122 - A New Compact Octagonal Split Ring Resonator based Tuning Fork-Hammer Shape Perfect Metamaterial Absorber for C-Band Applications**

Salah Uddin Afsar, Mohammad Rashed Iqbal Faruque, Bellal Hossain

Space Science Centre (ANGKASA), Institute of Climate Change (IPI), Universiti Kebangsaan Malaysia, Bangi 43600, Malaysia

Corresponding author: rashed@ukm.edu.my

A new compact octagonal split ring resonator based tuning fork-hammer shape perfect metamaterial absorber for C-band applications presented in this paper. It is a new combination of an octagonal split resonator with tuning fork-hammer shape metal strip. FR-4 (lossy) is selected as substrate material and copper (pure) is used for all metal stripes. The projected unit cell is assessed by a high frequency electromagnetic simulator like CST microwave studio. The proposed structure exhibits maximum absorption at 4.65GHz (98.86%) and 6.19GHz (95.42%). The simulated results are also validated by HFSS and equivalent circuit model which shows insignificant amount variation. Absorption individualities are also analyzed by different polarization angle, width and length of the structure. The anticipated design is optimized through the different types of parametric studies such as design optimization, unit cell size, substrate materials. This C-band absorber permits numerous applications like satellite communication, defense, security and stealth technology.



**ISRP 2021**  
**International Symposium on Radiation Physics**  
**Kuala Lumpur – Malaysia**  
**6 – 10 December 2021**

**A123 - Complex atomic fine structure across the copper K-edge: new results and opportunities**

Chanh Q. Tran<sup>1</sup>, Tony Kirk<sup>1</sup>, Christopher T. Chantler<sup>2</sup>, Paul di Pasquale<sup>1</sup>, Minh H. Dao<sup>1</sup>, Julian Ceddia<sup>1</sup>, Zwi Barnea<sup>2</sup>, Gerald Hinsley<sup>1</sup>, Grant van Riessen<sup>1</sup>, Cameron Kewish<sup>3</sup>, Martin de Jonge<sup>3</sup> and David Paterson<sup>3</sup>

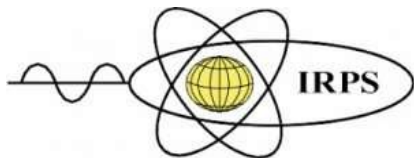
<sup>1</sup>Department of Chemistry and Physics, La Trobe Institute for Molecular Science, La Trobe University, Victoria, Australia

<sup>2</sup>School of Physics, University of Melbourne, Victoria, Australia

<sup>3</sup>XFM beamline, The Australian Synchrotron, ANSTO, Australia

Corresponding author: cq.tran@latrobe.edu.au

X-ray Absorption Spectroscopy has been one of the most powerful tools for probing atomic and molecular structures of materials. However, the measured fine structures in the absorption domain do not have adequate dimensionalities to extract three-dimensional structural information of the material of interest. In this presentation, we will describe a new technique that allows accurate measurements of the atomic fine structure in both the absorption and the phase domains, thereby opening exciting opportunities in a wide range of fundamental and applied research. New results of the complex atomic fine structure of copper across the K-edge will be discussed.



**ISRP 2021**  
**International Symposium on Radiation Physics**  
**Kuala Lumpur – Malaysia**  
**6 – 10 December 2021**

### **A126 - Development of FPGA-based Coincidence Module for TDCR Counting System**

Agung Agusbudiman<sup>1,2,3</sup>, Kyoung Beom Lee<sup>1,2</sup>, Jong Man Lee<sup>1,2</sup>, Sang Hoon Hwang<sup>1,2</sup>,  
Byoung Ju Kim<sup>2</sup>

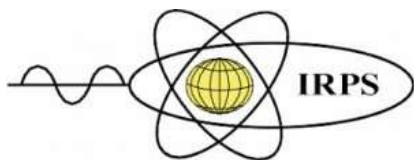
<sup>1</sup> Department of Science of Measurement, University of Science and Technology (UST), South Korea

<sup>2</sup> Radioactivity Metrology Team, Korea Research Institute of Standards and Science (KRISS), South Korea

<sup>3</sup> Radiation Metrology Division, National Nuclear Energy Agency (BATAN), Indonesia

Corresponding author: lee@kriss.re.kr

A new coincidence module for the Triple-to-Double Coincidence Ratio (TDCR) counting system has been developed at KRISS. The module is developed based on the Field-Programmable Gate Array (FPGA) to replace the MAC3 unit, a well-known coincidence module for a TDCR system. A cRIO controller, equipped with a Zynq-7020 FPGA, from the National Instrument is used to develop the FPGA code that realizes the same functionality as the MAC3 unit. The code is programmed to process pulses from three photomultiplier tubes (PMTs) and simultaneously generate the counting signals from the three channels. An extendable common dead-time correction is also applied in the FPGA code. Performance of the new module is tested by varying some measurement parameters, i.e., input pulse width, measurement time, dead-time, and resolving-time. A preliminary measurement result using <sup>14</sup>C and <sup>3</sup>H shows a difference of less than 0.5% between the FPGA and the MAC3, confirming the ability of the new coincidence module to replace the MAC3 unit.



**ISRP 2021**  
**International Symposium on Radiation Physics**  
**Kuala Lumpur – Malaysia**  
**6 – 10 December 2021**

### **A130 - Proton radioactivity of Dysprosium**

M.G.Srinivas<sup>1&3</sup>, N. Sowmya<sup>2\*</sup>, H C manjunatha<sup>2\*</sup>, P.S. Damodara Gupta<sup>2</sup>

<sup>1</sup>Department of Physics, Government First Grade College, Mulbagal, Karnataka, India.

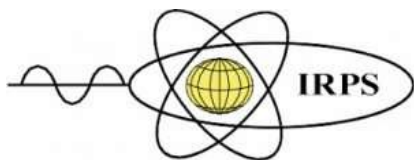
<sup>2</sup>Department of Physics, Government College for Women, Kolar, Karnataka, India.

<sup>3</sup>Department of Physics, St.Joseph's college, Affiliated To Bharathidasan University, Tiruchirappalli-620002,

Tamil-Nadu, India

Corresponding Author: manjunathhc@rediffmail.com, sowmyaparakash8@gmail.com

The one proton radioactivity of all possible isotopes of Dysprosium are investigated theoretically. Using effective liquid drop model (ELDM), the possible barriers limiting one proton emission are studied using the molecular phase of the dinuclear system. The mass excess values are taken from the reference [Chinese Physics C Vol. 45, No. 3 (2021) 030003]. The penetration probability is evaluated using Wentzel–Kramers–Brillouin (WKB) integral. The half-lives obtained from the present work were compared with the available experimental values. The half-lives of possible isotopes with positive decay energy in the isotopes of Dysprosium are predicted. The predicted decay energies along with the corresponding half-lives were useful in diagnosis and radiotherapy.



**ISRP 2021**  
**International Symposium on Radiation Physics**  
**Kuala Lumpur – Malaysia**  
**6 – 10 December 2021**

**A136 - Dose Assessment in CT Examination of Pelvis and Establishment of Provincial Diagnostic Reference Levels in Taif, Saudi Arabia**

Khaled AlQahtanii<sup>1</sup>, Hamid Osman<sup>2</sup>, Amin Elzaki<sup>2</sup>, Mayeen Uddin Khandaker<sup>3</sup>, Ahmed Yaqinuddin<sup>4</sup>

<sup>1</sup>King Abdul Aziz Specialist Hospital (KAASH) Radiology, Taif Saudi Arabia.

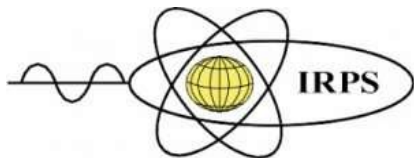
<sup>2</sup>Department Radiological Sciences, College of Applied Medical Sciences, Taif University Taif, Saudi Arabia.

<sup>3</sup>Centre for Applied Physics and Radiation Technologies, School of Engineering and Technology, Sunway University, Bandar Sunway 47500, Malaysia.

College of Medicine, Alfaisal University P. O. Box 50927, Takhassusi Road Riyadh 1153, Kingdom of Saudi Arabia

Corresponding author: A/Prof Hamid Osman, ha.osman@tu.edu.sa

Generally, Computed Tomography (CT) procedure makes a higher dose to patient compared to other conventional imaging procedures. Diagnostic Reference Levels (DRLs) are widely used to determine the unusual high patient doses from radiologic examinations. Because of its high radio-sensitivity, even a low radiation dose to pelvis may carry a greater risk to individual or descendant. The purpose of this study is to estimate the pelvis radiation dose and establish provincial DRLs. Several imaging parameters such as tube voltage, current as well as pitch and number of slices, CT dose index and dose length product (DLP) were recorded for 275 patients exposed at different radiology departments in Taif City, Saudi Arabia. Patients' characteristics (age, body mass index and number of CT examinations) were also recorded. In calculation of effective dose (ED), the Monte Carlo methods and DLP-based conversion coefficients were used. The use of any contrast media examinations was excluded from the calculation. The mean  $CTDI_{vol}$ , DLP, ED and DRL for the current study was estimated to be 20mGy, 600 mGy-cm, 8.9 mSV and 14.4 mSV, respectively. The third quartile was introduced to estimate the DRL for the pelvis examinations. The results show similar values with the recent studies available in the literature. The obtained provincial DRLs may allow an effective reduction in patient dose without resulting in degradation of image quality. Recommendations: Further CT studies are recommended for other organs, specifically CT examinations that carried out with contrast media where higher photoelectric absorption were occurred and consequently pose a higher dose and DRLs .



**ISRP 2021**  
**International Symposium on Radiation Physics**  
**Kuala Lumpur – Malaysia**  
**6 – 10 December 2021**

**A139 - Development of flexible radiation shielding materials from natural rubber/  
Sb<sub>2</sub>O<sub>3</sub> composites**

Supakit Yonphan<sup>1,2</sup>, Ekwipoo Kalkornsuraanee<sup>3</sup>, Pruittipol Limkitjaroenporn<sup>1,2</sup>, Suchart Kothan<sup>4</sup>, Siriprapa Kaewjaeng<sup>4</sup>, Jakrapong Kaewkhao<sup>1,2</sup>

<sup>1</sup>Physics program, Faculty of Science and Technology, Nakhon Pathom Rajabhat University, Nakhon Pathom 73000, Thailand

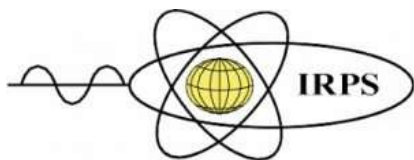
<sup>2</sup>Center of Excellence in Glass Technology and Materials Science (CEGM), Nakhon Pathom Rajabhat University, Nakhon Pathom, 73000, Thailand

<sup>3</sup>Department of Materials Science and Technology, Faculty of Science, Prince of Songkla University, Hat-Yai, Thailand

<sup>4</sup>Center of Radiation Research and Medical Imaging, Department of Radiologic Technology, Faculty of Associated Medical Sciences, Chiang Mai University, Chiang Mai, Thailand

Corresponding author: supakit.sc.phy@gmail.com

In this paper, the flexible materials from natural rubber (NR) has been developed for possible application in radiation shielding. Composites of natural rubber (NR) were prepared by incorporating Antimony oxide (Sb<sub>2</sub>O<sub>3</sub>) with various loading levels. Crosslink density and mechanical properties such as Modulus at 100% elongation, tensile strength, elongation at break, hardness and a specific gravity of the NR composites were investigated. For the gamma ray shielding properties, were measured in energy range 0.223 MeV–0.662 MeV using Compton scattering technique for variation the energy from Cs-137 source. From the results, the increasing of Sb<sub>2</sub>O<sub>3</sub> concentrations in the NR composites helped to increase the values of mass attenuation coefficient ( $\mu_m$ ), effective atomic number ( $Z_{eff}$ ), effective electron density ( $N_e$ ) and lead equivalent, While the half value layer (HVL) values of all samples were decreased with the increasing of Sb<sub>2</sub>O<sub>3</sub> concentrations. For the X-ray radiation attenuation properties, the linear attenuation coefficient ( $\mu$ ) and lead equivalent (dPb) were increased with increased Sb<sub>2</sub>O<sub>3</sub> add in NR and show the decreasing of X-ray energies range. These results reflect that the NR/Sb<sub>2</sub>O<sub>3</sub> composites are suitable for flexible radiation shielding materials.



**ISRP 2021**  
**International Symposium on Radiation Physics**  
**Kuala Lumpur – Malaysia**  
**6 – 10 December 2021**

**A141 - Simultaneous X-ray Scattering and Spectroscopy Computed Tomography – Monte Carlo Simulation and Experiment**

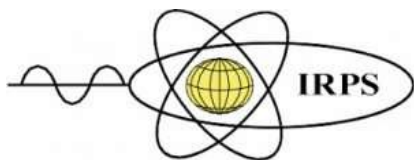
Andre L. C. Conceicao<sup>1</sup>, Marcelo Antoniassi<sup>2</sup>, Sylvio Haas<sup>1</sup>

<sup>1</sup>Deutsches Elektronen-Synchrotron DESY, Notkestraße 85, D-22607 Hamburg, Germany

<sup>2</sup>Federal University of Technology–Paraná, Curitiba 80230-901, Brazil

Corresponding author: andre.conceicao@desy.de

Simultaneous imaging of multiple and complementary probes represents a substantial step toward high specificity and large length-scale imaging. In this work, we combine the element-specific nature of X-ray Fluorescence with the ability of X-ray Compton scattering to provide information about the low atomic number matrix of materials by using the Rayleigh-to-Compton ratio technique (R/C), coupled with the capability of the Small-angle X-ray Scattering (SAXS) technique to probe particle sizes, shapes and orientations in the nano- to the mesoscopic range (up to about 1  $\mu\text{m}$ ). The simulations were performed using the Monte Carlo approach XRMC and a python-based in-house collagen fibril simulator. The simulations were compared against the experiment results for a phantom, specially design for this study. Finally, it will be shown the potential of exploiting the complementarity between X-ray scattering and spectroscopy techniques tomographically acquired, to map simultaneously three-dimensionally relevant features of the sample.



**ISRP 2021**  
**International Symposium on Radiation Physics**  
**Kuala Lumpur – Malaysia**  
**6 – 10 December 2021**

### **A142 - Barium Sulfate and Concrete Mixture as High Energy X-ray Radiation Shielding**

I. H. Hashim<sup>1,2</sup>, E. K. Lai<sup>1</sup>, M. S. M. Sanusi<sup>1</sup>, A. K. Ismail<sup>1</sup>, Y.J. Unn<sup>3</sup>

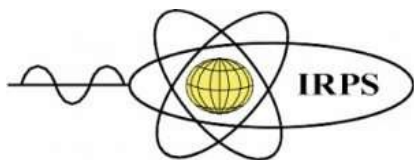
<sup>1</sup>Department of Physics, Faculty of Science, Universiti Teknologi Malaysia, 81310 Johor Bahru, Johor.

<sup>2</sup>National Centre Particle Physics, Universiti Malaya, 50603 Kuala Lumpur.

<sup>3</sup>Billion Prima Sdn Bhd, PTB 1587, Jalan Sengkang, Kawasan Perusahaan Sri Sengkang, 81000 Kulai, Johor

Corresponding author: izyan@utm.my

High energy X-ray penetrates most matter without any problem and the common shielding for X-ray is lead or concrete with various thickness. Betatron is a promising compact accelerator that are capable of producing high energy X-ray for industrial cargo scanner. Present work highlights the MCNP5 simulation of barium sulfate ( $\text{Ba}_2\text{SO}_4$ ) and concrete mixture radiation shielding for 9 MeV betatron at Billion Prima Sdn Bhd. Several points are marked within layers of the shielding materials to observe the radiation absorption and dose. Within the MCNP5 framework, the density of materials involved are set to  $1.2930 \times 10^{-3} \text{ g/cm}^3$  for air,  $3.35 \text{ g/cm}^3$  for well-mixed concrete barite,  $4.5 \text{ g/cm}^3$  for barite and  $2.35 \text{ g/cm}^3$  for cement. Based on our observation, combination design of well-mixed barite concrete shows the good shielding property as the radiation dose reading outside the inspection room shows the lowest reading which is  $4.1600 \mu\text{Sv}$ . The used of well mixed concrete and  $\text{Ba}_2\text{SO}_4$  as radiation shielding effectively reduced the incident X-ray absorption and backscattered X-ray during cargo scanning procedure.



**ISRP 2021**  
**International Symposium on Radiation Physics**  
**Kuala Lumpur – Malaysia**  
**6 – 10 December 2021**

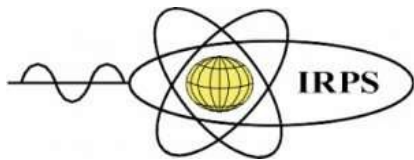
**A143 - Fourier Transform Holography with Extended Reference: a step toward the use of photons of higher energy**

Minh H. Dao<sup>1</sup>, Chanh Q. Tran<sup>1</sup>, Tony Kirk<sup>1</sup>, Paul Di Pasquale<sup>1</sup>

Department of Chemistry & Physics, La Trobe Institute for Molecular Science, La Trobe University, Australia

Corresponding author: [h.dao@latrobe.edu.au](mailto:h.dao@latrobe.edu.au)

Fourier Transform Holography (FTH) is a single-shot imaging technique that can determine both the absorption and phase of a sample. However, there are major practical challenges in fabricating the FTH object mask. Consequently, FTH related studies have only been demonstrated in the Extreme UV regime. In this presentation, we will present a simulation study of a new approach, which makes it possible to use FTH with photons of higher energy region (i.e., x-ray).



**ISRP 2021**  
**International Symposium on Radiation Physics**  
**Kuala Lumpur – Malaysia**  
**6 – 10 December 2021**

**A145 - Relation between energy dependence and dosimeter size: An experimental study on glass TLDs**

Farhad Moradi<sup>1</sup>, Ghafour Amouzad Mahdiraji<sup>2</sup> Khadijeh Rezaee Ebrahim Saraee<sup>1</sup>

Mayeen Uddin Khandaker<sup>3</sup> Faisal Rafiq Mahamd Adikan<sup>4</sup> David Bradley<sup>3,5</sup>

<sup>1</sup>Faculty of Physics, University of Isfahan, Isfahan, Iran

<sup>2</sup>Flexilicate Sdn. Bhd., University of Malaya, Kuala Lumpur, Malaysia

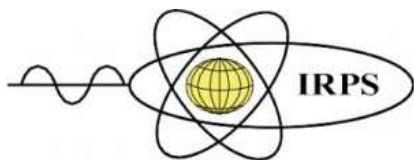
<sup>3</sup>Centre for Biomedical Physics, School of Healthcare and Medical Sciences, Sunway University, Bandar Sunway, Selangor, Malaysia

<sup>4</sup>Integrated Lightwave Research Group, Department of Electrical Engineering, Faculty of Engineering, University of Malaya, Kuala Lumpur, Malaysia

<sup>5</sup>Department of Physics, University of Surrey, Guildford, Surrey, UK

Corresponding author: morfar1982@gmail.com

Practical Use of a dosimeter in a range of photon energies necessitates recognition of the radiation field as well as energy response of the dosimeter. Energy dependence is caused by the unequal absorption properties of the material from various radiation energies. The emphasis on the tissue equivalence of a dosimeter is also mainly due to energy dependent response of non-tissue equivalent materials. The aim in this work was to measure the energy dependence of the response of capillary glass silica fibre thermoluminescent dosimeters and to check whether there is a relation between energy dependence and the size of the dosimeter. Irradiations were performed in free-in-air condition at the secondary standard dosimetry laboratory (SSDL) of the Malaysian Nuclear Agency using X-ray narrow beam series spectra and gamma rays from a <sup>137</sup>Cs source as the reference photon energy. Small size TLDs of hollow rod shape with the external/internal diameters of 870/544, 386/241 and 127/79  $\mu\text{m}$  and 3 mm length prepared by a precision cutting process and preconditioning were irradiated at various photon energies. Theoretical energy dependence calculated from the ratio of mass energy absorption coefficients as well as the results from the Monte Carlo (MC) simulations using the MCNPX code were also used for the comparison. The results show an increasing energy dependence trend with the dosimeter size in the studied range. This can be explained based on the cavity theory, MC simulation results and size-dependence of the luminescence efficiency at various photon energies.



**ISRP 2021**  
**International Symposium on Radiation Physics**  
**Kuala Lumpur – Malaysia**  
**6 – 10 December 2021**

**A147 - Dosimetry audit of megavoltage photon beams under non-reference conditions:  
Comparison of fabricated Ge-doped optical fibres and TLD-100 systems**

Muhammad Safwan Ahmad Fadzil<sup>1,2</sup>, Noramaliza Mohd Noor<sup>2</sup>, Nizam Tamchek<sup>3</sup>, Ung Ngie Min<sup>4</sup>, Norhayati Abdullah<sup>5</sup>, Mohd Taufik Dolah<sup>5</sup>

<sup>1</sup>Diagnostic Imaging and Radiotherapy Programme, Centre for Diagnostic, Therapeutic and Investigative Studies, Faculty of Health Sciences, Universiti Kebangsaan Malaysia, 50300, Kuala Lumpur, Malaysia

<sup>2</sup>Department of Radiology, Faculty of Medicine and Health Sciences, Universiti Putra Malaysia, 43400, Serdang, Selangor, Malaysia

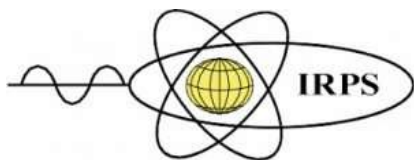
<sup>3</sup>Department of Physics, Faculty of Science, Universiti Putra Malaysia, 43400, Serdang, Selangor, Malaysia

<sup>4</sup>Clinical Oncology Unit, Faculty of Medicine, University of Malaya, 50603, Kuala Lumpur, Malaysia

<sup>5</sup>Radiation Safety and Health Division, Malaysian Nuclear Agency, Bangi, 43000 Kajang, Selangor, Malaysia

Corresponding author: safwanfadzil@ukm.edu.my

The present study compares the feasibility of fabricated Ge-doped optical fibres as a potential remote dosimeter for radiotherapy postal dosimetry audit in non-reference conditions to a commercial thermoluminescence dosimetry (TLD-100) system. The optical fibres system was made up of two types of fibres: cylindrical (CF) and flat fibres (FF). The dosimetric characteristics of the systems were studied and compared, with particular attention paid to dose linearity, energy dependency, reproducibility, and fading. Methods for measuring absorbed doses of CF, FF, and TLD-100 were developed, as well as uncertainty budgets. A preliminary audit was performed under non-reference conditions to assess the variations in absorbed doses measured by CF and FF over TLD-100. For both 6 MV and 10 MV photon beams, CF, FF, and TLD-100 exhibit linear dose-response from 1 Gy to 3 Gy with a coefficient of determination ( $R^2$ ) greater than 0.99, minimum energy dependency, and good reproducibility of 2.2%, 2.9%, and 1.8%, respectively. The highest fading rate were determined to be 37.6%, 63.4%, and 14.2% for CF, FF, and TLD-100, respectively, over the 106<sup>th</sup> day following irradiations. Several correction factors have been established for the absorbed dose formalism utilizing these two dosimetry systems. For irradiation with a 6 MV photon beam, the combined relative standard uncertainty in the absorbed dose determined from CF, FF, and TLD-100 measurements were estimated to be 4.3%, 5.56%, and 0.74%, respectively. The preliminary audit for the absorbed dose measurement under non-reference conditions observed no significant differences ( $p > 0.05$ ) in the absorbed dose measured by CF, FF, and TLD-100. The fabricated Ge-doped optical fibre systems have commensurate dosimetric performance to TLD-100 and can be utilized as a potential remote dosimeter for postal dosimetry audits with appropriate correction factors applied to the absorbed dose measurements.



**A148 - X ray spectrometry methodologies for sustainable cancer tissue analysis – recent advances and limitations**

Sofia Pessanha<sup>1,2</sup>, Patrícia M. Carvalho<sup>1,2,3</sup>, Delfim Doutel<sup>4,5</sup>, Eva Marguí<sup>6</sup>, Daniel Braga<sup>1</sup>, Alexandre Veiga<sup>1</sup>, António A. Dias<sup>1,2</sup>, Diogo Casal<sup>2,4</sup>, Diogo Pais<sup>b,d</sup>, José Paulo Santos<sup>1,2</sup>, Maria Luísa Carvalho<sup>1,2</sup>, Ana Félix<sup>4,5</sup>, Jorge Machado<sup>1,2</sup>

<sup>1</sup>NOVA School of Science and Technology, Campus Caparica, 2829-516, Caparica, Portugal

<sup>2</sup>LIBPhys, Laboratory of Instrumentation, Biomedical Engineering and Radiation Physics

<sup>3</sup>Institute for Nanostructures, Nanomodelling and Nanofabrication (i3N), Physics Department, University of Aveiro, 3810-193 Aveiro, Portugal

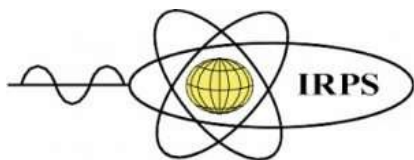
<sup>4</sup>NOVA Medical School, Campo dos Mártires da Pátria 130, 1169-056 Lisboa

<sup>e</sup>Instituto Português de Oncologia de Lisboa Francisco Gentil (IPOLFG)

<sup>5</sup>Department of Chemistry, University of Girona (UdG), C/M.Aurèlia Capmany, 69, 17003 Girona

Corresponding author: sofia.pessanha@fct.unl.pt

Trace elements play an important role in biological processes and an association between the levels of trace elements and the presence of diseases such as cancer has already been established. Thus, the understanding of the mechanisms of assimilation of trace elements may be indicative of the genesis or progression of the disease. Energy Dispersive X-ray Fluorescence technique (EDXRF) might be the innovative technique for screening analysis as it constitutes the ideal compromise for a non-destructive, of simple instrumentation and good sensitivity technique for the elements of interest. For these reasons, this technique has already been tested in research regarding to the characterization of tumour tissues. However, there is always a great impairment to statistically significant conclusions: the extremely reduced number of samples. The research here presented intends to overcome this obstacle by taking advantage of the vast repository of human tissue samples, fixed in formalin and embedded in paraffin, that is stored in Portuguese hospitals. However, there is a major disadvantage when using these samples, namely the type of substrate (formalin and/or paraffin), that increases the factor of greatest uncertainty in the quantification by EDXRF: the characterization of the dark matrix of the sample. This methodology will be based on the analysis and characterization of "fresh" normal tissues by the techniques already established suitable: EDXRF, but also with Total Reflection X-Ray Fluorescence (TXRF) and Inductively Coupled Plasma Optical Emission Spectrometry (ICP-OES). This way, we will obtain an accurate elemental quantification of the tissues, that we will then parameterize as we go through the paraffin inclusion steps. The final samples will be analysed again by EDXRF, in order to create a matrix correction model.



**ISRP 2021**  
**International Symposium on Radiation Physics**  
**Kuala Lumpur – Malaysia**  
**6 – 10 December 2021**

**A154 - COMBAT algorithm for the coordination of delineation of multiple radiologists of nodule boundaries in lung computed tomography images**

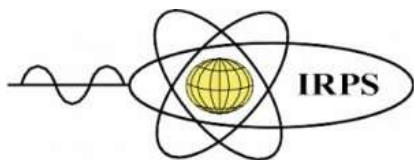
Xiaolei Zhang<sup>1,2</sup>, Xianling Dong<sup>2</sup>, M. Iqbal bin Saripan\*<sup>1</sup>

<sup>1</sup>Faculty of Engineering, Universiti Putra Malaysia, Malaysia

<sup>2</sup>Department of Biomedical Engineering, ChengDe Medical University, China

Corresponding author: 721867783@qq.com

The global incidence of malignant tumors is increasing every year, and 70% of them receive radiotherapy. The accuracy of tumor boundary delimitation greatly influences the success of radiotherapy. Nodule boundaries are usually marked by experienced radiologists. However, marking is highly subjective and may lead to errors. Therefore, research to further improve the accuracy of marking and automatically correct radiologists' marking errors is ongoing. In this study, 340 nodules were selected from computed tomography (CT) images of lung nodules. Center on the centroid direction gradient (CDG) of the boundary drawn by each radiologist on the CT image. The direction is drawn from the centroid of the polygon to the boundary point of the polygon. The centroid direction gradient (CDG) of the boundary drawn by each radiologist on the CT image was considered as the center. The COMBAT method was used to coordinate the CDG, and the boundary of the nodule was redrawn according to the newly obtained direction gradient. The results showed that the COMBAT method increases the accuracy of delineation of the tumor boundary, and at the same time, it can clean the error points of the data set. Analysis of variance showed that significant differences between the CDGs of each expert disappeared after coordination. this method can be used to correct delineation errors, making delineation of the tumor boundary more accurate.



**ISRP 2021**  
**International Symposium on Radiation Physics**  
**Kuala Lumpur – Malaysia**  
**6 – 10 December 2021**

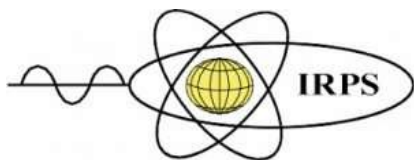
### **A155 - Overview of methods for determining the depth distribution of elements in X-ray fluorescence analysis**

Ladislav Musilek, Radek Prokes, Tomas Trojek

Faculty of Nuclear Sciences and Physical Engineering, Czech Technical University in Prague, Czech Republic

Corresponding author: musilek@fjfi.cvut.cz

X-ray fluorescence analysis is a frequently used analytical method in a number of areas, including the research of objects of cultural heritage. Especially in this area, the irreplaceable advantage is the fact that the measurement can be performed non-destructively and non-invasively on the examined object as a whole. If it is to be used in a non-destructive manner, it only affects a relatively thin layer at the surface of the object under investigation, nevertheless, this layer can have a complex structure (various coatings, gilding or other metallization, etc.). Information about it can be a valuable contribution both to historical knowledge and to restoration work. During the development of the method, therefore, several procedures were elaborated to estimate the homogeneity or possible inhomogeneities of the investigated layer. In principle, the simplest one is to measure at different beam angles. However, this also changes the depth in the material into which the radiation penetrates. Without changing the measurement geometry, it is possible to use simultaneous detection of two different energy lines of the characteristic radiation of the investigated element (e.g.,  $K_{\alpha}$  and  $K_{\beta}$ ) and to evaluate the depth distribution on the basis of their ratio. Finally, the most sophisticated, but also the most informative, is the confocal arrangement of the spectrometer, where the focus, i.e. the intersection of the beams of incident and emitted radiation very narrowly collimated the by the capillary optics, shifts to the depth of the measured material. The review paper summarizes the principles and possibilities of these methods, their advantages and limitations, and thus gives instructions for their use for specific needs. The use is illustrated by examples of specific measurements of art objects, realized in various laboratories, but especially in the laboratory of the authors of this paper.



**A156 - New analysis method for neutron dosimetry with Fluorescent Nuclear Track Detectors**

Anna Becker<sup>1,2</sup>, Oliver Jäkel<sup>1,3,4</sup>, José Vedelago<sup>1,3</sup>

<sup>1</sup>Department of Medical Physics in Radiation Oncology, German Cancer Research Center (DKFZ), Im Neuenheimer Feld 280, Heidelberg 69120, Germany

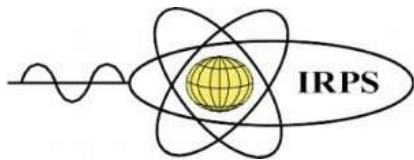
<sup>2</sup>Department of Physics and Astronomy, Heidelberg University, Im Neuenheimer Feld 226, Heidelberg 69120, Germany

<sup>3</sup>Heidelberg Institute for Radiation Oncology (HIRO), National Center for Radiation Research in Oncology (NCRO), Heidelberg, Germany

<sup>4</sup>Heidelberg Ion Beam Therapy Center (HIT), University Hospital Heidelberg, Im Neuenheimer Feld 450, Heidelberg 69120, Germany

Corresponding author: [anna.becker@dkfz.de](mailto:anna.becker@dkfz.de)

The production of secondary neutrons and their contribution to the non-target dose remains a general concern in the field of heavy ion therapy. Due to the high relative biological effectiveness of neutrons, their broad energy distribution and their large range in tissue, even small doses might be relevant. A precise determination of secondary neutron dose is required for the correct estimation of potential risks. Fluorescent Nuclear Track Detectors (FNTDs) are biocompatible passive detectors based on doped aluminium oxide and a promising tool for personal dosimetry, especially for the high-energy neutrons resulting from ion beams used for cancer treatment. They allow for single particle track detection on a microscopic scale while offering several superior characteristics compared to other available dosimeters in use. In this work, FNTD technology was implemented for neutron dosimetry using a standard Am-241/Be neutron source for irradiation and a confocal laser scanning microscope for detector readout. Acquired images were evaluated in terms of track density of recoil proton signals behind a polyethylene neutron converter that was placed between the neutron source and FNTD detectors during irradiation. The proton track density is found to be linear to dose and was therefore used to obtain a calibration curve of the FNTDs for neutron dosimetry. This study presents a new methodology for the post-irradiation data analysis, based on the intensity threshold parameter during the track reconstruction process. By doing this, it was possible to reduce the influence of the sensitivity differences between FNTDs, and the obtained calibration curve is in agreement with previous publications. This methodology will be used for experimental measurements of secondary neutrons at the Heidelberg Ion Beam Therapy Center (HIT), Heidelberg, Germany, along with other experimental techniques for comparison reasons.



**A159 - Sonologist occupational exposure and ambient dose resulted from patients underwent nuclear medicine procedure**

Gada Khouqeer\*<sup>1</sup>, H. Salah<sup>2,3\*</sup>, A Sulieman<sup>4</sup>, M. Alkhorayef<sup>5,6</sup>, N. Tamam<sup>7</sup>, and D.A. Bradley<sup>6,8</sup>

<sup>1</sup>Department of Physics, College of Science, Imam Mohammed bin Saud Islamic University, Riyadh, Saudi Arabia

<sup>2</sup>INAYA Medical Collage, Nuclear Medicine Department, Riyadh, Saudi Arabia

<sup>3</sup>College of Medical Radiologic Science, Sudan University of Science and Technology, Khartoum, Sudan

<sup>4</sup>Prince Sattam Bin Abdulaziz University, College of Applied Medical Sciences, Radiology and Medical Imaging Department, Alkharj, Saudi Arabia

<sup>5</sup>Department of Radiological Sciences, College of Applied Medical Sciences, King Saud University, Riyadh, Saudi Arabia

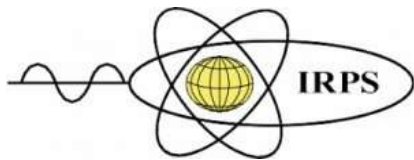
<sup>6</sup>Centre for Nuclear and Radiation Physics, Department of Physics, University of Surrey, Guildford, Surrey GU2 7XH, United Kingdom

<sup>7</sup>Department of Physics, College of Sciences, Princess Nourah Bint Abdulrahman University, Riyadh, Saudi Arabia

<sup>h</sup>Centre for Applied Physics and Radiation Technologies, School of Engineering and Technology, Sunway University, 47500, Bandar Sunway, Selangor, Malaysia.

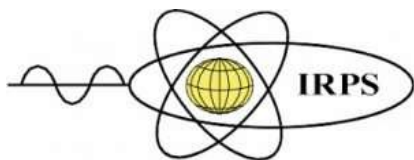
\*Corresponding author: gkhouqeer@gmail.com

Ultrasound personnel was exposed occupationally to ionizing radiation from radioisotopes during Ultrasound imaging. Thus, radiation safety assessment is required to ensure that the Ultrasound physician's practice conforms with the international guidelines and dose limits are not exceeded. This study aims to measure staff exposure during certain ultrasound investigations on patients who received radioactive material in molecular imaging procedures, including positron emission tomography (PET) and single-photon emission computed tomography (SPECT) procedures, and estimate the biological risk of occupational exposure. Occupational doses and ambient dose were monitored for Ultrasound physicians' personnel over one year and at King Faisal Specialist Hospital and Research Center (KFSHRC), Riyadh, Saudi Arabia. Occupational dose equivalent was measured in terms of Hp(10) (deep dose), Hp(0.07) (skin dose) using calibrated thermos-luminescent dosimeters (TLDs), TLD-200 (CaF<sub>2</sub>:Dy). TLDs were read using an automatic TLD reader (Harshaw 6600) in a nitrogen gas environment. The overall mean of Hp(10), Hp(0.07) for an annual occupational dose 0.4 mSv and ambient dose (mSv) were (M) in ultrasound room, Hot Lab were (Hp(10)=1.7 and Hp(0.07)=1.72 mSv) and in the Stress Room were (Hp(10)=0.4 and Hp(0.07)=0.02 mSv) respectively. Occupational exposure exceeded the annual dose limits (20.0 mSv) for some practitioners. The



**ISRP 2021**  
**International Symposium on Radiation Physics**  
**Kuala Lumpur – Malaysia**  
**6 – 10 December 2021**

extremities dose is below the annual dose limits (500 mSv). Staff exposure, which depends on radioisotopes characteristics and protection measures, can vary significantly for different personnel. Careful assessment of working conditions is recommended to ensure that occupational exposure is below the annual dose limits.



**A163 - Aluminum oxide crystals for high spatial resolution dosimetry of photon beams**

Roua Abdulrahim<sup>1,2</sup>, Oliver Jäkel<sup>1,3,4</sup>, José Vedelago<sup>1,3</sup>

<sup>1</sup>Department of Medical Physics in Radiation Oncology, German Cancer Research Center (DKFZ), Im Neuenheimer Feld 280, Heidelberg 69120, Germany

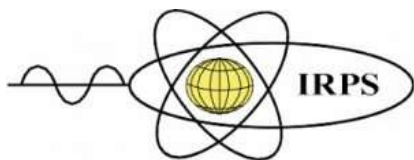
<sup>2</sup>Medical Faculty Mannheim, Heidelberg University, Theodor-Kutzer-Ufer 1-3, Mannheim 68167, Germany

<sup>3</sup>Heidelberg Institute for Radiation Oncology (HIRO), National Center for Radiation Research in Oncology (NCRO), Heidelberg, Germany

<sup>4</sup>Heidelberg Ion Beam Therapy Center (HIT), University Hospital Heidelberg, Im Neuenheimer Feld 450, Heidelberg 69120, Germany

Corresponding author: j.vedelago@dkfz.de

Microbeam Radiation Therapy (MRT) is a pre-clinical concept in radiation therapy that uses collimated arrays of micrometer width beams. A similar concept is minibeam radiation therapy, which uses millimeter-sized beam widths. Both techniques can deliver very high doses at the peak region and shallow doses at the valleys and have demonstrated equivalent tumor control to conventional radiation therapy and better sparing of healthy tissue. An accurate dose measurement of these beams requires a micro-scale detector with high spatial resolution and a wide dynamic range to account for the dose variation between the peak and the valley. In this work, the performance of Fluorescent Nuclear Track Detectors (FNTDs), based on aluminum oxide crystal doped with carbon and magnesium, was examined as a dose verification tool for photon sources such as Cesium 137 and X-ray beams, and MRT spatially collimated beams. The FNTDs were read out using a confocal laser microscope which provides sub-micrometer resolution and multiple non-destructive detector readouts. For data analysis, three methods were used to quantify the fluorescence signal from the detectors, namely, the image mean intensity, the fluorescence count rate, and the frequency domain analysis by means of the power spectrum integral. The results obtained with the three methodologies agree with previous studies in the dose range of 0.1 Gy to 100 Gy. A preliminary MRT dosimetry application was achieved with a range of doses from 2 Gy up to 50 Gy, and it was possible to estimate the full width at half maximum (FWHM) and the peak-to-valley dose ratio (PVDR) as the main parameters of the spatially fractionated dose resulting from the MRT beams.



**ISRP 2021**  
**International Symposium on Radiation Physics**  
**Kuala Lumpur – Malaysia**  
**6 – 10 December 2021**

**A164 - Effective dose and radiogenic risk during certain computed tomography examinations**

A. Sulieman<sup>1</sup>, N. Tamam<sup>2</sup>, Abdelrahman Elnour<sup>3</sup>, Alkhorayef<sup>4,5</sup>, Mayeen Uddin Khandaker<sup>6</sup>, David A. Bradley<sup>5,6</sup>

<sup>1</sup>Prince Sattam Bin Abdulaziz University, College of Applied Medical Sciences, Radiology and Medical Imaging Department, P.O.Box 422, Alkharj 11942, Saudi Arabia

<sup>2</sup>Physics Department, College of Sciences, Princess Nourah Bint Abdulrahman University, P.O. Box 84428, Riyadh 11671, Saudi Arabia

<sup>3</sup>Radiologic Science Department, College of Radiology and Nuclear Medicine, The National Ribat University, Khartoum, Sudan

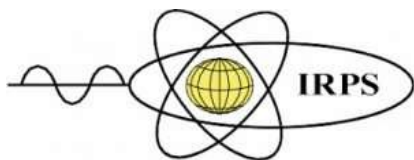
<sup>4</sup>Department of Radiological Sciences, College of Applied Medical Sciences, King Saud University, P.O. Box 10219 Riyadh 11433, Saudi Arabia

<sup>5</sup>Centre for Nuclear and Radiation Physics, Department of Physics, University of Surrey, Guildford, Surrey GU2 7XH, UK

<sup>6</sup>Centre for Applied Physics and Radiation Technologies, School of Engineering and Technology, Sunway University, 47500, Bandar Sunway, Selangor, Malaysia.

Corresponding author: E mail: [abdelmoneim\\_a@yahoo.com](mailto:abdelmoneim_a@yahoo.com)

Radiation exposure from computed tomography (CT) examinations contributed to more public exposure from medical procedures. Establishing the diagnostic reference levels (DRL) is recommended as an effective dose optimization method for patients' doses. This study aims to measure patient's doses and establish the DRL for CT brain and paranasal sinuses procedures. Sixty-six patients underwent CT procedures at 7 CT departments equipped with CT modalities from different vendors. The Scheffe test was used to analyze variable differences. Patient age ranges were 19- to 70 years. The radiation dose ranges for paranasal sinuses procedure (PNS) were 185 mGy.cm to 587 mGy.cm, and 12.6 mGy to 55 mGy in terms of dose length product (DLP) and volume CT dose index (CTDIvol) in that order. There are statistically significant differences at the level of significance (0.05) or less in the variables (tube current-time product (mAs), DLP, and CTDI) attributable to hospitals. There are no statistically significant differences at the significance level (0.05) or less in the variable (age) attributable to hospitals. In addition to that, there are statistically significant differences at the level of significance (0.05) or less in the variable (CTDIvol) attributable to the number of CT slices. DRLs are proposed for all of the investigated CT procedures. The patient radiation doses observed herein are more significant than those typically seen in other studies worldwide.



**A166 - Carbon isotope composition ( $^{14}\text{C}$  and  $^{13}\text{C}$ ) of the atmospheric  $\text{CO}_2$  at several locations in Croatia**

Ines Krajcar Bronić<sup>1</sup>, Damir Borković<sup>1</sup>, Emma Hess<sup>2</sup>, Tjaša Kanduč<sup>3</sup>, Jadranka Barešić<sup>1</sup>,  
Andreja Sironić<sup>1</sup>

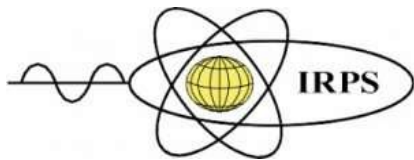
<sup>1</sup>Department of Experimental Physics, Ruđer Bošković Institute, Zagreb, Croatia

<sup>2</sup>Department of Physics (student), University of Rijeka, Rijeka, Croatia

<sup>3</sup>Department of Environmental Sciences, Jožef Stefan Institute, Ljubljana, Slovenia

Corresponding author: krajcar@irb.hr

Radiocarbon ( $^{14}\text{C}$ ) is both the cosmogenic and anthropogenic isotope. Anthropogenic sources of  $^{14}\text{C}$  are atmospheric nuclear bomb tests, various nuclear facilities and fossil fuel combustion. The bomb-produced  $^{14}\text{C}$  has been globally distributed across the planet and can be considered as a new-natural level (clean-air sites). Combustion of fossil fuels that do not contain  $^{14}\text{C}$  causes increase of atmospheric  $\text{CO}_2$  concentration and depletion of local  $^{14}\text{C}$  levels, while nuclear sources increase local or regional atmospheric  $^{14}\text{C}$  level. Naturally produced  $\text{CO}_2$  and that formed by fossil fuel combustion are characterized by different content of the stable isotope  $^{13}\text{C}$  ( $\delta^{13}\text{C}$  values) in addition to their different  $^{14}\text{C}$  content. Therefore, the carbon isotope composition ( $^{13}\text{C}$  and  $^{14}\text{C}$ ) of the atmospheric  $\text{CO}_2$  can indicate sources of  $\text{CO}_2$  at each location, if it is far from nuclear facilities.  $^{14}\text{C}$  activity in the atmospheric  $\text{CO}_2$  in Zagreb, Croatia, has been monitored since 1985. Recently we have been monitoring carbon isotope composition at several other locations in Croatia (city of Rijeka and rural areas around Zagreb and Rijeka) with the aim of determining influence of fossil fuel combustion on atmospheric  $^{14}\text{C}$  activity and  $\delta^{13}\text{C}$  values at different locations with the hypothesis that the urban sites are affected by fossil fuel uses. Rural locations show higher  $^{14}\text{C}$  activities (by about 2 pMC – percent Modern Carbon) and higher  $\delta^{13}\text{C}$  values than the urban sites in accordance with the hypothesis. The difference is larger during winter (about 2.4 pMC) due to more intense fossil fuel combustion in the cities.



**A168 - A Markov Random Field Approach for CT Image Lung Classification using Image Processing**

K. A. A. Aziz<sup>1,2</sup>, M. I. Saripan<sup>1</sup>, F. F. A. Saad<sup>3</sup>, R. S. A. R. Abdullah<sup>1</sup>

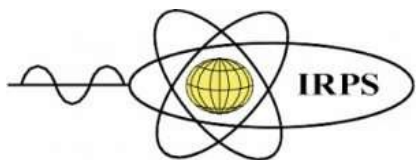
<sup>1</sup> Faculty of Engineering, Universiti Putra Malaysia, Malaysia

<sup>2</sup> Faculty of Electrical and Electronic Engineering Technology, Universiti Teknikal Malaysia Melaka, Malaysia

<sup>3</sup> Faculty of Medicine and Health Sciences, Universiti Putra Malaysia, Malaysia

Corresponding author: iqbal@upm.edu.my

In this study, the performance of computed tomography lung classification using image processing and Markov Random Field were investigated. For lung classification, the process must first be going thru lung segmentation process. Lung segmentation is important as an initial process before lung cancer segmentation and analysis. Image processing was employed to the input image. We propose multilevel thresholding and Markov Random Field to improve the segmentation process. Three setting for Markov Random Field was used for segmentation process that is Iterated Condition Mode, Metropolis algorithm and Gibbs sampler. The output from the experiments were analysed and compared to get the best performance. The results revealed that for CT image lung classification, Markov Random Field using Metropolis algorithm gives the best results. In view of the result obtained, the average accuracy is 94.75% while the average sensitivity and specificity are 76.34% and 99.80%. The output from this study can be implemented in lung cancer analysis research and computer aided diagnosis development.



**A175 - Pediatric radiation dosimetry and radiogenic risk estimation from computed tomography examinations**

N. Tamam<sup>3\*</sup> <sup>1</sup>, Abdelmoneim Sulieman<sup>2\*</sup>, Abdulrahman Elnour<sup>3</sup>, Mohammed Alkhoaryef<sup>4</sup>,  
Mayeen Uddin Khandaker<sup>5</sup>, David Bradley<sup>5,6</sup>

<sup>1</sup>Physics Department, College of Sciences, Princess Nourah Bint Abdulrahman University, P.O Box 84428, Riyadh 11671, Saudi Arabia

<sup>2</sup>Prince Sattam bin Abdulaziz University, College of Applied Medical Sciences, Radiology and Medical Imaging Department, Alkharj, Saudi Arabia

<sup>3</sup>Radiology Department, College of Radiological Sciences and Nuclear Medicine, National Ribat University, Khartoum, Sudan.

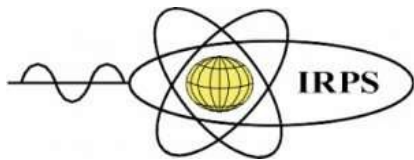
<sup>4</sup>Department of Radiological Sciences, College of Applied Medical Sciences, King Saud University, P.O Box 10219 Riyadh 11433, Saudi Arabia

<sup>5</sup>Centre for Nuclear and Radiation Physics, Department of Physics, University of Surrey, Guildford, Surrey GU2 7XH, UK

<sup>6</sup>Centre for Applied Physics and Radiation Technologies, School of Engineering and Technology, Sunway University, 47500, Bandar Sunway, Selangor, Malaysia.

Corresponding author: E mail: nmtamam@pnu.edu.sa

Pediatrics are vulnerable to ionizing radiation exposure due to their rapidly dividing cells compared to adults. Computed Tomography is one of the most imaging modalities used in hospitals worldwide. It contributes up to 72% of the collective dose for the whole population from medical procedures. Although the task is essential, few studies were performed in Saudi Arabia regarding medical exposure patients' doses. The objectives of this study were to evaluate the radiation dose for patients during CT scan of the brain, Chest, Abdomen, and CAP :( chest, abdomen, and pelvis in one scanning) and estimate the effective dose for the patients undergoing CT exams. Two hundred eighty-two patients were examined from five hospitals using five multi-detector CT machines. The radiation dose parameters were presented in terms of CTDIvol (mGy) and DLP (mGy.cm). The mean CTDIvol (mGy) was 51, 9, 10, and 11 mGy for the head, chest, abdomen, and CAP, respectively. The mean DLP (mGy.cm) was 912, 428, 604, and 738 for head, chest, abdomen, and CAP, in that order. Patients have been exposed to the highest dose during head CT procedures while the lowest was during CT chest. Patient doses depend on imaging protocol and the anatomy of the organ of interest. Patient doses showed wide variations due to technologist selection of exposure parameters. The patient doses were higher compared to most of the previous studies.



**ISRP 2021**  
**International Symposium on Radiation Physics**  
**Kuala Lumpur – Malaysia**  
**6 – 10 December 2021**

**A179 - Primary scintillation in gaseous xenon for x-rays and alpha-particles**

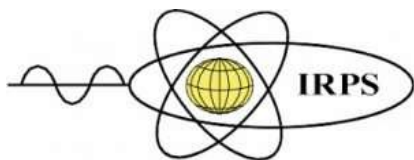
Carlos A. O. Henriques<sup>1</sup>, Joana M. R. Teixeira<sup>1</sup>, Pedro A. O. C. Silva<sup>1</sup>, Rui D. P. Mano<sup>1</sup>, Diego González-Díaz<sup>2</sup>, Cristina M. B. Monteiro<sup>1</sup>

<sup>1</sup>LIBPhys, Physics Department, University of Coimbra, Portugal

<sup>2</sup>Instituto Gallego de Física de Altas Energías, University of Santiago de Compostela, Spain

Corresponding author: henriques@uc.pt

Xenon scintillation has been widely used in rare event detection experiments, such as double beta decay and double electron capture, with or without neutrino emission, as well as dark matter. However, information on the primary scintillation yield in the absence of recombination is still scarce and dispersed. The mean energy required to produce a vacuum ultraviolet scintillation photon ( $W_{sc}$ ) in gaseous xenon has been measured in the range of 30-120 eV. Lower  $W_{sc}$ -values are often reported for alpha particles compared to electrons produced by gamma or x-rays, being this difference not understood. We carried out a systematic study of the absolute primary scintillation yield in Xe at 1.2 bar, using a Gas Proportional Scintillation Counter. The simulation model of the detector's geometric efficiency was benchmarked through the primary and secondary scintillation signals produced at different distances from the photosensor.  $W_{sc}$ -values were obtained for gamma and x-rays with energies in the range 5.9-25 keV, and for 2-MeV alpha particles. No significant differences were found between alpha particles and electrons.



**ISRP 2021**  
**International Symposium on Radiation Physics**  
**Kuala Lumpur – Malaysia**  
**6 – 10 December 2021**

**A181 - Contribution to the economic heavy minerals of East El- Arish coastal sediments, North Sinai, Egypt.**

M. Awad<sup>1,\*</sup>, A. M. El Mezayen<sup>2</sup>, A. El Azab<sup>1</sup>, S.M.a Alfi<sup>1</sup>, M I Sayyed<sup>3,4</sup>, Mayeen Uddin Khandaker<sup>5</sup>, H. H. Ali<sup>1</sup>, M.Y. Hanfi<sup>1,6</sup>

<sup>1</sup>Nuclear Materials Authority. P.O. Box 530, El Maadi, Cairo, Egypt

<sup>2</sup>Geology Department.Faculty of Science. Al Azhar University Nasr City, Cairo, Egypt.

<sup>3</sup>Department of Physics, Faculty of Science, Isra University, Amman – Jordan

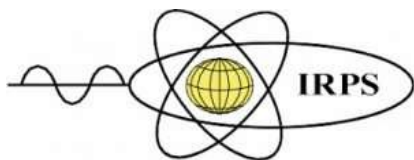
<sup>4</sup> Department of Nuclear Medicine Research, Institute for Research and Medical Consultations (IRMC), Imam Abdulrahman bin Faisal University (IAU), PO Box 1982, Dammam, 31441, Saudi Arabia

<sup>5</sup>Center for Applied Physics and Radiation Technologies, School of Engineering and Technology, Sunway University, 47500 Bandar Sunway, Selangor Darul Ehsan, Malaysia

<sup>6</sup>Ural Federal University, Mira Street 19, 620002, Ekaterinburg, Russia

Corresponding author: awad026@yahoo.com

The Egyptian beach black sands and sand dune placer deposits are discontinuously distributed along the Mediterranean Sea Coast including El- Arish coastal area, North Sinai, Egypt. Several drill hole (well) samples representing the main two geomorphologic units in the studied area; beach sand and sand dune were homogeneously mixed and collected to give one composite sample for individual well. Separation of economic heavy minerals using heavy liquid technique are considered. The total heavy minerals (THM) of beach sand varies from 2.7 to 11.39%, with an average 4.5%, while the mean content of total heavy minerals in sand dune is 2.89%. The opaque minerals, especially magnetite, ilmenite and leucoxene, represent more than 40% of the economic heavy minerals content. There is a wider variation in the non-opaque minerals that are dominated by zircon, rutile, apatite, monazite, garnet group, and silicates minerals (including amphiboles, pyroxenes, muscovite and biotite). Mineralogical examinations including XRD and ESEM, were done with an emphasis on the more radioactive minerals that comprise monazite and zircon. The ESEM analyses of monazite indicate that Th and U content with an average of 11.24% and 2.17% respectively are the main minerals responsible of the radioactivity in the studied area.



**ISRP 2021**  
**International Symposium on Radiation Physics**  
**Kuala Lumpur – Malaysia**  
**6 – 10 December 2021**

**A182 - Radiological Hazards associated to a raw material of Um Bogma area, southwestern Sinai, Egypt**

El Saeed R. Lasheen<sup>1</sup>, Mostafa S. Elstohy<sup>2</sup>, M. Y. Hanfi<sup>2,3</sup>, M I Sayyed<sup>4,5</sup>, Mayeen Uddin Khandaker<sup>6</sup>

<sup>1</sup>Geology Department, Faculty of Science, Al-Azhar University, Cairo, P.O. Box 11884, Egypt.

<sup>2</sup>Nuclear Materials Authority, P.O. Box 530, Maadi, Cairo, Egypt.

<sup>3</sup>Institute of Physics and Technology, Ural Federal University, Ekaterinburg, Russia.

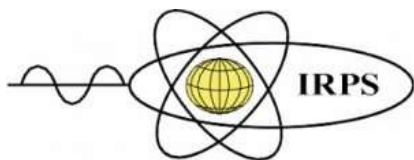
<sup>4</sup>Department of Physics, Faculty of Science, Isra University, Amman – Jordan

<sup>5</sup>Department of Nuclear Medicine Research, Institute for Research and Medical Consultations (IRMC), Imam Abdulrahman bin Faisal University (IAU), PO Box 1982, Dammam, 31441, Saudi Arabia

<sup>6</sup>Center for Applied Physics and Radiation Technologies, School of Engineering and Technology, Sunway University, 47500 Bandar Sunway, Selangor Darul Ehsan, Malaysia

Corresponding author: [elsaeedlasheen@azhar.edu.eg](mailto:elsaeedlasheen@azhar.edu.eg)

Uranium represents the main heavy minerals that are used in nuclear applications. The aim of the current study is to assess the exposure of Um Bogma formation from three localities (Allouga, Abu Thor and Wadi Naseib) as a raw material that could be used in industrial and construction applications and their environmental implications. Multichannel NaI gamma-ray spectrometer was used to measure the radionuclides ( $^{238}\text{U}$ ,  $^{226}\text{Ra}$  (eU),  $^{232}\text{Th}$  and  $^{40}\text{K}$ ) contents of the collected samples. The average values of  $^{238}\text{U}$ ,  $^{226}\text{Ra}$  (eU) activities of Allouga (7285, 5089 Bq/kg), Abu Thor (894.67, 757.3 Bq/kg) and Wadi Naseib (3076.33, 1237.67 Bq/kg) are higher than the recommended average values. Six radiological hazard indices: rate of absorbed dose ( $D_{\text{air}}$ ), radium equivalent ( $R_{\text{aeq}}$ ) activity, annual effective dose (AED), external ( $H_{\text{ex}}$ ) and internal ( $H_{\text{in}}$ ) hazard indices, as well as activity gamma ( $I_{\gamma}$ ) were estimated based on radionuclide activity concentrations. These indices exhibit that the examined samples have values higher than the recommended permissible values, reflecting that they cannot be used for industrial applications due to their impact on human-beings.



**ISRP 2021**  
**International Symposium on Radiation Physics**  
**Kuala Lumpur – Malaysia**  
**6 – 10 December 2021**

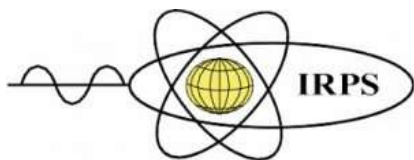
### **A185 - New studies on Neutral Bremsstrahlung in Xenon optical TPCs**

Cristina Monteiro<sup>1</sup>, on behalf of NEXT Collaboration

<sup>1</sup>LIBPhys, Physics Department, University of Coimbra, Portugal

Corresponding author: cristinam@uc.pt

We have ambiguously measured, in pure Xe, non-excimer-based secondary scintillation, Neutral Bremsstrahlung (NBrS), in fully-controlled conditions in a dedicated setup based on a Gas Proportional Scintillation Counter. We reveal the presence of NBrS in the NEXT-White TPC, at present the largest optical HPXe-TPC in operation worldwide. NBrS is emitted by drifting electrons scattering on neutral atoms and occurs, unlike electroluminescence (EL), even for electric field values below the gas excitation threshold. Moreover, for field values above 1 kV/cm/bar, the typical field intensities used for EL-based signal amplification, there is solid evidence that NBrS is present with an intensity that is about two orders of magnitude lower than conventional, excimer-based EL. Our results are in excellent agreement with the NBrS yield values obtained with a recently developed simulation toolbox based on Magboltz and Python (Pyboltz). Even being less intense than EL in pure xenon, this new source of scintillation has to be accounted for in Xe optical TPCs and may play an important role in future single-phase LXe TPCs, especially in view of the forthcoming ton-scale detector experiments.



**ISRP 2021**  
**International Symposium on Radiation Physics**  
**Kuala Lumpur – Malaysia**  
**6 – 10 December 2021**

### **A190 - Development of a KRISS Rn-mini radon detector at KRISS**

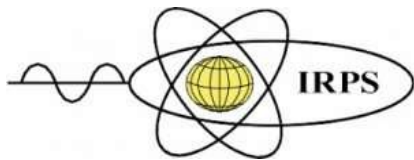
Sanghoon Hwang<sup>1,2</sup>, Minji Han<sup>1,2</sup>, Byungju Kim<sup>1</sup>, B.C. Kim<sup>1</sup>, K.B. Lee<sup>1,2</sup>, J.M. Lee<sup>1,2</sup>, and D. H. Heo<sup>1</sup>

<sup>1</sup>Ionizing Radiation Metrology Group, Korea Research Institute of Standards and Science (KRISS), Daejeon, Republic of Korea

<sup>2</sup>University of Science & Technology (UST), Daejeon, Republic of Korea

Corresponding author: shhwang@kriss.re.kr

Recently, Radon ( $^{222}\text{Rn}$ ) and Thoron ( $^{220}\text{Rn}$ ) made an issue in Republic of Korea, since the mattresses from domestic manufactures release the radon at levels that exceed safety standards, which is 1 mSv per year for the radiation dose of the general public by processed products. Radon emanation found in several living goods, such as a natural latex, a mask, a sanitary pad, a health care instrument, construction materials and so on. Most types of the radon mitigation use the ventilation the inner gases. This method causes some loss of the heated or air conditioned air, which increase the operation cost of the system. Korea Research Institute of Standards and Science (KRISS) is developing a new concept of an active radon reduction system by an interworking technology with a highly sensitive radon monitor system and a ventilation system. We employ an electrostatic radon detection method and the radon detector counts an alpha emitting from the radon daughters ( $^{218}\text{Po}$ ,  $^{214}\text{Po}$ ,  $^{216}\text{Po}$  and  $^{212}\text{Po}$  from  $^{222}\text{Rn}$  and  $^{220}\text{Rn}$ ) with a silicon detector. KRISS is developing a highly sensitive radon detector, KRISS Rn-mini, with a micro controller and own developed signal processing circuit. The electric field has been optimized by the 3D electric field calculation by finite element method. The mock-up model of the radon collection cell has been fabricated by the 3D printer and the sensitivity is found to be 4.5 times high by comparing with RAD7. In this presentation, the development of the KRISS Rn-mini will be discussed.



**A192 - Time-resolved radiation dosimetry using a Cerium and Terbium co-doped YAG crystal scintillator**

A. Basaif<sup>1</sup>, Adebiyi Oresgun<sup>1</sup>, Zubair H. Tarif<sup>1,5</sup>, Hafiz Zin<sup>2</sup>, K. Y. Choo<sup>1</sup>, S. A. Ibrahim<sup>1</sup>, H. A. Abdul-Rashid<sup>1\*</sup>, D. A. Bradley<sup>3,4</sup>, Tingyu Wang<sup>6</sup>, Jianxiang Wen<sup>6</sup>, Dingpeng Gang<sup>7</sup>, Elfed Lewis<sup>8</sup>

<sup>1</sup>Fibre Optics Research Centre, Faculty of Engineering, Multimedia University, Jalan Multimedia 63100, Cyberjaya, Malaysia.

<sup>2</sup>Advanced Medical and Dental Institute, Universiti Sains Malaysia (USM), Bertam 13200, Kepala Batas, Penang, Malaysia

<sup>3</sup>Centre for Applied Physics and Radiation Technologies, Sunway University, 46150 PJ, Malaysia.

<sup>4</sup>Department of Physics, University of Surrey, Guildford, GU2 7XH, UK.

<sup>5</sup>Lumisysns Technology Sdn Bhd, Cyberjaya 63100, Selangor, Malaysia

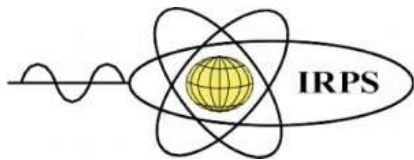
<sup>6</sup>Key Laboratory of Specialty Fiber Optics and Optical Access Networks, Joint International Research Laboratory of Specialty Fiber Optics and Advanced Communication, Shanghai Institute for Advanced Communication and Data Science, Shanghai University, 99 Shangda Road, Shanghai, 200444, China

<sup>7</sup>School of Electrical Engineering & Telecommunications, The University of New South Wales, NSW 2052, Australia

<sup>8</sup>Optical Fiber Sensors Research Group, School of Electrical and Electronic Engineering, Liverpool John Moores University, Liverpool, UK

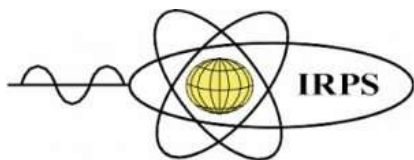
Corresponding author: hairul@mmu.edu.my

One of the determinants of quality delivery of patient prescribed doses in radiotherapy is the ability to make time-resolved radiation dosimetry. Doped silica optical fibres scintillators reported earlier, used in radioluminescence (RL) based dosimetry, have indicated advantages: an ability for real-time measurements, robustness, high spatial resolution, and versatility. Using a suitable scintillator with fast rise and decay time adds on to the advantages above leading to the time-resolved radiation dosimetry capability. Such capability provides the high temporal resolution required to ensure quality assurance through pulse-by-pulse radiation dosimetry. We report on the potential of cerium and terbium co-doped YAG crystal derived optical fibres as a suitable scintillator for a time-resolved radiation dosimetry system. The samples were irradiated in a high-energy clinical X-ray beams (6 MV) radiotherapy facility. The RL responses were recorded for dose-rates between 100 MU/min and 600 MU/min, delivered by a Varian 2100 C/D linear accelerator. The gating time in the photon-counting circuit was set at 1  $\mu$ s. The fluorescence lifetime analysis demonstrates a calculated rise time of 590.1 ns and a



**ISRP 2021**  
**International Symposium on Radiation Physics**  
**Kuala Lumpur – Malaysia**  
**6 – 10 December 2021**

decay time of  $0.423 \mu\text{s}$ . This indicates superior performance compared to other scintillator forms reported earlier. The scintillator samples demonstrated linear RL response, with minimal observable memory, afterglow and plateau effects. These results demonstrate the potential for the cerium and terbium co-doped YAG crystal derived optical fibre scintillators for time-resolved radiation dosimetry.



**ISRP 2021**  
**International Symposium on Radiation Physics**  
**Kuala Lumpur – Malaysia**  
**6 – 10 December 2021**

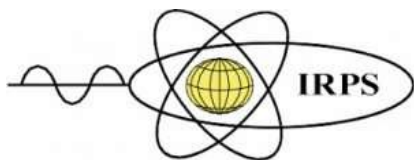
**A193 - Enhancing Information Learned from Auger Processes**

Eric L. Shirley<sup>1</sup>, Joseph C. Woicik<sup>2</sup>, C. Weiland<sup>2</sup>

<sup>1</sup>Sensor Science Division, NIST, USA

<sup>2</sup>Materials Measurement Science Division, NIST, USA

Auger electrons are a secondary form of radiation emitted following high-energy excitation of a physical system. Auger emission spectra can identify the element of an excited atom that decays by the Auger process. In addition, close examination of peak intensities can furnish information about the component of a core hole's angular momentum along the emission direction. Such analysis can provide information about the process by which the core hole came about. This therefore allows one to sense information regarding more than one step in a multi-step radiation-absorption process without the need to resort to coincidence spectroscopy. Here, resonant Auger spectra for several systems are re-analyzed in this light to better understand phenomena that occur in the low-energy portion of a cascade event. This includes better knowledge of angular and energy distributions of Auger electrons.



**ISRP 2021**  
**International Symposium on Radiation Physics**  
**Kuala Lumpur – Malaysia**  
**6 – 10 December 2021**

**A194 - Thermoluminescence characteristics of customised Ge-doped optical fibres (CusOF) under Am-Be neutron source as a potential to be used for space radiation detector**

Farid Bajuri<sup>1</sup>, Salasiah Mustafa<sup>2</sup>, Nizam Tamchek<sup>3</sup>, Fathinul Fikri Ahmad Saad<sup>2,4</sup>, Norkhairunnisa Mazlan<sup>1</sup>, David Andrew Bradley<sup>5,6</sup>, Noramaliza Mohd Noor<sup>2,4,7</sup>

<sup>1</sup>Department of Aerospace Engineering, Faculty of Engineering, Universiti Putra Malaysia, Malaysia

<sup>2</sup>Centre for Diagnostic Nuclear Imaging, Universiti Putra Malaysia, Malaysia

<sup>3</sup>Department of Physics, Faculty of Science, Universiti Putra Malaysia, Malaysia

<sup>4</sup>Department of Radiology, Faculty of Medicine and Health Sciences, Universiti Putra Malaysia, Malaysia

<sup>5</sup>Centre for Biomedical Physics, School of Healthcare and Medical Sciences, Sunway University, Malaysia

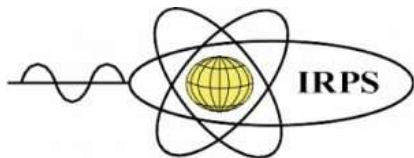
<sup>6</sup>Department of Physics, University of Surrey, United Kingdom

<sup>7</sup>Medical Physics Unit, Hospital Pengajar Universiti Putra Malaysia, Universiti Putra Malaysia, Malaysia

Corresponding author: [noramaliza@upm.edu.my](mailto:noramaliza@upm.edu.my)

While primary cosmic ray particles mainly consist of protons, the complex interactions of the particles with the neutral atoms that exist in the Earth's upper atmosphere may produce neutrons. Some of the neutrons possess enough energy and with the right direction are able to penetrate into the low Earth orbit (LEO). These neutrons are called albedo neutrons. This work focuses on the possibility of Ge-doped optical fibres (GOF) to be used as passive dosimeters for neutron detection in LEO environment. In order to feasibility toward neutron radiation detection, various types of GOF with different concentration of Ge and shapes were irradiated using Am-Be neutron source up to 72 hours with three distances of 0 cm, 15 cm and 30 cm from the location of the source. The irradiation was conducted at Radiation Teaching Laboratory, University of Surrey, United Kingdom. The GOF used were commercial GOF (ComOF) that is generally used for communication application and customised GOF (CusOF) to be used as a passive dosimeter. The TL signal from the GOF were compared with TLD-100, TLD-600 and TLD-700 as reference. Upon normalising with the core volume, flat fibre (FF) with 2.3 mol% Ge dopant had the highest average reading of  $49.7 \times 10^{11}$  nC/m<sup>3</sup>. Both cylindrical fibres (CF) with 6 mol% Ge and 604 micron diameter irradiated at 0 cm from source have linear R-squared value of 0.98 and linearity index in the ranges between 0.96 and 1.03. Finally, after 304 days upon irradiation, 483 micron CF with 6 mol% Ge had the least fading of 5% compared to the original reading. From this work, we conclude that GOF has the potential to be used as a neutron dosimeter.

ORAL PRESENTATIONS|



**A195 - The Impact of Tube Current and Iterative Reconstruction Algorithm on Dose and Image Quality of Infant CT Head Examination : A Phantom Study**

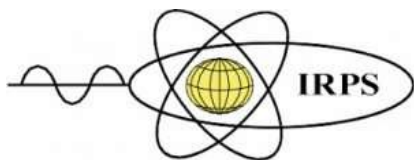
N. A Muhammad<sup>1\*</sup>, M.K.A Karim<sup>2</sup>, H.H. Harun<sup>2</sup>, R.N.R.M. Azlan<sup>1</sup>, N.F.Sumardi<sup>1</sup>

<sup>1</sup>College of Health Sciences University Malaya Medical Centre (UMMC), 59200 Kuala Lumpur, Malaysia

<sup>2</sup>Department of Physics, Faculty of Science, Universiti Putra Malaysia, 43400 Serdang, Selangor, Malaysia

Corresponding author: N. A Muhammad

Computed Tomography (CT) scan examinations have been acknowledged for its higher radiation doses contribution when compared to other imaging modalities. Hence, the public's recently has raised a concern of radiation burden, especially to paediatric patients. The purpose of this study is to investigate the influence of CT acquisition parameters on radiation dose in the selected radiosensitive organs of infant CT head examination and its repercussion on the image quality. This study utilized a 1-year-old anthropomorphic phantom and thermoluminescent dosimeter (TLD) for organ dose assessment. The examination was performed by using 128 multi-slice CT Ingenuity Core (Philips Koninklijke, Amsterdam, and The Netherlands) with adopting tube potential and iterative reconstruction algorithm (Ingenuity-128 with iDose4). The tube potential was fixing at 100 kVp with various tube current reference values (ref.mAs). 5 different CT protocols (P1 to P5) were employed during the process. 3 TLD chips were inserted into the phantom slab no 2, 4, and 7 to represent brain, lens, and thyroid respectively. The objective image quality in terms of signal to noise ratio (SNR) and contrast to noise ratio (CNR) and subjective image quality using the Visual Grading Analysis technique in terms of sharpness, noise and artefact were assessed from each protocol. As a result, the dose was declined up to 30% along with reducing tube current. Meanwhile, the SNR and CNR values were improved with iterative reconstruction. In conclusion, optimization of CT acquisition parameter led to reduced radiation dose in radiosensitive organ in CT brain examination.



**ISRP 2021**  
**International Symposium on Radiation Physics**  
**Kuala Lumpur – Malaysia**  
**6 – 10 December 2021**

## **A205 - Dosimetric characteristics of fabricated Germanium doped optical fibres for electron beam therapy audit**

N Abdullah<sup>1,2</sup>, N Mohd Noor<sup>1,3</sup>, Andrew Nisbet<sup>4</sup>, Z Kamarul Zaman<sup>5</sup>

<sup>1</sup>Faculty of Medicine and Health Sciences, Universiti Putra Malaysia, 43400 Serdang, Selangor, Malaysia

<sup>2</sup>Radiation Metrology Group, Malaysian Nuclear Agency, 43000 Kajang, Selangor, Malaysia

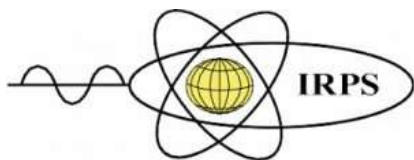
<sup>3</sup>Medical Physics Unit, Teaching Hospital Universiti Putra Malaysia, Universiti Putra Malaysia, 43400 Serdang, Selangor, Malaysia

<sup>4</sup>Department of Medical Physics and Biomedical Engineering, Faculty of Engineering Science, University College London, England

<sup>5</sup>Medical Physics Unit, University of Malaya Medical Centre, 59100 Kuala Lumpur, Malaysia

Corresponding author: hayatie@nuclearmalaysia.gov.my

In this study, the dosimetric characteristics of Germanium (Ge) doped optical fibres were investigated for their potential use as an alternative dosimeter for electron beam therapy postal audits. The dosimetric characteristics of 6mol% Ge-doped optical fibres fabricated in a cylindrical shape were examined in terms of fading effect, dose-response, energy dependence and dose rate dependence subject to electron beams using a medical linear accelerator located at Royal Surrey Hospital, England. The fibres were then used in the pilot study of electron beam therapy audit for reference and non-reference conditions in accordance with the International Atomic Energy Agency (IAEA) standard irradiation procedures. The results show that the fading effect of the Ge-doped optical fibres was reduced by 26% at 120 days post-irradiation and the dose-response was linear within the dose range of 1 to 3 Gy, with the least determination coefficient,  $R^2$  of 0.994 at 12 MeV. The responses for electron beam energy between 6 to 20 MeV and dose rate within 100 to 400 cGy demonstrate significant deviations at a maximum of 6% and 3%, respectively. The results of the electron beam therapy audit were satisfactory within the IAEA's acceptance limit of 5%, except for the 6 MeV electron beam in the reference condition, in which a deviation relative to the measured dose of 6% was obtained. In conclusion, the Ge-doped optical fibres are suitable to be used as a transfer dosimeter in electron beam therapy postal audit.



**A206 - Radiological and Environmental studies on granitic rocks of Abu Furad area used in construction purposes and ceramic industry**

S. A. Taalab<sup>1</sup>, M. Y. Hanfi<sup>2,3</sup>, M.I.Sayyed<sup>4,5</sup>, Mayeen Uddin Khandaker<sup>6</sup>

<sup>1</sup>Faculty of Science, Al-Azhar University, Cairo, P.O. Box 11884, Egypt

<sup>2</sup>Nuclear Materials Authority, P.O. Box 530 El-Maadi, Cairo, Egypt

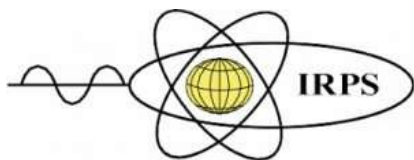
<sup>3</sup>Institute of Physics and Technology, Ural Federal University, Ekaterinburg, Russia

<sup>4</sup>Department of Physics, Faculty of Science, Isra University, Amman – Jordan

<sup>5</sup> Department of Nuclear Medicine Research, Institute for Research and Medical Consultations (IRMC), Imam Abdulrahman bin Faisal University (IAU), PO Box 1982, Dammam, 31441, Saudi Arabia

<sup>6</sup>Center for Applied Physics and Radiation Technologies, School of Engineering and Technology, Sunway University, 47500 Bandar Sunway, Selangor Darul Ehsan, Malaysia

Abu Furad area lies in the Central Eastern Desert, Egypt. The main outcrops include metasediments, metavolcanics, metagabbros, syn- to late-orogenic granites, and post-orogenic granites, in addition to numerous dykes and veins of different shapes and composition intruded and invading all the older rocks in the study area. Altered syenogranite at Abu Furad area is affected by multistages of hydrothermal alteration processes along brittle structures, this alteration comprises silicification, hematitization, sericitization, saussuritization, chloritization and muscovitization. These rocks were used as ornamental stones and inter in ceramic industry. The  $^{238}\text{U}$ ,  $^{232}\text{Th}$ ,  $^{226}\text{Ra}$  and  $^{40}\text{K}$  activities were measured in Abu Furad granitic rocks using a NaI (Tl) gamma-ray spectroscopy system. The activities are ranged from 31 to 351.33 Bqkg<sup>-1</sup>, 22.2 to 102.35 Bqkg<sup>-1</sup>, 22.2 to 168.35 Bqkg<sup>-1</sup> and 881.49 to 1460.67 Bqkg<sup>-1</sup>, for  $^{238}\text{U}$ ,  $^{232}\text{Th}$ ,  $^{226}\text{Ra}$  and  $^{40}\text{K}$ , respectively. The lowest activities of these radioelements were recorded in syn- to late-orogenic granites while the highest values in the altered granites and pegmatites. Absorbed Dose Rate (D), annual effective dose equivalent (AEDE), radium equivalent activity (Raeq), external (Hex) and internal (Hin) hazard index, in addition to activity gamma index (I<sub>γ</sub>) caused by gamma emitting natural radionuclide are determined from the obtained values of  $^{226}\text{Ra}$ ,  $^{232}\text{Th}$  and  $^{40}\text{K}$ . Fairly, the studied altered granites and pegmatites do not agree the international limits. This could be attributed to the presence of radioactive and U-bearing minerals such as thorite, fergusonite, samarskite, columbite, zircon, monazite, xenotime, apatite, fluorite and sphene.



**ISRP 2021**  
**International Symposium on Radiation Physics**  
**Kuala Lumpur – Malaysia**  
**6 – 10 December 2021**

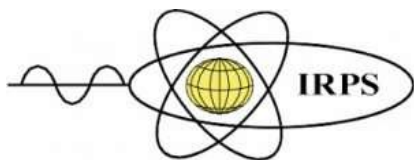
**A207 - Effect of different source-to-image distance on radiation dose and the quality of image in posteroanterior hand X-ray examination**

Inayatullah Shah Sayed<sup>1</sup> and Nik Noor Izzati Nik Lah<sup>1</sup>

<sup>1</sup>Department of Diagnostic Imaging and Radiotherapy, Kulliyyah of Allied Health Sciences, International Islamic University Malaysia, Kuantan Campus, 25200 Kuantan, Pahang, Malaysia

Corresponding author: [inayatullah@iium.edu.my](mailto:inayatullah@iium.edu.my); [s\\_ishah@yahoo.co.uk](mailto:s_ishah@yahoo.co.uk)

In clinical settings, the source-to-distance (SID) is adjusted using measuring tape attached to the x-ray tube. However, this method is ignored when hand extremities X-ray examinations are involved. Variation in SID can affect radiation dose to hand and quality of image. In this study upper extremities of the hand area were included. It is because the number of hand injuries cases at the hospitals is higher compared to other upper extremities such as the forearm, elbow and humerus. The purpose of this work was to investigate the effect of different SID on entrance surface dose (ESD) and quality of image for posteroanterior (PA) projection. The Siemens Multix Top system was used selecting 55 kVp and 1.6 mAs. The SID selected was 95, 100, 105, 110 and 115 cm. The anthropomorphic hand-wrist phantom was placed over the cassette with the third metacarpophalangeal joint as the centre of the anatomical structure. Twelve nanoDot OSLDs at various locations on the phantom were positioned. The ESD readings were repeated for three times at each SID in order to record an average value. Five images of PA hand X-ray examinations were produced in order to measure signal-noise-ratio (SNR) using ImageJ for image quality evaluation. The mean ESD value at the centre of anatomical structure, which is the metacarpophalangeal (MCP) joint of the third digit decreased as SID increased. There is a significant difference between the mean ESD at MCP joint of the third digit and SID ( $p < 0.05$ ). However, inconsistent ESD values at other locations were observed. In terms of image quality, the results also show inconsistent pattern of SNR for each image. To conclude, the increase in SID, lowers the ESD and image quality. It is suggested that the SID need to be adjusted manually when upper extremities of the hand X-ray examinations are performed.



**ISRP 2021**  
**International Symposium on Radiation Physics**  
**Kuala Lumpur – Malaysia**  
**6 – 10 December 2021**

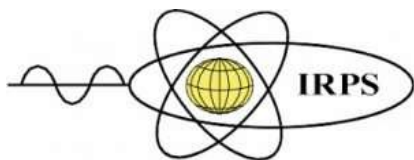
### **A208 - The Auger Effect and its Applications**

Jonathan W. Dean, Christopher T. Chantler

School of Physics, University of Melbourne, Australia

Corresponding author: [jonathan.dean@unimelb.edu.au](mailto:jonathan.dean@unimelb.edu.au)

The Auger Effect is the name given to a secondary ionisation of an atom due to an initial inner shell vacancy. While first discovered almost a century ago, there are still many active investigations into this phenomenon as well as newly found applications. Practical applications include cancer research, semiconductor and quantum dot studies, microelectronics, functional electroluminescence, and materials science. Furthermore, Auger Electron Spectroscopy has been a key analytical tool for decades. Despite this, there is a lack of theoretical understanding of the Auger Effect within the framework of relativistic quantum mechanics. Plenty of publications mention the need for a greater understanding of the Auger Effect. However, very few theoretical works exist which lead to a lack of understanding the fundamental atomic processes. This is unfortunate and we aim to bridge the gap in the literature. Two recent publications from our group include an analysis of the Auger Effect. The work considers the relative intensity, K-edge, Auger edge, and peak energy, as parameters to define the shape of an Auger energy profile. There is no consensus in the literature as to what profile one should use when considering an Auger emission profile, guesses range from non-contiguous and piecewise profiles to broad Gaussians. This is an issue in many radiation physics subfields, as the Auger Effect is always present to some degree in X-Ray physics experiments.



**A211 - Performance of Ge-doped silica optical fiber radioluminescence scintillators for radiotherapy dosimetry**

A. Oresegun<sup>1</sup>, A. Basaif<sup>1</sup>, Z.H. Tarif<sup>1,2</sup>, H.A. Abdul-Rashid<sup>1,\*</sup>, Hafiz Zin<sup>3</sup>, D.A. Bradley<sup>4,5</sup>

<sup>1</sup>Fibre Optics Research Centre, Faculty of Engineering, Multimedia University, Jalan Multimedia, 63100, Cyberjaya, Malaysia

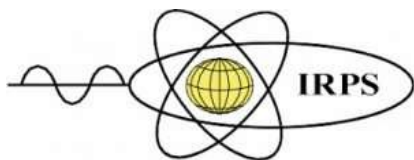
<sup>2</sup>Lumisysns Technology Sdn Bhd, Cyberjaya, 63100, Selangor, Malaysia

<sup>3</sup>Advanced Medical and Dental Institute, Universiti Sains Malaysia (USM), Bertam, 13200, Kepala Batas Penang, Malaysia

<sup>4</sup>Centre for Applied Physics and Radiation Technologies, School of Engineering and Technology, Sunway University, 46150, PJ, Malaysia.

<sup>5</sup>Department of Physics, University of Surrey, Guildford, GU2 7XH, UK  
Corresponding author: hairul@mmu.edu.my (H.A. Abdul-Rashid).

Investigation has been made on the performance of Ge-doped silica optical fiber radioluminescence (RL) scintillators used for radiotherapy dosimetry. The samples under study were differentiated by the core and cladding diameter and Ge dopant concentration. The small core samples have a relatively smaller core to cladding ratio compared to the larger core samples. In the characterization, the samples were subjected to 6 and 10 MV photon beams from a linear accelerator in a radiotherapy facility. Each sample were exposed under a set of similar conditions, with a fixed surface distance (SSD) of 100 cm and field size of 10 x 10 cm<sup>2</sup>. Dosimetric performance investigation included radioluminescence yield, dose-rate dependency, energy dependency, angular dependency and percentage depth dose profile. The radioluminescence yield was observed to be linear with increasing dose with the smaller core samples demonstrating a higher total radioluminescence yield. The sample with core diameter of 134 μm and core to cladding ratio of 0.069 demonstrated the highest sensitivity of 2.73 x 10<sup>6</sup> counts/ Gy. The higher RL yield is contributed by the higher number of color centers in the pure silica network (cladding) compared to the color centers in the Ge-doped silica network (core). The higher Ge-dopant concentration in the large core samples influenced the RL yield through photon trapping, reducing the overall RL yield in such samples. The RL response indicated dose-rate independence, indicating potential for Ge-doped silica optical fiber scintillators for radiotherapy dosimetry.



**A223 - Tomographic gamma-ray imaging of industrial processes and equipment**

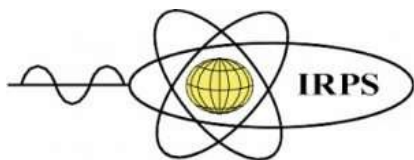
Geir Anton Johansen<sup>1</sup>, Bjørn Tore Hjertaker<sup>1</sup>, Reza Hashemi<sup>2</sup>, Ryan Spelay<sup>2</sup>

<sup>1</sup>University of Bergen, Norway,

<sup>2</sup>Saskatchewan Research Council, Saskatoon, Canada.

Corresponding author: geiranton.johansen@uib.no

Over the past decades there has been an increase in the development of tomography systems for cross sectional imaging of industrial processes and equipment. The motivation is typically to obtain better insight and understanding of the process dynamics to enable process optimization, and to carry out integrity measurements of process equipment such as pipes. At the University of Bergen, we concentrated on the development of gamma-ray imaging systems with multiple sources and detectors even though electrical tomographic imaging systems also were considered. There are several trade-offs in the design of these systems. For instance, to reveal the dynamics of multiphase flows, high speed imaging is required, preferably in combination with high spatial resolution. The first gamma tomograph system developed at the University of Bergen has five <sup>241</sup>Am sources with fan beam collimation so that each source faces a detector array of 17 CdZnTe semiconductor detectors and a total of 85 detectors / beams. The system has been applied to provide data which has been used to design efficient multiphase flow meters. The second gamma-ray tomograph was based on the system in Bergen and developed for and by Saskatchewan Research Council in Canada. The system utilises five pixelized CdZnTe detectors with a total of 4480 elements. The unit has been used to study the dynamics of solid-liquid, oil-water and oil-water-solid multiphase pipe flows and has been instrumental in better understanding the underlying physics and mechanisms that govern these type of flows. Tracerco has developed Discovery<sup>TM</sup>, a unique non-intrusive external inspection tool which can be clamped onto process equipment such as pipes for integrity measurements. The Discovery<sup>TM</sup> technology can measure defects to within a 2 mm resolution, provide a tomographic wall thickness and build up map of each scanning location, inspect pipe-in-pipelines to measure the wall thickness of both inner and outer pipes, provide accurate results unaffected by multiphase flow, and inspect non intrusively by ROV deployment.



**A225 - Flattening filter design for intraoperative radiotherapy with 12 MeV electron beam with large applicators using Monte-Carlo simulations**

Sandra Oliver<sup>1</sup>, Belén Juste<sup>1</sup>, Rafael Miró<sup>1</sup>, Gumersindo Verdú<sup>1</sup>, Javier Vijande<sup>2,5,6</sup>, Facundo Ballester<sup>2,6</sup>, Natalia Tejedor<sup>3</sup>, José Pérez-Calatayud<sup>3,4,6</sup>

<sup>1</sup> Instituto de Seguridad Industrial, Radiofísica y Medioambiental, Universitat Politècnica de València, Spain

<sup>2</sup> Departamento de Física Atómica, Molecular y Nuclear, Universitat de Valencia, Spain<sup>3</sup> Hospital Universitari i Politènic La Fe de València, Spain

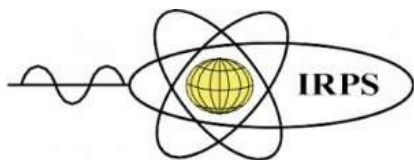
<sup>4</sup> Hospital Clínica Benidorm Alicante, Spain

<sup>5</sup> Instituto de Física Corpuscular, IFIC (UV-CSIC), Burjassot, Spain

<sup>6</sup>Unidad Mixta de Investigación en Radiofísica e Instrumentación Nuclear en Medicina (IRIMED), Instituto de Investigación Sanitaria La Fe (IIS-La Fe)—Universitat de Valencia (UV), Valencia, Spain

Corresponding author: [bjuste@upv.es](mailto:bjuste@upv.es)

Intraoperative electron radiotherapy treatments consist on the irradiation of the tumour bed during the surgical intervention after tumour extirpation to remove the remaining cancer cells. Due to the collaboration between the institutions the authors belong to, it has been possible to carry out the study of the beams emitted by the Liac HWL Sordina accelerator, using state-of-the-art Monte-Carlo (MC) simulations. During experimentation with 12 MeV electron beam and 10 cm diameter applicator, in a water phantom, it has been observed by the hospital medical physicist that the dose profile presents a significant inhomogeneity. To homogenise the field, the collaboration group has proposed the design of a flattened filter made of PMMA. MC simulations has been performed independently by two research groups using MCNP6v2 and PENELOPE/PenEasy. The applicator geometry was modelled and incorporated to the simulation, which was executed using as a source a phase space file at the exit of the accelerator, provided by the manufacturer. First, the dose distributions obtained in a water phantom located at the exit of the Liac, were compared with experimental data provided by the hospital. Once this verification was done, the PMMA filter attenuation in layers of different thicknesses and shapes was studied, applying these results to the filter design. After adding the proposed filter to the applicator geometry some simulations were performed to check its effectiveness on the field homogeneity. The results showed that the designed filter achieves the proposed objective, obtaining a flat dose profile at the depth of interest in the water phantom. Moreover, the fluence and dose distribution around the accelerator system have been studied to verify that the filter does not generate scatter that increase the peripheral dose around the Unit. The designed filter will be manufactured to be validated in a water phantom by performing experimental measurements. Its potential use for specific patients will be evaluated.



**ISRP 2021**  
**International Symposium on Radiation Physics**  
**Kuala Lumpur – Malaysia**  
**6 – 10 December 2021**

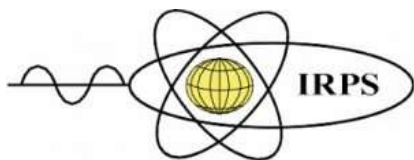
**A227 - Development of a unique neutron irradiation facility for medical radionuclides and advanced nuclear technologies**

Allan Simpson<sup>1</sup>, Bethany Slingsby<sup>1</sup>

<sup>1</sup>National Nuclear Laboratory, United Kingdom

Corresponding author: [allan.simpson@uknln.com](mailto:allan.simpson@uknln.com)

The UK's National Nuclear Laboratory is a centre of expertise for nuclear fuel cycle technologies. NNL is leading an ambitious project to deliver unique research facilities that will enable the requisite research and development for myriad applications of radiation and nuclear technology in the future. This project, called STELLAR, aims to deploy a high flux, high fluence neutron irradiation source at NNL's Central Laboratory located at the Sellafield nuclear fuels complex in the UK. It is expected that STELLAR will operate with a continuous flux in excess of  $10^{11}$  neutrons/cm<sup>2</sup>/s at energies of up to 14.1 MeV. By locating the system at Central Laboratory, STELLAR offers the opportunity to make use of high activity pre and post irradiation analytical facilities, enabling a range of unique experiments to be considered with STELLAR making use of materials that couldn't be handled at other facilities. Applications proposed to date include the development of novel radionuclide production processes for improved targeting of radiation in medical treatments, materials testing for advanced nuclear technologies across fission and fusion and investigating the transmutation of nuclear waste. Such a facility will enable the development of more hands-on skills for the UK and global nuclear sectors. To ensure the development of a flexible and suitable facility for these applications, feedback on the proposed facility is welcome as well as expressions of interest for future use of the facility. A summary of the facility specification and more detailed experimental concepts will be shared.



**ISRP 2021**  
**International Symposium on Radiation Physics**  
**Kuala Lumpur – Malaysia**  
**6 – 10 December 2021**

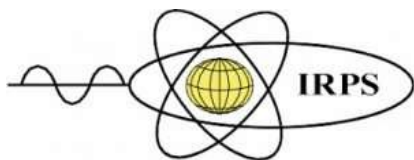
**A228 - Medical radionuclide prioritisation and the development of the Production Rate Assessment Tool**

Bethany Slingsby<sup>1</sup>, Duncan Horne<sup>1</sup>, Allan Simpson<sup>1</sup>, Howard Greenwood<sup>1</sup>

<sup>1</sup>National Nuclear Laboratory, United Kingdom

Corresponding author: [bethany.slingsby@uknnl.com](mailto:bethany.slingsby@uknnl.com)

In the UK many radionuclides are imported from abroad with the UK having a limited radionuclide production capability. Due to strict import conditions and the difficulty transporting short-lived radionuclides there is a gap in the UK's nuclear skills and facilities capability to meet this demand. A part of meeting this demand is not only the development of production facilities, but the identification of novel medical radionuclide and novel production routes aimed at increased effectiveness whilst limiting damage to healthy tissues. To accomplish this, a review was undertaken to develop a method of prioritising novel radionuclides and novel production routes of interest for medical applications. Once the method was established, radionuclides identified would be evaluated in the newly developed Production Rate Assessment Tool. This tool utilises the UK's fission product inventory code FISPIN as a calculation kernel to model the rate of production of nuclides generated when a target material is exposed to an incident neutron flux. FISPIN is used routinely for industrial applications on the Sellafield site and makes use of well-established and validated nuclear data. The unique attributes of FISPIN when used within this tool enable it to handle mixed nuclide inputs, multiple irradiation and cooling steps and both reactor and accelerator irradiations within one flexible model. The Production Rate Assessment Tool therefore allows the user to make quick assessments to enable effective decision making based on theoretical feasibility of production routes of radionuclides of interest. Through this work we have demonstrated a transfer of knowledge and understanding for this area of interest through the review of nuclear physics considerations and the method of prioritisation. The Production Rate Assessment Tool has also expanded the capability a reputable and well validated code for a novel application to enable assessment of prioritised radionuclides in a structured manner.



**ISRP 2021**  
**International Symposium on Radiation Physics**  
**Kuala Lumpur – Malaysia**  
**6 – 10 December 2021**

### **A230 - Wavefield Characterisation of MHz XFEL Pulses**

Trey Guest<sup>1,2</sup>, Brian Abbey<sup>1</sup>, Adrian Mancuso<sup>1,2</sup>, David Paganin<sup>3</sup>, Richard Bean<sup>2</sup>, Grant van Riessen<sup>1</sup>

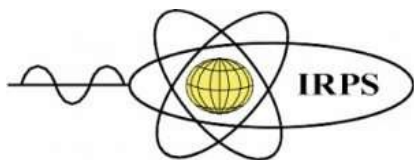
<sup>1</sup>La Trobe Institute for Molecular Sciences, La Trobe University, Victoria 3086, Australia.

<sup>2</sup>European XFEL GmbH, Albert-Einstein-Ring 19, 22761 Hamburg, Germany

<sup>3</sup>School of Physics, Monash University, Victoria 3800, Australia

Corresponding author: [twgust@students.latrobe.edu.au](mailto:twgust@students.latrobe.edu.au)

X-ray Free Electron Laser (XFEL) light sources present new opportunities in the imaging of single particles and biomolecules. However, the interpretation and analysis of XFEL data depends critically on a fundamental understanding of the characteristics of the inherently stochastic XFEL pulses delivered to the instrument. Exploiting the unique MHz repetition rate of the European XFEL to image single particles requires an improved understanding of both the inter- and intra-train fluctuations in pulse structure and beam pointing, which are frequently implicated in the loss of information in XFEL single particle imaging (SPI) and other classes of coherent diffraction experiment. Failure to account for fluctuations of the electron bunch phase-space and/or trajectory within a pulse train can result in deviations of the recorded wavefront and intensity statistics from theoretical behaviour and lead to conflation of the structure of the source and sample in single particle reconstruction. Contrary to expectations, X-ray optical data collected at the SPB-SFX instrument of the European XFEL demonstrates a sensitivity of inter- and intra-train variations in beam pointing to beam delivery parameters – We present this data in comparison to a partially coherent wave optical simulation of the SPB-SFX instrument, through which photon diagnostics have been designed and developed, with the goal of improving the stability and subsequent imaging quality of the user-end photon beam. We discuss these results within the scope of developing a novel phase-retrieval method applicable to the study of MHz repetition rate XFEL sources using nearfield speckle-tracking measurements.



**A231 - Glass microspheres as a novel targeting vector for proton-boron therapy**

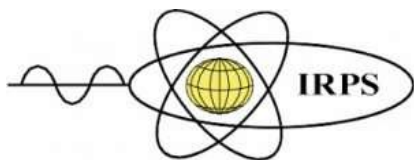
Fiona Pearce<sup>1</sup>, Lee J. Evitts<sup>1</sup>, Simon C. Middleburgh<sup>1</sup>, Michael J. D. Rushton<sup>1</sup>, P. Rautiyal<sup>1</sup>, M. Ghardi<sup>1</sup>, F. Davison<sup>1</sup>, W. E. Lee<sup>1,2</sup>

<sup>1</sup>Nuclear Futures Institute, Bangor University, Gwynedd, LL57 2DG, UK

<sup>2</sup>Institute for Security Science and Technology, Imperial College London, London, SW7 2AZ, UK

Corresponding author: f.pearce@bangor.ac.uk

Proton-boron capture enhanced proton therapy is an exciting area of development in cancer treatment. By introducing  $^{11}\text{B}$  into the treatment area of the proton beam three alpha particles can be produced in the  $^{11}\text{B}+p\rightarrow 3\alpha$  reaction. Highly ionising alpha particles result in large equivalent doses deposited in small treatment volumes. An increased dose produced within the treatment area would allow for a lower proton beam exposure, reducing the dose to healthy tissue and improving outcomes for patients. The reduction in damage to healthy tissue is particularly important for the treatment of tumours close to highly radiosensitive structures within the body, which currently limits the applications of proton therapy. To take advantage of the reaction cross-section, a high boron concentration is needed for the dose from the alpha particles to become significant. Previous research into the effectiveness of proton-boron capture therapy has focused on the use of boron containing pharmaceuticals. As the boron is free to interact in the body, the amount of boron that can be delivered to a tumour is limited by the boron toxicity level. By encasing the boron in inert glass microspheres, the boron concentration in the tumour location can be safely increased beyond this limit. This work will present glass microspheres doped with  $^{11}\text{B}$  as an alternative delivery vector to proton-boron capture therapy. A glass with the maximum amount of boron without leaching above the toxicity limit is being developed, produced and tested at Bangor University. Leaching levels are measured by simulating an in vivo environment and testing for all glass components to ensure biocompatibility. The effectiveness of proton-boron capture therapy compared to proton therapy for this delivery vector will be assessed experimentally by examination of cell culture damage. A detailed explanation of the methodologies and initial results will be given.



**ISRP 2021**  
**International Symposium on Radiation Physics**  
**Kuala Lumpur – Malaysia**  
**6 – 10 December 2021**

**A234 - Radiation treatment in ensuring traceability and biosafety of aquatic food and its environment**

Subha Bhassu<sup>1</sup>, Ming Tsuey Chew<sup>2</sup>, David Andrew Bradley<sup>2,3</sup>

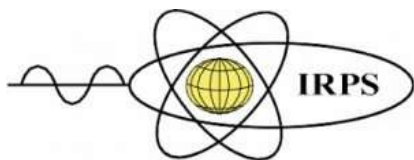
<sup>1</sup>Animal Genetics and Genome Evolutionary Biology Lab, Institute of Biological Sciences, Faculty of Science and Centre for Research in Biotechnology for Agriculture, 50300, University Malaya, Malaysia

<sup>2</sup>Research Centre for Applied Physics and Radiation Technologies, School of Engineering and Technology, Sunway University, Selangor, Malaysia.

<sup>3</sup>Department of Physics, University of Surrey, United Kingdom.

Corresponding authors: subhabhassu@um.edu.my and mtchew@sunway.edu.my

In aquaculture, as for all other sectors of the food industry, food safety is a major concern, there being a necessity for both transparency and traceability. In particular it is imperative for the consumer to have access to details of where (traceability) and how (transparency) the food has been produced. Importantly, the food industry including the aquaculture sector needs to be accountable in terms of seeking possible solutions towards ensuring food safety compliance. Forming the background to present work is the issue of the presence of anti-microbial resistance (AMR) bacteria in aquatic food and its environment, a matter of major and growing concern. Radiation treatment is one approach that can confront resistant microorganisms found in aquatic environments, combating their potential appearance in fresh market produce. This is an issue that has been little addressed in developing nations. In this paper, systematic controls and measures using radiation treatment will be compared to biological and chemical approaches such as phage therapy, lactic acid bacteria therapy and nano-sensors, also other existing controls such as the use of light (photovoltaic and blue and UV light). In recent studies radiation methods have been successful in inactivating microorganisms at the DNA level, with minimal damage to surrounding cells, being highly effective in eradication of harmful microorganisms. Ensuring aquatic food safe to health contributes to the UN Sustainable Development Goals (SDGs), addressing the 3<sup>rd</sup> goal 'good health and well-being' and the 12<sup>th</sup> SDG of 'responsible consumption and production'. In this review, the focus is on AMR radiation treatment, adopting the systematic control measures familiar in the medical field, offering a potential solution towards environmental and safety concerns in the aquatic food production sector.



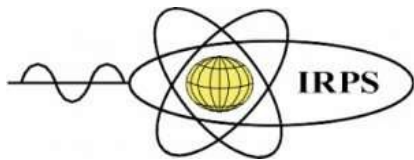
**A239 - Determination of the radon diffusion coefficient of thin polyethylene and aluminium foils**

Beatriz Ruvira<sup>1</sup>, Beatriz García-Fayos<sup>1</sup>, Belén Juste<sup>1</sup>, José Miguel Arnal<sup>1</sup>, Gumersindo Verdú<sup>1</sup>

<sup>1</sup>Institute for Industrial, Radiophysical and Environmental Safety (ISIRYM), Universitat Politècnica de Valencia, Spain

Corresponding author: bearuqui@upv.es

Radon is a radioactive noble gas that is exhaled from the soil and can reach high concentrations in enclosed spaces. As elevated concentrations cause serious health problems, legislation has been put in place in many countries to regulate the concentration limit and to establish mitigation techniques, the most effective for new buildings being the installation of radon barriers. One of the parameters that determine whether the barrier is adequate to protect against radon is the diffusion coefficient, whose measurement methodology is standardised in ISO/TS 11665-13:2017. The experimental setup consists of two stainless steel airtight chambers, 2 mm thick and with a volume of 0.801 litres each, placed one on top of the other. The radon source is placed in the lower chamber, the materials to be studied are positioned between the two chambers and the setup is sealed by means of an O-ring and several screws. Two continuous detectors (Durrigde RAD7) are used to measure the evolution of the radon concentration in both chambers every 30 minutes for 48 hours and, with these results, the radon diffusion coefficient is calculated. The materials to be studied are 10 micron sheets of polyethylene (PE) and 15 micron sheets of aluminium (Al), testing in each case 1, 2 and 3 layers of each material. In addition, combinations of the two materials, i.e., PE-Al-PE and PE-Al-PE-Al-PE, are also studied. The diffusion coefficients obtained vary around  $2 \cdot 10^{-12}$  m<sup>2</sup>/s for PE; in the case of Al the diffusion coefficient decreases with increasing number of layers and a lower value is obtained than for PE (around  $10^{-14}$  m<sup>2</sup>/s), making it a very good material for reinforcing polymeric barriers; and the combination of both materials gives very good results, the diffusion coefficient being very low. Radon reductions achieved range from 70-87.5% for PE to more than 98% for Al and the materials combinations. The excellent radon shielding capacity of aluminium is observed, which grows with increasing material thickness. Furthermore, it can be stated that the use of multilayer materials of different nature is very effective in reducing the radon concentration reaching an enclosed space, and that the use of aluminium in some of the layers is essential to achieve a greater shielding effect.



ISRP 2021

International Symposium on Radiation Physics

Kuala Lumpur – Malaysia

6 – 10 December 2021

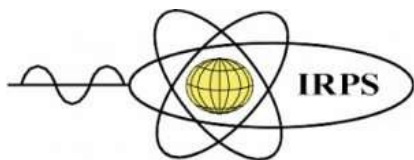
### A243 - First results from FATIMA within the DESPEC collaboration at FAIR-0

S. Jazrawi<sup>1,2</sup>, M. Poletti<sup>3,4</sup>, A. Yaneva<sup>5,6</sup>, M.M.R.Chishti<sup>1</sup>, B. Das<sup>7</sup>, A. Banerjee<sup>5</sup>, N. Hubbard<sup>5,8</sup>, A.K. Mistry<sup>5,8</sup>, M. Rudigier<sup>8</sup>, H.M. Albers<sup>5</sup>, R. Shearman<sup>4</sup>, M. Gorska<sup>5</sup>, J. Gerl<sup>5</sup>, P.H. Regan<sup>1,2</sup>, B. Cederwall<sup>7</sup>, J. Jolie<sup>6</sup>, S. Alhomaidhi<sup>5,8</sup>, T. Arici<sup>5</sup>, G. Benzoni<sup>4</sup>, P. Boutachkov<sup>5</sup>, T. Davinson<sup>9</sup>, T. Dickel<sup>5</sup>, E. Haettner<sup>5</sup>, O. Hall<sup>9</sup>, H. Heggen<sup>5</sup>, P.R. John<sup>8</sup>, I. Kojouharov<sup>5</sup>, N. Kurz<sup>5</sup>, B.S. Nara Singh<sup>10</sup>, S. Pietri<sup>5</sup>, Zs. Podolyak<sup>3</sup>, E. Sahin<sup>5,8</sup>, H. Schaffner<sup>5</sup>, C. Scheidenberger<sup>5</sup>, A. Sharma<sup>11</sup>, J. Vesic<sup>12</sup>, H. Weick<sup>5</sup>, H.J. Wollersheim<sup>5</sup>, U. Ahmed<sup>8</sup>, O. Aktas<sup>7</sup>, A. Algora<sup>13</sup>, C. Appleton<sup>9</sup>, J. Benito<sup>14</sup>, A. Blazhev<sup>6</sup>, A. Bracco<sup>3,4</sup>, A.M. Bruce<sup>15</sup>, M. Brunet<sup>1</sup>, R. Canavan<sup>1,2</sup>, A. Esmaylzadeh<sup>6</sup>, L.M. Fraile<sup>14</sup>, H. Grawe<sup>5</sup>, G. Häfner<sup>6,16</sup>, D. Kahl<sup>9</sup>, V. Karayonchev<sup>6</sup>, R. Kern<sup>8</sup>, G. Kosir<sup>12</sup>, R. Lozeva<sup>16</sup>, P. Napiralla<sup>8</sup>, R. Page<sup>17</sup>, C. M. Petrache<sup>16</sup>, J. Petrovic<sup>7</sup>, N. Pietralla<sup>8</sup>, J.-M. Régis<sup>6</sup>, P. Ruotsalainen<sup>18</sup>, L. Sexton<sup>9</sup>, V. Sanchez-Temble<sup>14</sup>, M. Si<sup>16</sup>, J. Vilhena<sup>19</sup>, V. Werner<sup>8</sup>, J. Wiederhold<sup>8</sup>, P. Woods<sup>9</sup> and G. Zimba<sup>18</sup>

<sup>1</sup>Department of Physics, University of Surrey, Guildford, GU2 7XH, UK; <sup>2</sup>National Physical Laboratory, Teddington, Middlesex, TW11 0LW, UK; <sup>3</sup>Dipartimento di Fisica, Università degli Studi di Milano, Italy; <sup>4</sup>INFN, Sezione di Milano, Italy; <sup>5</sup>GSI, Darmstadt, Germany; <sup>6</sup>Institut für Kernphysik der Universität zu Köln, Germany; <sup>7</sup>KTH Royal Institute of Technology Stockholm, Sweden; <sup>8</sup>Institut für Kernphysik, Technische Universität Darmstadt, Germany; <sup>9</sup>School of Physics and Astronomy University of Edinburgh, EH9 3FD, UK; <sup>10</sup>School of Computing, Engineering & Physical Sciences, University of the West of Scotland, UK; <sup>11</sup>Department of Physics, Indian Institute of Technology Ropar - Rupnagar, India; <sup>12</sup>Jozef Stefan Institute, Ljubljana, Slovenia; <sup>13</sup>Instituto de Fisica Corpuscular, CSIC-Universidad de Valencia, Valencia, Spain; <sup>14</sup>Universidad Complutense de Madrid, E-28040 Spain; <sup>15</sup>University of Brighton, UK; <sup>16</sup>Univeristé Paris-Saclay, IJCLab, CNRS/IN2P3 – F-91405 Orsay, France; <sup>17</sup>Department of Physics, University of Liverpool, L69 7ZE, UK; <sup>18</sup>University of Jyväskylä - Seminaarinkatu 15, 40014, Finland

Corresponding authors: s.jazrawi@surrey.ac.uk & p.regan@surrey.ac.uk

**Abstract:** The NuSTAR collaboration, based at the Facility for Antiproton and Ion Research (FAIR) radioactive-ion beam facility, under construction near Darmstadt, Germany, focusses on investigations of radioactive species with unusual combinations of protons and neutrons. The DEcay SPECtroscopy (DESPEC) research programme within NuSTAR includes instrumentation development for operation at FAIR, such as the FASt TIMing Array (FATIMA) of 36 LaBr<sub>3</sub>(Ce) scintillation  $\gamma$ -ray detectors; and the AIDA, position sensitive implantation detector. The commissioning run of the DESPEC at FAIR-0 umbrella took place in March 2020 and focussed on spectroscopy of neutron-deficient residues resulting from the projectile fragmentation of a 982 MeV/u <sup>124</sup>Xe primary beam. We report on the analysis of these first experimental data, including measurement of electromagnetic transition rates between excited states in neutron-deficient palladium (Z=46) isotopes. We use previously reported isomeric decays in <sup>94,96</sup>Pd to determine the in-situ operational characteristics of the FATIMA array, including full-energy peak efficiency and timing resolution, which are compared with a detailed GEANT4 simulation package developed within the DESPEC collaboration.



**ISRP 2021**  
**International Symposium on Radiation Physics**  
**Kuala Lumpur – Malaysia**  
**6 – 10 December 2021**

**A245 - Gamma-gamma coincidence method for determination of Fe and Tb in Montana II Soil and Coal Fly Ash sample**

Truong Van Minh<sup>1</sup>, Duong Thanh Tai<sup>2</sup>, Pham Dinh Khang<sup>3</sup>, Nguyen Xuan Hai<sup>4</sup>, Nguyen Ngoc Anh<sup>4</sup>, Hiba Omer<sup>5</sup>

<sup>1</sup>Department of natural science, Dong Nai University, Dong Nai, Viet Nam

<sup>2</sup>Department of Industrial Electronics - Biomedical Engineering, Faculty of Electrical and Electronics Engineering HCM University of Technology and Education, Ho Chi Minh, Vietnam.

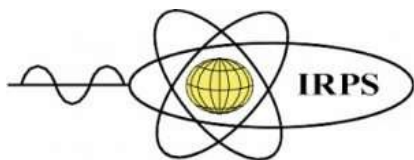
<sup>3</sup>Nuclear Research Institute, Dalat, Vietnam,

<sup>4</sup>Department of Nuclear Engineering and Environmental Physics, Hanoi University of Science and Technology, Hanoi, Vietnam

<sup>5</sup>Department of Basic Sciences, Deanship of Preparatory Year and Supporting Studies, Imam Abdulrahman Bin Faisal University, Saudi Arabia

Corresponding author: tvminh@dnpu.edu.vn; taidt@hcmute.edu.vn

In neutron activation analysis (NAA), the gamma–gamma coincidence method (GGC) is commonly employed in experimental studies of nuclear structure. In order to conduct an accurate measurement, requiring complex de-convolution peak methods must be applied to the resulting gamma-ray spectrum. This work applied GGC method for investigation of Fe and Tb in Montana II Soil and Coal Fly Ash sample. Measuring was done using an event–event gamma coincidence spectrometer (Dalat Nuclear Research Institute, Vietnam). This system has two semiconductor detectors (GMX35, Ortec, USA). Montana II Soil and Coal Fly Ash sample were provided by National Institute of Standards & Technology (NIST, USA). It is shown that the peak to background ratios have been improved and concentration of Fe and Tb in samples was determined with better accuracy when the GGC method applied. It has been demonstrated that the gamma–gamma coincidence method may accurately determine Fe and Tb in geological and environmental samples.



**A258 - Characterisation of Cadmium Telluride Zinc photon counting detector for soft tissue imaging**

K.Hameed<sup>1</sup>, R.Zainon<sup>1,2</sup>, M.Tamal<sup>3</sup>

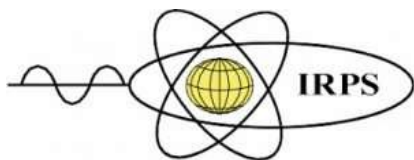
<sup>1</sup>Oncological and Radiological Sciences Cluster, Advanced Medical and Dental Institute, Universiti Sains Malaysia, SAINS@BERTAM, 13200 Kepala Batas, Pulau Pinang, Malaysia

<sup>2</sup>School of Physics, Universiti Sains Malaysia, 11800 Gelugor, Pulau Pinang, Malaysia

<sup>3</sup>Department of Biomedical Engineering, Imam Abdulrahman Bin Faisal University, PO Box 1982, Dammam 31441, Saudi Arabia.

Corresponding author: rafidahzainon@usm.my

Recent advances in photon counting detection technology have led to significant research interest in X-ray imaging. Photon-counting detectors are new technology for Computed Tomography (CT) scanner, with the potential to overcome major limitations of conventional CT detectors. The performance and sensitivity of semiconductor detector material in photon counting detectors in differentiating soft tissue contrast are still under investigation. The purpose of this study was to characterize the Cadmium Zinc Telluride photon counting detector's linearity and its sensitivity in distinguishing various type of tissues in imaging. The X-ray tube voltage and current were set at 25 keV, 35 keV and 0.5 mAs, 1.0 mAs respectively to find the optimum (FPS) Frame rate per second. The X-ray tube current was then set with the ranges from 0.1 mAs to 1 mAs and the detector energy thresholds were set in small steps from 15 KeV to 35 KeV to find the relationship between the voltage and current of the X-ray source and counts per second (CPS) and energy thresholds by keeping the optimum FPS fixed. A stair-step chamber was fabricated from Plexiglass with a dimension of 21 cm x 21 cm to place the fat, liver, muscle, paraffin wax and contrast media for six different thicknesses. The transmission of X-rays at six different thicknesses of samples were also evaluated to investigate the effect on Count per seconds (CPS) for varies tissue thickness at five different energy thresholds (21 keV, 25 keV, 29 keV, 31 keV, and 45 keV). This study found that the optimum FPS follows the X-ray source spectrum, The CPS has linear relationship with X-ray tube current. The sample thickness also affects the X-ray transmission at different energy thresholds. The high sensitivity and linearity of the detector make it suitable to be used in X-ray based medical applications as well as for preclinical applications.



**ISRP 2021**  
**International Symposium on Radiation Physics**  
**Kuala Lumpur – Malaysia**  
**6 – 10 December 2021**

### **A259 - Simulation of $K\alpha$ X-ray emission lines in metallic Cu from first principles**

Mauro Guerra<sup>1</sup>, Jorge Machado<sup>1</sup>, Jorge M. Sampaio<sup>2,3</sup>, Pedro Amaro<sup>1</sup>, Daniel Pinheiro<sup>1</sup>, César Godinho<sup>1</sup>, José P. Marques<sup>2</sup>, Fernando Parente<sup>1,2</sup>, Paul Indelicato<sup>4</sup>, José Paulo Santos<sup>1</sup>

<sup>1</sup> Laboratório de Instrumentação, Engenharia Biomédica e Física da Radiação (LIBPhys-UNL), Physics department, NOVA School of Science and Technology, Monte da Caparica, 2892-516 Caparica, Portugal.

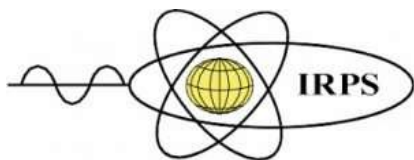
<sup>2</sup> BioISI – Biosystems & Integrative Sciences Institute, Faculdade de Ciências da Universidade de Lisboa, Campo Grande, C8, 1749-016 Lisboa, Portugal.

<sup>3</sup> LIP – Laboratório de Instrumentação e Física Experimental de Partículas, Av. Elias Garcia 141D, 1000-149 Lisboa, Portugal.

<sup>4</sup> Laboratoire Kastler Brossel, UPMC-Sorbonne Universités, CNRS, ENS-PSL Research University, Collège de France, France.

Corresponding author: mguerra@fct.unl.pt

High precision X-ray spectrometry has pushed the boundaries of electronic structure calculation, as with increased energy resolution the emission line shapes reveal asymmetries that sometimes fail to be explained by theory. Among the possible parameters that might hinder a good agreement between theory and experiments are X-ray fundamental parameters, such as fluorescence and Coster-Kronig yields, shake-off and shake-up probabilities as well as transition energies and rates. To this date, the analysis of experimental spectra requires multi peak fitting including up to 12 or more parameters depending on the complexity of the system and whether satellite lines are present. These parameters include not only experimental features such as spectrometer energy resolution and transfer functions but also energy shifts, natural transition widths, spectator intensities and broadening. In this work, we have performed simulations of high accuracy X-ray spectra of Cu where there is still inconsistencies between theory and experiment, namely on  $K\alpha_2/K\alpha_1$  intensity ratios and widths. These ab initio calculations included relativistic and quantum electrodynamics corrections such as self-energy and vacuum polarization using the MultiConfiguration Dirac-Fock (MCDF) method. The simulation of the spectrum is then free of any fitting parameters, requiring only as input the experimental energy resolution, background intensity and any energy offset due to solid state effects. Noteworthy is the fact that the ratio between the diagram and the satellite lines intensities is not subject to any fitting, being obtained directly from their calculated relative intensities.



**ISRP 2021**  
**International Symposium on Radiation Physics**  
**Kuala Lumpur – Malaysia**  
**6 – 10 December 2021**

**A260 - X-ray phase contrast imaging with a simple prototype system: polyenergetic beam and a dental imaging detector.**

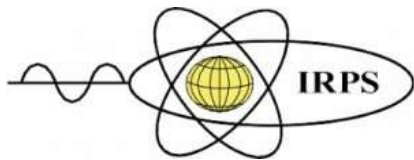
M.S.S. Gobo<sup>1</sup>, D.R. Balbin<sup>1</sup>, M.G. Hönnicke<sup>2</sup>, M.E. Poletti<sup>1</sup>

<sup>1</sup> Departamento de Física, Faculdade de Filosofia Ciências e Letras de Ribeirão Preto, Universidade de São Paulo, Brazil

<sup>2</sup> Instituto Latino-Americano de Ciências da Vida e da Natureza, Universidade Federal da Integração Latino-Americana, Brazil

Corresponding author: michelg@usp.br

Conventional X-ray images are obtained by placing an image receptor immediately after the object. The image contrast results from the variations on X-ray attenuation at structures within the object due to the different composition, density and thickness of these structures, as well as of the X-rays energies emitted from the source. Although this image modality is widely used in several applications, it can be limited when the attenuation characteristics of the structures and the surrounding medium are similar. However, if the image receptor is placed in a certain distance from the object, it's possible to detect phase changes after the X-rays refract in the object and travel a certain distance towards the image receptor. Thus, the phase contrast is formed. In this work, the propagation X-ray phase contrast imaging technique was studied and applied using a microfocus X-ray source (high spatial coherence), essentially polyenergetic, and a digital dental imaging detector, both compatible with conventional sources and detectors used clinically. Initially, all these elements were characterized and then the experimental setup was built and the influences of irradiation and geometric parameters on the images were investigated. Finally, several test phantoms (containing fibers and homogeneous materials with close attenuation characteristics) and animal tissues (bone, fibrous, adipose and mixed) were analyzed with this prototype system. The implemented prototype system showed great potential for biological and clinical applications, showing a significant increase in the contrast of biological and inorganic materials with similar attenuation characteristics, compared to the traditional X-ray images using the same energy spectrum.



**A261 - Proton therapy monitoring with orthogonal prompt-gamma imaging: the case of prostate irradiation**

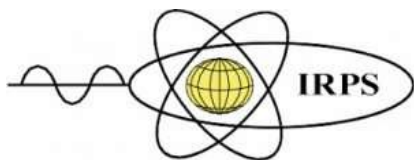
José Teodoro<sup>1,2</sup>, Valéria Lopes<sup>1,2</sup>, Andrey Morozov<sup>1</sup>, João Silva<sup>1,2</sup>, Paulo Crespo<sup>1,2</sup>, Hugo Simões<sup>1</sup>

<sup>1</sup>LIP – Laboratory of Instrumentation and Experimental Particle Physics, Coimbra, Portugal

<sup>2</sup>Department of Physics, University of Coimbra, Coimbra, Portugal

Corresponding author: hugo.simoies@coimbra.lip.pt

Proton therapy (PT) is growing worldwide since it can provide very conformational dose to the tumor being irradiated. However, diverse variables may compromise such conformational dose distribution, leading to undesirable situations that are suspected of being correlated with tumor recurrence. Several approaches have been suggested for in vivo proton beam range verification. One technique is based on detection of prompt-gamma rays (PG) originating from proton-nuclear interactions within the body. On one side, the emission of such PG rays occurs with higher intensity in the Bragg peak (BP) region. On the other side, PG emission should not occur after the BP since the protons are expected to stop at this point. Hence, LIP has addressed efforts to develop a multi-slat collimated system oriented orthogonally to the beam direction in order to detect the PG rays that escape the patient in the perpendicular direction. Such rays give an approximation of the proton's range into the patient. However, the neutrons produced during proton irradiation may interact with the patient and with the heavy structures inside the treatment room and produce secondary gamma rays that can mask the signal of interest. The number of neutrons increases as the proton energy increases, so the technique may be not suitable to assist in the irradiation of some anatomical regions, e.g. prostate irradiation, which requires protons with energies of 200 MeV or higher. Hence, a detailed study of this approach should include the simulation of real treatment plans. This task includes, on one hand, the adaptation of patient computed tomograms (which are proportional to electron density) into Geant4 (which includes tissue density and stoichiometry). On the other hand, some irradiation beam parameters (e.g. position, energy, direction, among others) should also be considered in the simulations. In this work, our latest developments on this topic will be presented.



**A262 - Polycapillary X-ray techniques for archeological studies: the Peltuinum excavation site**

V. Guglielmotti<sup>1,2</sup>, D. Hampai<sup>1</sup>, L. Migliorati<sup>3</sup>, A. Sperduti<sup>4</sup>, I. Fiore<sup>5</sup>, S. B. Dabagov<sup>1,6,7</sup>

<sup>1</sup> XLab Frascati, INFN–LNF, Italy

<sup>2</sup> Guglielmo Marconi University, Italy

<sup>3</sup> Dip. Scienze dell'Antichità, Sapienza University, Italy

<sup>4</sup> Museo delle Civiltà, Italy

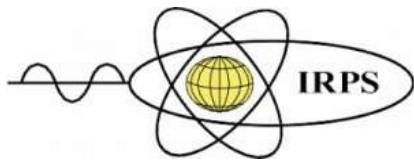
<sup>5</sup> Dip. Biologia Ambientale, Sapienza University, Italy

<sup>6</sup> National Research Nuclear University MEPhI, Russia

<sup>7</sup> RAS P.N. Lebedev Physical Institute, Russia

Corresponding author: [valeria.guglielmotti@lnf.infn.it](mailto:valeria.guglielmotti@lnf.infn.it)

The introduction of polycapillary optics into X-ray techniques has contributed to a huge improvement in terms of performances available with conventional lab setups, almost comparable to those achieved only with Synchrotron Radiation sources. At XLab Frascati, within the Laboratori Nazionali di Frascati (INFN-LNF), the expertise gained on X-ray techniques and on polycapillary lenses, has allowed researchers to carry out advanced X-ray spectroscopy and X-ray microscopy studies. We will show the results obtained on the characterization of building and crafting materials from the *Peltuinum* excavations (an archeological site located in Central Italy) to evaluate the temporal and geographical origin of the raw materials used for the production of these objects in an area characterized by the movement of goods and people linked to the presence of the sheep trail connecting Central and Southern Italy. Our focus is on the evaluation of the elemental composition and the structure materials coming from *Peltuinum*, as: a) tiles, to trace the origin of the clays used for the different productions; b) painted and unpainted plasters, mortars - characterized by the use of fine-grained gravel; c) limestone of different hardness, with different uses according to the context of destination; 4) ceramics, from the Roman age and archaic majolica productions, the latter being part of Abruzzo as early as the 14<sup>th</sup> century BCE; d) bone samples from domestic animal and people probably circulating along the sheep trail.



**A263 - High Resolution CT@XlabF: Future Tomographic Studies**

D. Hampai<sup>1</sup>, V. Guglielmotti<sup>1</sup> and S. B. Dabagov<sup>1,3,4</sup>

<sup>1</sup> INFN–LNF, XLab Frascati, Via E. Fermi, 40, I-00044 Frascati (Rome), Italy

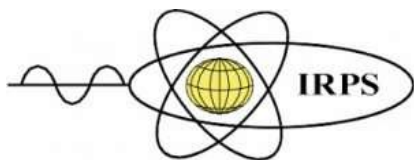
<sup>2</sup> Univ. Guglielmo Marconi, Department of Nuclear, Subnuclear and Radiation Physics, Rome Italy

<sup>3</sup> National Research Nuclear University MEPhI, Moscow, Russia

<sup>4</sup> RAS P.N. Lebedev Physical Institute, Moscow, Russia

Corresponding author: dariush.hampai@lnf.infn.it

Nowadays, x-ray Computed micro Tomography ( $\mu$ CT) is one of the most advanced high-resolution imaging techniques for the nondestructive analysis. Extreme penetration peculiarities of x-rays combined with beam shaping features of polycapillary x-ray optics allow contrast imaging of internal microstructures of various nontransparent objects and materials, becoming a basics for  $\mu$ CT. Measuring the three-dimensional (3D) X-ray attenuation coefficient, the distribution of areas with different densities and/or chemical compositions over the sample is typically visualized by virtual slicing or 3D volume rendering. Recently, at XLab Frascati (Dabagov laboratory at the National Institute for Nuclear Physics, Italy) a new dedicated facility, a Computed Tomography Station (CTS), has been installed offering to the users the accessibility to advanced  $\mu$ CT studies. Utilising a microfocus source with an advanced laboratory optics, CTS can provide a spatial resolution close to the focal spot size. Moreover, analysis enforced by the cross-section microstructure of the optics can result even in higher resolution without the radiation intensity increase. Furthermore, as known, performing phase-contrast microCT measurements is allowed independently of a limited spatial coherence with respect to the synchrotron radiation beam. Keeping in mind the growing request for the nondestructive analysis, x-ray CTS should represent a powerful investigation tool in the variety of applications, as for material science, geology, biomaterials and cultural heritage.



**ISRP 2021**  
**International Symposium on Radiation Physics**  
**Kuala Lumpur – Malaysia**  
**6 – 10 December 2021**

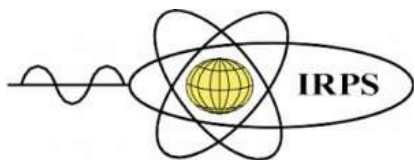
**A270 - Assessment Of Environmental Radioactivity In The Spacial Area Of Titanium Mining At Ha Tinh Province (Vietnam)**

Sy Minh Tuan Hoang<sup>1</sup>

<sup>1</sup>Institute of Applied Technology - Thu Dau Mot University, 6, Tran Van On, Phu Hoa Ward, Thu Dau Mot City, Binh Duong, Vietnam, 820000

Corresponding author: hoangsyminhtuan@tdmu.edu.vn

The assessment of the ambient dose rate from the natural background is always the main object of the environmental monitoring programs. Ky Anh, at coordinates of 18°07'35" N-106°15'27" E, is a rural district of Ha Tinh Province in the North Central Coast region of Vietnam. The titanium mineral itself has caused radioactive contamination to various degrees in the surrounding environments. Primarily, the mineral deposit at the mining area is located very close to even intermingling with residential areas; therefore, attention should be paid to investigating the status of radioactive contamination in the mine. The obtained values of the environmental gamma dose-rates were widely fluctuated in the range from 0.05 to 0.18 $\mu$ Sv/h, with the average value of 0.10  $\mu$ Sv/h. Approximately 86.2% of the obtained dose-rates within the range from 0.08 to 0.12  $\mu$ Sv/h equivalent to 0.70 to 1.05  $\mu$ Sv/year, and this range agrees with the natural radiation background in the entire world. In addition, the average values of the radioactivity of isotopes <sup>238</sup>U, <sup>226</sup>Ra, <sup>232</sup>Th, <sup>40</sup>K, and <sup>137</sup>Cs in the surface soil collected at 120 positions were 33.1, 21.1, 36.6, 279.0, and 0.42 Bq/kg, respectively and used to figure out the dose rate at 1m above the ground caused by these isotopes. The average calculated value was 0.048  $\mu$ Sv/h or 0.42 mSv/year.



**ISRP 2021**  
**International Symposium on Radiation Physics**  
**Kuala Lumpur – Malaysia**  
**6 – 10 December 2021**

**A276 - Resolution of ferrocene and deuterated ferrocene conformations using dynamic vibrational IR spectroscopy**

Nicholas Tran<sup>1</sup>, Ryan Trevorah<sup>1</sup>, Christopher Chantler<sup>1</sup>, Dominique Appadoo<sup>2</sup>, Feng Wang<sup>3</sup>

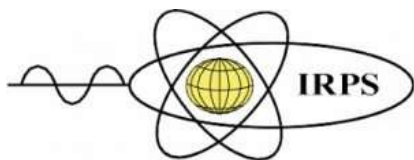
<sup>1</sup>School of Physics, The University of Melbourne, Australia

<sup>2</sup>Australian Synchrotron, Australia

<sup>3</sup>Department of Chemistry and Biotechnology, Swinburne University of Technology, Australia

Corresponding author: nicholast2@student.unimelb.edu.au

The signature of molecular vibrations and distortions in dynamic molecules gives a complex fingerprint which is insightful and can substantiate chemical hypotheses regarding molecular and conformer stability. Using high-accuracy experimental data of ferrocene (Fc) and deuterated ferrocene (dFc, Fc-d<sup>10</sup>) at temperatures from 7 K through to 388 K, we obtain complex spectral profiles which require an advanced reaction coordinate model to explain. We obtain compelling evidence that the single conformer model (staggered D<sub>5d</sub> or eclipsed D<sub>5h</sub>) used to interpret and explain many experimental results on ferrocene is invalid. We also present compelling evidence that mixed conformer models are invalid, where ferrocene is represented by an effective dihedral angle between the cyclopentadienyl (Cp) rings; or by a mixture of Boltzmann populations of the two conformers. We find no evidence for single or mixed conformer models despite covering almost all conclusions from past literature for gas, solution or solid phase Fc. A new principle based on the reaction coordinate is introduced using advanced spectroscopy and modelling for hypothesis testing, to articulate the nature of the potential surface, the reaction coordinate, and subtle conformational changes in dilute systems. Theoretical calculations of the infrared spectra of D<sub>5h</sub> and D<sub>5d</sub> with the B3LYP/m6-31G(d) functional highlights a significant difference between Fc conformations around 450–500 cm<sup>-1</sup> and early investigations provided key insight into the quantum dynamics of ferrocene. A new methodology for obtaining defined uncertainties with high quality Fourier Transform Infrared (FTIR) measurements allow for quantitative hypothesis testing for complex structural determination. Our experimental analysis shows that the lowest energy conformer is D<sub>5h</sub> for both Fc and dFc at low temperatures, but as temperature increases, the population of occupied vibrational modes increases towards the D<sub>5d</sub> conformation. We obtain agreement of the model with the complex spectral evolution of profiles.



**ISRP 2021**  
**International Symposium on Radiation Physics**  
**Kuala Lumpur – Malaysia**  
**6 – 10 December 2021**

### **A278 - Calculating Characteristic Spectral Profiles: Copper $K\alpha$ and $K\beta$**

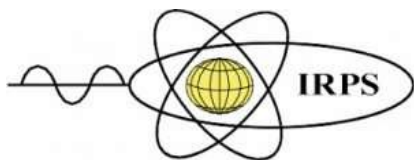
Hamish A. Melia, Truong V. B. Nguyen, Christopher T. Chantler

Institution: The University of Melbourne, Australia

Understanding fundamental atomic processes is key to advancing the field of radiation physics and spectroscopy. Copper is the most common source for laboratory X-Rays worldwide. Therefore, theoretical understanding of the copper characteristic X-Ray sources is vitally important to the field. There have been several high accuracy measurements of the copper  $K\alpha$  and  $K\beta$  spectrum recently. However, there is some discrepancy between these empirical investigations and the most recent theoretical studies.

Using a multiconfigurational Dirac-Hartree-Fock approach we have calculated the copper  $K\alpha$  and  $K\beta$  spectra. Results are the eigenenergies and relative amplitudes of the diagram and satellite lines. Novel results are the satellite lines and the shake-off probabilities for 1s, 2s, 2p, 3s, 3p, 3d, and 4s subshells. Convergence is monitored through gauge ratios and the evolution of energies with expansion to higher orbitals.

Theoretical investigations into fundamental X-Ray processes are essential for advancing the capabilities of computational relativistic quantum mechanics. Furthermore, by accounting for well-known and well-studied phenomena, such as shake-off events, to high accuracies we are able to make better claims on the consequences of lesser known features. For example, by characterising shake-events in various characteristic X-Ray spectra to greater precision, any discrepancies between theory and experiment can more strongly invoke other processes, such as the Auger Effect.



**ISRP 2021**  
**International Symposium on Radiation Physics**  
**Kuala Lumpur – Malaysia**  
**6 – 10 December 2021**

## **POSTER PRESENTATIONS**

Ordered by abstract number

### **A004 - A Study of the Neutron Induced Event Rate during Solar Eclipse Using Superheated Emulsion Detector**

Suraj Ali<sup>1,#</sup>, Mala Das<sup>1,\$</sup>

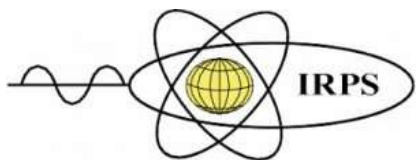
<sup>1</sup>Astroparticle Physics & Cosmology Division, Saha Institute of Nuclear Physics, Kolkata, India

<sup>#</sup>Present address : Department of Physics, Muralidhar Girls' College, India

<sup>\$</sup>Present address: High Energy Nuclear & Particle Physics Division, Saha Institute of Nuclear Physics, Kolkata , India

Corresponding author: mala.das@saha.ac.in

To observe the variation of neutron induced events, the experiments have been conducted on an annular solar eclipse day and a normal day using a Superheated Emulsion Detector (SED). The SED has been fabricated in the laboratory with R134a (C<sub>2</sub>H<sub>2</sub>F<sub>4</sub>) liquid of b.p. = -26.3 oC . The acoustic signals are produced in this detector by the shock wave created due to the energy deposition by the energetic particles. The present measurement has been carried out with R134a SED operated at 40oC at the laboratory (Kolkata, India) on 26 December 2019 which was an annular solar eclipse day that starts at 8:06 am (IST) and ends at 11:10 am (IST). Similar experiment has been carried out on a normal day. The calibration experiment has been carried out with <sup>241</sup>Am-Be neutron and <sup>137</sup>Cs gamma sources. We define the acoustic power, and Fundamental Frequency variables from the measured acoustic pulses. From the analysis with these variables it is observed that the maximum events during solar eclipse day were due to the neutrons. The expected event rate for neutrons has also been calculated for the interaction cross section of some specific energy of neutrons. The experimental count rate on the day of solar eclipse is found out to be  $7.75E-03 \pm 0.84E-03$  per second and on the normal day is  $2.16E-03 \pm 0.44E-03$  per second. The present study shows that there is an enhancement of the neutron flux during the solar eclipse. The effect of the small variation of gamma ray flux during the solar eclipse as reported earlier is not visible in this measurement.



### **A005 - Stability measurement of R-134a superheated emulsion detector**

Sunita Sahoo<sup>1,2</sup>, Mala Das<sup>1,2</sup>

<sup>1</sup>Astroparticle Physics & Cosmology Division, Saha Institute of Nuclear Physics, Kolkata 700064, India

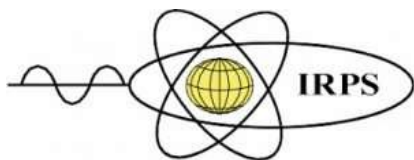
<sup>2</sup>Homi Bhabha National Institute, Training School Complex, Anushakti Nagar, Mumbai 400094, India

The superheated emulsion detector (SED) is based on the dispersion of superheated liquid droplets in an impurities-free gel base matrix. The SED performs well as a neutron detector in a mixed radiation field as it is sensitive to heavy ionizing particles at a specific temperature and pressure combination of the superheated liquid, but insensitive to low ionizing particles in the same thermodynamic regime [1]. This property of SED allows it to be used in dark matter direct search experiments, which is a challenging field of research these days [2]. The SED should run for a long time to detect the dark matter (DM) candidates as the cross-section of interaction of the DM with the detector nuclei is extremely small, on the scale of about  $10^{-41}$  cm<sup>2</sup> [3]. To run the SED for an extended period of time, one must know the superheated droplet stability feature. Superheated state is generally short lived in nature due to the presence of heterogeneous nucleation sites such as trapped air bubbles in gel base matrix, roughness of container, dissolved gas pockets etc. which can initiate nucleation to reach at stable vapour state. By removing such potential heterogeneous nucleation sites, the stability of the superheated state can be improved significantly. Another factor is that during SED fabrication process, stress is induced in the SED, which also promotes spontaneous nucleation so it requires curing for several days to be used in the experiment. In the present work, for different ranges of superheated droplet sizes, the stability of R-134a (C<sub>2</sub>H<sub>2</sub>F<sub>4</sub>, b.p. -26.3 °C) superheated liquid droplets has been investigated as a function of curing time. Here the curing time refers to the day from the SED fabrication. The gel matrix utilised in R-134 SED fabrication was properly degassed by vacuum pump to remove the trapped air bubbles. By adjusting the stirrer rotation speed of the high pressure reactor, different sized R-134a SEDs were created. The 900 rpm (rotation per minute) and 1400 rpm of the stirrer speed were used to fabricate the SEDs. To better understand the stability of the superheated droplets, the rate of bubble nucleation events was investigated in presence of a <sup>241</sup>Am-Be neutron source (10 mCi) with varying curing times. At 34 °C operating temperature, both SEDs (900 and 1400 rpm) were irradiated with the neutron source. It is observed that both the SEDs remain stable throughout the 5-months of curing period and enters into fragile region after an around 8 months of curing time.

[1] F. d'Errico, Nucl. Instr. Meth. Phys. B 184 (2001) 229.

[2] S. C. Roy, Radiat. Phys. Chem. 61 (2001) 271.

[3] C. Amole et al (PICO Collaboration), Phys. Rev. D 100 (2019) 022001.



**ISRP 2021**  
**International Symposium on Radiation Physics**  
**Kuala Lumpur – Malaysia**  
**6 – 10 December 2021**

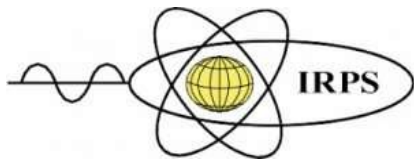
**A011 - Tomographic Voxel Deformable Phantom, Full Body Model for Radiation Protection Assessment**

Ali A Alghamdi<sup>1</sup>

<sup>1</sup>Department of Radiological Sciences, Imam Abdurhman Bin Faisal University, Kingdom of Saudi Arabia

Corresponding author: [alalghamdi@iau.edu.sa](mailto:alalghamdi@iau.edu.sa)

The purpose of this study is to build a model with similar characteristics to the average population of Saudi Arabia for radiation protection purpose, dosimetry, risk assessment and other related applications. A survey was conducted on the eastern province of Saudi Arabia among male volunteers only, recording their age, mass (weight) and height. A total of 3,404 data sets were collected. The data were used to find the average characteristics by which a volunteer was chosen to be the source of the computational phantom data. The tissues and organs according to ICRP 103 recommendation for radiation protection calculations were segmented from the phantom using open source software. A comparison of the dose calculation using MCNPX Monte Carlo code is presented with ICRP computational phantom for photon irradiation conditions. Results of implemented phantoms postures, one in a standing and the other walking are presented and discussed. The results showed that the phantom in walking posture may receive up to 2.96 times the dose of the standing one. In general, the organ dose in the walking phantom is in the order of 1.5 times that of the standing one. The radiation dosage estimation with the new phantom will be particularly relevant practical radiological situations. In addition the data from phantom will serve the implementation of the created computational virtual phantom for education purposes i.e. sectional anatomy teaching and advance images synthesising.



**A013 - Synthetic heavyweight concrete for low and mid-gamma ray energy protection applications**

K. A. Mahmoud<sup>1,2</sup>, M I Sayyed<sup>3,4</sup>, M Y. Hanfi<sup>1,2</sup>, Aljawhara H. Almuqrin<sup>5</sup>, K.A. Naseer<sup>6</sup>, O. L. Tashlykov<sup>1</sup>, Mayeen Uddin Khandaker<sup>7</sup>

<sup>1</sup>Ural Federal University, 19 Mira St, 620002, Ekaterinburg, Russia,

<sup>2</sup>Nuclear Materials Authority, P. O. Box 530 El-Maadi, Cairo, Egypt.

<sup>3</sup>Department of Physics, Faculty of Science, Isra University, Amman 11622, Jordan

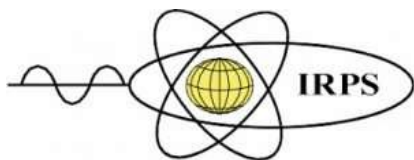
<sup>4</sup>Department of Nuclear Medicine Research, Institute for Research and Medical Consultations, Imam Abdulrahman bin Faisal University, Dammam 31441, Saudi Arabia

<sup>5</sup>Department of physics, college of science, Princess Nourah bint Abdulrahman University, Riyadh, Saudi Arabia

<sup>6</sup>Department of Physics, The Gandhigram Rural Institute - Deemed to be University, Gandhigram - 624 302, India

<sup>7</sup>Center for Applied Physics and Radiation Technologies, School of Engineering and Technology, Sunway University, 47500 Bandar Sunway, Selangor Darul Ehsan, Malaysia

The present study aims to fabricate a new concrete material that can be applied in radiation shielding applications. The fabricated concrete was prepared as a mixture of Portland cement, granite (coarse aggregate), and sand with ratios of 1: 3: 2 by volume. First, the mentioned components were mixed well, and then the water was added with different cement/water ratios 0.4, 0.6, and 0.8. Then the mixture with water content was mixed well and molded in the cubic molds with dimensions of  $7\text{ cm} \times 7 \times d$ , where  $d$  is the thickness and takes different values in the fabricated concretes. Three thicknesses were fabricated for each sample, and all samples were saved for 15 days to dry. After that, the preformed concretes density was measured using the volume ( $V$ ,  $\text{cm}^3$ ) and mass ( $M$ ,  $\text{g}$ ) of the samples were  $\rho = M/V$ , and the received results were confirmed by the density meter MH-300A. The density of the fabricated samples varied between 2.588 to 2.61  $\text{g}/\text{cm}^3$ . Also, the chemical composition of the concretes was measured. Then, the measured density and chemical. The chemical composition and density were applied to the Monte Carlo simulation to predict the fabricated concretes' attenuation characteristics in the energy range between 0.015 and 2 MeV. The predicted linear attenuation coefficient, transmission factor (TF), and half-value layer (HVL) were confirmed experimentally using the NaI detector.



**A014 - Study the radiation attenuation properties of ball clay-cement- slag iron composites by experimental and theoretical methods**

M. Almatari<sup>1,\*</sup>, M.G. Dong<sup>2</sup>, M.I.Sayed<sup>3,4</sup>, Mayeen Uddin Khandaker<sup>5</sup>, D. A. Bradley<sup>5,6</sup>, M.Elsafi<sup>7</sup>

<sup>1</sup>Department of Physics, Faculty of Sciences, Al-Balqa Applied University, Al-Salt 19117, Jordan

<sup>2</sup>Department of Resources and Environment, School of Metallurgy, Northeastern University, Shenyang 110819, China

<sup>3</sup>Department of Physics, Faculty of Science, Isra University, Amman – Jordan

<sup>4</sup>Department of Nuclear Medicine Research, Institute for Research and Medical Consultations (IRMC), Imam Abdulrahman bin Faisal University (IAU), PO Box 1982, Dammam, 31441, Saudi Arabia

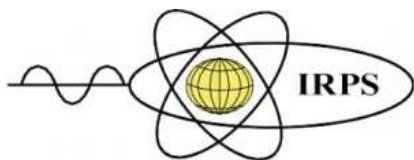
<sup>5</sup>Center for Applied Physics and Radiation Technologies, School of Engineering and Technology, Sunway University, 47500 Bandar Sunway, Selangor Darul Ehsan, Malaysia

<sup>6</sup>Department of Physics, University of Surrey, Guildford, Surrey GU2 7XH, UK

<sup>7</sup>Physics Department, Faculty of Science, Alexandria University, 21511 Alexandria, Egypt.

Corresponding author: matari@bau.edu.jo

The current work aimed to study the attenuation properties of ball clay-cement- slag iron as an alternative to concrete. The percentages between the three compounds were changed to obtain the best compound used to attenuate the photons. From this, 6 samples were designed as follows BCSI-x (where x represents values from 0 to 5). Experimentally the mass attenuation coefficient (MAC) was examined by using a HPGe detector. The measurement has been done using the collimated beam technique by different point sources (Am-241, Cs-137 and Eu-152). The experimental obtained results were compared with the results of XCOM program. The linear attenuation coefficient (LAC) as well as the half value layer (HVL) of the studied samples were calculated and compared with concrete and some types of ceramics and showed good results. This compound should be taken into consideration as a shield from radiation, especially that it does not cost as concrete or as a commercial shield, and has good mechanical and thermal properties.



**A015 - New recommended containers as a protection method against the intermediate level of radioactive wastes**

K.A. Mahmoud<sup>1,2</sup>, M.I. Sayyed<sup>3,4</sup>, Mayeen Uddin Khandaker<sup>5</sup>, O.L. Taslykov<sup>1</sup>

<sup>1</sup>Ural Federal University, 19 Mira St, 620002, Ekaterinburg, Russia,

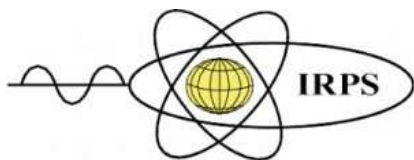
<sup>2</sup>Nuclear Materials Authority, P.O. Box 530 El-Maadi, Cairo, Egypt.

<sup>3</sup>Department of Physics, Faculty of Science, Isra University, Amman 11622, Jordan

<sup>4</sup>Department of Nuclear Medicine Research, Institute for Research and Medical Consultations, Imam Abdulrahman bin Faisal University, Dammam 31441, Saudi Arabia

<sup>5</sup>Center for Applied Physics and Radiation Technologies, School of Engineering and Technology, Sunway University, 47500 Bandar Sunway, Selangor Darul Ehsan, Malaysia

Nowadays the nuclear power plants are widely used in power generation. Thus, a huge amount of radioactive wastes was produced each year around the world. These radioactive wastes are classified according to their activity to high, intermediate, and low-level wastes. The high-level radioactive wastes represent around 95% of the detected total radioactive in the nuclear reactors. These type of radioactive wastes is hazardous. Thus, the radioactive waste has to cool off inside the reactor in deep pools for many years to be under control. On the other hand, the intermediate level wastes represent around 4% of the total radioactivity detected in the reactor. These wastes come from refurbishment waste, ion-exchange resins, and metal fuel cladding. The third is the low-level wastes which are not dangerous do not require shielding during handling and transport. The present work deals with the design of new containers to protect the ion-exchange resins and their adsorbate impurities (Co-60 and Cs-137) during the reactor cooling process. The Monte Carlo simulation was utilized to estimate the total absorbed dose received at 1 m from the container contains adsorbent and adsorbate. The recommended container consists of 3 layers. The outer wall is 15 cm of concrete, followed by empty space that can be filled with crushed rocks (filler). The inner layer (displacer) consists of a cylindrical container of different metals/alloys with thickness varied between 0.5 and 3 cm. The effect of displacer types, displacer thickness, and the filler type on the average absorbed dose was studied. The best lowest dose was received when using a displacer made up of (80PbO-20ZnO) alloys, the absorbed dose at 100 cm from the container reduced from 9.088 to 0.974  $\mu\text{Sv/h}$  with increasing the displacer thickness between 0.5 and 3 cm. on the other hand, the highest absorbed dose received was 22.143  $\mu\text{Sv/h}$ . This absorbed dose is received when the container consists of the concrete walls only without any displacer.



**ISRP 2021**  
**International Symposium on Radiation Physics**  
**Kuala Lumpur – Malaysia**  
**6 – 10 December 2021**

**A017 - An experimental technique for measuring the photon attenuation features of the glass system  $P_2O_5$ -CaO-K<sub>2</sub>O-N<sub>2</sub>O-PbO**

Nuha Al-Harbi<sup>1,2,\*</sup>, M. I. Sayyed<sup>3,4,\*</sup>, Ashok Kumar<sup>5,6</sup>, Mayeen Uddin Khandaker<sup>7</sup>, M.Elsafi<sup>8</sup>

<sup>1</sup>Department of Physics, Faculty of Science, King Abdulaziz University, Jeddah 21589, Kingdom of Saudi Arabia

<sup>2</sup>Department of Physics, Umm AL-Qura University, Makkah, Saudi Arabia

<sup>3</sup>Department of Physics, Faculty of Science, Isra University, Amman – Jordan

<sup>4</sup>Department of Nuclear Medicine Research, Institute for Research and Medical Consultations (IRMC), Imam Abdulrahman bin Faisal University (IAU), PO Box 1982, Dammam, 31441, Saudi Arabia

<sup>5</sup>University College, Benra- Dhuri, Punjab, India.

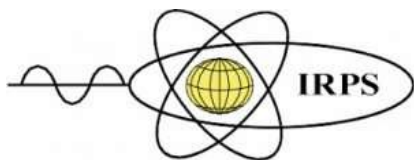
<sup>6</sup>Department of Physics, Punjabi University, Patiala, Punjab, India.

<sup>7</sup>Center for Applied Physics and Radiation Technologies, School of Engineering and Technology, Sunway University, 47500 Bandar Sunway, Selangor Darul Ehsan, Malaysia

<sup>8</sup>Physics Department, Faculty of Science, Alexandria University, 21511 Alexandria, Egypt.

Corresponding author: nallhibi0001@stu.kau.edu.sa

The photon shielding characterization of glass system  $40P_2O_5$  - $20CaO$  -  $10K_2O$  –  $(30-x) N_2O$  –  $x PbO$  (where x equal the values 0, 5, 10, 15 and 20 mol %) were determined. The experimental technique was applied to measure the linear-attenuation parameter (LAC) using NaI detector and multi radioactive point source (Cs-137, Co-60, Ba-133 and Am-241) to achieve a wide range of energies. The results of the experimental technique were compared with the theoretical results from online XCOM software and were found a fine agreement between the two results. The other deduced parameters of the LAC results were evaluated such as a half attenuator layer (HAL), mean free pass (MFP), Transmission factor (TF) and the photon protection efficiency (PPE). The present glass system was compared with recently published commercial glasses. The comparison showed the positive use of this glass as transparent and protective shield in places that use photons of X-ray or gamma ray.



**ISRP 2021**  
**International Symposium on Radiation Physics**  
**Kuala Lumpur – Malaysia**  
**6 – 10 December 2021**

**A018 - Comparison of radiation shielding ability of bulk and nanoparticle  $\text{Bi}_2\text{O}_3$  radiation shields**

M.I.Sayyed<sup>1,2,\*</sup>, M.Elsafi<sup>3</sup>, Mayeen Uddin Khandaker<sup>4</sup>, D. A. Bradley<sup>4,5</sup>

<sup>1</sup>Department of Physics, Faculty of Science, Isra University, Amman – Jordan

<sup>2</sup>Department of Nuclear Medicine Research, Institute for Research and Medical Consultations (IRMC), Imam Abdulrahman bin Faisal University (IAU), PO Box 1982, Dammam, 31441, Saudi Arabia

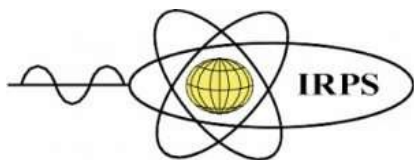
<sup>3</sup>Physics Department, Faculty of Science, Alexandria University, 21511 Alexandria, Egypt.

<sup>4</sup>Center for Applied Physics and Radiation Technologies, School of Engineering and Technology, Sunway University, 47500 Bandar Sunway, Selangor Darul Ehsan, Malaysia

<sup>5</sup>Department of Physics, University of Surrey, Guildford, Surrey GU2 7XH, UK

Corresponding author: mabualssayed@ut.edu.sa

The present work aims to study the attenuation ability of micro and nanoparticles of  $\text{Bi}_2\text{O}_3$ . To evaluate the attenuation parameters of two different  $\text{Bi}_2\text{O}_3$  types, the linear attenuation coefficient or LAC was determined experimentally for both types. The experiment was done using a narrow collimated beam method. A high pure germanium detector or, HPGe and different point sources have energies from 0.0595 up to 1.408 MeV. The experimental results of micro  $\text{Bi}_2\text{O}_3$  were compared with the results obtained from the XCOM online software and the results showed a good agreement which indicates the validity of the experimental values of nanoparticles. The mass and thickness, which required to attenuate the initial photon intensity to its half value ( $M_{1/2}$  and  $H_{1/2}$  respectively) were calculated. The results proved that the  $M_{1/2}$  be less in the case of nanoparticles. This means that using nanoparticles as an alternative to micro  $\text{Bi}_2\text{O}_3$ , which will provide the anti-radiation shield mass and have the same shielding efficiency at different energies.



**ISRP 2021**  
**International Symposium on Radiation Physics**  
**Kuala Lumpur – Malaysia**  
**6 – 10 December 2021**

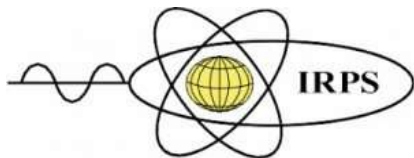
**A019 - Determination of 3D distribution of toxic chemical elements in historical plaster with surface and confocal X-ray fluorescence mapping**

Tomáš Trojek<sup>1</sup>, Martin Hložek<sup>1</sup>

<sup>1</sup>Department of Dosimetry and Application of Ionizing Radiation, Czech Technical University in Prague, Czech Republic

Corresponding author: tomas.trojek@fjfi.cvut.cz

Identification of toxic materials in historical objects is one of the many topics studied in the cultural heritage sciences. In this particular case, we have focused our attention on presence of such elements in coloured paints on historic plaster. The use of toxic elements in plaster is not only a recent problem but these elements can be found in historical buildings too. Thus, they represent a serious risk in the case of restoration, for instance. Heavier elements (e.g. lead or arsenic) are well measurable with X-ray fluorescence (XRF) analysis and the hand-held XRF instruments have been already used to identifying lead-based paints. However, such point XRF analysis can only provide information on the increased presence of the toxic element and it can estimate its amount if lead is distributed homogeneously. In this work, we tried to apply XRF mapping techniques to get 3D distributions of all heavier elements. The studied samples were taken from the walls of the rectory building in Potštát (Přerov district, Czech Republic), which are dated to the Baroque period, but may also be older because the building was built during the Renaissance. For the needs of restorers, samples are normally taken destructively from the walls of buildings, processed into the form of cut slides and studied by various types of microscopes. In our investigation, surface XRF scanning was firstly applied to a piece of wall with an aim to find areas containing toxic elements. Secondly, confocal 2D mapping was tested to visualize non-destructively the stratigraphy image of the selected parts of the sample. It made us possible to identify a structure of the sample which includes more layers with toxic elements. Another advantage of XRF mapping techniques is the contactless analysis without the more difficult sample preparation, which is unpleasant when working with toxic materials.



**ISRP 2021**  
**International Symposium on Radiation Physics**  
**Kuala Lumpur – Malaysia**  
**6 – 10 December 2021**

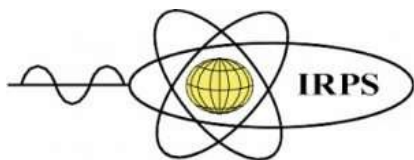
### **A020 - From counting-rate profile to $^{137}\text{Cs}$ profile**

Servo Kasi<sup>1</sup>

<sup>1</sup>IRPS, This Globe

Corresponding author: servo.kasi@aalto.fi

After Chernobyl accident (1986) the vertical distribution (profile) of  $^{137}\text{Cs}$  (30.17 a) I have measured in Finland with a new method. This method I have not seen in this connection elsewhere. What I have seen is to take samples and to measure their radioactivity in laboratory. Then the soil is destroyed. My method is nondestructive. The only gamma photon of  $^{137}\text{Cs}$  has the energy 661.7 keV.  $^{134}\text{Cs}$  (2.064 a) has been under consideration, because especially the 604.7 keV photon disturbs  $^{137}\text{Cs}$  measurements with the NaI(Tl) scintillator. I set scintillator in the tube, which had been in soil before 1986 (In peat I measured without tube). I measured the counting rate in different depths. The result is the counting-rate profile. The paper tells the inversion calculation from the counting-rate profile to the  $^{137}\text{Cs}$  density profile. In the calculation it is assumed that the  $^{137}\text{Cs}$  density only depends on the depth dimension. Soil density profile must be known well. Also element composition influences little. I have found that radioactive cesium (probably also  $^{135}\text{Cs}$ , 2.3 Ma) seems to be stabilized in mineral soil in few years. –This method has in the world been used in the borehole measurements of natural radioactivity (radioactive potassium, uranium, thorium).



**ISRP 2021**  
**International Symposium on Radiation Physics**  
**Kuala Lumpur – Malaysia**  
**6 – 10 December 2021**

**A022 - Assessment of radioactivity in the granite of granitoids at Nikeiba, south Eastern Desert, Egypt; radionuclides concentrations and radiological hazard parameters.**

Mohamed Y. Hanfi<sup>1,2§,\*</sup>, Ahmed E. Abdel Gawad<sup>1§</sup>, Khaled Ali<sup>1</sup>, Hassan Eliwa<sup>3</sup>, Mohamed I. Sayyed<sup>4,5</sup>, Mayeen Uddin Khandaker<sup>6</sup>

<sup>1</sup>Nuclear Materials Authority, P.O. Box 530 El-Maadi, Cairo, Egypt

<sup>2</sup>Institute of Physics and Technology, Ural Federal University, Ekaterinburg, Russia

<sup>3</sup>Geology Department, Faculty of Science, Minufiya University, Shebin El Kom, Egypt

<sup>4</sup>Department of Nuclear Medicine Research, Institute for Research and Medical Consultations (IRMC), Imam Abdulrahman bin Faisal University (IAU), P.O. Box 1982, Dammam, 31441, Saudi Arabia

<sup>5</sup>Department of physics, Faculty of Science, Isra University, Amman – Jordan

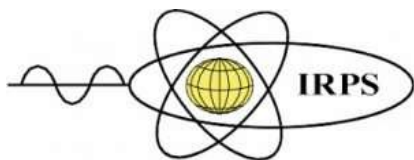
<sup>6</sup>Center for Applied Physics and Radiation Technologies, School of Engineering and Technology, Sunway University, 47500 Bandar Sunway, Selangor Darul Ehsan, Malaysia

<sup>7</sup>Department of Physics, University of Surrey, Guildford, Surrey, GU2 7XH, UK

<sup>§</sup> Ahmed E. Abdel Gawad, and Mohamed Y. Hanfi contributed equally to this work

Corresponding author: Mokhamed.Khanfi@urfu.ru

The present study aims to study the petrographical characteristics and evaluating the natural radionuclides  $^{238}\text{U}$ ,  $^{232}\text{Th}$ , and  $^{40}\text{K}$  and their activities in the collected granitoid samples from the Nikeiba, south Eastern Desert of Egypt. The geological investigation revealed the granites are metavolcanics, syenogranite, alkali feldspar granite and quartz syenite intruded by microgranite dikes and quartz veins. Moreover the mineral analysis illustrated the granites are bearing by radioactive minerals such as uranotorite as well as monazite, zircon and yttracolumbite. The mean activity concentrations of  $^{238}\text{U}$ ,  $^{232}\text{Th}$  and  $^{40}\text{K}$  are  $83.2 \pm 20.8$ ,  $75.2 \pm 23.3$  and  $1012.4 \pm 172.5 \text{ Bq kg}^{-1}$ , respectively which exceeded the worldwide average 33, 45 and  $412 \text{ Bq kg}^{-1}$ , respectively. The public exposure to emitted gamma radiation is detected by estimating various radiological hazard indices like radium equivalent content ( $R_{\text{eq}}$ ), external and internal hazard indices ( $H_{\text{ex}}$  and  $H_{\text{in}}$ ), annual effective dose (AED), annual gonadal dose equivalent (AGDE) and excess lifetime cancer (ELCR). The obtained results of radiological hazards parameters depicted that public exposure to emitted gamma radiation can induce various dangerous health effects. Thus, the application of the investigated sediments in different building materials and infrastructures fields is not safe. The multivariate statistical analysis is applied to detect the correlation of radionuclides with the radiological hazard parameters.



**ISRP 2021**  
**International Symposium on Radiation Physics**  
**Kuala Lumpur – Malaysia**  
**6 – 10 December 2021**

**A024 - The efficacy of WCu composites in shielding of ionizing radiation; experimental and theoretical studies.**

M.G. Dong<sup>1,\*</sup>, M.Y. Hanfi<sup>2,3</sup>, Daria Tishkevich<sup>4,5</sup>, Vladimir S. Semenishchev<sup>6</sup>, M.I. Sayyed<sup>7,8</sup>, Suying Zhou<sup>1</sup>, Alex Trukhanov<sup>4,5</sup>, Sergey S. Grabchikov<sup>4</sup>, Mayeen Uddin Khandaker<sup>9</sup>, Xiangxin XUE<sup>1</sup>

<sup>1</sup>Department of Resource and Environment, School of Metallurgy, Northeastern University, Shenyang 110819, PR China

<sup>2</sup>Ural Federal University, Mira St., 19, 62002, Yekaterinburg, Russia

<sup>3</sup>Nuclear Materials Authority, El Maadi, Cairo, Egypt

<sup>4</sup>Laboratory of Magnetic Films Physics, Scientific-Practical Materials Research Centre of National Academy of Sciences of Belarus, 220072 Minsk, Belarus

<sup>5</sup>Laboratory of Single Crystal Growth, South Ural State University, 454080 Chelyabinsk, Russia

<sup>6</sup>Department of Radiochemistry and Applied Ecology, Ural Federal University, 19, Mira Street, Yekaterinburg, Russia 620002

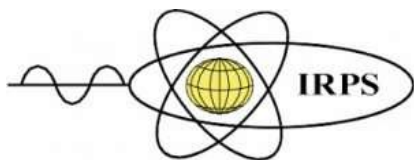
<sup>7</sup>Department of physics, Faculty of Science, Isra University, Amman 11622, Jordan

<sup>8</sup>Department of Nuclear Medicine Research, Institute for Research and Medical Consultations, Imam Abdulrahman bin Faisal University, Dammam 31441, Saudi Arabia

<sup>9</sup>Center for Applied Physics and Radiation Technologies, School of Engineering and Technology, Sunway University, 47500 Bandar Sunway, Selangor Darul Ehsan, Malaysia

Corresponding author: mg\_dong@163.com

A comprehensive study of the present work aimed to investigate the radiation shielding features for WCu composites materials with high density. The solid-phase synthesis was applied to obtain W85Cu15 and W75Cu25 composites with various thickness (0.6, 0.9, 1.2, 1.5 and 2.7 cm). The linear attenuation coefficient (LAC) was detected experimentally using a NaI detector at various incoming photon energy. The obtained results are confirmed by the theoretical data were detected by the Phy-X/PDS software program. The highest value of LAC ( $7.05 \text{ cm}^{-1}$ ) is found at low energy 0.266 MeV while the lowest value ( $0.86 \text{ cm}^{-1}$ ) is observed at high energy 1.25 MeV. The Mass attenuation coefficient ( $\mu_p$ ), the half-value layer (HVL) and the radiation protection efficiency (RPE) were also computed. The shielding ability is tested by comparing the mean free path of the studied composites with the commercial ones. Finally, it can deduce the discussed fabricated WCu composites are suitable to apply in diverse applications of radiation protection.



**A025 - Effect Of Bi<sub>2</sub>O<sub>3</sub> Addition On Radiation Shielding And Elastic Properties Of Mixed Ionic-Electronic 98[20Li<sub>2</sub>O-XBi<sub>2</sub>O<sub>3</sub>-(80-X)TeO<sub>2</sub>]-2Ag Glass System**

M.S. Sutrisno<sup>1,3</sup>, M.A. Yahya<sup>2</sup>, R. Hisam<sup>1</sup>

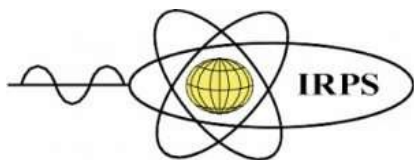
<sup>1</sup>Faculty of Applied Sciences, Universiti Teknologi MARA, 40450 Shah Alam, Selangor, Malaysia

<sup>2</sup>Universiti Teknologi Mara Cawangan Perak, Kampus Tapah, 35400 Tapah Road, Perak, Malaysia

<sup>3</sup>University of Cyberjaya (UoC), Persiaran Bestari, Cyber 11, 63000 Cyberjaya, Selangor Darul Ehsan, Malaysia

Corresponding author: rosdiyana@uitm.edu.my

The mixed ionic electronic 98[20Li<sub>2</sub>O-*x*Bi<sub>2</sub>O<sub>3</sub>-(80-*x*)TeO<sub>2</sub>]-2Ag glasses were prepared by melt-quenching method to determine the effect of Bi<sub>2</sub>O<sub>3</sub> addition on radiation shielding and elastic properties of the glass system. The simulation done in Phy-X/PSD software on the glass samples showed a minimum Linear Attenuation Coefficient (LAC) at *x*= 7 and 11 mol% with increasing Bi<sub>2</sub>O<sub>3</sub> concentration which may be associated with mixed ionic electronic effect (MIE). However, a maximum were observed at *x*= 7 and 11 mol% of Half Value Layer (HVL) and Mean Free Path (MFP). In addition, photon shielding abilities in relation to MAC, LAC, HVL, and MFP in the glass samples also have been observed to be photon energy dependent. Meanwhile, the electron shielding properties of the glass samples were simulated using ESTAR software which revealed that as kinetic energy rises, the electron total stopping power ( $\Psi_e$ ) values and continuous slowing down range approximation (CSDA) range ( $\Phi_e$ ) also increase. Bond compression model approach was used for elastic moduli determination which a maximum at *x*= 7 mol% is observed at all elastic moduli (longitudinal,  $L_{bc}$  shear,  $G_{bc}$  bulk,  $K_{bc}$  and Young's modulus,  $E_{bc}$ ) together with average force constant,  $F$  and average cross link density  $\bar{n}_c$  due to structural changes in term of BO/NBO thereby indicated the mixed ionic-electronic effect in elastic properties.



**ISRP 2021**  
**International Symposium on Radiation Physics**  
**Kuala Lumpur – Malaysia**  
**6 – 10 December 2021**

**A027 - Modified irradiation technique for transfusable blood using a clinical linear accelerator**

Janatul Madinah Wahabi<sup>1,2</sup>, Noor Zati Hani Abu Hanifah<sup>1,3</sup>, Suhairul Hashim<sup>3,4,\*</sup>

& David Andrew Bradley<sup>5,6</sup>

<sup>1</sup>Department of Radiotherapy and Oncology, Hospital Sultan Ismail, Malaysia

<sup>2</sup>Department of Biomedical Imaging, University of Malaya, Malaysia

<sup>3</sup>Department of Physics, Faculty of Science, Universiti Teknologi Malaysia, Malaysia

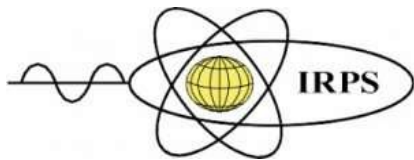
<sup>4</sup>Ibnu Sina Institute for Scientific and Industrial Research (ISISIR), Universiti Teknologi Malaysia, Malaysia

<sup>5</sup>Centre for Applied Physics and Radiation Technologies, Sunway University, Malaysia

<sup>6</sup>Department of Physics, University of Surrey, United Kingdom

Corresponding author: suhairul@utm.my

Whole blood irradiation prior to blood transfusion mitigates the risk of Transfusion Associated Graft versus Host Disease (TA-GvHD) to the receiver. This study aimed to improve dose homogeneity, also to benefit from a faster technique and a simplified blood irradiation workflow. An acrylic box accommodating eight units of blood has been fabricated, build-up material being used to ensure dose homogeneity. A linear accelerator dose distribution treatment plan for blood bag irradiations has been evaluated, measurement of dose using nanoDot optically stimulated luminescent dosimeters (OSLD) allowing comparison with calculated dose. By using build-up material, dose distribution was within 95% to 107% of the prescribed dose. With all eight units of blood accommodated in the box, an irradiation time of 20 minutes per box has been needed. Compared to a previously adopted procedure, use of the acrylic box and build-up material maintains dose homogeneity, also simplifying the workflow, the technique also being easy to undertake by the operators.



**ISRP 2021**  
**International Symposium on Radiation Physics**  
**Kuala Lumpur – Malaysia**  
**6 – 10 December 2021**

**A029- The amplitude and phase distributions of cosmic ray anisotropy at different conditions of Forbush decrease**

A Sh M Elshoukrofy<sup>1</sup>, S El Shalaby<sup>1</sup>, H A Motaweh<sup>1</sup>, M. Y. Hanfi<sup>2,3</sup>, M.I. Sayyed<sup>4,5</sup>, Mayeen Uddin Khandaker<sup>6</sup>, A A Darwish<sup>7</sup>.

<sup>1</sup> Faculty of Science, Damanhur University, Damanhur, El beheira, Egypt

<sup>2</sup>Ural Federal University, Mira St., 19, 62002, Yekaterinburg, Russia

<sup>3</sup>Nuclear Materials Authority, El Maadi, Cairo, Egypt

<sup>4</sup>Department of Physics, Faculty of Science, Isra University, Amman 11622, Jordan

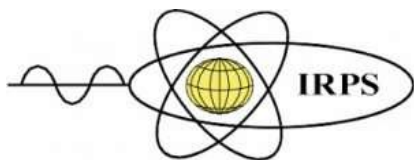
<sup>5</sup>Department of Nuclear Medicine Research, Institute for Research and Medical Consultations, Imam Abdulrahman bin Faisal University, Dammam 31441, Saudi Arabia

<sup>6</sup>Center for Applied Physics and Radiation Technologies, School of Engineering and Technology, Sunway University, 47500 Bandar Sunway, Selangor Darul Ehsan, Malaysia

<sup>7</sup> Faculty of Science, Alexandria University, Alexandria, Egypt

Corresponding author: sama.shalaby2018@gmail.com

A comprehensive study of the Forbush effects of galactic cosmic rays has been going on for more than half a century. This increased interest is primarily due to the fact that the Forbush effects of cosmic rays are associated with grandiose phenomena occurring on the Sun, in particular, with chromospheric flares that cause strong electromagnetic disturbances of the solar wind in interplanetary space. Such disturbances of the solar wind, spreading with colossal speed (1000 km / sec and more), pass through the Earth's Magnetosphere and Atmosphere, causing geophysical, biophysical and technological effects. Magnetic clouds and shock waves that arise in interplanetary space as a result of chromospheric flares on the Sun differ from each other both in their geometry and in their internal structure. Naturally, the Forbush effects caused by them are of a different nature. In this research Forty-eight Forbush decline occurrences were divided into four categories according on their shapes, we had gathered and used data on cosmic ray intensity from six different neutron monitor sites from 1990 until 2020. We found that there is an annual diminishing of cosmic intensity with a similar shape at the same time every year on 25th or 26th November due to the Forbush phenomena and there is no forbush reduction occurs in December of every year. An unexpectedly severe geomagnetic storm on September 6, 2017 and August 26, 2018 are revealed itself as a peculiar Forbush drop.



**ISRP 2021**  
**International Symposium on Radiation Physics**  
**Kuala Lumpur – Malaysia**  
**6 – 10 December 2021**

### **A030 - Dose Assessment Level in Industrial Betatron Electron Beam**

Y.J. Lee<sup>1</sup>, R. S. Omar<sup>1</sup>, S. Hashim<sup>2,3</sup>, D. A. Bradley<sup>4,5</sup>, N. Z. H. A. Hanifah<sup>2</sup> and C.L Goh<sup>1</sup>

<sup>1</sup>Billion Prima Sdn. Bhd., PTB 157, Jalan Sengkak, 81000 Kulai, Johor Baru, Malaysia.

<sup>2</sup>Department of Physics, Faculty of Science, Universiti Teknologi Malaysia, 81310 Johor Bahru, Malaysia.

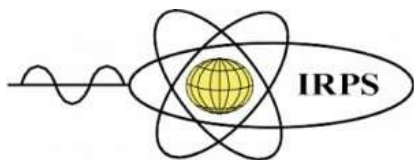
<sup>3</sup>Ibnu Sina Institute for Scientific and Industrial Research (ISISIR), Universiti Teknologi Malaysia, Johor, 81310 UTM, Skudai, Malaysia

<sup>4</sup>Centre for Applied Physics and Radiation Technologies, School of Engineering and Technology, Sunway University, Malaysia.

<sup>5</sup>Centre for Nuclear and Radiation Physics, University of Surrey, Guildford, Surrey, GU2 7XH, United Kingdom

Corresponding author: yuhjiunn@billionprima.com.my

The safety and hazardous radiation dose in betatron electron beam have emerged as a high concern for industrial and security applications. High power x-rays in the 3 to 20 MeV range are needed for rapid screening of cargo containers and vehicles for security applications. This study focused on the dose assessment level in 7.5 MeV (approximately 8.5 R/min at 1 meter) high energy x-ray betatron in cargo security full scan applications (scanning including driver). TLD-100<sup>TM</sup> rod type dosimeters, RadEye B20-ER alpha-beta-gamma survey meters and Polimaster PM1610B were used to measure the organ equivalent dose assessment and scanner boundary dose assessment, respectively. The results from the 12s operating x-ray ON setting for scanner boundary recorded an optimum achievable standard and were found below the control limit (below 0.5  $\mu\text{Sv/h}$  for the public area). The results ranged between 0.015 to 0.295  $\mu\text{Sv/h}$ . For organ dose assessment using Anthropomorphic Alderson Radiation Therapy phantom, the organ equivalent dose assessment for gonad, brain (left and right), and lens (left and right) shown an acceptable limit which lied in below 1 mSv annual dose limit for public exposure, which the results lied in a range between 0.010 to 0.080  $\mu\text{Sv}$ . Thus, the study proves that the betatron is safe to perform full scan in cargo scanning application to fill up the security gap in the driver cabin.



**A031 - Evaluation of Organ Dose Mapping in 128-Slice Multi-Detector Computed Tomography**

R. S. Omar<sup>1</sup>, S. Hashim<sup>1,2</sup>, D. A. Bradley<sup>3,4</sup>, M. K. A. Karim<sup>5</sup>, N. D. Shariff<sup>6</sup>

<sup>1</sup>Department of Physics, Faculty of Science, Universiti Teknologi Malaysia, 81310 Johor Bahru, Malaysia.

<sup>2</sup>Ibnu Sina Institute for Scientific and Industrial Research (ISISIR), Universiti Teknologi Malaysia, Johor, 81310 UTM, Skudai, Malaysia

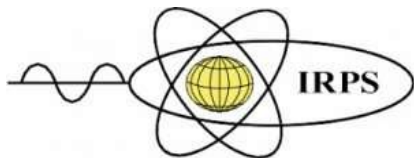
<sup>3</sup>Centre for Applied Physics and Radiation Technologies, School of Engineering and Technology, Sunway University, Malaysia.

<sup>4</sup>Centre for Nuclear and Radiation Physics, University of Surrey, Guildford, Surrey, GU2 7XH, United Kingdom

<sup>5</sup>Department of Physics, Faculty of Science, Universiti Putra Malaysia, 43400 UPM Serdang, Selangor Darul Ehsan, Malaysia.

<sup>6</sup>Hospital Sultanah Aminah, Johor Bahru, 80100, Malaysia. Corresponding author: ratnasuffhiyanni@gmail.com

This study of organ dose profiles depends on a method enabling acquisition of densely sampled dose measurements, acquired via modified nanoDot™ OSLDs and a standard anthropomorphic Alderson Radiation Therapy phantom (ARTM 1092 model). The CT scan parameters were based on an adult chest-abdomen and head region CT protocols using a Siemen Somatom Definition AS+ located in Hospital Sultanah Aminah, Johor. The tube voltage and exposure time values were varied significantly in examining the scanned region, the modulation techniques strongly affecting the dose distribution. From overall protocol, the greatest dose was detected in the thyroid. The doses to the thyroid showed larger values (34.528 mGy) and larger variations than the brain. The per-slice average absorbed dose in the brain and thyroid ranged from 3.469 to 33.645 mGy and 3.372 to 34.528 mGy, respectively. The radiation dose trends agree with similar examinations and modality, with differences depending on factors such as tube voltage, exposure time, tube current, slice collimation, and pitch factor. In CT head-neck examinations, dose dependence upon tube voltage and exposure time is of particular note. The modification of routine protocols to assure optimised image quality and the absorbed dose is of particular importance.



**A034 - Dose Assessment with NORM added Consumer Products Using Geant4 Monte Carlo Simulations**

Halmat J. Hassan<sup>1,2\*</sup>, S.Hashim<sup>1,3</sup>, N. Z. H. Abu Hanifah<sup>1</sup>, M. S. M. Sanusi<sup>1</sup>, M. R. Fahmi<sup>4</sup>, R. M. Tahar<sup>5</sup> and D. A. Bradley<sup>6,7</sup>

<sup>1</sup>Department of Physics, Faculty of Science, Universiti Teknologi Malaysia, Johor, 81310 UTM, Skudai, Malaysia

<sup>2</sup>Department of Physics, College of Education, University of Sulaimani, Sulaimani, 46001, Kurdistan-Iraq

<sup>3</sup>Ibnu Sina Institute for Scientific and Industrial Research (ISISIR), Universiti Teknologi Malaysia, Johor, 81310 UTM, Skudai, Malaysia

<sup>4</sup>School of Physics, Universiti Sains Malaysia, 11800 Gelugor, Pulau Pinang, Malaysia

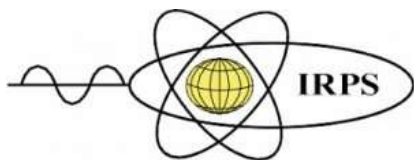
<sup>5</sup>Atomic Energy Licensing Board, Jalan Dengkil, 43000, Selangor, Batu 24, Dengkil

<sup>6</sup>Centre for Applied Physics and Radiation Technologies, School of Engineering and Technology, Sunway University, 47500, Selangor, Bandar Sunway, Malaysia

<sup>7</sup>Department of Physics, University of Surrey, GU2 7XH, Guilford, United Kingdom

Corresponding author: halmat.hassan@univsul.edu.iq

Radioactive consumer products (RCP) are widely marketed for everyday use. The study herein was conducted on 23 commercially available RCP, such as glass infused discs, energy cards, scalar energy products and anti-radiation stickers which were purposefully designed to contain naturally occurring radioactive material (NORM). The goal of this study is to assess the potential risk of NORM-added consumer products in the living environment, as the presence of such products in the living environment could expose members of the public to unnecessary radiation exposure. A Pb-shielded high purity Ge (HPGe) spectrometer was used to perform the analysis. Simulations were performed using Geant4 Monte Carlo simulations to estimate the equivalent organ doses and annual effective dose (AED) in the use of such products. The total activity in such radioactive consumer products ranges from  $2 \pm 0.1 - 7413 \pm 576$  Bq,  $1.2 \pm 0.2 - 1168 \pm 131$  Bq, and  $14.2 \pm 3 - 574 \pm 103$  Bq, for  $^{232}\text{Th}$ ,  $^{238}\text{U}$ , and  $^{40}\text{K}$ , respectively. It was found that RCP contains monazite, which relatively gives the high concentration of uranium and thorium. The radiological risk posed by the use of such items as healthcare products is assessed, with the daily external and internal exposure doses of particular concern. Dose assessments of the organ equivalent and average effective doses were performed by measuring the activity of  $^{238}\text{U}$ ,  $^{232}\text{Th}$ , and  $^{40}\text{K}$  using the aforementioned products for various exposure duration scenarios. Accordingly, sample A15 scalar energy necklace offered the greatest concentration, with mean percentages of  $1.54 \pm 0.008\%$  and  $26.54 \pm 0.08\%$  for U and Th, respectively, giving rise to estimate annual effective dose exposure of 2.59 mSv, considerably in excess of the public dose limit of 1 mSv/y.



**A035 - The Naturally Occurring Radioactivity of Tourmaline-based Healthcare Products and Associated Radiation Risk**

N.N. Yusof<sup>1\*</sup>, S.Hashim<sup>1,2</sup>, Halmat J. Hassan<sup>1,3</sup>, N. Z. H. Abu Hanifah<sup>1</sup>, M. S. M. Sanusi<sup>1</sup>, M. R. Fahmi<sup>4</sup>, R. M. Tahar<sup>5</sup> and D. A. Bradley<sup>6,7</sup>

<sup>1</sup>Department of Physics, Faculty of Science, Universiti Teknologi Malaysia, Johor, 81310 UTM, Skudai, Malaysia

<sup>2</sup>Ibnu Sina Institute for Scientific and Industrial Research (ISISIR), Universiti Teknologi Malaysia, Johor, 81310 UTM, Skudai, Malaysia

<sup>3</sup>Department of Physics, College of Education, University of Sulaimani, Sulaimani, 46001, Kurdistan-Iraq

<sup>4</sup>School of Physics, Universiti Sains Malaysia, 11800 Gelugor, Pulau Pinang, Malaysia

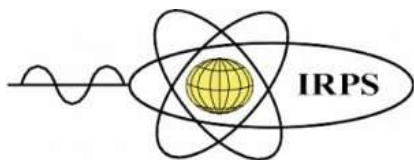
<sup>5</sup>Atomic Energy Licensing Board, Jalan Dengkil, 43000, Selangor, Batu 24, Dengkil, Malaysia

<sup>6</sup>Centre for Applied Physics and Radiation Technologies, School of Engineering and Technology, Sunway University, 47500, Selangor, Bandar Sunway, Malaysia

<sup>7</sup>Department of Physics, University of Surrey, GU2 7XH, Guilford, United Kingdom

Corresponding author: nnbyutm7@gmail.com

The study investigates 24 commercially available tourmaline-based healthcare products that contain naturally occurring radioactive material (hot spa stone, face mask, waist supporter slimming belt, arm relief belt, socks, sole, soap, and comb) (NORM). Self-heating products are claimed to provide health benefits by releasing negative ions and heating body parts. The assessment of the radiological risk posed by the use of such products for therapy and healthcare, with the daily external exposure dose being of particular concern. Gamma spectroscopy analysis and Geant4 Monte Carlo simulations are being used for evaluation. Organ doses from these have been simulated using male and female human phantoms, with dose conversion factors (DCFs) included. Tourmaline sock coded T21 was found to contain the greatest activity at  $2.41 \pm 0.2$  and  $28 \pm 1.3$  Bq g<sup>-1</sup>, for <sup>238</sup>U and <sup>232</sup>Th, respectively, while the magnetic therapy face mask coded T02 recorded the least activity, at  $0.04 \pm 0.01$  and  $0.1 \pm 0.01$  Bq g<sup>-1</sup>, again for <sup>238</sup>U and <sup>232</sup>Th, respectively. The range for <sup>40</sup>K was  $0.16 \pm 0.01 - 16.4 \pm 1.1$  Bq g<sup>-1</sup> among the tourmaline products. Accordingly, sample T21 tourmaline sock offered the greatest concentration, with mean percentages of  $0.65 \pm 0.1$ ,  $0.02 \pm 0.001$  for Th and U, respectively. Given the assumption of exposure for a period of 8 h per day, wearing tourmaline sock T21 gives rise to an annual effective dose of 0.79 mSv/y below the public annual dose limit of 1 mSv/y. However, some samples have relatively high doses, and the activity concentration limits are necessary as a screening tool. In brief, the use of these healthcare products led to elevated unnecessary radiation exposure doses to the environment.



**ISRP 2021**  
**International Symposium on Radiation Physics**  
**Kuala Lumpur – Malaysia**  
**6 – 10 December 2021**

**A036 - A study of proton small field collimator-scattering function into the Geant4 (PTSim) simulation**

Selvaraj Balaji<sup>1</sup>, Chung-Chi Lee<sup>1, 2, 3</sup>, Kang-Hsing Fan<sup>2</sup>, Shen-Hao Lee<sup>2</sup>, Hsiao-Chieh Huang<sup>2</sup>, Tsi-Chian Chao<sup>1, 2, 3</sup>.

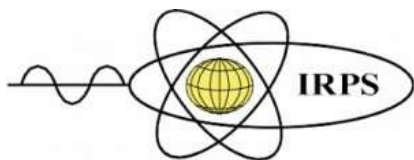
<sup>1</sup>Department of Medical Imaging and Radiological Sciences, College of Medicine, Chang Gung University, Taoyuan, Taiwan

<sup>2</sup>Department of Radiation Oncology, Chang Gung Memorial Hospital, Kwei-Shan Taoyuan, Taiwan

<sup>3</sup>Institute for Radiological Research, Chang Gung University/Chang Gung Memorial Hospital, Linkou, Taoyuan, Taiwan

Corresponding author: chaot@mail.cgu.edu.tw

Beam modifiers such as apertures and multi-leaf collimators (MLCs) are commonly used in proton therapy to conform the radiation field for the passive scattered beam module. The scattered protons from the inner surfaces of these beam modifiers can cause Bragg peak degradation in a water phantom, especially for small-fields proton. In addition, the multiple coulomb scattering (MCS) would have a greater impact on small-field proton applications. In this study, a Monte Carlo toolkit, Geant4, was used to assess the scattering effects of beam modifiers for small proton fields. The Geant4-v10.05 is used to determine the particle tracks before and after beam modifiers for various circular fields ranging from 5 mm to 30 mm in diameter, and under 190 MeV proton irradiation with different Geant4 dRoverRange values. The simulation results showed that the Geant4 dRoverRange (0.2) default value incorrectly calculated the scattered doses and ranges from beam modifiers and that different dRoverRange values do influence these calculations. Next, simulation results also indicated that the scattered dose from beam modifiers of 30 mm field is largest (about 17.5% in the surface) among these small fields, and the total scattered dose was reduced as the field size reduced. Overall, the beam modifiers such as MLCs and brass apertures generate significant scattered protons in the shallow region for small fields from 5 mm to 30 mm diameter circular fields. Finally, our results suggest that the Geant4 dRoverRange value should be 0.5 or less in order to more accurately calculate the scattering dose in water or homogeneous phantoms.



**ISRP 2021**  
**International Symposium on Radiation Physics**  
**Kuala Lumpur – Malaysia**  
**6 – 10 December 2021**

**A037 - Temporal (spatial) resolution of a neutron probe for C/O nuclear well logging**

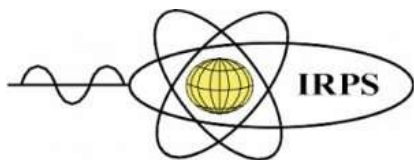
J. Batur<sup>1</sup>, D.Sudac<sup>1</sup>, I.Meric<sup>2</sup>, H.E.S.Pettersen<sup>3</sup>, V. Valkovic<sup>1</sup>, J.Obhodas<sup>1</sup>, K.Nad<sup>1</sup>, Z.Orlic<sup>1</sup>, M.Uroic<sup>1</sup>, D.Rentic<sup>1</sup>,

<sup>1</sup>Rudjer Boskovic Institute, Bijenička c.54, 10000 Zagreb, Croatia

<sup>2</sup>Department of Computer Science, Electrical Engineering and Mathematical Sciences, Western Norway University of Applied Sciences, 5020 Bergen, Norway

<sup>3</sup>Department of Oncology and Medical Physics, Haukeland University Hospital, 5021 Bergen, Norway

Temporal and spatial resolutions of a neutron probe (NP) specially designed for C/O nuclear well logging were obtained. The NP contains an alpha detector as well as a gamma-ray detector with high energy resolution, both designed for operation in a high temperature environment (up to 175 °C). Measurements with the NP were conducted by irradiating diesel fuel bottles with fast (14 MeV) neutrons. Bottles were placed on several equi-spaced (around 10 cm) positions parallel to the NP and time spectra of the probe in each case was obtained. The start signal for TAC (time-to-amplitude converter) was the detection pulse of alpha particles from deuterium-tritium reaction whereas the stop signal was the detection pulse of the characteristic carbon gamma-rays emitted from the irradiated diesel fuel sample. The peak in the time spectra for two adjacent positions was shifted for about 2 ns. It was also shown that the spatial resolution of the NP is about 10 cm. Experimental results were substantiated by Monte-Carlo simulations of the problem geometry, carried out using the MCNP6.2 software.



**ISRP 2021**  
**International Symposium on Radiation Physics**  
**Kuala Lumpur – Malaysia**  
**6 – 10 December 2021**

**A043 - Absorption and fluorescence spectra of an EGFR inhibitor AG-1478 using TD-DFT methods**

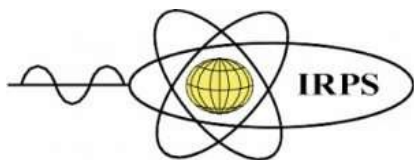
Sallam Alagawani,<sup>1</sup> Vladislav Vasilyev<sup>2</sup> and Feng Wang<sup>1\*</sup>

<sup>1</sup>Department of Chemistry and Biotechnology, Swinburne University of Technology, Melbourne, Australia

<sup>2</sup>National Computational Infrastructure, Australian National University, Canberra, ACT 0200, Australia

Corresponding author: fwang@swin.edu.au

Absorption and fluorescence spectra are sensitive to chemical environment and conformation of fluorophores and therefore, are ideal optical probes for biomolecule conformation in solvents. Epidermal growth factor receptor (EGFR) tyrosine kinase inhibitors (TKI) with a quinazolinone scaffold such as AG-1478 are fluorophores. Conformers of AG-1478 have been confirmed computationally and experimentally. In a recent solvent benchmarking study of a number of important DFT functionals, it is discovered that when combined with 6-311++G(d,p) basis set, B3LYP and B3PW91 functionals are top performers for accurately determination of maximum absorption and emission spectral transitions, as well as Stokes shift. It is further discovered that the absorption spectrum dominates by local excitation (LE) transfer while the geometry of the ground electronic state remains planar; whereas the emission spectrum is largely twisted intramolecular charge transfer (TICT). The results are helpful for understanding the mechanism of the TKI inhibitors and EGFR binding.



**A045 - Optimization of Tumour Segmentation Threshold in Gallium-68 PET/CT Neuroendocrine Imaging**

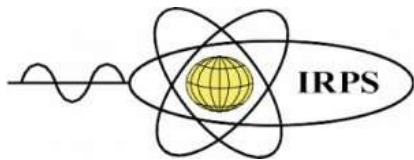
Puvanesuawary Morthy<sup>1</sup>, Marianie Musarudin<sup>1</sup>, Mohamad Aminudin Said<sup>2</sup>

<sup>1</sup>School of Health Sciences, Health Campus, Universiti Sains Malaysia, Kelantan, Malaysia

<sup>2</sup>Nuclear Medicine Department, Institut Kanser Negara, Putrajaya, Malaysia

Corresponding author: marianie@usm.my

Numerous methods to segment neuroendocrine tumours (NETs) using Gallium-68 (<sup>68</sup>Ga) in Positron Emission Tomography/Computer Tomography (PET/CT) imaging have been introduced. Up to now, manual tumour segmentation technique has been the gold standard, however, it is time-consuming, subjective, subject to inter- and intra-observer variability and prone to segmentation errors. An adaptive threshold-based is preferable to a fixed threshold-based approach for forecasting accurate and precise tumour volume in real-patient studies, as several researchers reported that threshold-based segmentation methods are more resistant to noise and resolution. This study aimed to determine the optimal adaptive threshold for NET segmentation in different tumour-to-background ratios (TBRs) in <sup>68</sup>Ga PET/CT imaging. A phantom with spheres of different volumes (0.5-27.02 ml) was filled with <sup>68</sup>Ga-DOTA-Phe<sup>1</sup>-Tyr<sup>3</sup>-Octreotide (<sup>68</sup>Ga-DOTA-TOC) at different TBRs (TBR: 2.5-10) and scanned for different acquisition periods (t: 120-240 s). MIM Encore Software was used to perform image registration of PET and CT images, followed by contouring and tumour segmentation. A set of different adaptive thresholds (T<sub>adaptive</sub>: 20%-50%) was applied to each sphere in each TBR image of the phantom using tri-dimensional automatic segmentation tool. Lin's concordance correlation coefficient ( $\rho_c$ ) statistical analysis was employed to assess the strength of agreement between measured sphere volume (V<sub>m</sub>) and actual sphere volume (V<sub>a</sub>) for each T<sub>adaptive</sub> relative to TBRs. The optimal T<sub>adaptive</sub> determined in TBRs of 2.5:1, 5:1 and 10:1 image is 35% ( $\rho_c = .991$ ), 45% ( $\rho_c = .999$ ) and 40% ( $\rho_c = .998$ ), respectively. The optimal threshold among the TBRs with maximum tolerance for delineation differences (% deviation = 10.93%) is 40%. As TBR is the most significant predictor of T<sub>adaptive</sub>, 40% T<sub>adaptive</sub> is recommended as the optimized T<sub>adaptive</sub> for tumour delineation because it demonstrated perfect accuracy and precision in tumour volume estimation in higher TBR images using an adaptive threshold-based approach and is thus successful for NET segmentation.



**ISRP 2021**  
**International Symposium on Radiation Physics**  
**Kuala Lumpur – Malaysia**  
**6 – 10 December 2021**

**A048 - Least square optimization for modelling ridge filters in the proton wobbling nozzle**

Luu Dang Hoang Oanh<sup>1</sup>, Tsi Chian Chao<sup>1,2,3</sup>, Chung Chi Lee<sup>1,2,3</sup>, Shen Hao Lee<sup>2</sup>, Hsiao Chieh Huang<sup>2</sup>

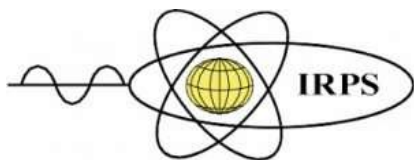
<sup>1</sup>Department of Medical Imaging and Radiological Sciences, College of Medicine, Chang Gung University, Guishan, Taoyuan, Taiwan

<sup>2</sup>Department of Radiation Oncology, Chang Gung Memorial Hospital, Guishan, Taoyuan, Taiwan

<sup>3</sup>Institute for Radiological Research, Chang Gung University/Chang Gung Memorial Hospital, Linkou, Taoyuan, Taiwan

Corresponding author: clee@mail.cgu.edu.tw

In proton therapy, the width of the pristine Bragg peak is too narrow to cover the entire tumour, and should be spread out into a uniform using Spread out Bragg peak (SOBP) techniques such as energy stacking, range modulator wheel (RMW), and ridge filter. The purpose of this study is to optimize the ridge filter modeling using the least square method in the proton wobbling nozzle. In this work, four different ridge filters (5 cm-LE, 5 cm-HE, 10 cm and 11 cm SOBP) of the proton middle wobbling nozzle at Chang Gung Memorial Hospital (CGMH) were simulated by PTSim Monte Carlo code. The thickness, height, and width of each ridge filter must be modelled into simulations. In our study, pristine Bragg peaks of different energies were simulated according to different step thickness. Least square method was used to generate the optimized weighting factors for these pristine Bragg peaks and then built up the optimized ridge filter from the G4MRidgeFilter class. These optimized ridge filters were then checked by the measurements performed by a PTW MP3 water tank and a Markus ionization chamber type 34045. Besides, the optimized ridge filters were also verified by proton beams other energy. The results showed a good agreement between the measured and simulated SOBP in various proton energies. Compared to the measurements, the deviation of these simulations of optimized ridge filters were less than 1.5 mm, 0.6 mm and 4 mm in range ( $R_{90d}$ ), distal dose fall-off ( $W_{80-20}$ ) and modulation width ( $W_{SOBP}$ ), respectively. And all their flatness were within 2.5 %. These data can be applied in practical and clinical uses.



**ISRP 2021**  
**International Symposium on Radiation Physics**  
**Kuala Lumpur – Malaysia**  
**6 – 10 December 2021**

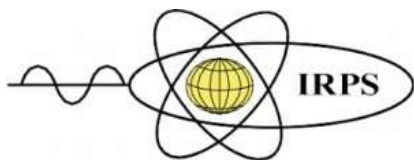
**A054 - Identify Malaysian residential buildings with high Radon concentration and their possibility for remedy**

Abdullah Mohd Noh<sup>1</sup>, Nordin Ayoub<sup>1</sup>, Siti Zurina Mat Noor<sup>1</sup>, Norhafizah Zahari<sup>1</sup>, Mardhiyati Mohd Yunus<sup>1</sup>

<sup>1</sup>Faculty of Health Sciences, Universiti Selangor, 40000 Shah Alam, Selangor, Malaysia

Corresponding author: [abdullahmnoh@gmail.com](mailto:abdullahmnoh@gmail.com)

It has been explained in many works of literature that some commercial and residential buildings have a high indoor Radon accumulation because of their layout design, building age, and other factors. A building with a possibility of high Radon accumulation may require finding some sort of remedial and rectification solutions to avoid its inhalation by the occupants. This unhealthy building may require more activities of Radon inspection and then provide solutions for its remediation that may save human lives in the long term. Radon monitoring was carried out for this study using two different Airthings detectors that are recently being used in many previous studies as Radon detectors. Its indoor concentration levels were measured passively and continuously for seven days inside a selected room of a building. The measurements were compared for both detectors to identify which rooms record a high level of Radon concentration when the room's door is being closed and then open. The amount of the average Radon concentrations and the graphs of Radon accumulation at each room showed some of the affected rooms require finding the most effective proposed solution to avoid its inhalation. One of the Radon accumulation graphs for the storeroom show high Radon concentration level of  $130 \text{ Bq/m}^3$  that exceed a healthy level of  $100 \text{ Bq/m}^3$  compared to other rooms in the same building that show within a healthy level. Any early hazard sign of Radon high concentration level should be avoided as it is known as one of the main causes of lung cancer. It should be given high attention in order to minimize any possibility of its contribution to respiratory disease that is being reported by the ministry of health in 2019 to be the second-highest cause of death in local government hospitals. This considerable percentage of mortality may only be controlled and reduced through radon monitoring and measurement which require the public to understand it as one of the disease preventives and practiced methods.



**ISRP 2021**  
**International Symposium on Radiation Physics**  
**Kuala Lumpur – Malaysia**  
**6 – 10 December 2021**

**A055 - Structural and Defect Changes in Black Carbon Charcoal Irradiated with Gamma**

K.S. Almugren<sup>1</sup>, S.F. Abdul Sani<sup>2\*</sup>, Irzwan Affendy Sulong<sup>2</sup>, F.H. Alkallas<sup>1</sup>, D.A. Bradley<sup>3,4</sup>

<sup>1</sup>Department of Physics, Princess Nourah Bint Abdulrahman University, Riyadh, Saudi Arabia.

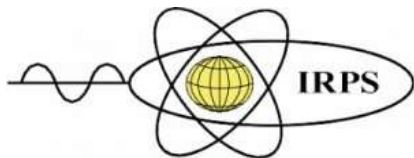
<sup>2</sup>Department of Physics, Faculty of Science, University of Malaya, 50603, Kuala Lumpur, Malaysia.

<sup>3</sup>Department of Physics, University of Surrey, Guildford, GU2 7XH, UK.

<sup>4</sup>Sunway University, Centre for Biomedical Physics, Jalan Universiti, 46150 PJ, Malaysia.

Corresponding author: s.fairus@um.edu.my

Effects of high energetic electromagnetic waves, neutrons, and heavy ions on structural defects and alterations in graphite have been extensively studied and well-established. However, recent studies on the effects of sub-kGy dose electromagnetic radiation (x-ray and gamma) over the dose range of a few mGy up to 200 Gy have shown to possess a potential for applications as novel material in passive radiation dosimetry. The graphite-rich materials produced promising dosimetric properties, including linear therapeutic dose-response and effective atomic number similar to bodily soft tissues. Present work revolves around exploring the utility of black carbon charcoal in complementing the use of graphite as a novel material for *in-vivo* radiation dosimeter. The structural alteration of charcoal irradiated by gamma within the dose range 0-10 Gy will be optically characterized, use being made of energy-dispersive x-ray (EDX), Raman spectroscopy and X-ray diffraction (XRD).



**A056 - Evaluation of Perturbation Effects in Small Field Dosimeter using Monte Carlo Simulation**

E.H. Uguru<sup>1,2</sup>, S.F. Abdul Sani<sup>1</sup>, M.H. Norazri<sup>1</sup>, F. Moradi<sup>1</sup>, N.M. Ung<sup>3</sup>, K.S. Almugren<sup>4</sup>, F.H. Alkallas<sup>4</sup>, D.A. Bradley<sup>5,6</sup>

<sup>1</sup>Department of Physics, Faculty of Science, University of Malaya, 50603, Kuala Lumpur, Malaysia.

<sup>2</sup>Department of Industrial Physics, Ebonyi State University, P.M.B. 053, Abakaliki, Nigeria

<sup>3</sup>Clinical Oncology Unit, Faculty of Medicine, University of Malaya, 50603 Kuala Lumpur, Malaysia.

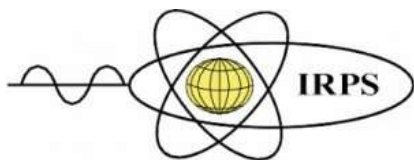
<sup>4</sup>Department of Physics, Princess Nourah Bint Abdulrahman University, Riyadh, Saudi Arabia.

<sup>5</sup>Department of Physics, University of Surrey, Guildford, GU2 7XH, UK.

<sup>6</sup>Sunway University, Centre for Biomedical Physics, Jalan Universiti, 46150 PJ, Malaysia.

Corresponding author: s.fairus@um.edu.my

The delivery of radiation dose treatments using small fields require precise and accurate measurement, noting the importance of dosimeter to possess high spatial resolution, small sensitive volumes, tissue equivalence, high sensitivity, dose rate and energy independence. Present work is aimed at investigating the application of small field radiation in reducing the perturbation effect in commercially available thermoluminescence dosimeter (TLD). The Monte Carlo (MC) simulation method was used in this study, which is directed to the linear accelerators (LINAC) treatment units for the determination of dosimetric parameter variations of photon and electron spectra, and dosimeter correction factors prior to achieving least perturbation in small fields. Different sizes of the dosimeter represented in diameter and thickness (D, T) mm were investigated at various radiation field sizes. The results show that perturbation region exist in all the dosimeter sizes. However, for dosimeters with  $2 \times 2 \text{ cm}^2$  square area field size, the maximum and minimum energy deposition of 0.0114 MeV and 0.00915 MeV is recorded on (4.5, 0.89) mm and (3, 0.38) mm, respectively. Similarly, for  $10 \times 10 \text{ cm}^2$  square area field size dosimeter, the lowest energy deposition is 0.0004 MeV for (3.6, 0.25) mm dosimeter while the highest energy of 0.00053 MeV is recorded on (4.5, 0.89) mm. This shows that the field size of  $10 \times 10 \text{ cm}^2$  has the lowest perturbation in comparison with other field sizes.



**ISRP 2021**  
**International Symposium on Radiation Physics**  
**Kuala Lumpur – Malaysia**  
**6 – 10 December 2021**

### **A057 - Optical Characterisation of Borosilicate Microscope Glass Slides**

A.A.Z. Ahmad Nazeri<sup>1</sup>, S.F. Abdul Sani<sup>1</sup>, K.S. Almugren<sup>2</sup>, , F.H. Alkallas<sup>2</sup>, D.A. Bradley<sup>3,4</sup>

<sup>1</sup>Department of Physics, Faculty of Science, University of Malaya, 50603, Kuala Lumpur, Malaysia

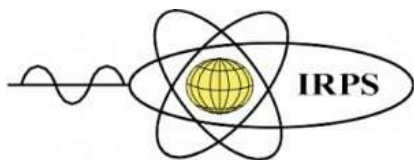
<sup>2</sup>Department of Physics, Princess Nourah Bint Abdulrahman University, Riyadh, Saudi Arabia.

<sup>3</sup>Department of Physics, University of Surrey, Guildford, GU2 7XH, UK.

<sup>4</sup>Sunway University, Centre for Biomedical Physics, Jalan Universiti, 46150 PJ, Malaysia.

Corresponding author: s.fairus@um.edu.my

The study herein provides analysis of structural changes of radiation-induced and the associated luminescence that originates from the energy absorption in the microscope glass slide samples exposed to <sup>60</sup>Co gamma-ray source. Using kVp and MV spectra, the photon response of several commercially available borosilicate microscope glass slide has already been the subject of investigation by this group, also in regard to the photoelectron generation enhancement resulting from high Z-material coatings (gold in particular). Encouraging results from such studies have paved the way for development of borosilicate glass slide radiation dosimeters specifically tailored to the task of dosimetry in therapeutics and diagnostic dose regimes. Not least, commercial borosilicate microscope glass slide offers a range of features of interest, including a relatively low softening point (820 °C), precluding need for a Pt-coil oven in fabrications, a spatially homogenous and mechanically robust constitution, ready availability in varying thicknesses, chemical inertness, and biocompatibility, also being inexpensive, reusable and easily sterilizable through either simple heating or use of an autoclave. Raman and Photoluminescence (PL) spectroscopy, and X-ray diffraction (XRD) analysis will be undertaken to characterise the alterations in order-disorder defect of microscope glass slide exposed to gamma radiation at relatively low doses from 0 up to 10 Gy.



**ISRP 2021**  
**International Symposium on Radiation Physics**  
**Kuala Lumpur – Malaysia**  
**6 – 10 December 2021**

**A061 - Evaluation of Dose-Area Product in pediatric interventional cardiology**

Hugo Schelin<sup>1</sup>, Akemi Yagui<sup>1</sup>, Paula Vosiak<sup>1</sup>, Luiza Costa<sup>1</sup>, Rosiane Mello<sup>1</sup>, Valeriy Denyak<sup>2,3</sup>, Sergei Paschuk<sup>3</sup>, Danielle Filipov<sup>3</sup>, Helen Khoury<sup>4</sup>

<sup>1</sup>Pelé Pequeno Príncipe Research Institute, Pequeno Príncipe Faculty, Brazil

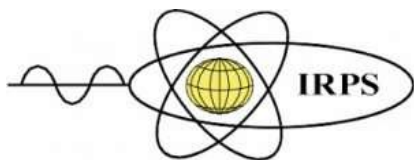
<sup>2</sup>National Science Center ‘Kharkov Institute of Physics and Technology’, Ukraine

<sup>3</sup>Federal University of Technology - Paraná, Brazil

<sup>4</sup>Federal University of Pernambuco, Brazil

Corresponding author: schelin2@gmail.com

Pediatric interventional cardiology procedures are performed to treat or diagnose congenital cardiac pathologies. The execution of these procedures involves the acquisition of radiological images in fluoroscopy mode and in cine mode. The cine mode requires images in more detail, as they will be used for later viewing. In pediatrics, it is important to perform radiological protection in radiological procedures, as children are more sensitive to radiation and can develop diseases due to stochastic effects throughout life. The objective of this study is to evaluate the DAP (Dose-Area product) values in the interventional (diagnostic and therapeutic) procedures of cardiology performed in a pediatric hospital in Curitiba, Brazil. Radiation Dose Structure Reports (RDSR), provided at the end of the procedures, were evaluated. In the procedures, the protocol used is generally the same for all patients, with low detail and 3.75 images/s for fluoroscopy mode and normal detail with acquisition of 30 images/s for cine mode. The anti-scatter grid was used in all procedures. The correction factor of the DAP value was obtained previously (0.65). The mean fluoroscopy time was  $1053 \pm 88$  s and the cine mode was  $38.4 \pm 1.9$  s in the procedures ( $1092 \pm 90$  s in total). The mean DAP value in fluoroscopy mode was  $1.72 \pm 0.42$  Gy.cm<sup>2</sup>, for cine mode was  $1.65 \pm 0.31$  Gy.cm<sup>2</sup>, and the total value was  $3.37 \pm 0.65$  Gy.cm<sup>2</sup>. These results demonstrate that, as described in the ICRP 135, fluoroscopy time is a weak dose indicator. The values obtained of mean DAP for the age groups were lower than the values found in other studies, despite our fluoroscopy times being higher.



**ISRP 2021**  
**International Symposium on Radiation Physics**  
**Kuala Lumpur – Malaysia**  
**6 – 10 December 2021**

**A065 - Bismuth tellurite glasses doped with CeO<sub>2</sub> for gamma radiation shielding and dosimetry application**

Ashwitha Nancy D'Souza<sup>1</sup>, K. Sharmila<sup>2</sup>, M. I Sayyed<sup>3,4</sup>, H.M Somashekarappa<sup>2</sup>, Aljawhara H. Almuqrin<sup>5</sup>, Mayeen Uddin Khandaker<sup>6</sup>, Sudha D. Kamath<sup>1,\*</sup>

<sup>1</sup>Department of Physics, Manipal Institute of Technology, Manipal Academy of Higher Education, Manipal, India

<sup>2</sup>Centre for application of Radioisotopes and Radiation Technology, Mangalore University, Mangalore, India

<sup>3</sup>Department of Physics, Faculty of Science, Isra University, Amman – Jordan

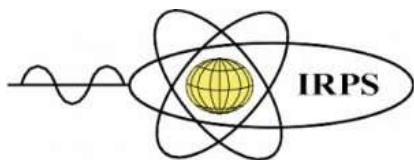
<sup>4</sup>Department of Nuclear Medicine Research, Institute for Research and Medical Consultations (IRMC), Imam Abdulrahman bin Faisal University (IAU), Dammam, Saudi Arabia

<sup>5</sup>Department of Physics, College of science, Princess Nourah bint Abdulrahman University, Riyadh, Saudi Arabia.

<sup>6</sup>Center for Applied Physics and Radiation Technologies, School of Engineering and Technology, Sunway University, 47500 Bandar Sunway, Selangor Darul Ehsan, Malaysia

Corresponding author: sudhakamath6@gmail.com

Glasses with matrix  $(50-x) \text{B}_2\text{O}_3 - 17.5\text{SiO}_2 - 0.5\text{CeO}_2 - x\text{TeO}_2 - 12\text{Bi}_2\text{O}_3 - 12\text{ZnO} - 8\text{BaO}$ ,  $x = 0, 10, 20, 30$  and  $40$  mol% and coded as BiTe were synthesized using melt-quench technique with purpose of investigating their radiation shielding and thermoluminescence (TL) properties. Photon Shielding and Dosimetry (Phy-X/PSD) software was utilized for theoretical calculation of parameters related to gamma and neutron radiation shielding. The current study reported highest density value of  $5 \text{ g/cm}^3$  for BiTe-40 glass leading to the occurrence of maximum linear attenuation coefficient, effective atomic number, and minimum half value layer, tenth value layer, mean free path values in  $0.015\text{-}15 \text{ MeV}$  range of gamma energy. BiTe-10 glass exhibited higher fast neutron removal cross-section ( $\Sigma_{\text{R}} = 0.1012 \text{ cm}^{-1}$ ), which is also greater than that of ordinary ( $0.093 \text{ cm}^{-1}$ ) and hematite serpentine concrete ( $0.096 \text{ cm}^{-1}$ ). Further, to assess the gamma dosimetry application, glasses were irradiated with  $3 \text{ kGy}$  dose of gamma radiation, which produced maximum intensity TL curve for BiTe-40. Deconvolution of this TL glow curve by Computerized Glow Curve Deconvolution (CGCD) technique resulted in higher activation energy and longer lifetime values ( $1.63 \text{ eV}$  and  $42.7 \times 10^5$  years) at  $559 \text{ K}$ , indicating the presence of deeper traps and low fading behaviour. Also, in the dose range of  $0.25\text{-}1 \text{ kGy}$ , the BiTe-40 sample displayed good linearity which makes it suitable for TL dosimetry application.



**ISRP 2021**  
**International Symposium on Radiation Physics**  
**Kuala Lumpur – Malaysia**  
**6 – 10 December 2021**

**A068 - Evaluation of radiation shielding characteristics of B<sub>2</sub>O<sub>3</sub>-K<sub>2</sub>O- Li<sub>2</sub>O - HMO (HMO = TeO<sub>2</sub>/ SrO /PbO/Bi<sub>2</sub>O<sub>3</sub>) glass system: A simulation study using Geant4 code**

Dalal Abdullah Aloraini<sup>1</sup>, M.I. Sayyed<sup>2,3</sup>, Anisha Jain<sup>4,5,\*</sup>, Ali Askin<sup>6</sup>, Aljawhara A.H. Almuqrin<sup>1</sup>, Ashok Kumar<sup>4,5</sup>, Mayeen Uddin Khandaker<sup>7</sup>

<sup>1</sup>Department of Physics, College of Science, Princess Nourah Bint Abdulrahman University, Riyadh, Saudi Arabia

<sup>2</sup>Department of Physics, Faculty of Science, Isra University, Amman 11622, Jordan

<sup>3</sup>Department of Nuclear Medicine Research, Institute for Research and Medical Consultations, Imam Abdulrahman bin Faisal University, Dammam 31441, Saudi Arabia

<sup>4</sup>University College, Benra- Dhuri, Punjab 148024, India.

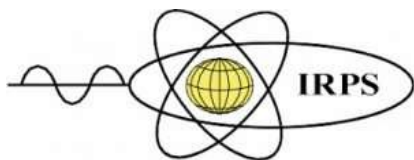
<sup>5</sup>Department of Physics, Punjabi University, Patiala, Punjab 147002, India.

<sup>6</sup>Munzur University, Faculty of Engineering, Department of Electrical and Electronics Engineering, 62000, Tunceli, Turkey

<sup>7</sup>Center for Applied Physics and Radiation Technologies, School of Engineering and Technology, Sunway University, 47500 Bandar Sunway, Selangor Darul Ehsan, Malaysia

\*Corresponding author: aishajain1011@gmail.com

The four borate glass samples have been fabricated by addition of 10 mol% of SrO, TeO<sub>2</sub>, PbO, and Bi<sub>2</sub>O<sub>3</sub> to the 10 Li<sub>2</sub>O - 20 K<sub>2</sub>O - 60 B<sub>2</sub>O<sub>3</sub> glass using the melt-quenching technique. The effect of addition of SrO, TeO<sub>2</sub>, PbO, and Bi<sub>2</sub>O<sub>3</sub> on the mechanical and the gamma ray shielding properties have been studied. The Makishima and Mackenzie (MM) were used to calculate the various mechanical properties. The variation of these parameters with percentage composition of each of heavy metal oxide have been studied. A number of bonds per unit volume and average cross-link density of the glasses have also been studied. The elastic moduli such as Young's modulus (E), bulk modulus (B), shear modulus (G), longitudinal modulus (L), Poisson's ratio ( $\sigma$ ), fractal bond connectivity (d) and hardness (H) have also been studied. For the proposed glasses, we used Geant4 simulation code to study the influence of the four heavy metal oxides (SrO, TeO<sub>2</sub>, PbO, and Bi<sub>2</sub>O<sub>3</sub>) on the radiation shielding features. The Geant4 code helped us to examine the radiation protection efficiency of these glasses. Also, it helped in determining the transmission of the photons through each glass sample. The radiation shielding parameters for the 10 Li<sub>2</sub>O - 20 K<sub>2</sub>O - 60 B<sub>2</sub>O<sub>3</sub> glass system with 10 mol% of SrO, TeO<sub>2</sub>, PbO, and Bi<sub>2</sub>O<sub>3</sub> were compared with other traditional radiation shielding materials.



**ISRP 2021**  
**International Symposium on Radiation Physics**  
**Kuala Lumpur – Malaysia**  
**6 – 10 December 2021**

**A071 - Structural and Optical Properties of graphite-rich media under low level neutron doses for radiation dosimetry**

S.N. Mat Nawi\*<sup>1</sup>, M.U. Khandaker<sup>1</sup>, S.S. Ismail<sup>1</sup>, S.F. Abdul Sani<sup>2</sup>, Julia A. Karim<sup>3</sup>, K.S. Almugren<sup>4</sup>, D.A. Bradley<sup>1,5</sup>

<sup>1</sup>Centre for Applied Physics and Radiation Technologies, School of Engineering and Technology, 47500, Bandar Sunway, Selangor, Malaysia.

<sup>2</sup>Department of Physics, Faculty of Science, University of Malaya, 50603, Kuala Lumpur, Malaysia.

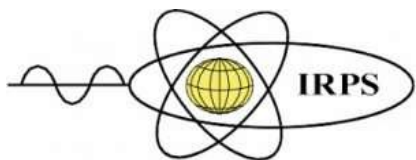
<sup>3</sup>Nuclear and Reactor Physics Section, Nuclear Technology Center, Technical Support Division, Malaysian Nuclear Agency, Kajang, Malaysia

<sup>4</sup>Department of Physics, Princess Nourah Bint Abdulrahman University, Riyadh, Saudi Arabia.

<sup>5</sup>Department of Physics, University of Surrey, Guildford, GU2 7XH, UK.

Corresponding author: sitinurasiah\_90@yahoo.com

A comprehensive understanding of radiation-induced effects has been made using commercially produced graphite, in the form of 0.3 mm thick rods of highly uniform 2B and HB grade polymer pencil lead graphite (PPLG) (approximately 91 wt % and 75 wt % graphite content, respectively), identifying variation in lattice structure and defects resulting from low level neutron dose range of 2 to 10 Gy. To understand the nature and distribution of defects in its crystal lattice that give rise to the luminescence signal, investigations have been made of thermoluminescence (TL) and photoluminescence dose dependence, also of alterations in Raman spectroscopic features. X-ray diffraction (XRD) study have focused on the atomic spacing, lattice constant and the degree of structural order of the irradiated samples, supported by crystallite size calculations. The results are clearly accepted to arise from irradiation changes that are happening at the microscopic level, supporting previous TL, Raman and photoluminescence research. Within the dose range studied, all samples showed excellent linear response, with 2B grade PPLGs showing greater sensitivity than HB. The reported findings demonstrate that graphite-rich commercially produced PPLG offers a lot of useful features to be used as a dosimetric medium for neutron radiation physics applications. Most specifically, the easily accessible PPLG can provide the basis of a low-cost yet highly effective system for studies of radiation-driven changes in carbon and all results when summed up, predict 2B grade to be a worth material for new generation radiation dosimetry.



**A073 - Time-division multiplexing in real-time radioluminescent dosimetry system for high energy photon**

Janatul Madinah Wahabi<sup>1,5</sup>, Ngie Min Ung<sup>2</sup>, Ghafour A. Mahdiraji<sup>3</sup>, Wu Yi Chong<sup>4</sup>, Jeannie Hsiu Ding Wong<sup>1</sup>

<sup>1</sup>Department of Biomedical Imaging, Faculty of Medicine, Universiti Malaya, Malaysia

<sup>2</sup>Clinical Oncology Unit, Faculty of Medicine, Universiti Malaya, Malaysia

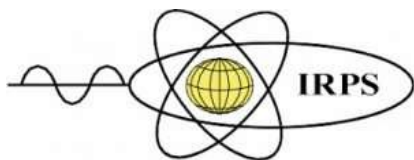
<sup>3</sup>Flexilicate Sdn. Bhd., Universiti Malaya, Malaysia

<sup>4</sup>Photonics Research Centre, Universiti Malaya, Malaysia

<sup>5</sup>Ministry of Health, Malaysia

Corresponding author: janatul9@gmail.com

Radioluminescent dosimetry system with plastic scintillator has the advantages of real-time dose measurement, tissue equivalent and high resolution. These advantages are desirable for radiation detectors in radiotherapy. This study developed and tested a multichannel radioluminescent dosimetry system by adapting the time-division multiplexing concept. This design provided real-time dose measurement with a compact assembly and retained the advantage of radioluminescent dosimetry. A prototype 2-channel system was developed, incorporating an optical switch in the readout system. Two optical fibres were prepared, where only one was coupled to a plastic scintillator and the other was not. These fibres were connected to the optical switch, and the switch was controlled via software. The switch was automatically set to acquire 100 ms at each channel in the looping sequence, and the switching duration was 3 ms. This procedure was repeated for different acquisition times ranging from 100 ms to 1000 ms, and the sampling time was set at 10 ms and 100 ms. The system was tested in the clinical linear accelerator, using 6 MV and 10 MV photon beams. The findings showed that channel 2 of the optical switch was systematically slower than channel 1, with a mean deviation of 4.0% and 51.8%, respectively, to the time set in the control software. Channel 1 showed an increase in deviation as time increased, and channel 2 showed the opposite trend. The measurements were reproducible with 2.5% variation when changing from sampling time 10 ms to 100 ms. In conclusion, the developed radioluminescent dosimetry system could measure high energy photon beams. This design allows for multiple channel measurement, an advantage for clinical radiotherapy application.



**ISRP 2021**  
**International Symposium on Radiation Physics**  
**Kuala Lumpur – Malaysia**  
**6 – 10 December 2021**

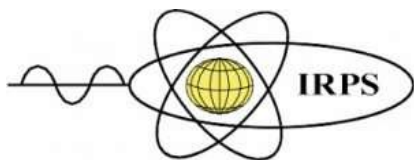
**A074 - Formation of a clavicle phantom for radiography using hydrated lime for the purposes of education and quality assurance**

Shyma M. Alkhateeb<sup>1</sup>

<sup>1</sup> Diagnostic Radiography Technology Department, Faculty of Applied Medical Sciences, King Abdulaziz University, Jeddah, Saudi Arabia

Corresponding author: [smalkhateeb@kau.edu.sa](mailto:smalkhateeb@kau.edu.sa)

Epidemiological studies indicate that clavicle fracture is a predominant fracture especially in males. Hydrated lime was found to be a suitable substance to mimic bone composition. It is durable and has a good X-ray image intensity compared with that of real bone. On the other hand, silicone shows a similar X-ray diffraction spectrum to that of soft tissue. In this paper, phantoms that compromise different sites of clavicle fractures are formed using hydrated lime for education and quality assurance purposes. Phantoms of left clavicle with different pathologies are formed using a many-step technique. The technique is easy to follow and reproduce in a home-based station. Clavicle phantoms were broken in different sites that represent most fractures in the literature. Clavicle phantoms were radiographed together with the real clavicle bone using an X-ray machine Definium 6000, General Electric, 2009 with imaging parameters set to 53kV, 100mA, 1.2mAs. This was done to compare their structures and densities. Mean grey values were 243.03, 248.97, and 253.53 for real bone, fabricated lime bone, and fabricated bone coated with silicone. This indicates 0.02 contrast between real and fabricated bone and 0.04 contrast between real and fabricated bone coated with silicone. Low contrast values between real bone and fabricated phantoms support the formation of a clavicle phantom for radiography using hydrated lime for the purposes of education and quality assurance.



**ISRP 2021**  
**International Symposium on Radiation Physics**  
**Kuala Lumpur – Malaysia**  
**6 – 10 December 2021**

**A078 - An annual effective dose due to  $^{222}\text{Rn}$  in spring and some surface waters of Johor state, Malaysia**

Rakiya Haruna<sup>1</sup>, Muneer Aziz Saleh<sup>2</sup>, Suhairul Hashim<sup>3,4</sup>

<sup>1</sup>Department of Physics, School of Secondary Education (Sciences), Federal College of Education, Zaria P.M.B 1041 Kaduna state, Nigeria

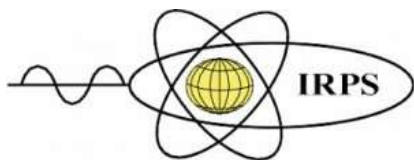
<sup>2</sup>Department of Energy Engineering, School of Chemical Engineering & Energy Engineering Universiti of Teknologi Malaysia, 81310 UTM Skudai, Johor, Malaysia

<sup>3</sup>Department of Physics, Faculty of Science, Universiti Teknologi Malaysia, 81310 UTM Skudai, Johor, Malaysia

<sup>4</sup>Centre for Sustainable Nanomaterials (CSNano), Ibnu Sina Institute for Scientific and Industrial Research (ISI-SIR), Universiti Teknologi Malaysia, 81310 UTM Skudai, Johor,

Corresponding author: hrakiy26@gmail.com

Ubiquitous nature, along with the detrimental health impact of radon ( $^{222}\text{Rn}$ ), has led to the investigation of its activity concentration in the various environmental medium, including bodies of water. This work was conducted to estimate the annual effective dose of inhalation due to  $^{222}\text{Rn}$  in spring and some surface waters in Johor state, Malaysia.  $^{222}\text{Rn}$  activity concentration was measured using RAD7 alpha detector. The annual effective dose for inhalation was evaluated using the measured  $^{222}\text{Rn}$  activity concentration in water. The activity concentration of  $^{222}\text{Rn}$  in water varies from  $80 \pm 110$  to  $5400 \pm 1100$   $\text{mBq l}^{-1}$  in surface and spring water respectively, with a mean value of  $1227$   $\text{mBq l}^{-1}$  from all samples. The measured activity concentrations in the samples were found to be below the EPA and WHO maximum permissible limit for  $^{222}\text{Rn}$  in Water of  $1100$   $\text{mBq l}^{-1}$  and  $10^5$   $\text{mBq l}^{-1}$  respectively. The highest value of  $^{222}\text{Rn}$  activity concentration was measured in spring water discharging from granitic rocks Aquifer. While the lowest value was measured in surface waters. The values of an annual effective dose of inhalation, due to  $^{222}\text{Rn}$  in spring water, were found to range from  $0.998$  to  $5.139$   $\mu\text{S y}^{-1}$  with a mean value of  $2.15$   $\mu\text{S y}^{-1}$ , while in the surface waters the values range from  $0.076$  to  $1.140$   $\mu\text{S y}^{-1}$  with a mean value of  $0.423$   $\mu\text{S y}^{-1}$ . The inhalation doses estimated were found to be well below the recommended limit set by UNSCEAR of  $1260$   $\mu\text{Sv y}^{-1}$ .



**ISRP 2021**  
**International Symposium on Radiation Physics**  
**Kuala Lumpur – Malaysia**  
**6 – 10 December 2021**

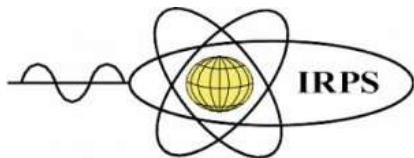
**A080 - Effects of Inorganic Salts and Maltose on the Dose-Response of HEMA Polymer Gel Dosimeters at the Diagnostic Range**

Umairah Mohd Zaki<sup>1</sup>, Iskandar Shahrim Mustafa<sup>1</sup>, Azhar Abdul Rahman<sup>1</sup>, Nuridayanti Che Khalib<sup>1</sup>

<sup>1</sup>School of Physics, Universiti Sains Malaysia, Malaysia

Corresponding author: iskandarshah@usm.my

The first polymer gel that contains maltose and inorganic salts, magnesium sulphate ( $\text{MgSO}_4$ ) has been introduced in this research work as a new low toxicity and sensitive polymer gel dosimeter. The assessment is based on the effect of magnesium sulphate and maltose towards the dose-response at the diagnostic range and the thermal stability of the polymer gel dosimeters. Various concentration (0.5 – 1.0 M) of magnesium sulphate ( $\text{MgSO}_4$ ) and (0.15 - 0.30 M) of maltose ( $\text{MgSO}_4$ ) were added to improve the basic composition of the polymer gel which consist of deionized water, gelatine, N,N'-Methylenebisacrylamide (BIS), ascorbic acid and 2-hydroxyethylmethacrylic acid (HEMA). The polymer gels were then exposed with X-ray at different (40-80 kVp; 5-100 mAs) modality energy setup. Upon irradiation, the absorption spectra of the polymer gel dosimeters were measured by using UV-visible spectrophotometer. Maltose is aid in the increments of the polymer gel melting point. Eventually, maltose is a type of sugar which has been demonstrated to improve the thermal stability and density of a polymer gel in order to obtain the desired tissue-equivalent properties. The use of inorganic salts as additives is to improve the dose-response of polymer gel dosimeters based on the indirect optical characterization. Polymerization was read based on absorption spectra in the wavelength range from 1000 nm to 200 nm. The dependency of polymerization with increasing of exposure dose was determined by changes in the optical energy band gap and Urbach energy. The results showed that the  $\text{MgSO}_4$  increase the dose sensitivity of the polymer gel dosimeter and maltose has helped in improving the mechanical properties of the polymer gel dosimeter upon irradiation. This observation is supported by the decreasing in the optical energy band gap for sample with addition of  $\text{MgSO}_4$ . This study has proved that addition of  $\text{MgSO}_4$  increase the sensitivity of polymer gel dosimeter towards radiation and maltose helped in improving the thermal stability of the polymer gel dosimeter.



**ISRP 2021**  
**International Symposium on Radiation Physics**  
**Kuala Lumpur – Malaysia**  
**6 – 10 December 2021**

**A082 - Scattering radiation exposure to eye lenses in the fluoroscopy-guided interventional procedures**

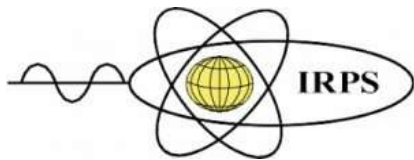
Asmah Bohari<sup>1</sup>, Suhairul Hashim<sup>1</sup>, Siti Norsyafiqah Mohd Mustafa<sup>2</sup>

<sup>1</sup>Department of Physics, Faculty of Science, Universiti Teknologi Malaysia, 81310 UTM Skudai, Johor, Malaysia

<sup>2</sup>Department of Radiology, Institut Kanser Negara, 62250 Putrajaya, Wilayah Persekutuan Putrajaya, Malaysia

Corresponding author: [asmahbohari@gmail.com](mailto:asmahbohari@gmail.com)

The scattering radiation distributed across the room during fluoroscopy-guided interventional (FGI) procedures were quantified using nanoDot Optically stimulated luminescence dosimeters. This research examines the radiation eye dose received by the staff involved in FGI procedures. Four types of fluoroscopic imaging were simulated using a radio-opaque Sawbones torso (Sawbones, WA) and carried out on a flat panel biplane (Phillips Allura XPer FD20/20, Netherlands). All the tube angulation imaging shows that the radiation spectrum resembled a single peak distribution. The right anterior oblique 45° shows the highest single peak distribution (16.80 mSv/h). The single peak distribution for standard anteroposterior, left anterior oblique 45° and left anterior oblique 90° imaging was 2.75, 2.94 and 11.99 mSv/h, respectively. The interventional radiologist position shows the highest eyes lens dose compared to other staff. During procedures, radiation doses differed significantly around the patient's table and with imaging angles. With the increased workload, a specific dosimeter for regular eye dosage monitoring is required. Radiation exposure limits must be understood in order to avoid negative consequences, especially amongst staff.



**A083 - The functionality assessment of fabricated automated radiopharmaceutical dispenser system**

Noorfatin Aida Baharul Amin<sup>1</sup>, Mohd Fadzil Ain<sup>2,3</sup>, Rafidah Zainon<sup>1,4</sup>

<sup>1</sup>Oncological and Radiological Sciences Cluster, Advanced Medical and Dental Institute, Universiti Sains Malaysia, SAINS@BERTAM, 13200, Kepala Batas, Pulau Pinang, Malaysia

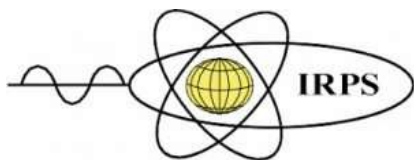
<sup>2</sup>School of Electrical and Electronic Engineering, Universiti Sains Malaysia, 11800 Gelugor, Pulau Pinang, Malaysia

<sup>3</sup>Collaborative Microelectronic Design Excellence Centre (CEDEC), Sains@USM Level 1, Block C, No. 10, Persiaran Bukit Jambul, 11900 Bayan Lepas, Pulau Pinang, Malaysia

<sup>4</sup>School of Physics, Universiti Sains Malaysia, 11800 Gelugor, Pulau Pinang, Malaysia

Corresponding author: rafidahzainon@usm.my

This paper presents the assessment of a fabricated automated radiopharmaceutical dispenser system using stepper motor peristaltic pump processing. The manual dispensing technique of the radiopharmaceutical in nuclear medicine involves manual withdrawal of activity from an elution vial, from a combination of the syringe and elution vial activities, and preparation of individual radiopharmaceutical doses to patients. Current evolution in the fields of control engineering and industrial automation has been driven by a revived interest in automatic methods of radiopharmaceutical activity measurements in nuclear medicine. In the proposed system, the stepper motor peristaltic pump transferred water, replacing the radiopharmaceutical from mother vial to the 1.5 cc and 10.0 cc control stroke syringes for volume accuracy and precision measurement. The required amount of water are set on the remote application controller of the automated dispenser radiopharmaceutical dispenser system and the measurement are carried out. This dispenser system is equipped with functionality of dispensing radiopharmaceutical and saline driven by customised 3 –way-stopcocks gears. The measurement are carried out for both functionality and time taken to dispense the water are also calculated. The percentage error calculated for both functionality of the automated radiopharmaceutical dispenser system are below 5% which in the range of 0.2-0.9 mL and 2.0 -10 mL volume dispensed. The precision of the automated radiopharmaceutical system are between 0.013-0.055. The proposed system offers a potential alternative to high-cost commercial radiopharmaceutical dispenser achieving a high precision and reducing operator's radiation exposure.



**ISRP 2021**  
**International Symposium on Radiation Physics**  
**Kuala Lumpur – Malaysia**  
**6 – 10 December 2021**

**A087 - Doped Plastic Scintillator Properties for Soft Tissue Dosimetry**

S. M. Tajudin<sup>1</sup>, Y. Namito<sup>2</sup>, T. Sanami<sup>2</sup>, H. Hirayama<sup>2</sup>, S. Hashim<sup>3,4</sup>

<sup>1</sup>Faculty of Health Sciences, Universiti Sultan Zainal Abidin (UniSZA), 21300 Kuala Nerus, Terengganu, Malaysia.

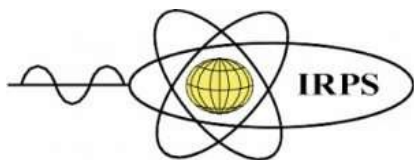
<sup>2</sup>High Energy Accelerator Research Organization (KEK), 1-1 Oho, Tsukuba, Ibaraki 305-0801, Japan.

<sup>3</sup>Department of Physics, Faculty of Science, Universiti Teknologi Malaysia (UTM), Johor, 81310 Skudai, Malaysia

<sup>4</sup>Ibnu Sina Institute for Scientific and Industrial Research (ISISIR), Universiti Teknologi Malaysia (UTM), Johor, 81310 Skudai, Malaysia

Corresponding author: [suffian@unisza.edu.my](mailto:suffian@unisza.edu.my)

For medical dosimetry, the dose to tissue is often the quantity of interest. Tissue-equivalent material is preferable to create dosimeters that directly represent the absorbed dose on human soft tissue. The materials used in plastic scintillators (PLS) have a density that is close to that of soft human tissue and a relatively energy-independent energy response. However, for photons below 200 keV, non-proportionality has to be taken into account to reproduce light output spectrum since it causes significant reduction on light output in this energy range. Several researchers have made an attempt to compensate the reduction or difference of plastic scintillator between soft tissue in response at low-energy photon region (< 200 keV). In this study, the effect of lead doping on the pulse height spectra for low and high energy photon will be measured and calculated in comparison to standard plastic scintillator. The influence of the optimal concentration of lead doping scintillator with soft-tissue dose will be discussed.



**ISRP 2021**  
**International Symposium on Radiation Physics**  
**Kuala Lumpur – Malaysia**  
**6 – 10 December 2021**

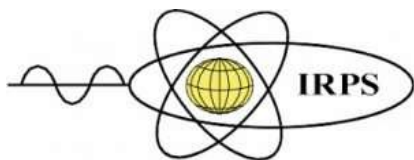
**A090 - The impact of gamma rays on the structural, optical and electrical properties of copper iodide (CuI) thin films prepared by SILAR technique**

Syed Mansoor Ali<sup>1</sup>, S. Aldawood<sup>1\*</sup>, M.S. AlGarawi<sup>1</sup>, S. S. AlGamdi<sup>1</sup>, S.A. Al Salman<sup>1</sup>,

<sup>1</sup>Department of Physics and Astronomy, College of Science, P.O. BOX 2455, King Saud University, Riyadh 11451, Saudi Arabia

Correspondence: Symali@ksu.edu.sa,

The influence of incident  $\gamma$ - rays, with different doses, on nano-structural, optical, and electrical properties of copper iodide (CuI) thin films, deposited via successive ionic layer adsorption and reaction (SILAR), have been investigated in this work. The prepared thin films were exposed to different  $\gamma$ - radiation doses (0-100 kGy) by using a  $^{60}\text{Co}$  gamma source, which has a dose rate of 7.33 kGy/h at room temperature. X-Ray diffraction (XRD) results confirmed the cubic phase structure with preferred growth direction corresponding to (111) diffraction peak. The Williamson and Hall (W-H) analysis were used to compute the effect of crystallite size and micro-strain on the peak enlargement after irradiation with various doses. The field emission scanning electron microscope (FESEM) morphological descriptions revealed the grain size decreased with increasing  $\gamma$ - radiation doses and agglomerated at high dose value. The energy dispersive X-rays (EDX) analysis confirmed the elemental composition of the pristine CuI thin films. The estimated energy band gap for the irradiated thin films varied from 2.43 to 2.66 eV with increasing dose value. The photoluminescence (PL) spectra of pristine and irradiated CuI thin films showed strong emissions at the energy around their band gaps and the intensity of the resulted peak decreased with increasing the  $\gamma$ - radiation doses. The irradiation dose enhances the conductivity, charge mobility as well as carrier concentration in CuI thin films as confirmed by Hall investigation. The obtained results suggested that the CuI thin films are suitable for radiation detection and dosimetric applications.



**ISRP 2021**  
**International Symposium on Radiation Physics**  
**Kuala Lumpur – Malaysia**  
**6 – 10 December 2021**

**A092 - Computerized glow curve deconvolution of proton-irradiated Ge-doped optical fibres**

Mohammad Faizal Hassan<sup>1</sup>, Wan Nordiana Rahman<sup>2</sup>, Takashi Akagi<sup>3</sup>, Nor Shazrina Sulaiman<sup>3</sup>, David Andrew Bradley<sup>4,5</sup>, Noramaliza Mohd Noor<sup>1</sup>

<sup>1</sup>Department of Radiology, Faculty of Medicine and Health Sciences, Universiti Putra Malaysia, 43400 UPM Serdang, Selangor, Malaysia

<sup>2</sup>Medical Radiation Programme, School of Health Sciences, Universiti Sains Malaysia, 16150 Kubang Kerian, Kelantan, Malaysia

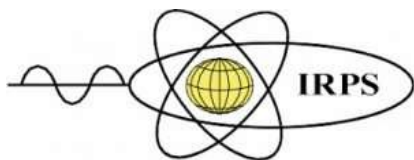
<sup>3</sup>Department of Radiation Physics, Hyogo Ion Beam Medical Center, 1-2-1 Koto, Shingu-cho, Tatsuno City, Hyogo 679-516, Japan

<sup>4</sup>Centre for Applied Physics and Radiation Technologies, School of Engineering and Technology, Sunway University, 47500 Bandar Sunway, Selangor, Malaysia

<sup>5</sup>Centre for Nuclear and Radiation Physics, Department of Physics, University of Surrey, Guildford, Surrey, GU2 7XH, United Kingdom

Corresponding author: [noramaliza@upm.edu.my](mailto:noramaliza@upm.edu.my)

While the thermoluminescence (TL) yield of Ge-doped optical fibres have been widely studied in respect of a wide range of radiation-based applications, detailed evaluation of the electron-trapping mechanism of this material for proton irradiations is still not well represented. Herein, for 150-MeV proton irradiations, we analysed key kinetic parameters; activation energy, peak integral and frequency factor of TL glow curves for locally fabricated Ge-doped optical fibres, use being made of the computerized glow curve deconvolution (CGCD) technique. For maximum readout temperatures ( $T_{\text{stop}}$ ) from 100 to 400 °C, the glow curves of the optical fibre were obtained using increments of 5 °C and a fixed heating rate of 30 °C s<sup>-1</sup>. For each  $T_{\text{stop}}$ , the irradiated optical fibre was heated to acquire gross TL glow curve and then reheated with similar readout parameters to obtain the remaining glow curve. The temperature of the maximum peak intensity ( $T_{\text{max}}$ ) of the glow curve was then recorded. A plot of the  $T_{\text{max}}$  against  $T_{\text{stop}}$  reveals five noticeable plateaus, indicating that the Ge-doped optical fibre is composed of five individual peaks. Through use of GlowFit CGCD fitting method, all glow peaks were shown to overlap each other, with figures of merit of better than 3%. The kinetic parameters of the fitted glow peaks were calculated, the data suggesting that the TL glow peaks of the proton-irradiated Ge-doped optical fibres obey second-order kinetics.



**ISRP 2021**  
**International Symposium on Radiation Physics**  
**Kuala Lumpur – Malaysia**  
**6 – 10 December 2021**

**A094 - Photo and X-ray induced luminescences behaviors of Dy<sup>3+</sup> ions doped alkaline borophosphate glasses**

N. Kiwsakunkran<sup>1,2\*</sup>, N. Chanthima<sup>1,2</sup>, H.J. Kim<sup>3</sup> and J. Kaewkhao<sup>1,2</sup>

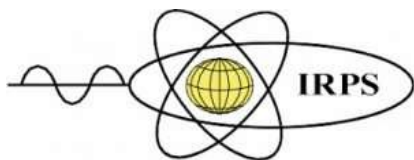
<sup>1</sup>Physics Program, Faculty of Science and Technology, Nakhon Pathom Rajabhat University, Nakhon Pathom 73000, Thailand

<sup>2</sup>Center of Excellence in Glass Technology and Materials science (CEGM), Nakhon Pathom Rajabhat University, Nakhon Pathom 73000, Thailand

<sup>3</sup>Department of Physics, Kyungpook National University, Daegu, 41566, Republic of Korea

Corresponding author: b\_njr\_kskk@hotmail.com

Dy<sup>3+</sup> ions doped alkaline borophosphate glasses have been prepared by melt quenching technique. The physical properties of present glasses like density ( $\rho$ ), molar volume ( $V_m$ ), X-ray diffraction (XRD) and refractive index ( $n$ ) were determined. Totally the absorption spectra are observed, which are assigned to the transitions from the ground state  $^6H_{15/2}$  to the higher energy levels. From the analysis of absorption spectra and JO parameters ( $\Omega_2$ ,  $\Omega_4$  and  $\Omega_6$ ), the radiative properties such as radiative transition probabilities, branching ratios and radiative lifetimes for the fluorescent levels of Dy<sup>3+</sup> ions were determined. The photoluminescence and X-ray induced luminescence were show four prominent emission bands that corresponds to the  $^4F_{9/2} \rightarrow ^6H_J$  ( $J = 15/2, 13/2, 11/2, 9/2$ ) transitions. The detailed revision of the present glasses reveals that these glasses could be useful solid-state lasers, LED's and scintillation materials applications.



**ISRP 2021**  
**International Symposium on Radiation Physics**  
**Kuala Lumpur – Malaysia**  
**6 – 10 December 2021**

**A098 - Potential of amino acid based vesicle as hydrogen peroxide radiosensitizer carrier**

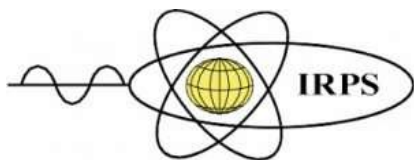
Nur Ratasha Alia Md. Rosli<sup>1,2</sup>, Faizal Mohamed<sup>1,2</sup>, Irman Abdul Rahman<sup>1,2</sup>, Hur Munawar Kabir Mohd<sup>1,2</sup>

<sup>1</sup>Nuclear Technology Research Centre, Faculty of Science and Technology, Universiti Kebangsaan Malaysia, Malaysia

<sup>2</sup>Department of Applied Physics, Faculty of Science and Technology, Universiti Kebangsaan Malaysia, Malaysia

Corresponding author: nralia2542@gmail.com

Incorporating low concentrations of hydrogen peroxide ( $H_2O_2$ ) as a radiosensitizer in radiotherapy has effectively enhanced the therapeutic outcome of the treatment, specifically towards hypoxic tumors. However, the current mode of delivery via intratumoral injection causes clinical patients to experience side effects such as inflammation, local pain, flare, fibrosis, sclerosis and edema acute phase. In this study, an amino acid based vesicle-hydrogen peroxide complex was synthesized and the properties that underline its potential as a radiosensitizer carrier alternative delivering method have been investigated. Vesicle- $H_2O_2$  complex was synthesized with sodium N-lauroulsarcosinate hydrate (SNLS) surfactant and decanol co-surfactant immersed in  $H_2O_2$  solution for passive loading. Formed vesicles were then extruded through a  $0.1 \mu\text{m}$  polycarbonate membrane. In terms of molecular conformation, the FTIR spectra amide transmission peak at  $1638 \text{ cm}^{-1}$  affirms the formation of the synthesized vesicles. The formed nanovesicles had spherical morphologies and were moderately stable upon synthesis. In vitro studies against hepatocellular carcinoma cell line Hep G2 demonstrated that through agent encapsulation in vesicles, the cytotoxicity of agent against cultured cell was reduced. This study elucidates that an amino acid based biosurfactant vesicle has the potential to function as a radiosensitizer carrier.



**ISRP 2021**  
**International Symposium on Radiation Physics**  
**Kuala Lumpur – Malaysia**  
**6 – 10 December 2021**

**A099 - Radiation induced alterations in carbon rich media**

D.A. Bradley<sup>1,2</sup>, Lam Siok Ee<sup>1</sup>, Siti Nurasih Mat Nawi<sup>1</sup>, Siti Fairus Abdul Sani<sup>3</sup>, Mayeen Khandaker<sup>1</sup>, Amal Alqhatani<sup>4</sup>, Eman Daar<sup>5</sup>, Ming Tsuey Chew<sup>1</sup>

<sup>1</sup>Centre for Applied Physics and Radiation Technologies, Sunway University, 46150, Petaling Jaya, Malaysia

<sup>2</sup>Department of Physics, University of Surrey, Guildford, GU2 7XH, UK

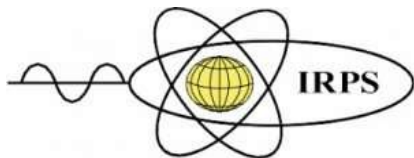
<sup>3</sup>Department of Physics, Faculty of Science, University of Malaya, 50603, Kuala Lumpur, Malaysia

<sup>4</sup>College of Medicine, Deanship of Preparatory Year and Supporting Studies, University of Imam Abdulrahman Bin Faisal, Dammam, Saudi Arabia

<sup>5</sup>Department of Physics, University of Jordan, Amman, Jordan

Corresponding author: [dbradley@sunway.edu.my](mailto:dbradley@sunway.edu.my)

We provide retrospective analysis of a set of confocal Raman microspectrometry and photoluminescence data for irradiated carbon rich media, in so-doing detecting low-dose alterations. Within the dose range 0.1 Gy to 200 Gy an effect is identified that potentially seeds material weakening, the pooled data covering independent x-, gamma-rays, and thermal neutron field irradiations. Categorised in terms of a number of key influencing factors, an emergent pattern of response for the various samples under study is observed, indicative of the cycling of radiation driven modifications and subsequent relaxation. This novel technique, referred to as defectroscopy, provides a probe of the generation of radiation-induced defects and internal annealing, the strength of the effects being strongly identified to arise from a combination of the ratio of sample surface to volume, fractional carbon content, linear energy transfer (LET), and strain within the initial material. Outcomes from the technique suggest applicability in determination of changes in materials of widespread importance in structural and functional roles in biology, including the collagen of skin and pericardium, also the viscosity of synovial fluid.



**A104 - Extraction and Purification of high-purity ThO<sub>2</sub> from monazite ores for thorium fuel-based reactor**

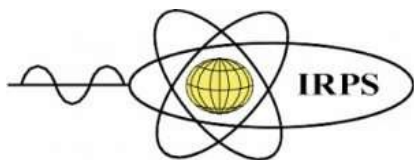
Aznan Fazli Ismail<sup>1,2</sup>, Ahmad Hayaton Jamely Mohd Salehuddin<sup>1</sup>, Eli Syafiqah Aziman<sup>1</sup>

<sup>1</sup>Nuclear Science Programme, Faculty of Science and Technology, Universiti Kebangsaan Malaysia, 43600 UKM Bangi, Selangor, Malaysia

<sup>2</sup>Nuclear Technology Research Centre, Faculty of Science and Technology, Universiti Kebangsaan Malaysia, 43600 UKM Bangi, Selangor, Malaysia

Corresponding author: [aznan@ukm.edu.my](mailto:aznan@ukm.edu.my)

The most commonly used solvent to extract thorium is tri-butyl phosphate (TBP). However, this chemical has drawbacks due to its high chemical consumption and the multi-extraction steps in achieving high-purity thorium and the aqueous solution of TBP tends to form a hazardous explosive red-oil chemical. Furthermore, TBP is a controlled chemical that could not be obtained in large quantities due to its utilization in plutonium uranium reduction extraction (PUREX) processing, which likely leads to nuclear weapon production. Therefore, the purpose of this study is to investigate the utilization of D<sub>2</sub>EHPA and Aliquat-336 as an alternative thorium extraction solvent. The present study aims to investigate the optimum parameter in producing high-purity thorium dioxide (ThO<sub>2</sub>) using Di-2-ethylhexyl phosphoric acid (D<sub>2</sub>EHPA) and Aliquat-336 as solvent materials. The extraction and purification process was performed using [Th-RE](OH)<sub>4</sub> compound which was selectively precipitated from the monazite leach solution. Several parameters such as types of acid (HCl, HNO<sub>3</sub> and H<sub>2</sub>(SO<sub>4</sub>)), acid molarity (1M–6M), and solvent ratio (10%–30%) were investigated. The findings indicate that different solvents require a distinctive aqueous medium to extract thorium. The optimum concentrations of D<sub>2</sub>EHPA and Aliquat-336 in extracting thorium were identified to be at 1M H<sub>2</sub>(SO<sub>4</sub>) and 4M HNO<sub>3</sub> with 30% and 20% ratio, respectively. The multi-stage extraction process was successfully extracted and purified thorium at a purity of 96.8% (D<sub>2</sub>EHPA) and 98.0% (Aliquat-336). Subsequent conversion to ThO<sub>2</sub> yielded a high-purity thorium dioxide at 99.1%. In general, the study elucidates that both solvents have the potential to be utilized as thorium extracting agents in preference to the conventional tri-butyl phosphate (TBP).



**ISRP 2021**  
**International Symposium on Radiation Physics**  
**Kuala Lumpur – Malaysia**  
**6 – 10 December 2021**

**A105 - Industrial Contamination Assessment of Natural Radionuclides and Heavy Metals to the Environment: Case Study of Unregulated Industry in Malaysia**

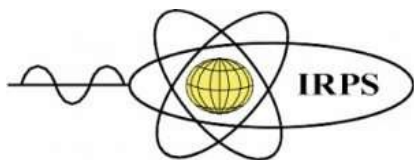
Muhammad Abdullah Rahmat<sup>1</sup>, Aznan Fazli Ismail<sup>1,2</sup>

<sup>1</sup>*Nuclear Science Programme, Faculty of Science and Technology, Universiti Kebangsaan Malaysia, 43600 UKM Bangi, Selangor, Malaysia*

<sup>2</sup>*Nuclear Technology Research Centre, Faculty of Science and Technology, Universiti Kebangsaan Malaysia, 43600 UKM Bangi, Selangor, Malaysia.*

Corresponding author: [aznan@ukm.edu.my](mailto:aznan@ukm.edu.my)

The tin tailing processing industry in Malaysia has operated with minimal regard and awareness for material management and working environment safety, impacting the environment and workers in aspects of radiation and heavy metal exposure. RIA was conducted where environmental samples were analysed, revealing concentrations of  $^{226}\text{Ra}$ ,  $^{232}\text{Th}$  and  $^{40}\text{K}$  between the range of 0.47 - 9.80, 0.22 – 25.30, and 0.23 - 5.60 Bq/g respectively, resulting in the AED exceeding UNCEAR recommended value and regulation limit enforced by AELB (1 mSv/y). Since employees fall outside of the definition of radiation workers, the dose small limit paired with the repercussion of the exemption order increases the likelihood of overexposure from the studies materials.  $R_{\text{aeq}}$  calculated indicates that samples collected pose a significant threat to human health from gamma-ray exposure. Assessment of heavy metal content via pollution indices of soil and sediment samples showed significant contamination and enrichment from processing activities conducted. As and Fe were two of the highest metals exposed both via soil ingestion with an average of  $4.61 \times 10^{-3}$  and  $1.44 \times 10^{-4}$  mg/kg-day and dermal contact with an average of  $5.59 \times 10^{-4}$  mg/kg-day and  $5.98 \times 10^{-4}$  mg/kg-day respectively. Exposure via accidental ingestion of soil and sediment samples could potentially cause adverse non-carcinogenic and Carcinogenic health effect towards workers in the industry. A correlation analysis was also carried out which shows the presence of a relationship between the concentration of NORM and trace elements indicating that the source of both radionuclides and heavy metals could potentially be from the same source.



**A106 - Radiation hazard indices of sediment and water samples in Amang processing plant in Perak state**

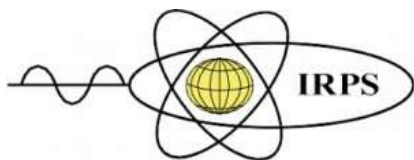
Nursyamimi Diyana Rodzi<sup>1</sup>, Aznan Fazli Ismail<sup>1,2</sup>

<sup>1</sup>Nuclear Science Programme, Faculty of Science and Technology, The National University of Malaysia, 436000 UKM Bangi, Selangor, Malaysia.

<sup>2</sup>Nuclear Technology Research Centre, The National University of Malaysia, 436000 UKM Bangi, Selangor, Malaysia.

Corresponding author: aznan@ukm.edu.my

Amang or by-product of tin minerals processing has been found to contain valuable heavy minerals which are significant to Malaysian economy in producing rare earth elements (REE) such as ilmenite, monazite, and xenotime. This study aims to provide indications of radiological hazard to authorities on the effect of the processing activity to close cycle water management. Seven amang processing plants in Perak were chosen as the study location. Sediment and water samples are collected from each processing plant retention pond before being processed and analysed using HPGe spectroscopy. The Uranium-238 (<sup>238</sup>U), Thorium-232 (<sup>232</sup>Th), and Potassium-40 (<sup>40</sup>K) concentration in sediment samples were 0.1-1.9 Bq/g, 0.2-3.2 Bq/g and 0.1-1.8 Bq/g respectively, with some of the sediment samples exceeds the limit stated by Atomiv Energy Licensing Board (AELB) of 1 Bq/g for <sup>238</sup>U and <sup>232</sup>Th and none exceeds the limits of 10 Bq/g for <sup>40</sup>K. The values are then used for radiological hazard indices calculation. The range values obtained from the sediment samples for Radium Equivalent Activity ( $R_{eq}$ ), Absorbed Dose Rates ( $D_R$ ), Annual Effective Doses (AED), External Hazard Index ( $H_{ex}$ ), Internal Hazard Index ( $H_{in}$ ) and Excess Lifetime Cancer Risk (ELCR) were found to be  $2416.5 \pm 2020$ ,  $1046.3 \pm 858.0$  nGy/h,  $2.6 \pm 2.0$  mSv/y,  $3.7 \pm 2.6$ ,  $6.4 \pm 5.3$  and  $10.0 \pm 7.5$ , respectively. These reported results are compatible with those values in previous study in amang processing plant. Whereas, for water samples, the activity concentration of Radium-226 (<sup>226</sup>Ra), Radium-228 (<sup>228</sup>Ra), and <sup>40</sup>K was found to be in ranged of 2.4-34.9 Bq/l, 0.8-14.7 Bq/l and 19.5-299.4 Bq/l respectively. Further analysis on water samples using Inductively Coupled Plasma-Mass Spectrometry (ICPMS) to assess the heavy metals concentration found that the concentration of Cadmium (Cd), Chromium (Cr), Arsenic (As), Plumbum (Pb), Nickel (Ni), and Zinc (Zn) is 0-0.003 mg/l, 0.001-0.2 mg/l, 0.01-0.3 mg/l, 0.001-0.2 mg/l, 0.003-0.1 mg/l and 0.004-0.3 mg/l respectively. Findings shows that the the amang processing activity has enhanced the natural radionuclides concentrations in sediment and water samples.



**A107 - Radiological Dose Assessment of internal exposure due to Radon in Groundwater affected by Tin Mining in Doguwa, Kano State, Nigeria**

Abdu Nasiru Muhammad<sup>1,2</sup>, Aznan Fazli Ismail<sup>1,3</sup>, Nuraddeen Nasiru Garba<sup>4</sup>

<sup>1</sup>Nuclear Science Program, Faculty of Science and Technology, University Kebangsaan Malaysia (UKM), Bangi, Malaysia.

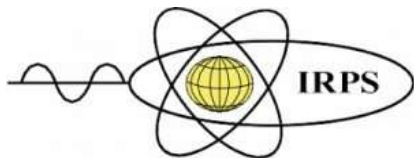
<sup>2</sup>Nigerian Nuclear Regulatory Authority (NNRA), Plot 564/565 Airport Road, Central Business District, Abuja

<sup>3</sup>Nuclear Technology Research Centre, Faculty of Science and Technology, University Kebangsaan Malaysia (UKM), Bangi Malaysia.

<sup>4</sup>Department of Physics, Ahmadu Bello University, 810211 Zaria, Nigeria.

Corresponding author: [aznan@ukm.edu.my](mailto:aznan@ukm.edu.my)

Unregulated mining activities usually enhances the background radiation level in an environment, thereby exposing its inhabitants to unnecessary radiation doses, which can increase the chances of cancer and non-cancer induction. This work measured the activity concentrations of <sup>222</sup>Rn in ground water from the tin mining areas in Doguwa, Kano State, Nigeria. A total of 40 ground water samples were collected and analysed using a liquid scintillation counter (Tri-Carb-LSA1000). The measured <sup>222</sup>Rn concentrations in the study area lies within the range of 0.75-14.08 Bq/L with a mean value of 12.36Bq/L which is slightly higher than the 11 Bq/L set by USA-EPA. The average annual effective dose due to radon inhalation in ground water in the study area was found to be 0.31 $\mu$ Sv/yr while the average annual effective dose due to radon ingestion in ground water within the study area by adult, children and infant was found to be 90.885, 136.328 and 159.049 $\mu$ Sv/year respectively. These values are lower than the safety limit of 0.1 mSvy<sup>-1</sup> set by WHO for drinking water. This signifies that the water in the study area is safe for consumption and other domestic activities.



**ISRP 2021**  
**International Symposium on Radiation Physics**  
**Kuala Lumpur – Malaysia**  
**6 – 10 December 2021**

**A108 - Occupational dose and technical parameters in pediatric upper gastrointestinal series**

Gracielly Nunes<sup>1</sup>, Rosangela Jakubiak<sup>1</sup>, Renato Doro<sup>2</sup>, João Setti<sup>1</sup>, Valeriy Denyak<sup>1,3</sup> Hugo Schelin<sup>4</sup>

<sup>1</sup>Federal University of Technology – Paraná, Curitiba, Brazil

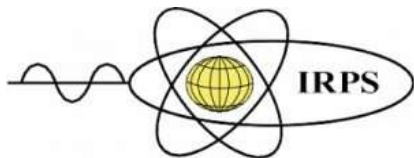
<sup>2</sup>BrasilRad – Innovation and Quality in Medical Physics, Florianópolis, Brazil

<sup>3</sup>National Science Center ‘Kharkov Institute of Physics and Technology’, Kharkiv, Ukraine

<sup>4</sup>Pelé Pequeno Príncipe Research Institute, Curitiba, Brazil

Corresponding author: denyak@gmail.com

The present study had as main goal to estimate the dose received by the professionals involved in pediatric upper gastrointestinal series. We compared all five exam positions in filming sequence and studied certain variables that influence dose: field size on the table, distance from the ionization chamber to the isocenter, lead apron, additional filtration. The polyethylene mannequin filled with water were used to simulate the patient’s body and another assistant. The equipment used to measure dose rate was a parallel plate ionization chamber calibrated with accuracy of 1.8%. For different exam positions, the difference in dose rate reaches 15% and the doses in radiography differ by a factor of up to 2.8. The contribution of the radiographic images may reach 30%. The dose rate dependence on distance follows the inverse square law with the precision better than 1%. For tube voltage of 83 kV, lead apron decreases the dose rate of scattered radiation similar to the monochromatic radiation of 49 keV. The application of additional filtration reduces the dose rate by tens of percent. The dose values in one examination are somewhat smaller but comparable with typical patient doses in chest radiography. The annual effective dose may exceed the limit in the case of hundreds of procedures. This is the first study of the “dynamic” of occupational exposure in upper gastrointestinal series: dose rate in fluoroscopy and dose in radiographic image production for each exam position.



**A111 - Screening in bremsstrahlung at high-energies**

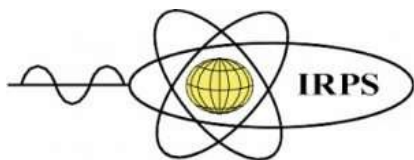
Alessio Mangiarotti<sup>1</sup>, Marcos Nogueira Martins<sup>1</sup>, Doris Jakubassa-Amundsen<sup>2</sup>

<sup>1</sup>Instituto de Física, Universidade de São Paulo, Brazil

<sup>2</sup>Mathematics Institute, University of Munich, Germany

Corresponding author: [alessio@if.usp.br](mailto:alessio@if.usp.br)

The screening correction in bremsstrahlung at high energies is customary handled using the complete screening approximation of the Bethe-Heitler (BH) expression. By including the Coulomb correction, this approach allows introducing the radiation length as the only parameter characterizing each element. Although such approximations are justified at high energies of the impinging electron and low energies of the emitted photon, they have to fail along the evolution of the radiated spectrum since no screening is present at the short-wavelength-limit (SWL). Recently, new high precision data have been collected at MAMI with a systematic uncertainty of 1.6% to verify the Bethe-Maximon discovery that higher order non-radiative corrections tend to vanish in the high energy limit. These measurements fully validated an approach where the Coulomb correction is evaluated at the leading order with the Furry-Sommerfeld-Maue wave-functions and the screening correction is taken into account with the Maximon-Olsen-Wergeland additivity rule in the first-Born approximation using realistic atomic form factors. Here the same theoretical approach will be used to test the accuracy of the complete screening high-energy limit of the BH expression. Calculations for 500 MeV, 1 GeV, 2 GeV and 5 GeV impinging electrons will be presented (going above 500 MeV for the first time). While the complete-screening high-energy limit of the BH expression is not particularly good in the higher half of the spectrum for 500 MeV, the discrepancy is progressively confined closer to the SWL as the energy is increased to 5 GeV. The experimental data will be compared with non-relativistic and relativistic atomic form factors, showing that the current experimental uncertainties do not allow to distinguish the two. Finally, these form factors will be used in the low photon-energy limit to compare with the radiation length values routinely employed by the whole high energy physics community.



**A112 - Dosimetric Comparison in Adjuvant Radiotherapy for Early Stage and Advance Stage for Left-Side Breast Cancer using Volumetric Modulated Arc Therapy**

Yi-Chi Liu<sup>1</sup>, Tsung-Shuo Yen<sup>2</sup>, Hsin-Hon Lin<sup>3</sup>, Lu-Han Lai<sup>4</sup>

<sup>1</sup>Department of Radiation Oncology, Wei Gong Memorial Hospital, Taiwan

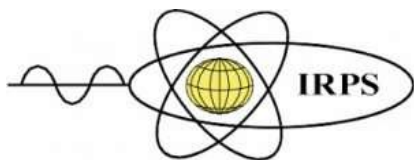
<sup>2</sup>Department of Radiology, Wei Gong Memorial Hospital, Taiwan

<sup>3</sup>Department of Medical imaging and Radiological Sciences, Chang Gung University, Taiwan

<sup>4</sup>Department of Medical Imaging and Radiological Technology, Yuanpei University of Medical Technology, Taiwan

Corresponding author: llai@mail.ypu.edu.tw

Breast cancer is the most common cancer among women worldwide. The purpose of this study is to demonstrate the critical organ dose for various irradiation ranges with the left sided breast cancer. The common lymph node metastasis includes the supraclavicular fossa (SCF), axillary lymph node (AXLN), internal mammary node (IMN). The treatment toxicity for the critical organs would depend on the irradiation range significantly. The irradiation ranges were divided into four groups: whole breast irradiation (group 1), whole breast with the SCF irradiation (group 2), whole breast with the SCF and the AXLN (group 3), whole breast with the SCF and AXLN and IMN irradiation (group 4). Each group has 20 patients. VMAT treatment plan was consist of two partial arcs. We would analyze dose parameters for various irradiation ranges in the treatment planning retrospectively. The prescription dose was 45 Gy in 25 fractions to the planning target volume (PTV). The critical organs included the whole lungs, heart, trachea, esophagus, liver, stomach and spinal cord. Figures of merits such as the conformity index (CI) and homogeneity index (HI) were calculated to evaluate the quality of the treatment plan. In terms of left lung, the mean dose in the group 1,2,3,4 was 6.2, 7.4, 9.1 and 11.2 Gy. The mean  $V_{5Gy}$ ,  $V_{10Gy}$ ,  $V_{20Gy}$  of left lung were 30.0, 34.5, 41.2 and 48.8 % for the above four groups. As for heart, the average dose in the group 1,2,3,4 were 2.8, 2.9, 3.3, 4.8 Gy, respectively. The mean  $V_{30Gy}$  of the heart were 1.0, 1.3, 2.0, 5.9 % in the four groups. This is the first research to collect complete dosimetric data for the left sided breast cancer with various lymph node irradiations. The dosimetric results of critical organs may have an effect on the decision of the physicians' irradiation range.



**ISRP 2021**  
**International Symposium on Radiation Physics**  
**Kuala Lumpur – Malaysia**  
**6 – 10 December 2021**

**A116 - Influence of Bi<sub>2</sub>O<sub>3</sub> content on structural, optical and radiation shielding properties of transparent Bi<sub>2</sub>O<sub>3</sub>-Na<sub>2</sub>O-TiO<sub>2</sub>-ZnO-TeO<sub>2</sub> glass ceramics**

W.L. Fong<sup>1</sup>, S.O. Baki<sup>2,\*</sup>, M.K.A. Karim<sup>3</sup>, Kh.A. Bashar<sup>1</sup>, M.A. Mahdi<sup>1</sup>, M.H.M. Zaid<sup>3</sup>, B.T. Goh<sup>4</sup>

<sup>1</sup>Wireless and Photonic Networks Research Centre, Faculty of Engineering, Universiti Putra Malaysia, Serdang, Selangor 43400, Malaysia

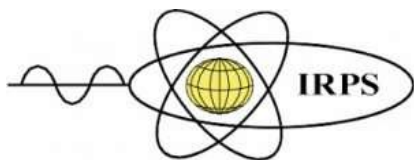
<sup>2</sup>Physics Division, Centre of Foundation Studies for Agricultural Science, Universiti Putra Malaysia, UPM, Serdang, Selangor 43400, Malaysia

<sup>3</sup>Department of Physics, Faculty of Science, Universiti Putra Malaysia, UPM, Serdang, Selangor 43400, Malaysia

<sup>4</sup>Low Dimensional Materials Research Centre, Department of Physics, Faculty of Science, University of Malaya, UM, Kuala Lumpur 50603, Malaysia

Corresponding author: sharudinomar@upm.edu.my

This paper summarises the physical and structural properties of the  $x\text{Bi}_2\text{O}_3\text{-}5\text{Na}_2\text{O-}5\text{TiO}_2\text{-}10\text{ZnO-}(80\text{-}x)\text{TeO}_2$  glass ceramics, where  $x = 5, 8, 10, 12,$  and  $15$  mol% using the conventional melt quenching technique and controlled heat treatment. This paper also discusses the effects of Bi<sub>2</sub>O<sub>3</sub> content on the radiation shielding properties. The glass stability was found to decrease as Bi<sub>2</sub>O<sub>3</sub> content increased. UV-Vis spectrophotometer show that the optical band gap decreased as the period of controlled heat treatment prolonged. A low energy band gap indicates the high polarizability of the sample glass due to the high polarizability of non-bridging oxygen. The physical and ionizing shielding features were investigated for current glass samples. The shielding properties were examined within the energy range of 0.015 until 15 MeV. The sample S5 has the optimum shielding features as a result of the addition of Bi<sub>2</sub>O<sub>3</sub>. Hence, the composition attributes a new glass system that can be used in various applications such as optical communication applications, radiation dosimeter and photon shielding materials.



**ISRP 2021**  
**International Symposium on Radiation Physics**  
**Kuala Lumpur – Malaysia**  
**6 – 10 December 2021**

**A124 - The effect of BaO on the luminescence and radiation shielding properties of borosilicate glass system**

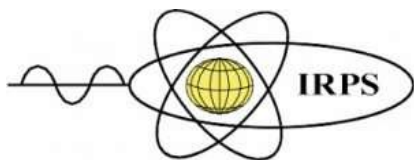
W. Cheewasukhanont<sup>1,2</sup>, P. Limkitjaroenporn<sup>1,2</sup>, J. Kaewkhao<sup>1,2</sup>

<sup>1</sup> Physics program, Faculty of Science and Technology, Nakhon Pathom Rajabhat University, Nakhon Pathom 73000, Thailand

<sup>2</sup> Center of Excellence in Glass Technology and Materials Science (CEGM), Faculty of Science and Technology, Nakhon Pathom Rajabhat University, Nakhon Pathom, 73000, Thailand

Corresponding author: wasu.kotzen@gmail.com

This experimental research aimed to investigate the photoluminescence (PL) and radioluminescence (RL) spectra results of the BaO–ZnO–Al<sub>2</sub>O<sub>3</sub>–B<sub>2</sub>O<sub>3</sub>–SiO<sub>2</sub> (BZABS) glass systems that doped with Dy<sup>3+</sup> (1.5 mol%) ions, and studied varying the BaO concentrations that affected the radiation shielding properties as parameters the mass attenuation coefficients (MAC), effective atomic number ( $Z_{\text{eff}}$ ), and electron density ( $N_{\text{eff}}$ ) by using direct gamma-ray energy from the Compton scattering technique. The result found that the intensity of PL and RL increases with the increasing BaO contents, and also affected increasing the radiation shielding properties.



**ISRP 2021**  
**International Symposium on Radiation Physics**  
**Kuala Lumpur – Malaysia**  
**6 – 10 December 2021**

**A125 - Evaluation of radiation-exposed graphite sheets for passive dosimetry and damage studies**

S.E. Lam<sup>1,\*</sup>, D.A. Bradley<sup>1,2</sup>, M.U. Khandaker<sup>1</sup>, S.N. Mat Nawi<sup>1</sup>, S.F. Abdul Sani<sup>3</sup>, S.S. Ismail<sup>1</sup>

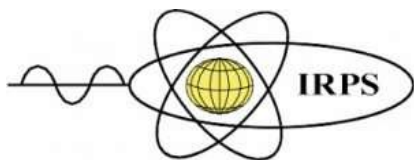
<sup>1</sup>Research Centre for Applied Physics and Radiation Technologies, School of Engineering and Technology, Sunway University, 47500 Bandar Sunway, Selangor, Malaysia

<sup>2</sup>Department of Physics, University of Surrey, Guildford, GU2 7XH, UK

<sup>3</sup>Department of Physics, Faculty of Science, University of Malaya, 50603 Kuala Lumpur, Malaysia

Corresponding author: [siokeel@sunway.edu.my](mailto:siokeel@sunway.edu.my)

Effective clinical use of ionizing radiation has evolved in intimate association with a range of complex dosimetric procedures in diagnostic and therapeutic applications, which necessitates a need to optimize dose delivery against the best clinical outcome. Ongoing intensive research into adaptation of carbon-rich compounds for a wide variety of applications offers ample opportunities in multidisciplinary fields beyond conventional uses. Of late, use has been made of a number of state-of-the-art analytic techniques, investigating the novel use of rod type pencil-lead graphite for passive radiation dosimetry. Current work, aiming to further research, presents the results of 0.1 mm, 0.3 mm and 0.5 mm thick graphite sheets and activated carbon beads, including the effective atomic numbers, dose linearity and sensitivity, radiation-induced structural alterations in Raman spectroscopic features and dose-dependent photoluminescence. All samples were irradiated to Co-60 gamma doses up to 20 Gy. The graphite sheets with a greater carbon purity in excess of 90% are near tissue equivalent, also easy to work with, demonstrating enormous potential to provide for dermal dose evaluation.



**ISRP 2021**  
**International Symposium on Radiation Physics**  
**Kuala Lumpur – Malaysia**  
**6 – 10 December 2021**

### **A128 - Raman and FTIR spectroscopy of synovial fluid after gamma irradiation**

Hur Munawar Kabir Mohd<sup>1</sup>, Irman Abdul Rahman<sup>1,2</sup>, Faizal Mohamed<sup>1,2</sup>, Kenton Paul Arkill<sup>3</sup>, Nur Ratasha Alia Md Rosli<sup>1</sup>

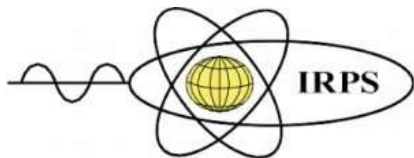
<sup>1</sup>Department of Applied Physics, Faculty of Science and Technology, Universiti Kebangsaan Malaysia, Bangi, 43600, Selangor, Malaysia

<sup>2</sup>Nuclear Technology Research Centre, Faculty of Science and Technology, Universiti Kebangsaan Malaysia, Bangi, 43600, Selangor, Malaysia

<sup>3</sup>Division of Cancer and Stem Cells, School of Medicine, Biodiscovery Institute, University of Nottingham, Nottingham, NG7 2RD, United Kingdom

Corresponding author: hur\_kabir@yahoo.com

Synovial fluid is a viscous fluid that provides lubrication to joints. Recent studies showed that radiation might cause a functional decline in joint health associated with the degradation of synovial fluid post cancer radiation treatment. In this preliminary study, Raman spectroscopy and Fourier transform infrared (FTIR) spectroscopy were used to investigate the effect of gamma irradiation on the synovial fluid and the potential of such technique to detect changes in synovial fluid was evaluated. Bovine synovial fluid samples were irradiated at 10Gy, 25Gy, 50Gy and 100Gy doses at room temperature. The synovial fluid Raman spectral band intensity, post irradiation, slightly decreased compared to the unirradiated sample. The Raman spectra using the 532nm laser line also showed three carotenoid-specific bands at  $1003\text{cm}^{-1}$ ,  $1157\text{cm}^{-1}$  and  $1521\text{cm}^{-1}$ , which could be used as a biochemical marker to correlate with radiation induced degradation. FTIR spectra of synovial fluid samples show no significant changes in overall chemical composition pre and post irradiation as FTIR spectroscopy could not identify individual components in synovial fluid. This early study also suggests that enhancement needs to be done to the Raman and FTIR technique to further analyze synovial fluid biochemical effect post irradiation.



**ISRP 2021**  
**International Symposium on Radiation Physics**  
**Kuala Lumpur – Malaysia**  
**6 – 10 December 2021**

**A129 - Radioactivity and hazard risk analysis of soil samples taken from former mining area in Klang Valley**

S.S. Shamsuri<sup>1</sup>, M.K.A. Karim<sup>1\*</sup>, M.M.A Kechik<sup>1</sup>, Y.Yaakob<sup>1</sup>, M.H.A Mhareb<sup>2,3</sup>

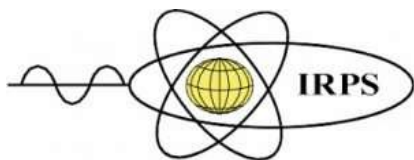
<sup>1</sup>Department of Physics, Faculty of Science, Universiti Putra Malaysia, 43400 Serdang, Selangor, Malaysia

<sup>2</sup>Department of Physics, College of Science, Imam Abdulrahman Bin Faisal University, P.O. Box 1982, Dammam 31441, Saudi Arabia;

<sup>3</sup>Basic and Applied Scientific Research Center, Imam Abdulrahman Bin Faisal University, P.O. Box 1982, Dammam 31441, Saudi Arabia.

Corresponding author: mkhalis@upm.edu.my

Radioecology until now considered significant field in monitoring and observe the impact of natural or man made radiation to human population. Hence, this study aimed to evaluate the radioactivity from the former mining soils of Klang Valley and to determine its associated risk. 20 soil samples have been collected systematically and analyzed by using the High Purity Germanium (HPGe) gamma spectrometer (Canberra, Australia). The <sup>226</sup>Ra, <sup>232</sup>Th and <sup>40</sup>K were predetermined from the soil samples and the activity concentration were ranged from 11.91-54.09 Bq/kg, 8.95-49.50 Bq/kg and 974.64 Bq/kg, respectively. The risk of radiation hazard to human being were analyzed and categorized based on studied area and several parameters such as radium equivalent activity, radiation hazard index, external hazard index and total air absorbed dose rate were found to be  $305.90 \pm 111.84$  Bq/kg,  $2.25 \pm 0.85$ ,  $0.30 \pm 0.84$  and  $139.5 \pm 49.42$  nGy/h, respectively. These values were compared with the recommendation by United Nations Scientific Committee on the Effect of Atomic Radiation (UNSCEAR) international standard safe limit. Locations P2, P6, P16 and P17 were observed to have highest potential risk and has a radioactive element that can endanger the health of the surrounding population on external exposure through either the food chain or daily use. Overall, the mean annual effective dose outdoors received by an individual at studied area was estimated to be  $0.17 \pm 0.01$  mSv/y, which is far below than the annual dose limit of 1 mSv/y of the public.



**ISRP 2021**  
**International Symposium on Radiation Physics**  
**Kuala Lumpur – Malaysia**  
**6 – 10 December 2021**

**A131 - A study on Competition between proton and beta decay for some  $\beta$ -therapeutic nuclides**

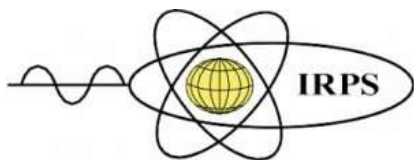
N. Sowmya<sup>1\*</sup>, H.C. Manjunatha<sup>1\*</sup>, K.N.Sridhar<sup>2</sup>

<sup>1</sup>Department of Physics, Government College for Women, Kolar, Karnataka, India.

<sup>2</sup>Department of Physics, Government First Grade College, Kolar, Karnataka, India.

Corresponding Author: manjunathhc@rediffmail.com, sowmyaparakash8@gmail.com

Proton decay and  $\beta$ -decay half-lives of  $\beta$ -therapeutic nuclides such as  $^{177}\text{Lu}$ ,  $^{90}\text{Sr}$ ,  $^{153}\text{Sm}$ ,  $^{153}\text{I}$ ,  $^{137}\text{Cs}$ ,  $^{201}\text{Au}$ ,  $^{165}\text{Dy}$ ,  $^{99}\text{Mo}$ ,  $^{89}\text{Sr}$ ,  $^{59}\text{Fe}$ ,  $^{32}\text{P}$ ,  $^{166}\text{Ho}$ ,  $^{92}\text{Sr}$ ,  $^{188}\text{Re}$ ,  $^{90}\text{Y}$ ,  $^{147}\text{Pr}$ ,  $^{60}\text{Co}$  and  $^{42}\text{K}$  have been studied using formulated theoretical models. Competition between proton and beta decay is studied. Branching ratios corresponds to the proton decay and beta decay are presented. Evaluated half-lives are compared with the that of experiments. Decay chains of these therapeutic nuclides are also presented. A detailed study of branching ratio of proton decay with respect to beta-decay confirms the dominant decay mode in the  $\beta$ -therapeutic nuclides. Present work is useful in radiotherapy and dosimetry.



**ISRP 2021**  
**International Symposium on Radiation Physics**  
**Kuala Lumpur – Malaysia**  
**6 – 10 December 2021**

**A132 - Synthesis and characterisation of  $\text{CuFe}_2\text{O}_4$  for X-ray/gamma radiation shielding**

B.Chinnappa Reddy<sup>1&2</sup>, L.Seenappa<sup>3\*</sup>, H.C.Manjunatha<sup>3\*</sup>, Y.S.Vidya<sup>4</sup>, K.N.Sridhar<sup>5</sup>,  
U.Mahaboob Pasha<sup>1</sup>

<sup>1</sup>Department of Physics, Presidency University, Bengaluru-560064 Karnataka, India

<sup>2</sup>Department of Physics, Government First Grade College, Srinivasapur-563135 Karnataka, India

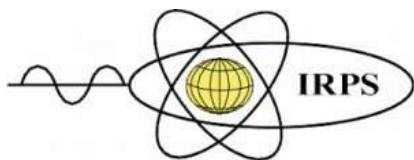
<sup>3</sup>Department of Physics, Government College for women, Kolar-563101, Karnataka, India

<sup>4</sup>Department of Physics, Lal Bahadur Shastri Government First Grade College, RT Nagar, Bangalore-560032, Karnataka, India

<sup>5</sup>Department of Physics, Government First Grade College, Kolar-563101 Karnataka, India

Corresponding authors: seenappakolar@gmail.com, manjunathhc@rediffmail.com

X-ray/gamma radiation have many applications in various fields like agriculture, engineering, medicine, archeology, aviation and so on. Copper ferrite ( $\text{CuFe}_2\text{O}_4$ ) is a spinel ferrite with great potential technological applications. Nanoscale  $\text{CuFe}_2\text{O}_4$  is less toxic and cost effective material compared to other radiation shielding materials. Hence the study of radiation shielding properties of  $\text{CuFe}_2\text{O}_4$  in radiation dosimetry is important.  $\text{CuFe}_2\text{O}_4$  nanoparticles was synthesized by solution combustion method using Urea as fuel. The mixture containing  $\text{Cu}(\text{NO}_3)_2 \cdot 5\text{H}_2\text{O}$ ,  $\text{Fe}(\text{NO}_2)_3 \cdot 9\text{H}_2\text{O}$  and fuel Urea [ $\text{CH}_4\text{N}_2\text{O}$ ] in the stoichiometric ratio with distilled water were taken in a cylindrical crucible. Using magnetic stirrer, the mixture was stirred well for half an hour at 400 rpm. Then the crucible was placed in preheated muffle furnace maintained at a temperature of  $500 \pm 10^\circ\text{C}$ . This resulted product was calcined at  $500^\circ\text{C}$  for 3 hrs in the muffle furnace and then it is cooled to the room temperature and collected. The resulting  $\text{CuFe}_2\text{O}_4$  was characterized by using Shimadzu Powder X-ray diffractometer (PXRD). The particle size and morphological features were studied by scanning electron microscopy and transmission electron microscopy respectively. By using Perkin Elmer Forntier FTIR spectrometer the FTIR studies of the nanoparticles were performed. The UV-Visible absorption spectrum was recorded on PerkinElmer UV Visible Spectrophotometer. The measured radiation shielding parameters like mass attenuation coefficient, linear attenuation coefficients, half value layer, tenth value layer, mean free path, effective atomic number ( $Z_{\text{eff}}$ ), effective electron density ( $N_e$ ), energy build-up factor (EBF) and specific absorption fraction of energy ( $\phi$ ) in the energy range 0.081-1.332 MeV using NaI (TI) detector and multi channel analyzer were measured. The measured values for  $\text{CuFe}_2\text{O}_4$  are found to be useful in radiation dosimetry and hence it can be used as the shielding material for X-rays and gamma rays.



**ISRP 2021**  
**International Symposium on Radiation Physics**  
**Kuala Lumpur – Malaysia**  
**6 – 10 December 2021**

### **A133 - X-ray/gamma radiation absorption studies in transition metal doped ZnO**

K.N. Sridhar<sup>3</sup>, H.C. Manjunatha<sup>1\*</sup>, Y.S.Vidya<sup>2</sup>, L. Seenappa<sup>1\*</sup>

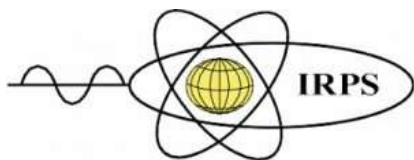
<sup>1</sup>Department of Physics, Government College for Women, Kolar-563101, Karnataka, India

<sup>2</sup>Department of Physics, Lal Bahadur Shastri Government First Grade College, RT Nagar, Bangalore–560032, Karnataka, India

<sup>3</sup>Department of Physics, Government First Grade College, Kolar-563101, Karnataka, India

Corresponding authors: seenappakolar@gmail.com, manjunathhc@rediffmail.com

The radiations such as X-ray/gamma have useful and harmful effects depending on the exposure and dose. X-rays/gamma used medical diagnosis, cancer treatment, food irradiation and airport security scanners. Prolonged exposure to these radiations cause cell mutations. Sometimes cells die, or can lead to cancer. The amount of damage depends on the dose of radiation received. So unwanted exposure to radiation results in health issues. In order to prevent harmful effects of these radiations, lead based shielding materials are used. The disposal of lead based materials is an environmental issue. Hence, it is a search for alternate materials for blocking these radiations, thus protecting both health and environment. In this work, the X-ray/gamma radiation shielding parameters like mass attenuation coefficient (MAC), linear attenuation coefficient (LAC), mean free path ( $\lambda$ ), half value layer (HVL), tenth value layer (TVL), effective atomic number ( $Z_{eff}$ ) and electron density ( $N_e$ ) are studied in zinc oxide doped with transition metals such as titanium, vanadium, cadmium and platinum. The literature survey on the studies of shielding properties of ZnO doped with other elements prompted us to study the shielding properties of different concentrations (2%, 4%, 6% & 8%) of the above dopants with ZnO. Theoretically, shielding parameters such as LAC, HVL, TVL,  $\lambda$ ,  $Z_{eff}$  &  $N_e$  were computed with the aid of MAC which was generated using WINXCOM program in the energy range 1 keV -100 GeV for ZnO doped with transition metals such as (a)Ti, (b) V, (c) Cd & (d) Pt with 2, 4, 6 & 8% molar concentration of dopants. The computed data revealed that MAC, LAC,  $Z_{eff}$ ,  $N_e$  are larger whereas HVL, TVL &  $\lambda$  are smaller for 8% Cd doped ZnO when compared to the other ZnO compounds. This clearly indicates that 8% Cd doped ZnO is a good absorber of X-rays/gamma radiation.



**ISRP 2021**  
**International Symposium on Radiation Physics**  
**Kuala Lumpur – Malaysia**  
**6 – 10 December 2021**

### **A134 - Radioactivity of Radon**

A.M.Nagaraja<sup>1&2</sup>, N. Sowmya<sup>1\*</sup>, H.C. Manjunatha<sup>1\*</sup>, N.Manjunatha<sup>1</sup>, L. Seenappa<sup>1</sup>

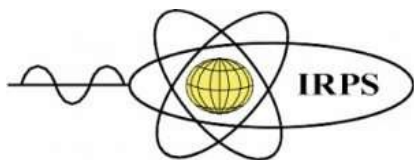
<sup>1</sup>Department of Physics, Government College for Women, Kolar, Karnataka, India.

<sup>2</sup>Department of Physics, St.Joseph's college, Affiliated To Bharathidasan University, Tiruchirappalli-620002,

Tamil-Nadu, India

Corresponding Author: manjunathhc@rediffmail.com, sowmyaparakash8@gmail.com

Using modified generalised liquid drop model, the cluster and alpha radioactivity of isotopes of Thorium are studied. The effect of deformation parameter and angular momentum were also included in order to evaluate total potential. The key role of preformation factor and penetration probability using Wentzel–Kramers–Brillouin (WKB) integral were used to evaluate decay constant of cluster/alpha radioactivity. The half-lives of cluster/alpha is evaluated using the reciprocal of decay constant. Present work is compared with the available experiments. The cluster emissions such as <sup>9</sup>Be, <sup>10,11</sup>B, <sup>12</sup>C, <sup>14</sup>N, <sup>16</sup>O, <sup>19</sup>F, <sup>20-23</sup>Ne, <sup>23</sup>Na, <sup>24-26</sup>Mg, <sup>27</sup>Al, <sup>28-30</sup>Si, <sup>31</sup>P, <sup>32-34</sup>S, <sup>35</sup>Cl, <sup>36,38,40</sup>Ar, <sup>39,41</sup>K and <sup>40</sup>Ca. Relative yield and total kinetic energy of the possible decay mode is identified.



**ISRP 2021**  
**International Symposium on Radiation Physics**  
**Kuala Lumpur – Malaysia**  
**6 – 10 December 2021**

### **A138 - Gamma and X-ray shielding properties of Gallium alloys**

K.V. Sathish<sup>1,4</sup>, L. Seenappa\*<sup>1</sup>, H.C. Manjunatha\*<sup>1</sup>, Y.S.Vidya<sup>2</sup>, K.N. Sridhar<sup>3</sup>, S. Alfred Cecil Raj<sup>4</sup>

<sup>1</sup>Department of Physics, Government College for Women, Kolar-563101, Karnataka, India

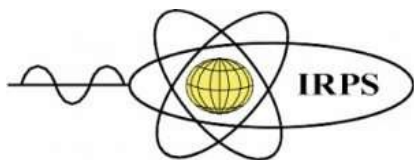
<sup>2</sup>Department of Physics, Lal Bahadur Shastri Government First Grade College, RT Nagar, Bangalore-560032, Karnataka, India

<sup>3</sup>Department of Physics, Government First Grade College, Kolar-563101, Karnataka, India

<sup>4</sup>Department of Physics, St. Joseph's College, Trichy-620020 Tamil Nadu, India

Corresponding authors: seenappakolar@gmail.com, manjunathhc@rediffmail.com

Gallium alloys are less toxic and cost effective material compared to lead. Due to the importance of gallium alloys in radiation shielding, the study of an interaction of X-rays and gamma radiation in these alloys becomes important. The X-ray and gamma interaction parameters such as mass attenuation coefficient, linear attenuation coefficient, Half Value Layer (HVL), Tenth Value Layer (TVL), effective atomic number, electron density, buildup factors, kerma coefficient and radiation protection efficiency are studied in gallium alloys of different composition such as Gallium alloy [Al-50% , Ga-50%], Galfenol [Fe-30% , Ga-70%] and Galinstan [Ga-68.5% , In-21.5%, Sn-10%]. In the present work, the mass attenuation coefficients and photon interaction cross sections in the energy range from 1 keV to 100 GeV are generated using WinXCom and its composition. The total linear attenuation coefficient ( $\mu$ ) is evaluated by multiplying density of compounds to mass attenuation coefficients. The total linear attenuation coefficient ( $\mu$ ) is used in the calculation of Half Value Layer (HVL) and Tenth Value Layer (TVL). The photon mean free path is determined by the reciprocal of linear attenuation coefficient. The effective atomic number is evaluated by taking the ratio between atomic cross section and electronic cross section. We have estimated energy absorption buildup factors using geometric progression (GP) fitting method. Kerma coefficient is determined by multiplying energy of radiation with the mass energy transfer coefficient of the material for this radiation. For the studied gallium alloys, the measured values of mass attenuation coefficient, linear attenuation coefficient, effective atomic number, electron density, buildup factors, kerma coefficient and radiation protection efficiency are large and HVL, TVL are small for the gallium alloy Galinstan. From this results we can conclude that among the studied gallium alloys, Galinstan alloy is the good shielding material and good absorber for X-ray and gamma radiation



**ISRP 2021**  
**International Symposium on Radiation Physics**  
**Kuala Lumpur – Malaysia**  
**6 – 10 December 2021**

**A140 - Simulated Technique to Calculate the Coincidence Summing Factor for a voluminous  $\gamma$ -ray Sources**

Mahmoud I. Abbas<sup>1,\*</sup>, Mohamed.Elsafi<sup>1</sup>, M.I. Sayyed<sup>2,3</sup>, Mayeen Uddin Khandaker<sup>4</sup>

<sup>1</sup>Physics Department, Faculty of Science, Alexandria University, 21511 Alexandria, Egypt.

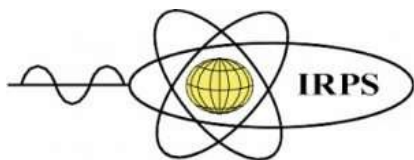
<sup>2</sup>Department of Physics, Faculty of Science, Isra University, Amman 11622, Jordan

<sup>3</sup>Department of Nuclear Medicine Research, Institute for Research and Medical Consultations, Imam Abdulrahman bin Faisal University, Dammam 31441, Saudi Arabia

<sup>4</sup>Center for Applied Physics and Radiation Technologies, School of Engineering and Technology, Sunway University, 47500 Bandar Sunway, Selangor Darul Ehsan, Malaysia

Corresponding author: mabbas@physicist.net

Geant4 simulation (GS) was used to correct the coincidence summing (CS) effect in detecting a volumetric  $\gamma$ -ray sources, and this technique was applied to a  $^{152}\text{Eu}$  standard sources. The sources were a liquid cylindrical, rectangular and Marinelli beaker shapes of different volume for each one. The full energy peak (FEP) or photopeak efficiency was calculated using two options of GS. Radionuclide track (RT) including coincidence summing and Monoenergetic Track (MT) without coincidence summing. The results obtained from two methods compared with the experimental method and the modified KORSUM code for cylindrical  $\gamma$ -ray source. The comparison indicated that the present method is correct and useful for coincidence summing corrections for a voluminous  $\gamma$ -ray sources as well as this technique requires far less computation time than other techniques that depend on the calculation of total efficiency.



**ISRP 2021**  
**International Symposium on Radiation Physics**  
**Kuala Lumpur – Malaysia**  
**6 – 10 December 2021**

#### **A144 - Enhancement of $^{18}\text{F}$ -FDG PET phantoms imaging accuracy using MCNP5**

Nazreen Waeleh<sup>1,2</sup>, M. Iqbal Saripan<sup>1</sup>, Marianie Musarudin<sup>3</sup>, Fathinul Fikri Ahmad Saad<sup>4</sup>, Syamsiah Mashohor<sup>1</sup>

<sup>1</sup>Faculty of Engineering, Universiti Putra Malaysia, Selangor, Malaysia

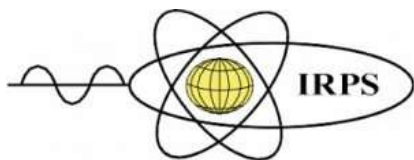
<sup>2</sup>Faculty of Electronic and Computer Engineering, Universiti Teknikal Malaysia Melaka (UTeM), Melaka, Malaysia

<sup>3</sup>School of Health Sciences, Universiti Sains Malaysia, Kelantan, Malaysia

<sup>4</sup>Centre for Diagnostic Nuclear Imaging, Universiti Putra Malaysia, Selangor, Malaysia

Corresponding author: nazreen@utem.edu.my

The image quality, readability, and accuracy of uptake quantification are crucial in nuclear medicine imaging systems for determining correct diagnosis. However, a negative correlation was observed between the detection of high energy photons and the patient's size. This result is due to photons' interaction with the medium as they move through the body. Thus, the current study aims to examine Monte Carlo N-Particle (MCNP) Positron Emission Tomography (PET) data attenuation correction simulations using the MCNP5 code for four different categories of patient groups with varying stages of cancer. The cylindrical volume of water was designed and calculated to replicate the shape of the National Electrical Manufacturers Association (NEMA) of the International Electrotechnical Commission (IEC) PET phantom to represent the patients. In addition, the attenuation maps for each phantom were generated from data acquired with a 511 keV positron-emitting source to correct the effect of photon attenuation along the line of response. As a result, four attenuation correction maps were developed for each patient category: underweight, normal weight, overweight, and obese. These maps were multiplied with the relevant PET sinogram to obtain the attenuation-corrected image during the image reconstruction procedure. Comparing images of the radiotracer distribution in each phantom demonstrates the quantifiable improvement in image quality following the attenuation correction method. The intensity profiles confirmed that the radiotracer concentration is greater near the edge than in the center before attenuation adjustment. The signal-to-noise ratio of attenuated corrected images were improved by nearly 80% for the early stage of cancer diagnosis known to be the most challenging stage. The results show the possibility of utilizing the MCNP5 code to correct the attenuation effect on PET data simulation. It improves the radiotracer distribution by having a good quality image quantitatively and qualitatively.



**ISRP 2021**  
**International Symposium on Radiation Physics**  
**Kuala Lumpur – Malaysia**  
**6 – 10 December 2021**

**A146 - Effect of gamma irradiation on lubricin concentration in synovial fluid**

Hur Munawar Kabir Mohd<sup>1</sup>, Irman Abdul Rahman<sup>1,2</sup>, Faizal Mohamed<sup>1,2</sup>, Kenton Paul Arkill<sup>3</sup>, Anuar Jonet<sup>4</sup>, Megan S Lord<sup>5</sup>, Nur Ratasha Alia Md Rosli<sup>1</sup>

<sup>1</sup>Department of Applied Physics, Faculty of Science and Technology, Universiti Kebangsaan Malaysia, Bangi, 43600, Selangor, Malaysia

<sup>2</sup>Nuclear Technology Research Centre, Faculty of Science and Technology, Universiti Kebangsaan Malaysia, Bangi, 43600, Selangor, Malaysia

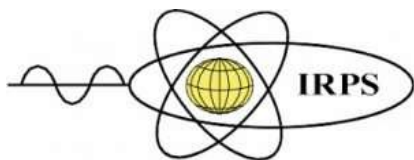
<sup>3</sup>Division of Cancer and Stem Cells, School of Medicine, Biodiscovery Institute, University of Nottingham, Nottingham, NG7 2RD, United Kingdom

<sup>4</sup>Department of Structural Biology and Biophysics, Malaysia Genome Institute, Kajang 43000, Selangor, Malaysia

<sup>5</sup>Graduate School of Biomedical Engineering, University of New South Wales, Kensington, New South Wales 2052, Australia

Corresponding author: irman@ukm.edu.my

Lubricin is a boundary lubricant component found in synovial fluid. There have been reports of joint pain post cancer radiation treatment and loss of lubricin has been reported as a potential factor that contributes to loss of joint lubrication, and subsequently the prevalence of joint pain. However, an effective lubricin isolation method and the trajectory underlining the radiation effects on lubricin component concentrations in the synovial fluid has yet to be discerned. This work describes the development of a lubricin purification technique using fast protein liquid chromatography (FPLC) through anion exchange chromatography via a HiTrap column that resulted in optimum yield of lubricin. Lubricin band was observed after sodium dodecyl sulphate-polyacrylamide (SDS-PAGE) electrophoresis with a molecular weight of approximately 350 kDa. Exposure to gamma irradiation decreased the detectable lubricin band intensity compared to the control sample, indicating that degraded lubricin was eluted in washing fractions during the purification process. Characterisation of the lubricin band was also carried out using LC-MS/MS. Both *N*- and *C*-terminal regions from the peptide sequence in the synovial fluid were identified, thus confirming the presence of purified lubricin. Western blot analysis demonstrated that the 350 kDa fragment amount was decreased post irradiation, indicating lubricin degradation. This study elucidates that gamma irradiation may cause the degradation of lubricin, which could affect the physiological lubrication function of synovial fluid as a whole.



**ISRP 2021**  
**International Symposium on Radiation Physics**  
**Kuala Lumpur – Malaysia**  
**6 – 10 December 2021**

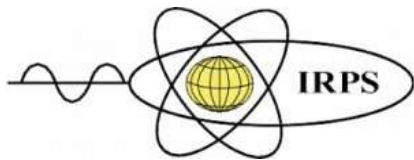
### **A149 - The Rhisotope Project; Using radioisotopes to devalue rhinoceros horn**

Professor James Larkin<sup>1</sup>,

<sup>1</sup>The Radiation and Health Physics Unit. University of Witwatersrand, South Africa

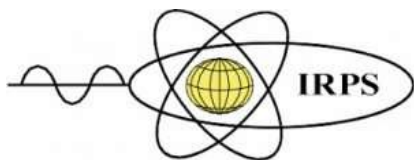
Corresponding author: james.larkin@wits.ac.za

South Africa is home to approximately 80% of the global population of both the white rhinoceros (*Ceratotherium simum*) that is considered endangered, and the black rhinoceros (*Diceros bicornis*) critically endangered. At current rates of poaching, in ten years the wild populations of both these species will cease to exist. The Rhisotope Project, established to counter this trend has been broken down into a few phases culminating in the development of a Radiological Safety Assessment. The initial stage was to insert L-Proline made using  $^{13}\text{C}$  and  $^{15}\text{N}$  into the horns of two test animals. This would allow the subsequent determination  $\delta^{13}\text{C}/^{12}\text{C}$ , and  $\delta^{15}\text{N}/^{14}\text{N}$  ratios in blood and faecal samples. Demonstrating whether there has been any movement of material from the horn into the animal. The next phase has been to determine the appropriate quantity of radioisotope that can be inserted into the horn that will set off installed radiation portal monitors; this has been done using various computer simulations of different potential exposure situations including horns being packed into shipping containers. Based on these results, computer based radiological assessments to the head of an animal have been carried out and efforts made to identify the more radiologically sensitive tissues. This has been necessary to set upper dose limits that are acceptable to both the regulator and other stakeholders in the welfare of these animals. Use has been made use of various mcnp-based software programs combined with CT scanner files to do the dose modelling. The results of this modelling have been compared to laboratory-based dose assessments done using a 3D life-sized phantom printed in the university's engineering faculty. Work continues on the development of a system that will determine the quantity of radioisotope that can be inserted into a horn, based on size, and shape, of the animal's horns. The Rhisotope Project has been established to try and reverse this trend. The project aims to insert small, measured quantities of a chosen radioisotope into the horns of these species with the aim of achieving two specific results. Firstly, reduce demand amongst the end-user population. This will be based on peoples' natural reticence to own and use items that are potentially radioactive. The reduction in the value and demand will then lead to a reduction in the illegal slaughter of these iconic mega-herbivores. The second aim of the project is to make it markedly easier to track and trace any horns that are taken by poachers. Globally there are between 10 and 11 thousand installed radiation portal monitors that have been established at many international border crossings, ports, and airports. In addition, there are many skilled customs agents, border control staff who routinely carry radiation detection equipment. This means that the number of people who are capable of interdicting rhinoceros horns that has been treated with radioactivity has vastly increased. This will significantly increase the risk of detection and interdiction of these illicit



**ISRP 2021**  
**International Symposium on Radiation Physics**  
**Kuala Lumpur – Malaysia**  
**6 – 10 December 2021**

wildlife goods, it will at the same time also expose other contraband that is routinely dispatched with rhinoceros horns to seizure. The penalties associated with the illegal



**ISRP 2021**  
**International Symposium on Radiation Physics**  
**Kuala Lumpur – Malaysia**  
**6 – 10 December 2021**

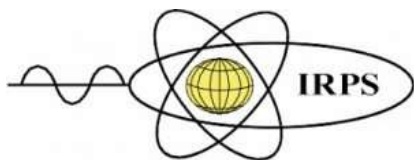
### **A150 - Gamma rays induced effects on the properties of CsPbBr<sub>3</sub> perovskite thin film**

S. Aldawood<sup>1\*</sup>

<sup>1</sup>Department of Physics and Astronomy, College of Science, P.O. BOX 2455, King Saud University, Riyadh 11451, Saudi Arabia

Correspondence: sdawood@ksu.edu.sa

In the last two decades, the family of metal halide perovskites has grabbed more attention in radiation detection application. In this work, radiation detection and dosimetric applicability of CsPbBr<sub>3</sub> thin film will be investigated. So, the impact of gamma irradiation dose on structural, morphological, optical and electrical properties of CsPbBr<sub>3</sub> thin film have been studied. The CsPbBr<sub>3</sub> thin film was synthesized by Thermal evaporation deposition technique. The deposited thin film were exposed to different gamma-ray doses (0 kGy, 25kGy, 50 kGy, 75kGy and 100 KGy) using a <sup>60</sup>Co gamma source, which has an activity of 7.328 KGy/h. The XRD analysis of CsPbBr<sub>3</sub> thin film confirmed the cubical crystal structure, also showed an increase in the crystalline and crystallite size, whereas the dislocation density ( $\delta$ ) and micro strain ( $\epsilon$ ) decreased as the gamma dose increases. The FE-SEM results revealed that surface morphology considerably change by gamma exposure. The optical properties exhibited that the value of energy band gap decreases from 2.35eV to 2.14eV with increasing the dose. This may be due to the increases in the crystallite size and the induced defects. The photoluminescence peaks shifted towards longer wavelength, intensity and FWHM of PL peaks increased with increasing the gamma dose (0 to 100 KGy), which was attributed to spectral broadening and enhancement in the recombination rate of electron-hole pair. Impedance spectroscopy of all irradiated samples showed the single semicircle feature, which is the same as the un-irradiated sample. The grain boundary resistance gradually reduced as the gamma dose increases. The achieved outcomes prove that the structural defects induced by gamma exposure has superficial influence on the structural, morphological optical, photoluminescence and impedance properties of CsPbBr<sub>3</sub> thin films. This blowing impact of gamma dose on the properties makes the CsPbBr<sub>3</sub> thin films significance for possible use in sensing materials.



**ISRP 2021**  
**International Symposium on Radiation Physics**  
**Kuala Lumpur – Malaysia**  
**6 – 10 December 2021**

**A151 - Determination of the Fetal Radiation Dose during Various-Row Multi-Detector Computed Tomography Imaging: Phantom Study**

Osman Günay<sup>1</sup>, Özcan Gündoğdu<sup>2</sup>, Mustafa Demir<sup>3</sup>, S. Hilmi Aksoy<sup>4</sup>, David A Bradley<sup>5,6</sup>

<sup>1</sup> Istanbul Okan University, Vocational School of Health Services, Istanbul, Turkey

<sup>2</sup> Kocaeli University, Faculty of Technology, Kocaeli, Turkey

<sup>3</sup> Istanbul University-Cerrahpasa, Cerrahpasa Faculty of Medicine, Department of Nuclear Medicine, Istanbul, Turkey

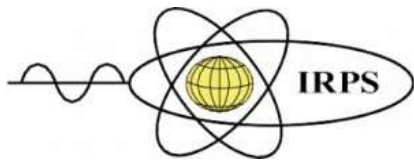
<sup>4</sup> Hisar Intercontinental Hospital, Department of Radiology, Istanbul Turkey

<sup>5</sup> Sunway University, Centre for Applied Physics and Radiation Technologies, 46150 Petaling Jaya, Malaysia

<sup>6</sup> Centre for Nuclear and Radiation Physics, University of Surrey, Guildford, GU4 8JU, UK

Corresponding author: osmangunay07@gmail.com

In computed tomography (CT), the image is obtained by rotating the x-ray tube around the patient in 360 degrees. The patient is exposed to certain amounts of ionizing radiation during CT imaging. In some cases, where pregnant women having a CT imaging are absolutely essential, both the pregnant woman and the fetus are exposed to ionizing radiation. It is therefore crucial to know the radiation dose level that the fetus is exposed to. This paper reports the radiation doses to which the fetus might be exposed. For this purpose, thermoluminescence dosimeters (TLD) were placed in the fetus area of The Alderson Radiation Therapy (ART) phantom and CT imaging was performed using 6-row, 16-row, 128-row and 320-row multi-detector CT (MDCT) for imaging. It was found that the radiation dose that fetus is exposed to in the pelvis of the expecting mother ranged from  $4.02 \pm 0.15$  to  $5.65 \pm 0.48$  mSv and the radiation dose in which the fetus was exposed to in the whole body imaging varied between  $3.75 \pm 0.28$  and  $5.46 \pm 0.32$  mSv.



**ISRP 2021**  
**International Symposium on Radiation Physics**  
**Kuala Lumpur – Malaysia**  
**6 – 10 December 2021**

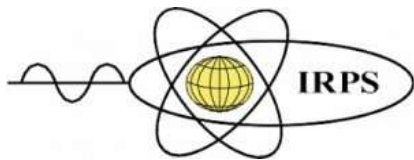
**A152 - Suppressing Moiré artefacts in grating-based X-ray phase-contrast imaging**

Zhili Wang

Department of Physics, Hefei University of Technology, China

Corresponding author: dywangzl@hfut.edu.cn

Grating-based X-ray phase-contrast imaging (GBXPCI) simultaneously retrieves the transmission, refraction (i.e., differential phase) and dark-field modalities of the investigated sample, and therefore is known to provide significant benefits for biomedical imaging. Phase stepping, the most common GBXPCI acquisition technique, involves translation of one of the gratings with high accuracy in regular submicron steps. Then three different modalities can be retrieved by standard least-squares- or FFT-based methods. However, stepping errors inevitably occur due to mechanical inaccuracies and/or thermal drift of the imaging system during the stepping process. As a result of these stepping errors, the standard processing of phase-stepping data with incorrect stepping positions can introduce Moiré artefacts to the retrieved modalities, especially the refraction and dark-field images. In this report, we propose an efficient approach for accurate information retrieval from phase stepping data with stepping errors. In this approach, we introduce an effective phase step number, and search its solution space to obtain the modulation amplitude of phase-stepping data with the minimum coefficient of variation. Then the three different modalities are retrieved using the searched effective phase step number. Numerical and experimental studies demonstrate that this approach can realize highly accurate transmission, refraction and dark-field retrieval consistently in diverse situations, compared to the standard retrieval methods. More importantly, the Moiré artefacts are greatly suppressed, leading to a significant improvement in image quality. Therefore, we anticipate that this approach may provide a powerful solution for accurate information retrieval in grating-based X-ray phase contrast imaging with realistic settings.



**A153 - Dosimetric comparison of renewable product-based composite phantoms**

Damilola Oluwafemi Samson <sup>1,\*</sup>, Mohd Zahri Abdul Aziz <sup>2,\*\*</sup>, Ahmad Shukri <sup>3</sup>, Mohd Zubir Mat Jafri <sup>3</sup>, Rokiah Hashim <sup>4</sup>, Siti Hajar Zuber <sup>3</sup>, and Mohd Fahmi Mohd Yusof <sup>5</sup>

<sup>1</sup>Department of Physics, University of Abuja, P.M.B. 117, Abuja, Nigeria

<sup>2</sup>Advanced Medical and Dental Institute, Universiti Sains Malaysia, 13200 Bertam, Malaysia

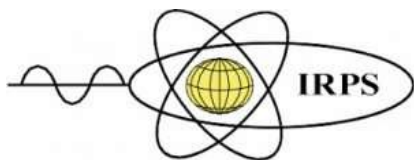
<sup>3</sup>School of Physics, Universiti Sains Malaysia, 11800 Penang, Malaysia

<sup>4</sup>School of Industrial Technology, Universiti Sains Malaysia, 11800 Penang, Malaysia

<sup>5</sup>School of Health Sciences, Universiti Sains Malaysia, 16150, Kelantan, Malaysia

Corresponding author: damilola.samson@uniabuja.edu.ng ; mohdzahri@usm.my

The present study aimed to compare the tissue substitute phantoms fabricated from renewable product composites based on the combination of soy protein concentrate (SPC – 25 wt%), soy protein isolate (SPI – 12 wt%), *Rhizophora spp. (Rh. spp.)*, sodium hydroxide (NaOH – 10 wt%), and curing agent itaconic acid polyamidoamine-epichlorohydrin (IA-PAE – 0, 5, 10, 15, and 20 wt%). Radiation interaction measurements were made at selected gamma photon energies of 0.662 – 1.250 MeV emitted from point sources of <sup>137</sup>Cs and <sup>60</sup>Co at an angle of 0° – 75° using a Ludlum NaI(Tl) detector and verified with the theoretical values obtained through the WinXcom program. For a quantitative analysis of the dosimetric parameters, samples with 15 wt% IA-PAE were evaluated by ionization chamber (IC) and Gafchromic EBT3 films at photons and electrons ranging from 6 – 10 MV and 6 – 15 MeV, and the results were compared with those of water and solid water phantoms. In addition, irradiation was made parallel to the beam for a static 10 x 10 cm<sup>2</sup> field size at 100 cm SSD and with a dose ranging from 0 – 700 cGy. Ludlum configuration technique obtained significantly more attenuation characteristics in SPI-based than SPC-based (p-values > 0.05), exhibiting the consistency of the SPI-based phantoms with those of reference phantoms for the majority of the energy range selected. There was good consistency between the computed tissue phantom ratio (TPR<sub>20,10</sub>) and percentage depth dose (PDD) that was performed in water and solid water phantoms with IC and Gafchromic EBT3 films for both photons and electrons. These results along with 15 wt% of IA-PAE suggest that the design of the new phantoms may be more advantageous in radiation dosimetry and therapy.



**ISRP 2021**  
**International Symposium on Radiation Physics**  
**Kuala Lumpur – Malaysia**  
**6 – 10 December 2021**

### **A157 - Development and characterization of a portable CT system for wooden sculptures analysis**

Renan Oliveira<sup>1</sup>, Anderson de Paula<sup>1</sup>, Fernando Gonçalves<sup>2</sup>, Regina Bueno<sup>3</sup>, Tereza Calgam<sup>3</sup>, Soraia Azeredo<sup>1</sup>, Olga Araújo<sup>1</sup>, Alessandra Machado<sup>1</sup>, Marcelino Anjos<sup>4</sup>, Ricardo Lopes<sup>1</sup>, Davi Oliveira<sup>1</sup>

<sup>1</sup>Laboratório de Instrumentação Nuclear, PEN/COPPE/UFRJ, Brazil

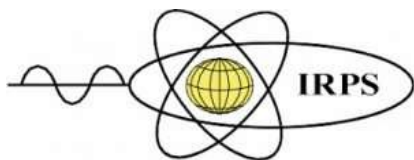
<sup>2</sup>Faculdade de Arquitetura e Urbanismo, IBMR, Brazil

<sup>3</sup>Ateliê Arte e Restauro, Brazil

<sup>4</sup>Instituto de Física, UERJ, Brazil

Corresponding author: [davifoliveira@coppe.ufrj.br](mailto:davifoliveira@coppe.ufrj.br)

In this work, a portable computed tomography system was developed and applied for the analysis of wooden sculptures. The CT system is composed by a portable 120 kV X-ray tube and a 410 x 410 mm a-Si flat panel detector with a pixel size of 200  $\mu\text{m}$ . An arduino controlled turntable was used for the angular movement of the part under analysis. A wooden piece was used for the characterization of the system and the CT images were compared with the ones acquired with a microCT equipment. This piece is a 300 x 160 x 90 mm (H x W x D) wooden block with several details that can be found in wooden sculptures, as thickness reductions, cracks, inclusions of metallic materials, assembling of different wooden parts etc. After the characterization, the system was used for the analysis of a 380 mm high wooden sculpture and the images were also compared with the microCT ones. After these steps, the system was applied for the in loco analysis of a 1450 mm high sculpture. The images acquired with the portable CT system showed similar results when compared with the microCT equipment, being able to detect small details with resolution lower than 500  $\mu\text{m}$ . Also, other characteristics of the piece were perfectly visualized, like growth rings, damages caused by xylophagous insects and assembling of different woods. The sculpture analysis revealed their structural conditions and their manufacturing process, as the types of glass eyes and the different wood densities used. The results showed that the portable CT system can be used for in loco analysis of wooden sculptures that can't be moved for in-lab evaluations, with qualitative and quantitative results equivalent to the microCT.



**ISRP 2021**  
**International Symposium on Radiation Physics**  
**Kuala Lumpur – Malaysia**  
**6 – 10 December 2021**

**A158 - XRF analysis of amorphous silicate slags in cremation remains from the Roman period**

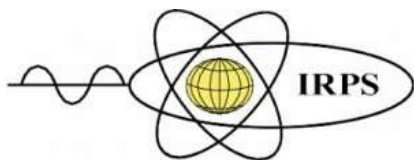
Martin Hložek<sup>1</sup>, Balázs Komoróczy<sup>2</sup>, Tomáš Trojek<sup>1</sup>

<sup>1</sup>Department of Dosimetry and Application of Ionizing Radiation, Czech Technical University in Prague, Czech Republic

<sup>2</sup>Institute of Archaeology of the Czech Academy of Sciences, Brno, Czech Republic

Corresponding author: mhlozek@seznam.cz

On Roman period burial grounds, burnt human remains and grave goods are usually placed into the ground in ceramic urns. Different types of artefacts such as spears, swords, knives and bronze vessels are often involved in the grave goods only after the cremation, but artefacts that were part of clothing ornaments such as brooches, amber artefacts, glass beads usually were influenced by the heat of the funeral pyre. In addition to many burnt bone fragments, the relics of shapeless silicate slags are often found during the conservation work or flotation of the infill of urns. The origin of these shapeless silicate slags, sometimes called cremation waste or cremation slag, is not sufficiently clarified so far. They are believed to be formed by reaction of clay, ashes from wood and straw, which were part of the cremation pyre under the influence of a high temperature of up to 1050 °C. In one of the cremation graves from the Roman period burial ground in Modřice – Sádky near Brno, the slags were obtained from the filling of the ceramic urn. However, there were also damaged glass artefacts (blue bead and game token) in this grave. It is possible that in this grave amorphous silicate slags originated by melting of the beads made from clear glass. We compare the chemical composition of damaged glasses and shapeless silicate slags using XRF analyses and other analytical methods. The methods help to specify the origin of these formations and to refine their archaeological interpretation at the same time.



**ISRP 2021**  
**International Symposium on Radiation Physics**  
**Kuala Lumpur – Malaysia**  
**6 – 10 December 2021**

**A160 - Evaluation of internal structure of concrete after gamma irradiation**

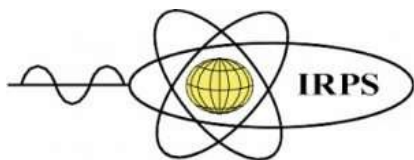
Luan Bastos<sup>1</sup>, Olga de Araujo<sup>1</sup>, Tâmara Teixeira<sup>1</sup>, Sebastião Calixto<sup>2</sup>, Alessandra Machado<sup>1</sup>, Marcelo Gonçalves<sup>2</sup>, Ricardo Lopes<sup>1</sup>, Davi Oliveira<sup>1</sup>

<sup>1</sup>Nuclear Instrumentation Laboratory, Federal University of Rio de Janeiro, Brazil

<sup>2</sup>Engineering and Technology Institute, Geraldo di Biase University, Brazil

Corresponding author: luanfbastos@gmail.com

Concrete is widely used in the world and is the main material for civil construction. Due to its properties, it has different uses such as structural, filling and shielding and interaction with gamma ray causes its internal structure to undergo changes. The aim of this work is to verify the modifications that occur in the concrete structure for three different traits (standardized sand, conventional sand and artificial sand) after an irradiation of 10 kGy and 30 kGy. For this, density, porosity and compressive strength values were determined experimentally. The results showed that after an irradiation of 30 kGy, there was a change in porosity of 21.34% for conventional, 25.44% for artificial sand and 30.29% for standardized sand, the same behavior could be observe for the open pores. The samples showed a variation in density less than 2%. The compressive strength increased 27.48% for conventional sand, 16.47% for artificial sand and 15.72% for standardized sand. It can be seen that the gamma ray promotes changes in internal structure of concrete that can increase its mechanical strength.



**ISRP 2021**  
**International Symposium on Radiation Physics**  
**Kuala Lumpur – Malaysia**  
**6 – 10 December 2021**

**A161 - Pediatric organ and effective doses and radiogenic risk during chest contrast enhanced computed tomography procedure**

H. Salah<sup>1,2\*</sup>, Mohammad Rabbaa<sup>3</sup>, Mohammad Abuljoud<sup>3</sup>, A Sulieman<sup>4</sup>, M. Alkhorayef<sup>5,6</sup>, N. Tamam<sup>7</sup>, and D.A. Bradley<sup>6,8</sup>

<sup>1</sup>INAYA Medical Collage, Nuclear Medicine Department, Riyadh, Saudi Arabia

<sup>2</sup>College of Medical Radiologic Science, Sudan University of Science and Technology, Khartoum, Sudan

<sup>3</sup>Radiology Department, Riyadh Care Hospital, Riyadh, Saudi Arabia

<sup>4</sup>Prince Sattam Bin Abdulaziz University, College of Applied Medical Sciences, Radiology and Medical Imaging Department, Alkharj, Saudi Arabia

<sup>5</sup>Department of Radiological Sciences, College of Applied Medical Sciences, King Saud University, Riyadh, Saudi Arabia

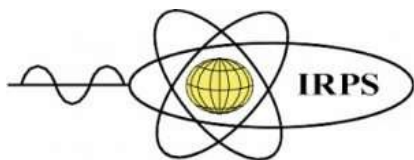
<sup>6</sup>Centre for Nuclear and Radiation Physics, Department of Physics, University of Surrey, Guildford, United Kingdom

<sup>7</sup>Department of Physics, College of Sciences, Princess Nourah Bint Abdulrahman University, Riyadh, Saudi Arabia

<sup>8</sup>Centre for Applied Physics and Radiation Technologies, School of Engineering and Technology, Sunway University, 47500, Bandar Sunway, Selangor, Malaysia.

Corresponding author: hassan.salah.ibrahim1@gmail.com

Children are sensitive to ionizing radiation exposure compared to adults. Currently, computed tomography (CT) is the primary source of medical radiologic examinations to patients and representing more than 70% of the collective doses to the overall population. CT chest with contrast is commonly performed for pediatric patients for various clinical indications. However, the high radiation dose from the procedure has raised severe public concern. Therefore, it is necessary to calculate this parameter to point to relative radiation risk. This study aimed to assess child exposure during diagnostic and estimate the radiation risk. A total of 10 child patients was calculated of radiation risk dose for whole years. The patient's exposure was measured using CT dose descriptors. The patients' doses per contrast-enhanced CT (CECT) procedures were CTDIvol (mGy) and DLP (mGy.cm)  $5.01 \pm 1.26$  (2.63-6.36) and  $218.13 \pm 50.86$  (118.8-265.3) for the Chest with contrast, respectively. After each study, the participating physicians obtained the parameters relevant to the radiation dose from the scan protocol generated by the CT system. Shielding of the radiosensitive organs (eye lens and thyroid) is necessary to reduce the radiation risk. In addition, optimizing the CT acquisition parameter is crucial to maximizing the benefit while reducing the risk of the procedure.



**ISRP 2021**  
**International Symposium on Radiation Physics**  
**Kuala Lumpur – Malaysia**  
**6 – 10 December 2021**

**A165 - Study of digital filters to 3D position-sensitive pixelated CdZnTe detector**

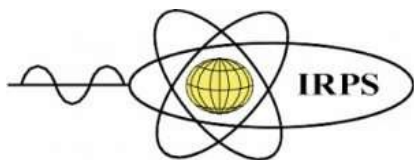
B.J.Kim<sup>1</sup>, K.B.Lee<sup>1,2</sup>, J.M.Lee<sup>1,2</sup>, S.H.Hwang<sup>1</sup>, D.H.Heo<sup>1</sup>

<sup>1</sup>Ionizing Radiation Center, Korea Research Institute of Standards and Science (KRISS), Daejeon, Rep. of Korea

<sup>2</sup>University of Science & Technology (UST), Daejeon, Rep. of Korea

Corresponding author: byungju@kriss.re.kr

Several research related to Cadmium Zinc Telluride (CZT) semiconductor detector have been recently conducted in the field of medical imaging and gamma-ray imaging. This is due to their capability of image reconstruction determining where the radiation source is. The easiest way to enhance the spatial resolution is by reduction of the electrode pitch, but this lead to higher cost owing to a large number of readout electronics. A good compromise is to use optimal digital filters to increase two dimensions of position sensitivity based on transient signal analysis, and, third dimension coming from signal ratio of the planar cathode to the pixelated anode or from the electron drift time for each pixel. In other words, sub-pixel spatial resolution can be obtained by the ratio between the neighboring pixel signals and the center pixel signal. The electron drift time is used to determine the interaction depth. The movement of the electrons in faraway from the anode have no effect on the anode signal because of the small pixel effect. Using two triggers on the cathode signal generated when the electron clouds start to move and anode signal generated when the electron clouds reach the anode vicinity, respectively, the electron drift time can be determined. In this work, we studied the performance several digital filters for energy determination and timing determination, respectively. The advantage of using digital filters is many filters with various parameter can be tested. For energy, the optimal filter, the trapezoidal filter, that can provide the best signal-to-noise ratio was chosen.



**ISRP 2021**  
**International Symposium on Radiation Physics**  
**Kuala Lumpur – Malaysia**  
**6 – 10 December 2021**

**A167 - Patients radiation dose reduction during contrast enhanced computed tomography urography examination**

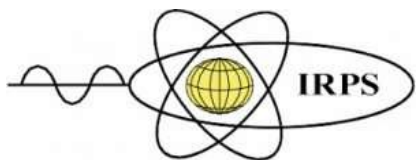
M Alkhorayef\*<sup>1</sup>, Loyal Jambi<sup>1</sup>, Mohammed Almuwanis<sup>1</sup>, Abdelmoneim Sulieman<sup>2</sup>, N.

<sup>1</sup>Department of Radiological Sciences, College of Applied Medical Sciences, King Saud University, P.O Box 10219 Riyadh 11433, Saudi Arabia

<sup>1</sup>Prince Sattam Bin Abdulaziz University, College of Applied Medical Sciences, Radiology and Medical Imaging Department, P.O.Box 422, Alkharj 11942, Saudi Arabia

\*Corresponding author: E mail: malkhorayef@ksu.edu.sa

The computed tomography urography (CTU) procedure is widely used to assess urinary system disorders. It was estimated that the prevalence of the renal disease is 13% on average globally. Patients frequently underwent repeatedly CTU procedures for follow-ups, thus receiving a higher radiation dose. Therefore, dose measurement and reduction are welcomed to prevent patients from unnecessary radiation risk. One hundred fifty-three patients underwent CTU examination at six radiological departments equipped with CT modalities from different vendors. The Scheffe test was used to analyze variable differences. Patient age ranges were 19- to 70 years. The patient's radiation dose in terms of dose length product (DLP) and volume CT dose index (CTDI<sub>vol</sub>) were quantified. The mean and range of patients' dose per CTU procedure were 3098 (647-5301) and 44.11(15-136) in terms of DLP (mGy.cm) and (CTDI<sub>vol</sub> (mGy)), respectively. There are statistically significant differences at the level of significance (0.05) or less in the variables (tube current-time product (mAs), DLP, and CTDI) attributable to hospitals. There are no statistically significant differences at the level of significance (0.05) or less in the variables (age, tube current-time product (mAs), and CTDI<sub>vol</sub>) attributable to gender. DRLs are proposed based on the third quartile of the median value, and radiogenic risk was quantified to be approximately 1 per 400 CTU procedures. Further reduction is recommended to ensure that the benefit from the CTU examination is maximized.



**A169 - Estimation of Breast radiation dose and radiogenic risk during PET/CT imaging procedures**

Huda Al-Mohammed \*<sup>1</sup>, A Sulieman<sup>2</sup>, Suha Eltahir<sup>3</sup>, M. Alkhorayef<sup>4,5</sup>, and D.A.Bradley<sup>5,6</sup>

<sup>1</sup>Department of Physics, College of Science, Imam Mohammed bin Saud Islamic University, Riyadh, Saudi Arabia

<sup>2</sup>Prince Sattam Bin Abdulaziz University, College of Applied Medical Sciences, Radiology and Medical Imaging Department, Alkharj, Saudi Arabia

<sup>3</sup>Radiation safety institute, Sudan Atomic Energy Commission, Khartoum, Sudan

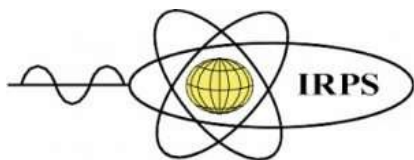
<sup>4</sup>Department of Radiological Sciences, College of Applied Medical Sciences, King Saud University, Riyadh, Saudi Arabia

<sup>5</sup>Centre for Nuclear and Radiation Physics, Department of Physics, University of Surrey, Guildford, Surrey GU2 7XH, United Kingdom

<sup>6</sup>Centre for Applied Physics and Radiation Technologies, School of Engineering and Technology, Sunway University, 47500, Bandar Sunway, Selangor, Malaysia.

Corresponding author: hialmohammad@pnu.edu.sa

Breast malignancy incidence increases worldwide due to numerous factors, including exposure to carcinogenic agents (radiation or chemicals). Breasts are radiosensitive organs and contribute 12% of whole-body sensitivity to ionizing radiation. It was estimated that breast cancer incidence in Saudi Arabia is 28% of all cancers in Saudi Arabia (22.4 per 100,000 women). With the increasing frequency of medical imaging procedures, female breasts receive high doses during diagnostic imaging procedures, although the breast is not the organ of interest. Therefore, assessment of breast cancer risk is recommended to increase practitioners' awareness and develop dose optimization. This study intended to evaluate breast doses and imaging protocol during PET/CT imaging procedures. Breast dose and effective dose per procedure were estimated using the administered activity (<sup>18</sup>F-FDG), and radiation dose resulted from CT exposures (GE PET/CT VCT). The mean and range of patients' age (years) and body mass index ((BMI), kg/m<sup>2</sup>) were 41.1±14.2 (18.0-71) and 24.3±6.9 (15.0-35.6), respectively. The mean and range of administered activity (MBq) and effective dose (mSv) were 451.9±80 (345.0-561.9) and 9.1±1.7 (6.6-11.1) in that order. The average breast equivalent dose (mGy) per PET/CT brain, chest, and abdomen procedures were 7.2±4, 32.2±11.0, and 12.6±6, respectively. The cancer risk is one cancer incidence per 500 per PET/CT procedure. The highest equivalent dose is during CT chest procedure because the breasts are within the primary X-ray beam. CT contributed up to 70% of the effective doses. Thus CT dose optimization will reduce the breast dose and radiation risk. In addition to that, proper shielding is also effective in breast dose reduction. During PET/CT imaging, the breast equivalent dose is up to 15 folds of the breast dose during the mammographic planar imaging procedure. Because young females have a higher risk, proper justification criteria and dose optimization are crucial to reducing over-exposure while maintaining image quality.



**ISRP 2021**  
**International Symposium on Radiation Physics**  
**Kuala Lumpur – Malaysia**  
**6 – 10 December 2021**

**A170 - Estimation of Effective dose and radiogenic risk during certain computed tomography examinations**

K.S. Al-Mugren\*<sup>1</sup>, N.Tamam<sup>1</sup>, A. Sulieman<sup>2</sup>, Omer Mahjoub<sup>3</sup>, Alkhorayef<sup>4,5</sup> Mayeen Uddin Khandaker<sup>6</sup>, David A. Bradley<sup>5,6</sup>

<sup>1</sup>Physics Department, College of Sciences, Princess Nourah Bint Abdulrahman University, P.O Box 84428, Riyadh 11671, Saudi Arabia

<sup>2</sup>Prince Sattam Bin Abdulaziz University, College of Applied Medical Sciences, Radiology and Medical Imaging Department, P.O.Box 422, Alkharj 11942, Saudi Arabia

<sup>3</sup>College of Medical Radiologic Science, Sudan University of Science and Technology, P.O.Box 1908, Khartoum 11111, Sudan

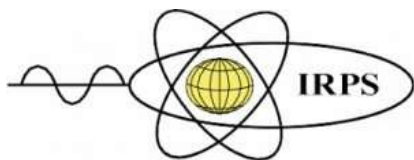
<sup>4</sup>Department of Radiological Sciences, College of Applied Medical Sciences, King Saud University, P.O Box 10219 Riyadh 11433, Saudi Arabia

<sup>5</sup>Centre for Nuclear and Radiation Physics, Department of Physics, University of Surrey, Guildford, Surrey GU2 7XH, UK

<sup>6</sup>Centre for Applied Physics and Radiation Technologies, School of Engineering and Technology, Sunway University, 47500, Bandar Sunway, Selangor, Malaysia.

Corresponding author: E mail: ksalmogren@pnu.edu.sa

Medical exposure is the largest source of artificial radiation to the general population. Computed tomography (CT) has tremendous benefits to human health. However, there is increasing concern regarding the risk of this radiation exposure. This study aims to quantify the patient dose in CT examination for brain, chest, and abdomen and estimate the effective patient dose and radiogenic risk resulting from these imaging procedures. The radiation dose was measured in five radiology departments equipped with different CT modalities from other vendors. In this study, the mean effective dose for hospital A was  $4.3 \pm 1.7$  mSv,  $20.5 \pm 6.6$  mSv, and  $62.3 \pm 32.5$  mSv for the brain, chest, and abdomen. The mean effective dose for hospital B was  $3.8 \pm 1.4$  mSv,  $28.1 \pm 36.5$  mSv, and  $46.2 \pm 34.2$  mSv for brain, chest, and abdomen, respectively. The mean effective doses for hospital C were  $2.7 \pm 1.4$  mSv,  $8.5 \pm 3.4$  mSv, and  $18.2 \pm 13.1$  mSv for the brain, chest, and abdomen. The mean effective dose for hospital C was  $3.2 \pm 1.6$  mSv,  $12.5 \pm 9.7$  mSv,  $36.9 \pm 20.6$  mSv for brain, chest, and abdomen in that order. The mean effective dose for hospital E was  $1.6 \pm 0.9$  mSv,  $3.2 \pm 1.8$  mSv, and  $8.7 \pm 5.7$  mSv for brain, chest, and abdomen, respectively. The radiation risk for cancer induction may reach  $3 \times 10^{-3}$ . Two departments equipped with 64 CT slices expose patients to higher doses than departments equipped with 16 CT slices. The radiation dose from these procedures is higher compared to previous international studies. A local diagnostic reference level was proposed, and actions were taken to ensure optimum radiation exposure.



**A171 - Patients' tissues and organs radiation equivalent doses in interventional orthopedic procedures**

Israa Abdullatif\*<sup>1</sup>, Abdelmoneim Sulieman<sup>2\*</sup>, N. Tamam<sup>3</sup>, Ali Abdelrazig<sup>4</sup>, Abdulrahman Elnour<sup>5</sup>, David Bradley<sup>6,7</sup>

<sup>1</sup>College of Medical Radiologic Science, Sudan University of Science and Technology, Khartoum, Sudan

<sup>2</sup>Prince Sattam bin Abdulaziz University, College of Applied Medical Sciences, Radiology and Medical Imaging Department, Alkharj, Saudi Arabia

<sup>3</sup>Physics Department, College of Sciences, Princess Nourah Bint Abdulrahman University, P.O Box 84428, Riyadh 11671, Saudi Arabia

<sup>4</sup>Radiology Department, University of Jazan, Jazan, Saudi Arabia.

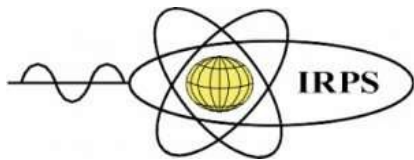
<sup>5</sup>Radiology Department, College of Radiological Sciences and Nuclear Medicine, National Ribat University, Khartoum, Sudan,

<sup>6</sup>Centre for Nuclear and Radiation Physics, Department of Physics, University of Surrey, Guildford, Surrey GU2 7XH, UK

<sup>7</sup>Centre for Applied Physics and Radiation Technologies, School of Engineering and Technology, Sunway University, 47500, Bandar Sunway, Selangor, Malaysia.

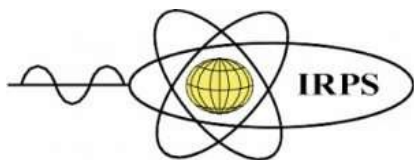
Corresponding author: E mail: [esra.abdallatif@uofg.edu.sd](mailto:esra.abdallatif@uofg.edu.sd)

Fluoroscopic guided intraoperative orthopedic surgery procedures are expanding rapidly due to their numerous advantages. Patients are exposed to repetitive ionizing radiation during the interventional and follow-up. The objective of this study is to evaluate the patients' radiation doses at four orthopedic departments. A total of 57 procedures (20 (35.1%) Female and 37 (64.9%) males) were evaluated at three orthopedic departments. The procedures include Kirschner wires, Dynamic hip screw (DHS), vertebral column, and lower extremities (knee, leg, and foot). Three C-arms fluoroscopic X-ray machines from different manufacturers were used equipped with kerma area product meter (KAP). The machines are equipped with a high-frequency generator and last image hold capability. Effective doses were estimated using computer software based on Monte Carlo simulation from the National Radiological Protection Board (NRPB SR262). The mean patient age was  $45 \pm 19$  (18.0-75.0) years. The mean and range of patient weight (kg) were  $75.2 \pm 14$  (48.0-110.0). The overall exposure parameters were  $59.1 \pm 13$  (42.0-82.0),  $2.0 \pm 0.5$  (1.5-2.7) and  $0.5 \pm 0.8$  (0.3-2.8) for the tube voltage (kVp) and tube current-time product (mAs) and fluoroscopic time (m), respectively. The mean and range of patient dose per procedure were 640 (40- 7580) mGy.cm<sup>2</sup>. The effective dose (mSv) 's overall mean and range ranged from 80 (0.01 to 122.0) per procedure. Patients' radiation dose per procedure showed wide variation up to 100 times due to variation in the clinical indication



**ISRP 2021**  
**International Symposium on Radiation Physics**  
**Kuala Lumpur – Malaysia**  
**6 – 10 December 2021**

and examined organ. Variation of patient doses among different departments attributed to the variation in the x-ray machines settings. The probability of future cancer induction has no threshold and is dose-dependent. Therefore, dose reduction is recommended for high dose procedures such as the DHS through proper equipment setting and establishment dose reference level (DRL).



**A172 - Prompt Gamma Spectroscopy of Metallic Implants in Proton Therapy: A Phantom Study**

Chun-Yu Liu<sup>1,2</sup>, Chung-Hao Su<sup>3</sup>, Chien-Yu Lin<sup>4</sup>, Chung-Chi Lee<sup>1</sup>, Tsi-Chian Chao<sup>1,2</sup>, Hsin-Hon Lin<sup>1,2</sup>

<sup>1</sup>Department of Medical Imaging and Radiological Sciences, Chang Gung University, Taiwan

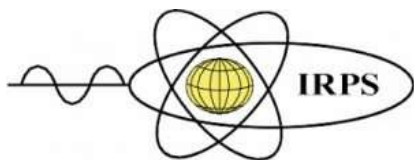
<sup>2</sup> Institute for Radiological Research, Chang Gung University, Taiwan

<sup>3</sup> Department of Oncology, National Taiwan University Hospital, Taiwan

<sup>4</sup> Department of Radiation Oncology, Chang Gung Memorial Hospital, Taiwan

Corresponding author: hh.lin@mx.nthu.edu.tw

The aim of this study is to explore whether the prompt gamma (PG) generated by metallic materials can be used as a surrogate signal for proton range verification so that it can be applied to proton therapy for accurate range verification. In the study, Monte Carlo simulation was first conducted to investigate the feasibility of the concept using the GATE/GEANT4 software. Three candidates of metallic materials including titanium, silver, and gold were selected and placed inside a water phantom with the irradiation of different energy proton beams. Two types of detectors (ideal detector and realistic detector) were simulated for detecting the PG signals in order to explore the most suitable PG energy peaks of different metals, and the relationship of PG yields and the relative metal position under different proton energies. Further, real measurements of the PG inside an HDPE phantom were performed with the irradiation of a 110-MeV proton beam. The measured results were then compared to the simulated spectra. Simulation results show that most metal-produced PGs belong to a low energy range and relatively readily to be detected by the modern detector. Regarding the ideal detector, the standard deviation (SD) of the range shifts from the three metals is within  $\pm 0.5$  mm. Regarding the realistic detector, the SDs were all below 1.0 mm for the low-energy proton, while the maximum SD would achieve  $\pm 8.4$  mm in titanium,  $\pm 0.89$  mm in silver, and  $\pm 2.09$  mm in gold when high-energy protons were employed. In the real PG measurement experiments, the energy peaks of titanium and silver can be effectively detected and identified. In conclusion, our study has indicated that the metal-produced PGs are detectable and have the potential for proton range verification.



**ISRP 2021**  
**International Symposium on Radiation Physics**  
**Kuala Lumpur – Malaysia**  
**6 – 10 December 2021**

**A174 - Dosimetric evaluation of an epitaxial silicon diode as an online dosimeter for orthovoltage photon beam radiotherapy**

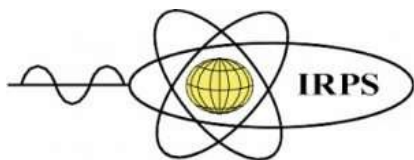
C. C. Bueno<sup>1</sup>, J. A. C. Gonçalves<sup>1</sup>, A. Mangiarotti<sup>2</sup>

<sup>1</sup>Instituto de Pesquisas Energéticas e Nucleares, São Paulo, Brazil

<sup>2</sup>Instituto de Física - Universidade de São Paulo, São Paulo, Brazil

Corresponding author: ccbueno@ipen.br

The response of a dosimetry system based on an epitaxial silicon diode as an online dosimeter for orthovoltage photon beam radiotherapy has been investigated in this work. To be used as a dosimeter, each diode is housed in a light-tight probe, and its readout electrode is directly connected to the Keithley 6517B electrometer. All current measurements are carried out in short-circuit mode with the diode unbiased and its backplane grounded. The data acquired by the electrometer are directly sent to a personal computer via a GBIP interface controlled by software developed in LabView to analyze the current signals. A Pantak/Seifert X-ray tube is used to irradiate the diode, placed 50.0 cm away in a radiation field of 8 cm, with 10, 25, 30, and 50 kV photons. The dose rate response is investigated for the 50 kV beam by varying the current tube from 2 to 20 mA. As expected, the induced current is linearly dependent on the dose rate within the range of 0.8 and 8.05 mGy/s. The current signals are quite stable, with a repeatability parameter of less than 0.2%. The dose-responses assessed offline by integrating the current signals are linear between 0.5 and 3.0 Gy despite being slightly dependent on the photon energy. However, in this dose range, no dose rate dependence is observed. These results are theoretically supported by dose and dose rate calculations performed assuming the diode is thin compared with the standard values of the minority carrier diffusion lengths in the epitaxial layer. Good agreement is found between calculations and experimental data. Investigations of possible radiation damage produced in the diode through dynamic measurements of dark current and capacitance as a function of the accumulated dose are currently in progress.



**A176 - Dose rate mapping in an industrial  $^{60}\text{Co}$  irradiator using an online photodiode-based dosimetry system**

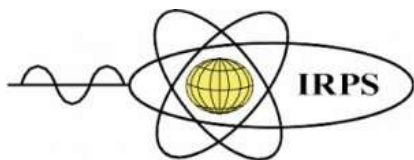
J. A. C. Gonçalves<sup>1</sup>, A. Mangiarotti<sup>2</sup>, C. C. Bueno<sup>1</sup>

<sup>1</sup>Instituto de Pesquisas Energéticas e Nucleares, São Paulo, Brazil

<sup>2</sup>Instituto de Física - Universidade de São Paulo, São Paulo, Brazil

Corresponding author: josemary@ipen.br

In the radiation processing field, any irradiation process is designed to irradiate products uniformly, but in practice, a reasonable variation in the absorbed dose through the product is accepted. However, the irradiation of inhomogeneous or irregularly shaped products gives rise to complex dose variations only assessed through dose mapping. It requires complementary dosimeters bearing good spatial resolution, prompt and easy readout, and cost-effectiveness. These features are found in silicon diodes that, despite all these advantages, are prone to radiation damage. This damage is mitigated with photodiodes whose thicknesses are much smaller than the minority carrier diffusion length at the anticipated accumulated dose. In this work, an in-house dosimetry system based on a thin photodiode is applied for online mapping dose rates, between 3.7 and 52.8 Gy/h, delivered by a Panoramic  $^{60}\text{Co}$  industrial facility. The operational principle of these dosimeters relies on the real-time acquisition of the induced currents from the irradiated diode operating in the short-circuit mode without externally applied voltage. Under this condition, the dose is assessed offline via the integration of these current signals. The radial mapping of the radiation field is performed by rotating the diode around the central axis of the panoramic irradiator, covering 360° at intervals of 10°. For comparative purposes, alanine dosimeters are also irradiated together with the diode. The experimental results are benchmarked with Monte Carlo simulations of the dose rate curves. Good agreement between the simulated values and the readings of both dosimeters is found. It reveals that the photodiode-dosimetry system is a reliable alternative to map dose rate fields and the effectiveness of Monte Carlo simulations as a predictive tool for dose rate measurements in an irradiator.



**A177 - Model to Estimate of cumulative dose in real-time**

Jose Carlos Lourenco<sup>1</sup>, Hugo Reuters<sup>2</sup>, Sergei Paschuk<sup>3</sup>, Edney Milhoreto<sup>3</sup>

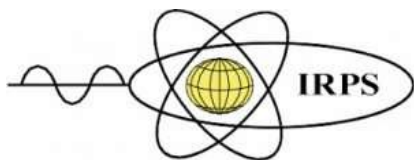
<sup>1</sup>Statistical Department, Londrina State University, Brazil

<sup>2</sup>Physics Department, Pele Pequeno Principe Research Institute, Brazil

<sup>3</sup>Physics Department, Federal University of Technology, Brazil

Corresponding author: jcl@uel.br

In interventionist procedures that use fluoroscopy, medical staff is exposed to ionizing radiation, often with doses exceeding the recommended limits. These doses are only observed at the end of the procedure, or after one month utilizing individual dosimeters. The objective of the present study was to develop a model to estimate doses of ionizing radiation in real-time. The performance of the remote-controlled fluoroscopy system in scattered radiation measurements was tested at 50 kV and 30 mA with a Ludlum 9DP ionization chamber and a PMMA phantom. Dose rates were collected by the ionization chamber for the gonad regions at 90 cm, for the hands at 109, for the chest at 128 and the lens of the eyes at 166 cm with the ground level about the beam distances main at 19, 38, 76 and 152 cm, around the 45 to 45-degree fluoroscopy table. The collected data were sent to the developed software to determine the estimated doses. We evaluated the estimate of the equivalent dose in a scattered object during an average time of exposure to scattered radiation in 20 minutes, we find, respectively, the following estimates in the scattered dimension object 30x30x15 cm: for the gonad region at 539, 159, 76, 42, and 22  $\mu\text{Sv}$ ; for hands at 858, 392, 172, 74 and 22  $\mu\text{Sv}$ ; for the chest at 539, 282, 152, 98 and 22  $\mu\text{Sv}$ ; and the lens of the eyes 221, 159, 110, 78 and 22  $\mu\text{Sv}$ , which correspond to the X-ray beam distances in 19, 38, 57, 76 and 152 cm respectively around the fluoroscopy table. The estimated dose in real-time helps the interventionist physician optimize their exposure to scattered radiation during the intervention procedure, allowing them to enhance personal protection and reduce the occupational dose.



**A178 - Cyclotron-based p(27)+Be neutron source for activation experiments**

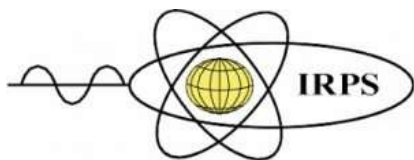
Milan Stefanik<sup>1,2</sup>, Eva Simeckova<sup>1</sup>, Jan Stursa<sup>1</sup>, Jaromir Mrazek<sup>1</sup>

<sup>1</sup>Nuclear Physics Institute of The Czech Academy of Sciences, Rez 130, Rez, 250 68, Czech Republic

<sup>2</sup>Czech Technical University in Prague, FNSPE, Brehova 7, Prague, 115 19, Czech Republic

Corresponding author: milan.stefanik@fjfi.cvut.cz

Nuclear Physics Institute (NPI) of The Czech Academy of Sciences (CAS) operates the accelerator-driven fast neutron sources of white and quasi-monoenergetic spectra using the charged particle beams (protons or deuterons) delivered by the isochronous cyclotron U-120M. In standard operation, proton induced reactions on thick beryllium or thin lithium targets are used for neutron field production within the fusion related research applications (e.g. cross-sections measurement and validation for IFMIF-DONES research program). Recently, the p + Be source reaction was investigated for 27 MeV proton beam and thick beryllium target at the NPI CAS in Rez near Prague, and new intensive neutron field of white spectrum up to 25 MeV was successfully developed. For neutron field determination of the p(27)+Be source reaction in close source-to-sample distances, the multi-foil activation technique was utilized. Sets of ten activation materials (Au, Co, Lu, Ti, In, Al, Y, Fe, Ni, Nb) were irradiated by neutrons from the p(27)+Be source, and activated dosimetry foils were analyzed by means of the nuclear gamma-ray spectrometry method (HPGe detector). From measured reaction rates, white neutron spectrum was reconstructed utilizing the modified version of SAND-II unfolding code. The study of Be(p,xn) source reaction with 27 MeV proton beam provided new spectral data for energy range that is characterized by a lack of empirical data (above 20 MeV). Obtained fast neutron field (with intensity of  $10^{10} \text{ cm}^{-2}\text{s}^{-1}$  at close source-to-sample position) extends the utilization of cyclotron-based fast neutron sources at the NPI and provides new experimental opportunities for future intensive irradiation experiments such as nuclear data validation, fast neutron activation analysis, radiation hardness tests of electronics and materials for nuclear energetics and aerospace industry.



**ISRP 2021**  
**International Symposium on Radiation Physics**  
**Kuala Lumpur – Malaysia**  
**6 – 10 December 2021**

**A180 - Assessment of the effective radiation dose and cancer induction probability in urographic imaging procedures**

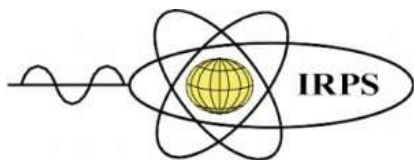
Loyal Jambi\*<sup>1</sup>, Mohammed Alkhorayef<sup>1</sup>, Mohammed Almuwanis<sup>1</sup>, Abdelmoneim Sulieman<sup>2</sup>

<sup>1</sup>Department of Radiological Sciences, College of Applied Medical Sciences, King Saud University, P.O Box 10219 Riyadh 11433, Saudi Arabia

<sup>2</sup>Prince Sattam Bin Abdulaziz University, College of Applied Medical Sciences, Radiology and Medical Imaging Department, P.O.Box 422, Alkharj 11942, Saudi Arabia

Corresponding author: E mail: [\\_ljambi@ksu.edu.sa](mailto:_ljambi@ksu.edu.sa)

Imaging procedures of the renal system (Intravenous Urography (IVU) and computed tomography urography (CTU)) are used frequently to evaluate the urinary system pathology. This study aimed to measure the radiation dose and estimate the risks resulting from exposure to X-rays during IVU and CTU procedures. A total of 82 patients were evaluated in three hospitals in five hospitals. The average age of the samples was  $39 \pm 14$  years, and the average height weight and body mass index (BMI) was  $1.7 \pm 0.1$ ,  $69 \pm 10$ , and  $24.3 \pm 4.1$  in that order. The mean of exposure factors kVp, mAs were  $74.04 \pm 3.1$  and  $33.64 \pm 4$ , respectively, and the average number of films per procedure was  $5.72 \pm 1.49$ . The mean ESAK was  $2.1 \pm 0.64$  mGy, and the mean effective dose was  $0.131 \pm 0.04$  mSv. The mean effective radiation dose per CTU procedure is  $61.0 \pm 33$  mSv. The overall cancer risk for IVU procedures was 5.85 per million procedures. The mean ESAK (mGy) and effective doses for the IVU procedure are comparable with previous studies. The effective dose from CTU and cancer risk is higher up to ten times compared to IVU procedures. The effective dose from the CTU procedure is higher compared to the previously published studies. More effort is recommended to reduce the patient dose to the published diagnostic reference level while maintaining the diagnostic findings and image quality.



**ISRP 2021**  
**International Symposium on Radiation Physics**  
**Kuala Lumpur – Malaysia**  
**6 – 10 December 2021**

**A183 - Evaluation of doses in dental radiographic units using 3d printed pediatric phantom**

Ladyjane Assemany<sup>1</sup>, Fernanda Pelegrini<sup>2</sup>, Erica Policarpo<sup>3</sup>, Kellen Daros<sup>4</sup>, Thiago Hirata<sup>5</sup>, Bruna Grechi<sup>6</sup>, Orlando Jr<sup>7</sup>, Maria da Penha Potiens<sup>8</sup>

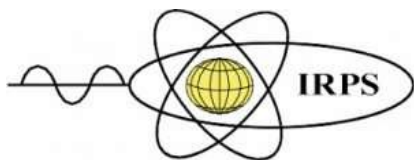
<sup>1,7,8</sup>Instituto de Pesquisas Energéticas e Nucleares, IPEN – CNEN/SP. Av. Prof. Lineu Prestes, 2242, Cidade Universitária – 05508-000. São Paulo – SP – Brasil

<sup>2,3,4</sup>Universidade Federal de São Paulo - Departamento de Diagnóstico por Imagem da Escola Paulista de Medicina da UNIFESP, Rua Napoleão de Barros, 800 - Vila Clementino - CEP 04024-002 - São Paulo – SP - Brasil.

<sup>4,5</sup>Rad Dimenstein - Rua Cardeal Arcoverde, 1749, Cj.57b, Blc2, Pinheiros – CEP 05407-002 São Paulo – SP – Brasil

Corresponding author: ladyjane.fontes@usp.br

In the healthcare field, additive manufacturing or 3D printing made it possible to reproduce anatomical parts for various applications, such as prostheses and anthropomorphic simulators. The possibility of using this technology as an alternative for making simulators for application in the area of ionizing radiation dosimetry attracted the scientific community's interest, mainly due to the low production cost, compared to the cost of anthropomorphic simulators available on the market. The great challenge is to establish the equivalence of available materials with human tissues and validate these simulators for clinical use. The study's objective was to evaluate the doses in dental radiology units using a 3D printed pediatric phantom and compare the values with literature data. Series of dose rate readings were taken in pediatric protocols predefined in the equipment, using a calibrated set of pencil-type ionization chamber and electrometer for the qualities of RQT radiation. The results found were satisfactory and showed slight variation to the dose values provided by the equipment. In addition, it was possible to compare doses in exams for the different modalities: CBCT and Panoramic/Cephalometric (Pano/Ceph). The variation between the doses was about 44%. This variation, according to the literature, can be up to 118%.



**ISRP 2021**  
**International Symposium on Radiation Physics**  
**Kuala Lumpur – Malaysia**  
**6 – 10 December 2021**

#### **A184 - Staff occupational exposure in the south region, Saudi Arabia**

Maher Alqurashi<sup>1</sup>, Ali Aamry\*<sup>2</sup>, Hussin Aamri<sup>3</sup>, Yehia H. Johary<sup>4</sup>, N. Tamam<sup>5</sup>, Abdelmoneim Sulieman<sup>6</sup>, David Bradley<sup>7,8</sup>

<sup>1</sup>Radiology Department, Ministry of Health, Riyadh, Saudi Arabia

<sup>2</sup>Nuclear Medicine Department, King Saud Medical City, Riyadh, Saudi Arabia

<sup>3</sup>Medical Physics Department, King Saud University Medical City (KSUMC), Riyadh, Saudi Arabia

<sup>4</sup>Medical Physics Department, General Directorate of Health Affairs in Aseer Region, Abha, Saudi Arabia

<sup>5</sup>Department of Physics, College of Sciences, Princess Nourah Bint Abdulrahman University, P.O Box 84428, Riyadh, 11671, Saudi Arabia

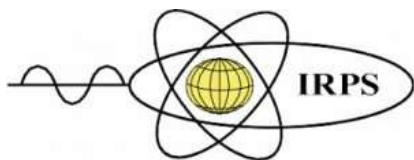
<sup>6</sup>Radiology and Medical Imaging Department, College of Applied Medical Sciences, Prince Sattam Bin Abdulaziz University, P.O.Box 422, Alkharj, 11942, Saudi Arabia

<sup>7</sup>Centre for Nuclear and Radiation Physics, Department of Physics, University of Surrey, Guildford, Surrey GU2 7XH, UK

<sup>8</sup>Centre for Applied Physics and Radiation Technologies, School of Engineering and Technology, Sunway University, 47500, Bandar Sunway, Selangor, Malaysia.

Corresponding author: E mail: [\\_a.aamry@ksmc.med.sa](mailto:_a.aamry@ksmc.med.sa)

Medical personnel at the radiology department are occupationally exposed to ionizing radiation. Staff exposure is regulated by the international atomic energy agency (IAEA) guidelines and the international commission on radiological protection (ICRP) recommendations. Staff working at the radiology department should not be exposed to an equivalent dose higher than 20 mSv per year or 100 mSv in five years to reduce the probability of the cancer effect. This study aims to measure staff radiation dose at radiology departments, south region, Saudi Arabia. A total of 204 staff working at the radiology department were monitored for two consecutive years. Occupational exposures were monitored calibrated Thermoluminescent dosimeters (LiF:Mg: Ti (TLD-100)). Staff exposure was quantified in terms of deep doses (Hp(10)) were evaluated. The TLD signal was obtained using an automatic TLD reader (Harshaw 6600). The overall annual dose for staff was 2.86 (2.51-3.18). The study revealed that the annual radiation exposure in the eight radiology departments is below the annual dose limits. However, Patients doses could be reduced if proper radiation protection is followed.



**ISRP 2021**  
**International Symposium on Radiation Physics**  
**Kuala Lumpur – Malaysia**  
**6 – 10 December 2021**

**A186 - Natural radioactivity in Sediments from Nile River and its tributaries in Khartoum State, Sudan**

Mohamed Dahab<sup>1</sup>, Ahmed Alhag<sup>2</sup>, Ibrahim Suliman<sup>3,\*</sup>

<sup>1</sup>Planning department, General Administration of Civil Defence, P.O. Box 5440, Khartoum, Sudan

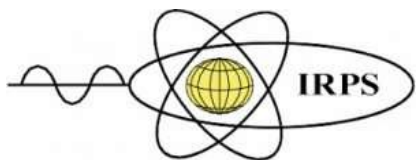
<sup>2</sup>Department, Institution, Country Nuclear Physics and Chemistry Institute, Atomic Energy Commission, P.O. Box 3001, Khartoum, Sudan

<sup>3</sup>Department of Physics, College of Science, Imam Mohammad Ibn Saud Islamic University (IMSIU), Riyadh 11642, Saudi Arabia

Corresponding author: iidris@imamu.edu.sa

Natural radioactivity is the most significant source of population exposure from ionising radiation. We determined the radioactivity concentration of natural radionuclides from thirty Sediments collected from the Nile River and its tributaries in Khartoum state, Sudan. Radioactivity measurements were performed using Na (TI) gamma-ray spectrometer. Energy and efficiency calibrations were performed using the International Atomic Energy Agency (IAEA) reference radionuclide mixture. Activity concentration of <sup>238</sup>U, <sup>232</sup>Th and <sup>40</sup>K were 21.29, 32.33 and 220.56 Bq.kg<sup>-1</sup>, respectively (in White Nile sediments); 21.59, 32.89 and 365.16 Bq.kg<sup>-1</sup>, respectively (in Blue Nile sediments); 18.93, 34.15 and 231.48 Bq.kg<sup>-1</sup>, respectively (in River Nile sediments). The mean outdoor absorbed doses rates were in the range were 38.63-45.18 nGyh<sup>-1</sup>, whereas the average effective doses were in the range 0.048-0.056 mSv.y<sup>-1</sup>. The annual gonadal dose equivalent (AGDE) values were found to be between 177.04 and 414.48 μGy.y<sup>-1</sup> with an average value of 286.16 μGy.y<sup>-1</sup>. These values obtained from the sediments were less than the recommended safe, and criterion limits UNSCEAR reports [1]. The study results showed an insignificant correlation between the radioactivity in the Nile River and its two tributaries.

1. United Nations Scientific Committee on the Effects of Atomic Radiation (UNSCEAR). Sources, Effects and Risks of Ionization Radiation; Report to The General Assembly, with Scientific Annexes B: Exposures from Natural Radiation Sources; UNSCEAR: New York, NY, USA, 2000.



**A187 - Survey on radon activity in the air of dwellings, water and soil of Carambeí rural region (Paraná State, Brazil)**

Sergei A. Paschuk<sup>1</sup>, Janine N. Corrêa<sup>1</sup>, Monique de Oliveira<sup>1</sup>, Silvia G. B. de Palma<sup>1</sup>, Aline Martin<sup>1</sup>, Amanda C. Malagi da Silva<sup>1</sup>, Hugo R. Schelin<sup>2</sup>, Francesco Antonelli<sup>3</sup>, Oderson Souza Filho<sup>4</sup>

<sup>1</sup>Physics Department, Federal University of Technology - Parana, UTFPR, Brazil

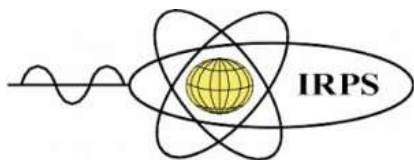
<sup>2</sup>Pelé Pequeno Príncipe Research Institute, Pequeno Príncipe Faculty, Brazil

<sup>3</sup>Department of Geology, Federal University of Parana, UFPR, Brazil

<sup>4</sup>CPRM -Geological Survey of Brazil, Curitiba, PR, Brazil

Corresponding author: spaschuk@gmail.com

Radon gas is recognized as an etiological agent of lung cancer, which is responsible for more than 50% of the exposure to natural radiation and is considered the second cause of lung cancer. Indoor human exposure to natural radiation is mainly due to inhalation of radon. The main objective of present research was focused on comparative measurements of <sup>222</sup>Rn indoor concentration in the region of Carambeí rural region, which was characterized by high rates of uranium, thorium and potassium in previous geological studies performed by the Federal University of Paraná (UFPR). Field recognition and subsequent measurements were performed using 40 detached houses in that rural area where the samples of artesian waters were collected with soil gas radon measurements, which were conducted using AlphaGUARD instant radon detector. Indoor radon measurements were performed using diffusion chambers with polycarbonate detectors (CR-39), which after the exposition period of 90 days were removed from dwellings and consequently submitted to chemical etching using 6.25 M NaOH solution plus 2% of ethyl alcohol at a temperature of 72° C for 14 hours. Obtained results show that indoor concentration levels of <sup>222</sup>Rn at Carambeí rural region ranged from 95+/-15 Bq/m<sup>3</sup> to 461+/-65 Bq/m<sup>3</sup>. In the case of detached houses with high (above 300 Bq/m<sup>3</sup>) radon activity levels, the mitigation measures were proposed to the proprietaries. Obtained results for initial radon concentrations in well waters ranged from 0.4+/-0.8 to 87+/-13 Bq/L as well as for radium activity the highest activity obtained was of 3.8+/-2.3 Bq/L, which is above the limit established by the Brazilian Ministry of Health. Such activity levels of alpha radioactivity shows that these artesian waters are improper for immediate for human consumption. Thus, the mitigation measures have been proposed to the population.



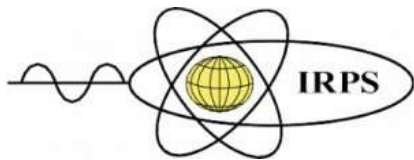
**A188 - Characterization of digital systems used in x-ray imaging**

Alessandra M. M. M. Perez<sup>1</sup>, Martin E. Poletti<sup>1</sup>

<sup>1</sup>Departamento de Física, Universidade de São Paulo, Brazil

Corresponding author: alessamm@usp.br

The physical characteristics of two clinical systems used in x-ray imaging have been investigated. Objective criteria such as signal transfer property (STP), modulation transfer function (MTF), noise power spectrum (NPS), noise equivalent quanta (NEQ) and detective quantum efficiency (DQE) were employed for this evaluation. The performance of computed radiography (CR) systems Carestream EHR-M3 and Carestream GP-2 (used in mammography and general radiography, respectively) was assessed by applying a method recommended in quality control protocols (IEC e EUREF). RQN-M and RQA-5 beam qualities were used, in the range of 1 to 1100  $\mu\text{Gy}$ . The dosimeters were RTI Piranha and PTW Unidos E with PTW Freiburg ionization chamber, respectively. CR systems showed a logarithmic response in the tested dose range ( $R^2 > 0.99$ ). The presampling MTF of the detector EHR-M3 was found to be 0.59, 0.23 and 0.15 at 2, 4 and 5  $\text{mm}^{-1}$ , respectively. For the detector GP-2, presampling MTF values for the same frequencies were 0.26, 0.08 and 0.06, respectively. Superior performance of EHR-M3 detector in terms of MTF was expected. NNPS increased as dose decreased for both detectors. NEQ relates acquisition dose level to the quality of the generated image and increased with dose. DQE increased with decreasing dose for both detectors. The findings show modest difference among data acquired in clinical conditions and those provided by the manufacturer. A quantitative technical characterization of digital systems was achieved for a variety of dose values, in the mammography and general radiography energy ranges.



**A191 - Evaluation of computed tomography imaging Protocol and pediatric doses to the sensitive organs**

Abdullah Almujaally\*<sup>1</sup>, Omer Serhan<sup>2</sup>, Khaled Alanazi<sup>2</sup>, Fares Alshalan<sup>2</sup>, Hesham Alshehy<sup>2</sup>, Abdullah Altowim<sup>2</sup>, N. Tamam<sup>3</sup>, Abdelmoneim Sulieman<sup>4</sup>, Mayeen Uddin Khandaker<sup>5</sup> David Bradley<sup>5,6</sup>

<sup>1</sup>King Faisal Specialist Hospital and Research Center, Riyadh, Saudi Arabia

<sup>2</sup>Radiology Department, King Khalid Hospital, Ministry of Health, Alkharj, Saudi Arabia

<sup>3</sup>Department of Physics, College of Sciences, Princess Nourah Bint Abdulrahman University, P.O Box 84428, Riyadh, 11671, Saudi Arabia

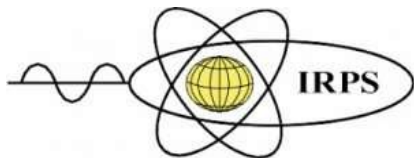
<sup>4</sup>Radiology and Medical Imaging Department, College of Applied Medical Sciences, Prince Sattam Bin Abdulaziz University, P.O.Box 422, Alkharj, 11942, Saudi Arabia

<sup>5</sup>Centre for Nuclear and Radiation Physics, Department of Physics, University of Surrey, Guildford, Surrey GU2 7XH, UK

<sup>6</sup>Centre for Applied Physics and Radiation Technologies, School of Engineering and Technology, Sunway University, 47500, Bandar Sunway, Selangor, Malaysia.

Corresponding author: E mail: [abdullah.almujaally@gmail.com](mailto:abdullah.almujaally@gmail.com)

Pediatric computed tomography (CT) procedures are frequently performed at the radiology department due to their ability to diagnose various clinical conditions. However, the price of accurate diagnosis is the increases the probability of cancer risk. However, the benefit of a justified CT examination outweighs by far the likelihood of malignancy. The objective of this study was to measure the patient dose and evaluate the imaging protocol according to the American College of Radiologists (ACR) guidelines. All pediatric patients underwent CT brain and abdomen procedures using a 128 slice CT machine installed at King Khalid Hospital and Prince Sultan Center for Health Services in Alkharj. A total of 33 patients were investigated (36.3% of the patients' undergone CT abdomen, and 72.7% undergone CT brain examination. The radiation dose parameters were presented in terms of CTDI<sub>vol</sub> (mGy) and DLP (mGy.cm). The effective and organ equivalent doses (mSv) were estimated using CTDOSE computer software based on Monte Carlo simulations. The mean CTDI<sub>vol</sub> (mGy) per procedure is 34mGy and 5.6 for CT brain and abdomen, respectively. The average DLP (mGy.cm) and effective dose (mSv) per procedure are 233 and 4.0, respectively. The main contributor to this high dose was using the adult protocol, which justifies the importance of using child CT protocol. Staff training on ACR imaging protocol is recommended to avoid unnecessary radiation risk of malignant tumors.



### **A203 - Proton radiography using Discrete Range Modulation method – A Monte Carlo study**

Yi-Chun Tsai<sup>1</sup>, Tsung-Lin Tsai<sup>2</sup>, Chung Chi Lee<sup>1,2,3</sup>, Chien-Yu Lin<sup>3</sup>, Tsi Chian Chao<sup>1,2,3</sup>,

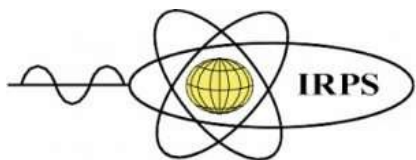
<sup>1</sup>Institute for Radiological Research, Chang Gung University/Chang Gung Memorial Hospital, Linkou, Taoyuan, Taiwan Department of Medical Imaging and Radiological Sciences, College of Medicine,

<sup>2</sup>Chang Gung University, Taoyuan, Taiwan

<sup>2</sup>Department of Radiation Oncology, Chang Gung Memorial Hospital, Kwei-Shan Taoyuan, Taiwan

Corresponding author: chaot@mail.cgu.edu.tw

The advantages of proton therapy are the Bragg peak, but its range uncertainties can also lead to a certain dose deviation. This deviation can sometimes lead to an even worse dose coverage than that of photon therapy. This problem can be solved by using proton radiography to determine water equivalent path length (WEPL). In this study, a Discrete Range Modulation (DRM) technique was used to generate proton radiography that benefits from the CGMH wobbling and layer stacking nozzle. The advantages of DRM over previously reported Continuous Range Modulation (CRM) technique are significant by quantitative assessing the image quality and range uncertainties. MCNPX 2.7.0 was used to simulate the depth dose distribution under a pencil beam geometry in a water phantom of 40 x 40 x 40 cm<sup>2</sup>. Energy selection system (ESS) were used to vary beam energies from 70 to 230 MeV at 2.5MeV/step. In DRM method, we used the parameter based on Bragg Peak characteristics, R<sub>80</sub>. The WEPL can be related to R<sub>80</sub> by using the relationship between the proton energy and energy deposition at 80% of the proximal fall off (E80) The E80 is quite independent with varying initial energy spread. For CRM method, a dose gradient plan was constructed to estimate relationship between WEPL and energy deposition. DRM and CRM were verified by different thickness of water phantoms, a step phantom and wedge phantoms. In DRM method, the difference of WEPL are < 2 mm, standard deviation in the images was found to be  $\sigma < 0.5$  mm. However, in CRM, difference of WEPL are >3mm,  $\sigma > 0.6$  mm. SNR of DRM is more than three times of CRM. Proton radiography obtained using DRM method is more accurate and precise than those using CRM method. DRM method also can solve mixed beam problem owing to multiple Coulomb scattering.



**ISRP 2021**  
**International Symposium on Radiation Physics**  
**Kuala Lumpur – Malaysia**  
**6 – 10 December 2021**

### **A209 - Accelerator selection for industry and medical applications**

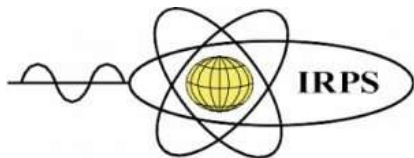
Leo Kwee Wah<sup>1</sup>, Siti A'iasah Hashim<sup>2</sup>

<sup>1</sup>Accelerator Development Center, Malaysian Nuclear Agency, Malaysia

<sup>2</sup>Director General Office, Malaysian Nuclear Agency, Malaysia

Corresponding author: leo@nm.gov.my

Accelerator is an advanced and promising technology that applies a variety of engineering techniques and science principles. Electromagnetic fields are used as static fields or AC field in the MHz to GHz range to accelerate the particles and deliver to the user for specific application. However, types of accelerator must be selected based on their applications which are basically determined by the accelerator parameters such as particle source and its energy. In this paper, we will concentrate accelerator selection criterion for industry and medical applications.



**A210 - Natural radioactivity analysis and radiological impact assessment of coal, bottom, and fly ash from a coal power plant**

Hassan Mohamed<sup>1</sup>, Nasuha Ahmad<sup>2</sup>, Anas Muhamad Pauzi<sup>3</sup>, Nashihah Ab Karim<sup>2</sup>, Mimi Nur Umaira Idham Wazir<sup>2</sup>, Mohd Idzat Idris<sup>2,\*</sup>

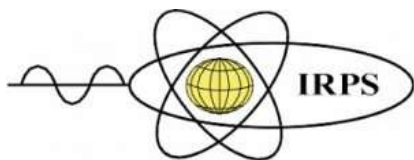
<sup>1</sup>Institute of Sustainable Energy, Universiti Tenaga Nasional, Malaysia

<sup>2</sup>Nuclear Technology Research Center, Faculty of Science and Engineering, Universiti Kebangsaan Malaysia, Malaysia

<sup>3</sup>College of Engineering, Universiti Tenaga Nasional, Malaysia

Corresponding author: idzat@ukm.edu.my

A coal-fired power plant produces by-products such as fly ash and bottom ash through coal combustion. Its by-products have significant amounts of radionuclides, including uranium, thorium, and potassium, that cause environmental contamination, leading to possible causes of health problems. This study aims to investigate the specific activity of naturally occurring radioactive materials (NORM) that stay in the coal, fly and bottom ashes at the coal-fired power plant and their radiological impacts. Coal, ashes, and soil were collected from a coal-fired power plant in Malaysia. The result indicates NORM's specific concentration, namely <sup>40</sup>K, <sup>232</sup>Th, <sup>238</sup>U, in each sample determined by gamma spectrometry. Radioactivity ranges in soil are between 22.7 to 150.7 Bq/kg, 20.7 to 153.6 Bq/kg, and 68.6 to 1594.4 Bq/kg for <sup>238</sup>U, <sup>232</sup>Th, and <sup>40</sup>K, respectively. In coal, fly ash, and bottom ash, they contain around 67.54 to 189.18 Bq/kg for <sup>238</sup>U, 50.2 to 134.57 Bq/kg for <sup>232</sup>Th, and between 327.54 to 1114.40 for <sup>40</sup>K. The radium equivalent activities ( $Ra_{eq}$ ) for coal, fly ash, and bottom ash are 164.55, 467.42, and 429.09 Bq/kg. Meanwhile, the absorbed dose rate in the air ranges from 76.04 to 217.44 nGy/h. Internal and external hazards range from 0.44 to 1.26 and 0.63 to 1.77, respectively. The annual gonadal dose equivalent (AGDE) value fluctuates between 521.28 to 1,496.99 with an average of 1,125.12  $\mu$ Sv. The excess lifetime cancer risk (ELCR) for indoor oscillates from  $1.30 \times 10^{-3}$  to  $3.75 \times 10^{-3}$  and for outdoor is between  $0.32 \times 10^{-3}$  to  $0.95 \times 10^{-3}$ . In conclusion, even though the other calculations exceed the global limit, the ECLR value is still under control and insignificant.



**ISRP 2021**  
**International Symposium on Radiation Physics**  
**Kuala Lumpur – Malaysia**  
**6 – 10 December 2021**

**A216 - Assessment of  $\gamma$ -radiation shielding behavior of some mixed nature clays**

Ahmed.M.El-khatib<sup>1</sup>, Mahmoud I. Abbas<sup>1</sup>, M.I. Sayyed<sup>2,3</sup>, Mayeen Uddin Khandaker<sup>4</sup>, Mohamed Abd-Elzaher<sup>5</sup>, Mona M Khalil<sup>1</sup>, Mohamed.Elsafi<sup>1</sup>, Mona M.Gouda<sup>1</sup>

<sup>1</sup>Physics Department, Faculty of Science, Alexandria University, 21511 Alexandria, Egypt.

<sup>2</sup>Department of Physics, Faculty of Science, Isra University, Amman 11622, Jordan

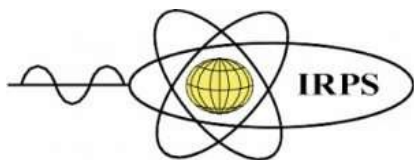
<sup>3</sup>Department of Nuclear Medicine Research, Institute for Research and Medical Consultations, Imam Abdulrahman bin Faisal University, Dammam 31441, Saudi Arabia

<sup>4</sup>Center for Applied Physics and Radiation Technologies, School of Engineering and Technology, Sunway University, 47500 Bandar Sunway, Selangor Darul Ehsan, Malaysia

<sup>5</sup>Department of Basic and Applied Sciences, Faculty of Engineering, Arab Academy for Science, Technology and Maritime Transport, Alexandria, Egypt.

Corresponding author: pro.monna2020@gmail.com

Attenuation parameters of the Clay samples Bentonite – red (BR), Bentonite – kaolin (BK), Bentonite – cement (BC), and Bentonite – ball (BB) was measured experimentally using sodium iodide scintillation detector NaI. The linear attenuation coefficient was calculated by obtaining area under each peak of the energy spectrum observed from Genie 2000 software in the presence and absence of the clay sample. The experimental results obtained were compared theoretically with XCOM software. The comparison was examined the validity of experimental results. The other dependent radiation shielding parameters on the LAC were estimated such as a half attenuator layer (HAL), mean free pass (MFP), Transmission factor (TF), and the photon protection efficiency (PPE). The mechanical properties of the samples were measured. Samples are also characterized by measuring Energy-dispersive X-ray (EDX), X-Ray diffraction (XRD) and Fourier transform infrared (FTIR).



**ISRP 2021**  
**International Symposium on Radiation Physics**  
**Kuala Lumpur – Malaysia**  
**6 – 10 December 2021**

**A217 - Full energy peak efficiency of a rectangular NaI (Tl) detector using standard non axial point sources**

Mohamed S. Badawi<sup>1</sup>, Mona M.Gouda<sup>2</sup>, Asmaa I. Shaaban <sup>2</sup>, Mahmoud I. Abbas<sup>2</sup>, M.I. Sayyed<sup>3,4</sup>, Mayeen Uddin Khandaker<sup>5</sup>, Salam Nouredine<sup>6</sup>, Ahmed.M.El-khatib<sup>2</sup>, Mohamed.Elsafi<sup>2</sup>

<sup>1</sup>Physics Department, Faculty of Science, Beirut Arab University, Beirut, Lebanon.

<sup>2</sup>Physics Department, Faculty of Science, Alexandria University, 21511 Alexandria, Egypt.

<sup>3</sup>Department of Physics, Faculty of Science, Isra University, Amman 11622, Jordan

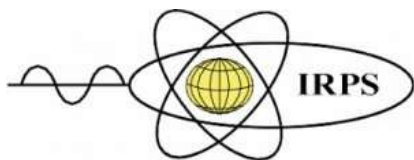
<sup>4</sup>Department of Nuclear Medicine Research, Institute for Research and Medical Consultations, Imam Abdulrahman bin Faisal University, Dammam 31441, Saudi Arabia.

<sup>5</sup>Center for Applied Physics and Radiation Technologies, School of Engineering and Technology, Sunway University, 47500 Bandar Sunway, Selangor Darul Ehsan, Malaysia.

<sup>6</sup>Physics Department, Faculty of Science, Lebanese University, Beirut, Lebanon.

Corresponding author: asmaaibrahim110@yahoo.com

Compared to standard cylindrical detectors, NaI (Tl) scintillation detectors with rectangular cross section provide a series of advantages like, are a cost-effective, easily stacked in arrays, only one PMT needed for a large crystal, increased efficiency according to large volume and excellent energy resolution similar to array of smaller detectors. In this work, the full energy peak efficiency of a rectangular NaI (Tl) detector using radioactive point sources placed at non – axial position was determined mathematically, experimentally and by Geant4. The mathematical calculations of efficiency depend on the energy transfer method and the effective solid angle. The attenuation of gamma rays through the NaI crystal or any material in between the crystal and the source are taken into consideration. The results show a good agreement between the three methods.



**ISRP 2021**  
**International Symposium on Radiation Physics**  
**Kuala Lumpur – Malaysia**  
**6 – 10 December 2021**

**A218 - The effect of FerroSilicon materials to enhance the radiation shielding ability of some clay**

Mohamed.Elsafi<sup>1</sup>, Ahmed.M.El-khatib<sup>1</sup>, Mahmoud I. Abbas<sup>1</sup>, Ahmed G. Shehata<sup>1</sup>, M.I. Sayyed<sup>2,3</sup>, Mayeen Uddin Khandaker<sup>4</sup>, Mona M.Gouda<sup>1</sup>

<sup>1</sup>Physics Department, Faculty of Science, Alexandria University, 21511 Alexandria, Egypt.

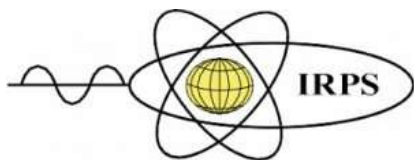
<sup>2</sup>Department of Physics, Faculty of Science, Isra University, Amman 11622, Jordan

<sup>3</sup>Department of Nuclear Medicine Research, Institute for Research and Medical Consultations, Imam Abdulrahman bin Faisal University, Dammam 31441, Saudi Arabia

<sup>4</sup>Center for Applied Physics and Radiation Technologies, School of Engineering and Technology, Sunway University, 47500 Bandar Sunway, Selangor Darul Ehsan, Malaysia

Corresponding author: ahmed\_shehata@alexu.edu.eg

In this work the attenuation properties of some clay (Bentonite, Kaolin and Ball clay) enhanced by some percentage of micro and nano size of both raw and waste ferrosilicon. The average size of micro ferrosilicon was  $100 \pm 20 \mu\text{m}$  while for nano ferrosilicon was  $40 \pm 5 \text{ nm}$ . The linear attenuation coefficient or LAC was experimentally calculated for the present samples by using a NaI scintillation detector and four radioactive point sources (Am-241, Cs-137, Co-60 and Eu-152). The results of experimental LAC for micro particle size were compared with XCOM results and a good agreement was noticed. The other radiation shielding parameters was determined such as the half value layer or HVL, mean free path or MFP and radiation protection efficiency or RPE. The results indicated that the effect of downsizing of ferrosilicon increase the attenuation ability for  $\gamma$ -ray.



**ISRP 2021**  
**International Symposium on Radiation Physics**  
**Kuala Lumpur – Malaysia**  
**6 – 10 December 2021**

**A220 - Estimation of Average Annual Committed Effective Dose Due to Intake of Medicinal Plants Collected from Chattogram, Bangladesh.**

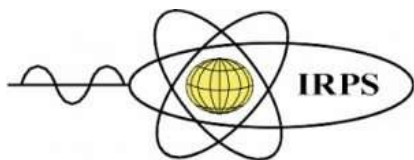
M. J. Hossen<sup>1</sup>, Md. Abu Haydar<sup>2</sup>, M. M. H. Miah<sup>1\*</sup>, Md. Idris Ali<sup>2</sup> and Debasish Paul<sup>2</sup>

<sup>1</sup>Department of Physics, University of Chittagong, Chattogram, Bangladesh

<sup>2</sup>Health Physics and Radioactive Waste Management Unit, Institute of Nuclear Science and Technology, Bangladesh Atomic Energy Commission, Savar, Dhaka.

Corresponding author: mhmiah\_85@yahoo.com

The natural as well as probable anthropogenic radioactivity in 21 medicinal plants collected from different areas of Chattogram district, Bangladesh were investigated by using a calibrated High Purity Germanium (HPGe) detector of relative efficiency of 20% and resolution of 2.0 KeV of FWHM for 1332KeV of <sup>60</sup>Co . This study showed that only naturally occurring radionuclides (e.g. <sup>226</sup>Ra, <sup>232</sup>Th and <sup>40</sup>K) were presented in the samples and no artificial radionuclides of <sup>137</sup>Cs have been identified in any of the analyzed samples. The activity concentrations of <sup>226</sup>Ra, <sup>232</sup>Th and <sup>40</sup>K were found to be ranged from  $13.87 \pm 1.03$  Bqkg<sup>-1</sup> to  $19.05 \pm 0.59$  Bqkg<sup>-1</sup>,  $4.5 \pm 0.78$  Bqkg<sup>-1</sup> to  $29.55 \pm 0.36$  Bqkg<sup>-1</sup>, and  $11.85 \pm 1.06$  Bqkg<sup>-1</sup> to  $241.68 \pm 1.06$  Bqkg<sup>-1</sup>, respectively with the corresponding average value of  $16.46 \pm 1.19$  Bqkg<sup>-1</sup>,  $15.51 \pm 3.90$  Bqkg<sup>-1</sup> and  $121.95 \pm 4.97$  Bqkg<sup>-1</sup>. Based on the concentrations of the mentioned radionuclides, the Average Annual Committed Effective Dose (AACED) were then calculated and found as 0.005 mSv/y, 0.004 mSv/y and 0.010 mSv/y, respectively with the average of them is 0.005 mSv/y. The Average Annual Committed Effective Dose (AACED) due to ingestion of the natural radionuclides in the medicinal plant samples are far below than the world average annual committed effective dose of 0.3 mSv/yr as per report of UNSCEAR 2000. The mean value of excess lifetime cancer risk for <sup>226</sup>Ra, <sup>232</sup>Th and <sup>40</sup>K are  $1.07E^{-06}$ ,  $1.06E^{-05}$  and  $8.35E^{-05}$  respectively which below the ELCR acceptable ( $0.29E^{-03}$ ) for radiological risk. Therefore the collected medicinal plants are safe for the human body in this region.



**ISRP 2021**  
**International Symposium on Radiation Physics**  
**Kuala Lumpur – Malaysia**  
**6 – 10 December 2021**

**A221 - Studies on the radiation absorption characteristics of different commercial granites collected from Saudi Arabia**

Neda Alohal<sup>1,2</sup>; Nidal Dwaikat<sup>3,4</sup>; M. I. Sayyed<sup>5,6</sup>; Mohammad Abu Mhareb<sup>1,2\*</sup>; Mouna Misfer AlQahtani<sup>1</sup>; Zahra Abdulaziz Al-Hulail<sup>1</sup>; Raghad Mofareh Yaanallah<sup>1</sup>; Y. S. Alajerami<sup>7</sup>, Mayeen Uddin Khandaker<sup>8</sup>

<sup>1</sup>Department of Physics, College of Science, Imam Abdulrahman Bin Faisal University, P.O. Box 1982, 31441 Dammam, Saudi Arabia

<sup>2</sup>Basic and Applied Scientific Research Center, Imam Abdulrahman Bin Faisal University, PO Box 1982, 31441 Dammam, Saudi Arabia

<sup>3</sup>Department of Physics, College of Engineering and Physics, King Fahd University of Petroleum & Minerals, Dhahran 31261, Saudi Arabia

<sup>4</sup>Interdisciplinary Research Center for Advanced Materials, King Fahd University of Petroleum & Minerals, Dhahran, Saudi Arabia

<sup>5</sup>Department of Physics, Faculty of Science, Isra University, Amman, Jordan

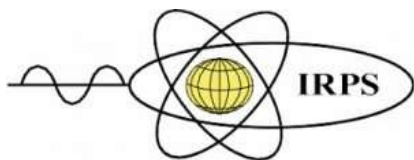
<sup>6</sup>Department of Nuclear Medicine Research, Institute for Research and Medical Consultations(IRMC), Imam Abdulrahman Bin Faisal University (IAU), P.O. Box 1982, 31441 Dammam, Saudi Arabia

<sup>7</sup>Medical Imaging Department, Applied Medical Sciences Faculty, Al Azhar University-Gaza, P.O. Box 1277, Gaza, Palestine

<sup>8</sup>Center for Applied Physics and Radiation Technologies, School of Engineering and Technology, Sunway University, 47500 Bandar Sunway, Selangor Darul Ehsan, Malaysia

Corresponding author: mhsabumhareb@iau.edu.sa

In this work, different commercial granites were collected from Saudi Arabia, and their radiation shielding characteristics were experimentally reported. The density of the collected granites varied between 2.5861 and 2.7557 g/cm<sup>3</sup>. The EDX was used to determine the weight fraction for each sample. Special attention was given to the strength, availability, and physical formation for selecting the investigated granites. The mass attenuation coefficient for the collected granites was measured using a narrow gamma-ray source and NaI detector for different energies ranging from 0.184 and 0.810 MeV. The experimental results were compared with the XCOM data to confirm the accuracy in the narrow beam condition, and we found a match between the experimental and XCOM data at all investigated energies. The mean free path demonstrated that as the energy goes up from 0.184 to 0.810 MeV, the probability of radiation interaction with the collected granites drops; hence more radiation can penetrate the granites. We also compared the attenuation ability of the collected granites with other granites used in other countries.



**ISRP 2021**  
**International Symposium on Radiation Physics**  
**Kuala Lumpur – Malaysia**  
**6 – 10 December 2021**

**A224 - The effect of gamma and electron beam irradiation on the properties of bioactive glass-polymer composite film patch for soft tissue healing**

Ruzalina Baharin<sup>1</sup>, Naurah Mat Isa<sup>2</sup>, Siti Fatimah Samsurrijal<sup>3</sup>, Siti Noor Fazliah Mohd Noor<sup>3</sup>

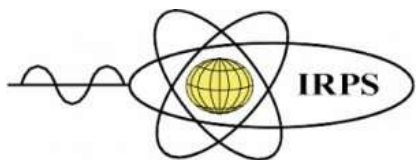
<sup>1</sup>Technical Support Division, Malaysian Nuclear Agency, Malaysia

<sup>2</sup>Radiation Processing Technology Division, Malaysian Nuclear Agency, Malaysia

<sup>3</sup>Craniofacial and Biomaterial Sciences Cluster, Advanced Medical and Dental Institute, Universiti Sains Malaysia, Malaysia

Corresponding author: ruzalina@nuclearmalaysia.gov.my

A common treatment for soft tissue and mucosal ulceration includes paste or gels which tend to dissolve or create painful taste and sensation. The use of plaster which most of the time not degradable creates the needs for patient to remove it and changed plaster dressing. This process will create a traumatic experience and put stress on the patient. To overcome this problem, a novel resorbable patch was developed to promote the generation of soft tissue has been put on evaluation for its performance. Prior to pre-clinical test, the patch containing bioactive glass-polymer composites has to go through a complete sterilisation process to ensure its sterility. One of the alternatives is by using radiation with doses of gamma and electron beam for sterilising the film patch that varies between 15 to 30 kGy. The absorbed dose for each of the radiation was verified using ceric cerous dosimeter (for gamma-ray) and cellulose triacetate (CTA) film dosimeter (for electron beam). The irradiated samples were then monitored for its morphological change via FESEM and TEM. Based on the finding, it was found that gamma and electron beam irradiation at the range of 25 to 30 kGy have kept the film patch structure at its best quality. Morphology of the irradiated film patch indicates that crosslinking event has occurred among the composition molecules improving the aesthetic structure. Dose uniformity ratio (DUR) of the irradiation process was noted below 2.0, and rise above 2.0, for gamma and electron beam, respectively. The values confirmed that gamma irradiation has better radiation penetration compared to electron beam irradiation, thus preferred for bulk sterilisation process. Further test should include analysing the cell responses of the sterilised patch.



**ISRP 2021**  
**International Symposium on Radiation Physics**  
**Kuala Lumpur – Malaysia**  
**6 – 10 December 2021**

**A127 - Development and establishment of medical Radiation Protection Officer certification program in Malaysia**

Z.Kayun<sup>1\*</sup>, M.K.A. Karim<sup>2</sup>, S. C Saifudin<sup>1</sup>, D.A Bradley<sup>3</sup> and M.T Chew<sup>3</sup>

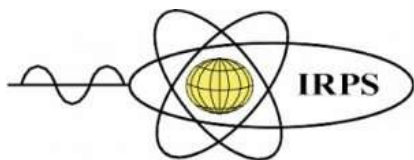
<sup>1</sup>Division of Medical Radiation Surveillance, Ministry of Health, Putrajaya

<sup>2</sup>Department of Physics, Faculty of Science, Universiti Putra Malaysia, UPM, Serdang, Selangor 43400, Malaysia

<sup>3</sup>Centre for Applied Physics and Radiation Technologies, School of Engineering and Technology, Sunway University, No 5, Jalan Universiti, Bandar Sunway, 47500 Petaling Jaya, Selangor, Malaysia

Corresponding author: [zunaide@moh.gov.my](mailto:zunaide@moh.gov.my)

Patients are exposed to ionizing radiation from individual radiographic or nuclear medicine procedures and from multiple procedures. There is increasing concern about the risks of cancer and other effects from the use of medical imaging procedures. There have been several studies on patient radiation exposure from all sources of ionizing radiation since the 1980s, especially from international bodies such as the National Council on Radiation Protection and Measurements (NCRP). The use of ionizing radiation to patients should be optimal in accordance with the principles of ALARA. To achieve those objectives, each facility need to have competent and qualified Radiation Protection Officer(RPO). The main role of RPO is to prevent unnecessary exposure to ionizing radiation and maintain necessary exposures as low as reasonably achievable (ALARA). The RPO is delegated broad authority throughout the organization by senior management. This authority includes permission to stop unsafe practices and identifying radiation protection problems, initiating, recommending, or providing corrective actions and verifying implementation of these actions. For each effectiveness of RPO efforts at each facility, Ministry of Health of Malaysia (MOH) has developed a medical RPO certification program in 2018. This program was developed following the IAEA's recommendations during the peer review audit mission in 2015. The implementation of this program is also in line with regulations under BSRP 2010. In this paper we want to discuss MOH mechanism in the RPO certification program and introduced available tools for the RPO to educate members of the medical community and senior management on the need to manage radiation doses to patients. Therefore, it is hoped that the implementation of this medical RPO program can ensure that the aim of radiation protection are achieved in line with increasing the growing practice and technology from time to time.



**ISRP 2021**  
**International Symposium on Radiation Physics**  
**Kuala Lumpur – Malaysia**  
**6 – 10 December 2021**

**A229 - Geant4 track structure simulation of electron beam interaction with a gold nanoparticle**

Farhad Moradi<sup>1</sup>, Mehrdad Jalili<sup>1</sup>, Khadijeh Rezaee Ebrahim Saraei<sup>1</sup>, Mayeen Uddin Khandaker<sup>2</sup> David Bradley<sup>2,3</sup>

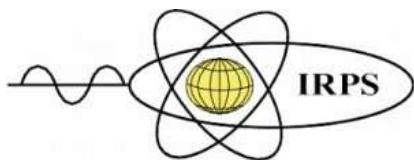
<sup>1</sup>Faculty of Physics, University of Isfahan, Isfahan, Iran

<sup>2</sup>Centre for Biomedical Physics, School of Healthcare and Medical Sciences, Sunway University, Bandar Sunway, Selangor, Malaysia

<sup>3</sup>Department of Physics, University of Surrey, Guildford, Surrey, UK

Corresponding author: mehrdad.jalili@live.com

Application of nanoparticles as radiosensitizer in various radiation therapy modalities have recently attracted considerable interest. However experimental findings have shown radiosensitization effect of gold nanoparticles (GNPs) when combining with electron irradiations, observing the recent literature reveals the lack of a comprehensive analysis regarding the modification effects caused by the presence of GNP on physical energy deposition pattern in electron fields. The aim of the current study is to evaluate and verify radioenhancement effects of NPs under electron beams. Monte Carlo track structure simulations that are the generally accepted approach for investigation of radiation effects in the nanometer scale were conducted by the use of Geant4-DNA code to track electrons down to the 10-eV energy. Macroscopic megavoltage energy electron spectrum from an intraoperative electron radiation source was used to irradiate a water phantom while particles were tracked to score the microscopic (nanometer) beam spectrum. Then, a single 50 nm gold nanoparticle was irradiated with the nanobeam where secondary electrons, energy deposition and ionization events were analysed. The results reveal a considerable dose escalation at close vicinities of the nanoparticle gradually decreasing at further distances caused by low energy electrons originated in the NP. Although, the amount of calculated dose enhancement strongly depends on the applied physics model, the current result provides a theoretical evidence in support of the physical dose enhancement in GNP aided electron radiotherapy.



**ISRP 2021**  
**International Symposium on Radiation Physics**  
**Kuala Lumpur – Malaysia**  
**6 – 10 December 2021**

**A232 - Evaluation of level of compliance of patients' doses and exposure parameters at a University Hospital (UNIMEDTH) in Nigeria during routine diagnostic imaging**

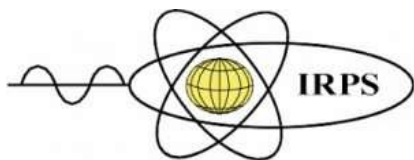
Christopher Olowookere<sup>1</sup>, Michael Olatunji<sup>1</sup>, Mayeen Khandaker<sup>2</sup>, Evelyn Osho<sup>1</sup>, Joseph Fatukasi<sup>1</sup>, Babatunde Salam<sup>1</sup>, David Bradley<sup>2</sup>

<sup>1</sup>Department of Physics, University of Medical Sciences, Ondo, Nigeria

<sup>2</sup>Centre for Biomedical Physics, Sunway University, Selangor, Malaysia

Corresponding author: colowookere@unimed.edu.ng

As the uses of radiation in healthcare services continue to expand, the need for radiation protection requires more attention during both conventional and computed radiodiagnosis. This necessitates the need for regular and consistent evaluation of the level of compliance of the practice of radiodiagnosis (dose and exposure parameters) with the guidance level recommended by the regulatory international bodies. This study investigated the doses received by patients examined at University of Medical Sciences Teaching Hospital (UNIMEDTH). The mean entrance surface doses (ESD) of chest PA, skull PA, lumbosacral AP, thoracolumbar AP and abdomen AP for adult patients are 0.73 mGy, 2.22 mGy, 0.46 mGy, 0.76 mGy and 1.08 mGy, respectively. The mean ESD for paediatric patients in chest PA, lumbosacral and shoulder lateral are 1.29 mGy, 0.48 mGy and 1.01 mGy, respectively. The obtained results for adult patients show that the value recorded in this study is lower than the UK (HPA) value in lumbosacral AP, thoracolumbar AP, and abdomen AP. However, the ESD value shows to be higher in chest PA and skull PA than the UK value. This shows that doses received by patients during chest PA and skull PA need to be optimised.



**ISRP 2021**  
**International Symposium on Radiation Physics**  
**Kuala Lumpur – Malaysia**  
**6 – 10 December 2021**

**A233 - Dosimetric characterization for experimental mouse irradiation using novel add-on collimator system combined with a standard cell irradiator**

AmirEntezam<sup>1, 2, 3</sup>, Andrew Fielding<sup>2, 4</sup>, Davide Fontanarosa<sup>1, 2</sup>

<sup>1</sup> School of Clinical Sciences, Queensland University of Technology, Brisbane, QLD, Australia

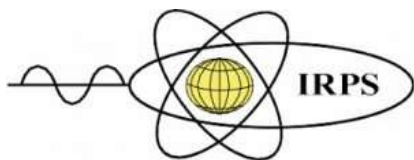
<sup>2</sup> Centre for Biomedical Technologies, Queensland University of Technology, Brisbane, QLD, Australia

<sup>3</sup> Diamantina Institute, Translational Research Institute, The University of Queensland, QLD, Australia

<sup>4</sup> Faculty of Science, School of Chemistry and Physics, Queensland University of Technology, Brisbane, QLD, Australia

Corresponding author: amir.entezam@hdr.qut.edu.au

In a previous study, we have demonstrated that our novel add-on collimator mounted into a Gammacell irradiator is an appropriate tool for mice irradiations. The objective of this study is to provide accurate dosimetric evaluation for a mouse irradiation, irradiated with our irradiation system, using a realistic Monte Carlo (MC) phantom. We generated a MC phantom from a micro-CT image set of a mouse with xenographic tumour model. MC modelling of the irradiation system for a specific experimental irradiation condition was performed and the calculated results were verified against dosimetric measurements using a physical phantom. The verified MC modelling was used to irradiate the MC mouse phantom and calculate the dose distribution. Also, dose volume histograms (DVHs) were generated for the tumour and organs at risk (OARs). The dose distribution calculations show that the dose to the normal tissue (the out of field dose) is of the order 7% of the maximum dose ( $D_{max}$ ) when irradiating the xenographic tumour of the phantom. DVHs analysis results suggest that the irradiation of the mouse phantom with our irradiation method can effectively deliver dose to the xenographic tumour volume while minimizing dose to other critical organs. The methodology of generating the MC mouse phantom and analysing dose distributions and DVHs calculations provides a quantitative method for dosimetric characterization of small animal irradiations.



**ISRP 2021**  
**International Symposium on Radiation Physics**  
**Kuala Lumpur – Malaysia**  
**6 – 10 December 2021**

**A235 - Tungsten carbide and tungsten carbide cobalt based epoxy resin composites for lead-free gamma ray radiation shielding in nuclear medicine**

Nadin Jamal Abualroos<sup>1</sup>, Mohd Idzat Idris<sup>2</sup>, Haidi Bin Ibrahim<sup>3</sup>, Rafidah Zainon<sup>1,4</sup>

<sup>1</sup>Oncological and Radiological Sciences Cluster, Advanced Medical and Dental Institute, SAINS@BERTAM, Universiti Sains Malaysia, 13200 Kepala Batas, Pulau Pinang, Malaysia.

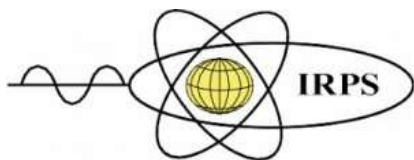
<sup>2</sup>Nuclear Technology Research Centre, Department of Applied Physics, Faculty of Science and Technology, Universiti Kebangsaan Malaysia, 43600 UKM, Bangi, Selangor, Malaysia

<sup>3</sup>School of Electrical and Electronic Engineering, USM Engineering campus, Jalan Transkrian, Bukit Panchor, 14300 Nibong Tebal, Pulau Pinang, Malaysia

<sup>4</sup>School of Physics, Universiti Sains Malaysia, 11800 Gelugor, Pulau Pinang, Malaysia.

Corresponding author: rafidahzainon@usm.my

**Introduction:** Radiation shielding in nuclear medicine is commonly accomplished with lead shields. However, lead is heavy, lacks durability, and its disposal is associated with environmental hazards. Epoxy resin is a hybrid thermostat polymer that well known for its excellent thermal and mechanical properties, chemical resistance, compatibility with organic and inorganic fillers, nontoxicity, and flexibility. **Purpose:** The aim of this study was to design a lead-free composite shield made of tungsten carbide epoxy resin and tungsten carbide cobalt epoxy resin for protection against gamma rays in the energy range of 0.6 MeV – 1.33 MeV in nuclear medicine. **Materials and Methods:** In this study, tungsten carbide epoxy resin and tungsten carbide cobalt epoxy resin composites were fabricated with four different weight percentages of epoxy resin (40wt %, 30wt %, 20wt % and 10wt %) and two different thicknesses (0.7 cm and 1.4 cm) just as the conventional lead shield thickness used in nuclear medicine department. Experimental measurements were carried out to assess the attenuation properties of the fabricated composites. Gamma attenuation study was performed using NaI (Tl) gamma ray spectrometer. The shielding parameters such as linear attenuation coefficient, mass attenuation coefficient, half value layer and mean free path were investigated. The distribution of the filler powder within the epoxy matrix was studied using Scanning Electron Microscopy (SEM). **Results:** Attenuation results reveal that, the effectiveness of gamma-ray shielding increases with increase in density of the composites. This is due to an increase in the weight percent of tungsten carbide powder. Hence, tungsten carbide and tungsten carbide cobalt epoxy resin composites can be used for gamma shielding applications in nuclear medicine. **Conclusion:** It can be concluded that the addition of tungsten carbide and tungsten carbide cobalt particles into epoxy matrix leads to improvement in radiation shielding characteristics, with potential applications in nuclear medicine.



**ISRP 2021**  
**International Symposium on Radiation Physics**  
**Kuala Lumpur – Malaysia**  
**6 – 10 December 2021**

**A236 - Towards real-time analysis of liquid jet alignment in SFX**

Jaydeep Patel<sup>1</sup>, Adam Round<sup>2</sup>, Andrew Peele<sup>3</sup>, Adrian Mancuso<sup>2</sup>, Brian Abbey<sup>1</sup>

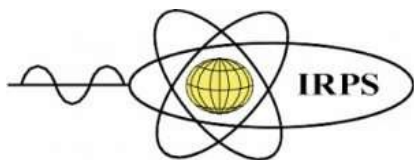
<sup>1</sup>Department of Chemistry and Physics, La Trobe Institute for Molecular Science,  
La Trobe University, Australia

<sup>2</sup>European XFELs, German Electron Synchrotron DESY, Germany

<sup>3</sup>Australian Synchrotron, Australian nuclear science and Technology, Australia

Corresponding author: j.patel2@latrobe.edu.au

Serial femtosecond crystallography (SFX) enables atomic scale imaging of protein structures via X-ray diffraction measurements from large numbers of small crystals intersecting intense X-ray Free Electron Laser (XFEL) pulses. Sample injection typically involves continuous delivery of crystals to the pulsed XFEL beam via a liquid jet. Due to movement of the jet, which is often focused to further reduce its diameter using a gas virtual dynamic nozzle (GVDN), repeated adjustment of the jet position during the experiment is often required. This can result in loss of beamtime and significant manual intervention. Here we present a novel approach to the problem of liquid jet misalignment in SFX based on machine vision. We demonstrate automatic identification and classification of when there is overlap ('hit') and when there is not overlap ('miss') between the XFEL beam and jet. Our algorithm takes as its input optical images from the 'side microscope' located inside the X-ray hutch. This algorithm will be incorporated into the control system at the SFX/SPB beamline at the European XFEL where it will be used for in-situ 'alignment correction' via a continuous feedback loop with the stepper motors controlling the location of the nozzle within the chamber. Full automation of this process will result in a larger volume of useful data being collected. By increasing the efficiency and reducing the per experiment operational cost of SFX at the European XFEL a higher volume of experiments can be performed. In addition, via analysis of the feedback metrology we anticipate that optimised nozzle designs and jetting conditions could be achieved further benefitting the end user.



**ISRP 2021**  
**International Symposium on Radiation Physics**  
**Kuala Lumpur – Malaysia**  
**6 – 10 December 2021**

**A237 - Establishing diagnostic reference levels based on clinical indications for enhanced computed tomography abdomen and pelvis examinations**

Entesar Zawam Dalah<sup>1&2\*</sup>, Jamila Salam Alsuwaidi<sup>1</sup>, Reem Salim AlKtebi<sup>3</sup>, Muna Abdellatif Ali AlMulla<sup>3</sup>, Priyank Gupta<sup>3</sup>.

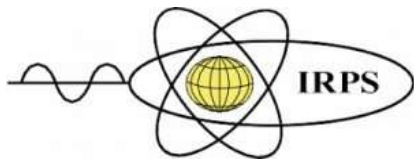
<sup>1</sup>HQ Diagnostic Imaging Department, Dubai Health Authority, Dubai, UAE

<sup>2</sup>Department of Clinical Support Services and Nursing Sector, Dubai Health Authority, Dubai, UAE

<sup>3</sup>Department of Radiology, Rashid Hospital, Dubai Health Authority, Dubai, UAE

Corresponding Author: edalah@dha.gov.ae

Computed tomography (CT) diagnostic reference levels (DRLs) are usually established based on anatomical location. Herein, we aim to establish DRLs based on clinical protocols for adult patients whom underwent CT abdomen & pelvis + contrast examinations. A second aim is to evaluate CT dose indices and patient dose metrics. CT dose indices for a total of 216 patients subjected to CT Abdomen & Pelvis + contrast examination were obtained and retrospectively analysed. DRLs were calculated using CT dose indices of dose length product per whole-scan (tDLPs) and volumetric CT dose index maximum (maxCTDI<sub>vol</sub>). Effective dose (E) was used to represent patient dose metric. Spearman coefficient and one-way ANOVA tests were used to check statistical differences between dose metrics and the different clinical protocols. In our institute, 10 common yet different clinical protocols were used to carry out CT abdomen & pelvis + contrast examinations. Among which, the clinical protocol of CT abdomen and pelvis tumors demonstrated the highest mean and median tDLPs across all 10 clinical protocols. CT abdomen and pelvis tumors protocol registered also the highest E followed by angio-abdomen-aorta-GI bleeding protocol, with a mean of 38.7 and 35.9 mSv, respectively. Significant differences ( $p < 0.0001$ ) were found between the tDLPs based on anatomical location and the routine clinical protocols of abdomen and pelvis +contrast and triphasic liver. Significant ( $r = 0.6941$ ,  $p < 0.0001$ ) correlation, despite the type of protocol, was seen between the tDLPs and the number of scan series using Spearman coefficient test. Wide range of CT dose indices and patient dose metrics were seen while relying on anatomical based DRLs. Patient dose optimizations require establishing clinical indication based DRLs rather than the anatomical location.



**ISRP 2021**  
**International Symposium on Radiation Physics**  
**Kuala Lumpur – Malaysia**  
**6 – 10 December 2021**

#### **A240 - Effective and Organ equivalent doses in Neck Computed Tomography Imaging**

Khalid Alzimami<sup>1\*</sup>, Layal Jambi<sup>1</sup>, Esam H. Mattar<sup>1</sup>, Ahmed Alenezi<sup>1</sup>, Abdulrahman Alfuraih<sup>1</sup>, H. Salah<sup>2,3\*</sup>, Mohammad Rabbaa<sup>4</sup>, Mohammad Abuljoud<sup>4</sup>, Khaled Alsafi<sup>5</sup>, Abdelmoneim Sulieman<sup>6</sup>, David .A.Bradley<sup>7,8</sup>

<sup>1</sup>Department of Radiological Sciences, College of Applied Medical Sciences, King Saud University, P.O Box 10219 Riyadh 11433, Saudi Arabia

<sup>2</sup>INAYA Medical Collage, Nuclear Medicine Department, Riyadh, Saudi Arabia

<sup>3</sup>College of Medical Radiologic Science, Sudan University of Science and Technology, Khartoum, Sudan

<sup>4</sup>Radiology Department, Riyadh Care Hospital, Riyadh, Saudi Arabia

<sup>5</sup>Department of Radiology, Medical Physics Unit, King Abdul Aziz University, Jeddah, Kingdom of Saudi Arabia

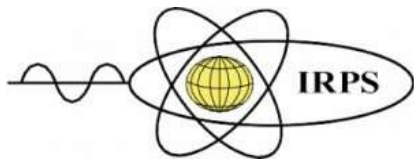
<sup>6</sup>Prince Sattam Bin Abdulaziz University, College of Applied Medical Sciences, Radiology and Medical Imaging Department, Alkharj, Saudi Arabia

<sup>7</sup>Centre for Applied Physics and Radiation Technologies, School of Engineering and Technology, Sunway University, 47500, Bandar Sunway, Selangor, Malaysia.

<sup>8</sup>Centre for Nuclear and Radiation Physics, Department of Physics, University of Surrey, Guildford, Surrey GU2 7XH, United Kingdom

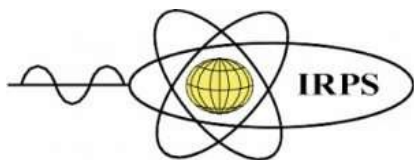
Corresponding author: kalzimami@ksu.edu.sa

Computed tomography (CT) is a leading source of ionizing radiation for medical purposes. It was estimated that in the United States, more than 84 million CT procedures are performed annually. CT for the neck region is frequently performed for a wide range of clinical indications because the neck region contains many organs and tissues with high sensitivity to ionizing radiation, such as the thyroid gland. Limited studies were conducted to assess the radiation dose for the radiosensitive organs in the primary beam. In total, 81 patients undergone CT procedures enhanced with contrast medium conducted at Riyadh Care Hospital using Multislice CT (MSCT) machine (Siemens Somatom Sensation 64 (64 slices/detector)). The mean and range of patient age (years) were  $41.5 \pm 15.5$  (21-73). Organ and effective doses were evaluated using computer software based on Monte Carlo simulation. The patient's radiogenic risk for a specific organ was extrapolated using the International Commission of Radiological Protection (ICRP) risk factors. The patients' radiation doses (mGy.cm) for CT neck examination were  $993.3 \pm 539.5$  (267.3-2441.7). The mean and range of volume CT dose per slice (CTDIvol (mGy)) were  $1.5 \pm 3.9$  (3.91-22.55). The overall effective dose (mSv) per procedure is ranged from 1.3 to 11.7 with a mean value equivalent to 4.8 mSv. Patients' CT neck procedures have been repeated the procedure up to 7 times during the treatment course. The risk of malignancy is  $1 \times 10^{-5}$  CT procedure. The study showed that patients received wide



**ISRP 2021**  
**International Symposium on Radiation Physics**  
**Kuala Lumpur – Malaysia**  
**6 – 10 December 2021**

discrepancies in patients' doses up to 9 times. Optimization of image acquisition protocol and scan length is necessary to reduce the unnecessary risk.



**ISRP 2021**  
**International Symposium on Radiation Physics**  
**Kuala Lumpur – Malaysia**  
**6 – 10 December 2021**

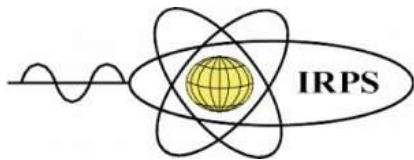
**A242 - Modelization of radon emanation generated by natural and artificial sources as a laboratory scale**

Aina Noverques, Belén Juste, María Sancho, Gumersindo Verdú

Institute for Industrial, Radiophysical and Environmental Safety (ISIRYM), Universitat Politècnica de València, Camino de Vera s/n 46022 Valencia (Spain)

Corresponding author: ainome@iqn.upv.es

The carcinogenic effects of radon gas, considered as responsible for 50% of the annual dose received, have promoted its study and the analysis of new forms of measurement, both in situ and from mathematical models that allow the prediction of radon levels in the air. The contribution to its exposure is mainly due to natural sources such as rocks and soils, but also from building materials or radioactive waste such as phospho-gypsum. The objective of this work is based on the measurement of radon emission from two sources: one of natural origin (pitchblende stone) and the other artificial (phospho-gypsum waste) obtained in the production of fertilizers. The objective of this work is based on the measurement of radon emission from two sources: one of natural origin and the other artificial (phospho-gypsum) obtained in the production of fertilizers. For this, a high density polyethylene radon accumulation box is designed, hermetically sealed. From the obtained results of air radon concentration inside the box, the fit of the mathematical model is analyzed. The model is based on the diffusive movement of gas during its emanation and release into the air. It is verified whether, for both the natural and artificial sources, the behaviour of radon is the same under laboratory conditions. Likewise, both sources are previously characterized with a germanium detector.



**A244 - Initial application of radiomics and deep learning in lung cancer diagnosis**

Duong Thanh Tai<sup>1</sup>, Zahra Alirezaei<sup>2</sup>, Abdelmoneim Suleiman<sup>3,4</sup>, Hiba Omer<sup>5</sup>, Le Cong Hieu<sup>7</sup>

<sup>1</sup>Department of Industrial Electronics and Biomedical Engineering, HCMC University of Technology and Education, Ho Chi Minh, Vietnam

<sup>2</sup>Radiology Department, Paramedical School, Bushehr University of Medical Sciences, Bushehr, Iran.

<sup>3</sup>Prince Sattam Bin Abdulaziz University, College of Applied Medical Sciences, Radiology and Medical Imaging Department, Saudi Arabia

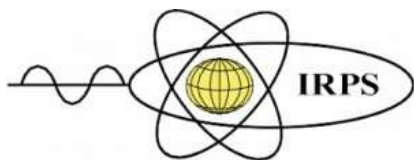
<sup>4</sup>Basic Science Department, College of Medical Radiologic Science, Sudan University of Science and Technology, Sudan

<sup>6</sup>Department of Basic Sciences, Deanship of Preparatory Year and Supporting Studies, Imam Abdulrahman Bin Faisal University, Saudi Arabia

<sup>7</sup>Faculty of Information Technology, Van Lang University, Ho Chi Minh, Vietnam

Corresponding author: taidt@hcmute.edu.vn

Accurate diagnosis, along with appropriate treatment planning, requires the exceptional experience of the clinicians. The application of deep learning in image processing can create tools to make the diagnosis process faster. This study aimed to apply Deep Learning and Radiomics in diagnosing lung cancer to build a supporting tool for clinicians in analyzing and making an appropriate treatment plan. CT images of 86 patients from Bach Mai Hospital and 1012 patients from the open-source library were used for this study. First, deep learning is applied in the segmentation process by U-NET and the cancer classification process by DenseNet Model. Then, the radiomics were used for measuring and calculating a diameter, surface area, and volume. Finally, hardware was also designed by connecting between Arduino Nano and MFRC522 module to read data from the tag. In addition, the displayed interface was created on a web platform using Python through Streamlight. Model of segmentation (train loss is 0.27 and Val loss is 0.498) and cancer classification (train accuracy is 0.98, validation loss is 0.78) were established. RFID Reader model and displayed interface were built on the web platform to meet objectives goal out initially. Initial research in the application of deep learning and radiomics in lung cancer diagnosis was successful in training models to classify, recognize tumors and diagnose cancer using CT image datasets for lung area of patients. The model is capable of storing patient data directly on the interface and updating the results directly after diagnosis on the patient information board to meet actual needs, support for examination methods, and traditional diagnosis. The basic functions in the Web are relatively satisfactory. The Web interface is easy to use and meets the security requirements.



**ISRP 2021**  
**International Symposium on Radiation Physics**  
**Kuala Lumpur – Malaysia**  
**6 – 10 December 2021**

**A246 - Chemical evaluation of vitrified spent resin with steel slag as a binder**

Shahrul Sazuan Ariffin<sup>1</sup>, Nur Fatin Humaira Jamaludin<sup>1</sup>, Syazwani Mohd Fadzil<sup>1,2</sup> & Rohyiza Ba'an<sup>3</sup>

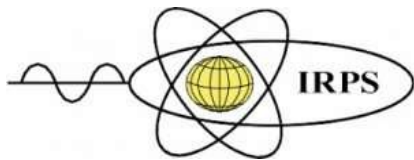
<sup>1</sup>Department of Applied Physics, Faculty of Science and Technology, Universiti Kebangsaan Malaysia, 43600 Bangi, Selangor, Malaysia

<sup>2</sup>Nuclear Technology Research Center, Faculty of Science and Technology, Universiti Kebangsaan Malaysia, 43600 Bangi, Selangor, Malaysia

<sup>3</sup>Waste and Technology Development Centre, Waste & Environmental Technology Division, Malaysian Nuclear Agency, Bangi, 43000, Kajang, Selangor, Malaysia

Corresponding author: syazwanimf@ukm.edu.my

In Malaysia, the spent ion exchange resins contribute a significant proportion of radioactive wastes which are generated from a research reactor. Following gazetted Act 304, spent resin have been classified as low-level radioactive waste, and intermediate-level radioactive wastes depend on the radioactivity level. Annually, 50 kg of spent ion exchange resin were generated which spur increment of radioactive wastes in Malaysia. Thus, a treatment and disposal method is required. For radiological evaluation, the samples were counted for 12 hours to determine the activity of radionuclides in the samples using a gamma spectrometry system with a High-purity Germanium (HPGe) detector coupled to a multi-channel analyser. Radionuclide <sup>60</sup>Co ( $751 \pm 2.19$  Bq/kg) and <sup>137</sup>Cs ( $0.68 \pm 0.34$  Bq/kg) reflect the highest and lowest activity concentration in spent resin, respectively. The product consistency test was used to analyse glass element release from the vitrified spent resin. The outcome depicts that the pH from vitrified composition of 15% spent resins + 10% steel slag + 75% glass at 1200°C is  $8.05 \pm 0.01$ , lower compared to the same composition at 1150°C. The binder (10% steel slag) concludes its capability to reduce the pH of leachate solvent in the vitrified resin from 8.10 to 8.05. The pH for vitrified composition of 10% spent resin + 15% steel slag + 75% glass is  $9.58 \pm 0.40$ , higher than vitrified composition of 15% spent resin + 10% steel slag + 75% glass which is  $8.20 \pm 0.14$ . The former composition displays a higher normalized release of element B and Na while the latter composition exhibits a higher normalized release of element Si. Eventually, the assessment of chemical evaluation of vitrified spent resin shows rather low and insignificant compared to previous studies. In conclusion, the binder plays an important role in the composition to retard the movement of hazardous elements from vitrified spent resin.



**ISRP 2021**  
**International Symposium on Radiation Physics**  
**Kuala Lumpur – Malaysia**  
**6 – 10 December 2021**

### **A248 - Benchmarking of Monte Carlo codes in Phantom Dose Distribution Simulation**

Sitti Yani<sup>1</sup>, Indra Budiansah<sup>2</sup>, Mohamad Fahdillah Rhani<sup>3</sup>, Duong Thanh Tai<sup>4</sup>, Freddy Haryanto<sup>5</sup>

<sup>1</sup>Department of Physics, Faculty of Mathematics and Natural Sciences, Bogor Agricultural University (IPB University), Indonesia

<sup>2</sup>SMA Darul Hikam Bandung, Indonesia

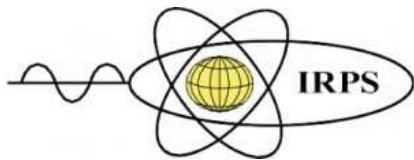
<sup>3</sup>Department of Radiology, Kathleen Kilgour Center, New Zealand

<sup>4</sup>Department of Industrial Electronics and Biomedical Engineering, HCMC University of Technology and Education, Ho Chi Minh, Vietnam

<sup>5</sup>Department of Physics, Faculty of Mathematics and Natural Sciences, Institut Teknologi Bandung, Indonesia

Corresponding author: [sittiyani@apps.ipb.ac.id](mailto:sittiyani@apps.ipb.ac.id)

Many Monte Carlo (MC) codes were developed to simulate the particle transport in medium, such as EGSnrc, MCNP, Geant4, PHITS, Fluka and PENELOPE. Each code has its own uniqueness distinguishing it with other codes. In this study, two Monte Carlo codes, EGSnrc and PHITS, were compared. The point and monoenergetic beam were used as a source located 1 cm from the phantom surface. The simulation parameters were set the same for all the simulations. The photon and electron cut-off energies were set to 10 keV and 521 keV, respectively in PHITS and EGSnrc simulation. The number of particles simulated (histories) is  $3 \times 10^7$  electrons. The dose distribution was collected from homogeneous (water) and heterogeneous phantom (water-lung-aluminium-water slices). At the end of the simulation, the percent depth doses (PDDs), dose profiles, isodose curve, and dose difference was evaluated. Dose profiles was scored at depth with maximum dose, depth = 5 cm, and depth = 10 cm from surface. Eight sets of simulations were done to compare these codes. Good agreement between codes was observed, except for out-of-field doses and toward the field edge for larger field size for beam energy less than 5 MeV. In the energy >5 MeV show the PDD shifted with deviation >5% especially in the beam axis. The cross-section data and radiation transport methodology of electron and photon in a medium applied in these codes was different causing the large deviation. The photon and electron cross-section data applied to PHITS simulation was from EPDL97 and EEDL database, respectively. Meanwhile, these cross-section data of the EGSnrc was derive from EGS4.



**ISRP 2021**  
**International Symposium on Radiation Physics**  
**Kuala Lumpur – Malaysia**  
**6 – 10 December 2021**

**A249 - Evaluation of impact of image reconstruction on  $^{18}\text{F}$ -FDG-PET/CT imaging radiomics features in head and neck cancer**

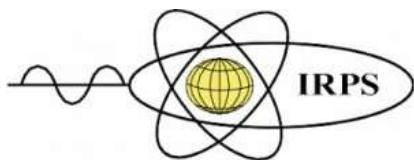
Noushin Anan<sup>1</sup>, Mahbubunnabi Tamal<sup>2</sup>, Rafidah Zainon<sup>1</sup>

<sup>1</sup>Oncological and Radiological Sciences Cluster, Advanced Medical and Dental Institute, SAINS@BERTAM, Universiti Sains Malaysia, 13200 Kepala Batas, Pulau Pinang, Malaysia

<sup>2</sup>Department of Biomedical Engineering, College of Engineering, Imam Abdulrahman Bin Faisal University, Dammam, Saudi Arabia

Corresponding author: rafidahzainon@usm.my

The diagnostic role of CT, integrated with fluorine-18 fluorodeoxyglucose positron emission tomography ( $^{18}\text{F}$ -FDG-PET/CT) imaging in head and neck cancer is evolving rapidly. Accuracy and reproducibility of the region of interest (ROI) delineation is an important parameter for analysing the progression of the tumour. Investigation of tumour metabolism, growth and treatment evaluation depends on the tumour segmentation technique. The absence of standardized technique inhibits the adaptation of  $^{18}\text{F}$ -FDG-PET/CT imaging as a biomarker. This study was aimed to investigate the impact of quantitative measures of image quality - size, contrast to noise ratio (CNR) and signal to noise ratio (SNR) on image reconstruction in order to attain a standardised image processing technique. Clinical images from the QIN Head and Neck collection stored in The Cancer Imaging Archive was employed in our study. 59 patients with head and cancer underwent  $^{18}\text{F}$ -FDG PET/CT scan. Manual and semi-automated segmentation were performed twice by three experienced radiologists to delineate the head and neck tumour, specifically the ROI to eliminate the intra-observer and inter-observer variability. Afterwards, maximum voting was determined to define a standard point of reference. Dice's coefficient was evaluated to analyse the overlap between maximum voting and the delineated region of interests. Our results showed that a higher Dice coefficient was achieved in the case of semi-automated segmentation method compared to the manual segmentation method. Additionally, delineation of the region of interest became more independent on the segmentation method with the increase of tumour size, CNR and SNR. Semi-automated segmentation method has higher accuracy compared to manual segmentation method. However, for a higher value of tumour size, SNR and CNR, dependency on segmentation method for delineation of the region of interest become lower. Imaging with high SNR and CNR leads to a more accurate region of interest delineation irrespective of the segmentation method.



**ISRP 2021**  
**International Symposium on Radiation Physics**  
**Kuala Lumpur – Malaysia**  
**6 – 10 December 2021**

**A250 - Investigation of the different nanoparticles effects on the mass attenuation coefficient in diagnostic radiology: A Monte Carlo study**

Khosravi Hossein<sup>1,\*</sup>, M. I. Sayyed<sup>2,3</sup>, Mayeen Uddin Khandaker<sup>4</sup>

Department of Radiology, Faculty of Para medicine, Hamadan University of Medical Sciences, Hamadan, Iran

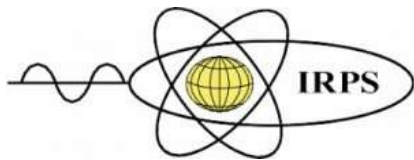
<sup>2</sup>Department of Physics, Faculty of Science, Isra University, Amman, Jordan

<sup>3</sup>Department of Nuclear Medicine Research, Institute for Research and Medical Consultations (IRMC), Imam Abdulrahman Bin Faisal University (IAU), P.O. Box 1982, 31441 Dammam, Saudi Arabia

<sup>4</sup>Center for Applied Physics and Radiation Technologies, School of Engineering and Technology, Sunway University, 47500 Bandar Sunway, Selangor Darul Ehsan, Malaysia

Corresponding author: [hkhosravi55@gmail.com](mailto:hkhosravi55@gmail.com)

The aim of this study was to determine the mass attenuation coefficient in diagnostic radiology for different nanoparticles to evaluate and compare the changes in bulk state. To calculate the mass attenuation coefficient in the presence of the target, nanoparticles were simulated in the target, using MCNPX Monte Carlo code. The following materials were used in this study: Pb, Bi, W, Pb NPs, Bi NPs, W NPs, PbO NPs, Bi<sub>2</sub>O<sub>3</sub> NPs and WO<sub>3</sub> NPs. The calculation data were then compared to theoretical results obtained using the XCOM software to examine the validity of the simulation values. According to the results, the protective attenuation of containing nanoparticles is better than bulk materials. Among of the selected nanoparticles, tungsten nanoparticles were more attenuated than the others. On the other hand, PbO, Bi<sub>2</sub>O<sub>3</sub> and WO<sub>3</sub> nanoparticles have a lower density and attenuation rate than Pb, Bi and W nanoparticles. Therefore, these nanoparticles are lightweight and have more flexibility than bulk materials. It is concluded that using nanoparticles in the protective materials leads to a significant mass attenuation coefficient enhancement for 10-100 keV x-ray photons.



**ISRP 2021**  
**International Symposium on Radiation Physics**  
**Kuala Lumpur – Malaysia**  
**6 – 10 December 2021**

### **A251 - Literacy challenges for nuclear science and technology in Thailand**

Phanee Saengkaew<sup>1,2\*</sup>, Supitcha Chanyotha<sup>1</sup>, Phongphaeth Pengvanich<sup>1</sup>, Chainarong Cherdchu<sup>2</sup>, Usa Kullaprawithaya<sup>2,3</sup>, Pantip Ampornrat<sup>2,3</sup>, Dhanaj Saengchantr<sup>4</sup>, Rieko Takaki<sup>5,7</sup>, and Takeshi Iimoto<sup>6,7</sup>

<sup>1</sup>Department of Nuclear Engineering, Faculty of Engineering, Chulalongkorn University, Phatumwan, Bangkok, 10330, Thailand

<sup>2</sup>Nuclear Society of Thailand (NST), 16 Vibhavadi Rangsit Rd., Bangkok, Bangkok 10900, Thailand

<sup>3</sup>Office of Atoms for Peace (OAP), Ministry of Higher Education, Science, Research and Innovation, 16 Vibhavadi Rangsit Rd., Bangkok, Bangkok 10900, Thailand

<sup>4</sup>Thailand Institute of Nuclear Technology (TINT), 16 Vibhavadi Rangsit Rd, Ladyao, Chatuchak, Bangkok 10900, Thailand

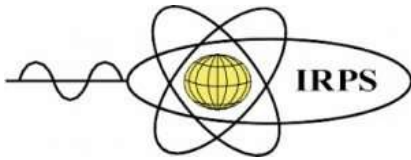
<sup>5</sup>Energy Communication Planning, 4-27-507 Onimaracho, Saga-shi, Saga 840-0021, Japan

<sup>6</sup>The University of Tokyo, 7-3-1 Hongo, Bunkyo-ku, Tokyo 113-8654, Japan

<sup>7</sup>JN-HRD.net

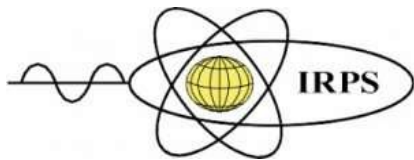
Corresponding author: phanee.s@chula.ac.th

Even though nuclear human resource development has been introduced in Thailand since 1962, but public communication in Nuclear Science and Technology (NST) has not yet been successfully done as expected. At present, NST is also not yet perceived as a promising professional in Thailand. Nevertheless, there are many outreach activities organized by each nuclear-related entity. Unfortunately, these conducted activities are not always sustainable and mostly do not involve with students and teachers in school levels. In addition, the outreach activities are not holistic, not focusing on delivery the same important messages, and not been published in the media frequently and widely. This article is proposed feasible solutions by having all nuclear-related organizations build a tightly strong national cooperation to deliver powerful messages, the same keywords sending to targeted audiences. Mass media should also play an important supporting role by having a program to broadcast basic knowledge and information on NST for daily life, regularly and continually. Level of public acceptance in nuclear technology utilizations is still different in medicine, industry, and agriculture. Public acceptance is quite positive for medical applications such as x-ray radiography, CT-scan, and PET-scan. These medical applications are accepted as one of necessary treatments for health care system. Thai people are rather more familiar with the word “radiation” than the word “nuclear”. They may not recognize technical differences between these two words, but they have perceived the word “radiation” more comfortably due to it more frequently mentioned in their daily life. Therefore, the possible solutions to solve these root problems are to have the



**ISRP 2021**  
**International Symposium on Radiation Physics**  
**Kuala Lumpur – Malaysia**  
**6 – 10 December 2021**

national science curriculum and the course syllabus reviewed and revised, having more nuclear-related topics, and more hands-on experiments to make NST more convincing and attractive to students to learn it. By doing so, it is expected that young students and Thai people will be more familiar with NST. The NST curriculum should enhance their NST literacy through these technical and strategic plans. Gradually, the nuclear human resource knowledge development (HRKD) will be successful step by step and ultimately gain long-term public acceptance in Thailand.



**ISRP 2021**  
**International Symposium on Radiation Physics**  
**Kuala Lumpur – Malaysia**  
**6 – 10 December 2021**

**A252 - Development of a methodology for dose optimization in abdominal exams using two Computerized Radiology (CR) systems**

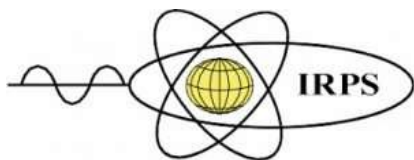
Marcos Alves<sup>1</sup>, Bruna Mota<sup>2</sup>, Érica policarpo<sup>3</sup>, Tiago Jornada<sup>4</sup>, Ladyjane Assemany<sup>5</sup>, Kellen Daros<sup>6</sup>.

<sup>1,2,3,4,6</sup> Universidade Federal de São Paulo - Departamento de Diagnóstico por Imagem da Escola Paulista de Medicina da UNIFESP, Rua Napoleão de Barros, 800 - Vila Clementino - CEP 04024-002 - São Paulo/SP.

<sup>5</sup>Instituto de Pesquisas Energéticas e Nucleares, IPEN – CNEN/SP. Av. Prof. Lineu Prestes, 2242, Cidade Universitária – 05508-000. São Paulo – SP – Brasil

Corresponding author: [alves.marcos@unifesp.br](mailto:alves.marcos@unifesp.br)

Optimization in radiological protection, is based on the principle (ALARA) which determines that doses in procedures should be as low as reasonably achievable. In the imaging process, quality is controlled by exposure factors (mAs and kV). With the replacement of the film screen system by computerized radiography (CR), the visual ability to distinguish underexposed or overexposed images was reduced. In CR systems, exposure analysis is performed through noise levels. The objective of the study is to optimize the doses in radiographs of the abdominal region, using image quality tools, through the analysis of the contrast-to-noise signal ratio (CNR). To perform the study, different exposure conditions were analyzed in CR systems from different manufacturers, called “A and B”. The images were acquired with 20 cm of PMMA to simulate the thickness of a typical adult abdomen and 0.5 mm of aluminum for contrast analysis. To estimate the Entrance Skin Air Kerma (ESAK), a calibrated set from the manufacturer Radcal®, consisting of a detector model 10X6-06 and an electrometer model 2068 was used. After standardization of the image acquisition protocol, the ESAK was reduced by approximately 10% in system A and 23.24% in system B, without a significant reduction in image quality.



**ISRP 2021**  
**International Symposium on Radiation Physics**  
**Kuala Lumpur – Malaysia**  
**6 – 10 December 2021**

**A254 - Monte Carlo simulation of the experimental beamline of the Particle Physics and Beam Delivery Core Laboratory at the Chang Gung Memorial Hospital**

Chun-Hui Hsing<sup>3</sup>, Tsi Chian Chao<sup>1,2,3</sup>, Chung Chi Lee<sup>1,2,3</sup>

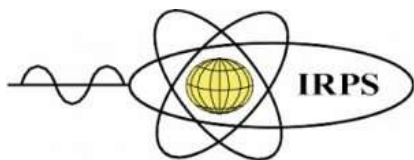
<sup>1</sup>Department of Medical Imaging and Radiological Sciences, College of Medicine, Chang Gung University, Taoyuan, Taiwan

<sup>2</sup>Department of Radiation Oncology, Chang Gung Memorial Hospital, Kwei-Shan Taoyuan, Taiwan

<sup>3</sup>Institute for Radiological Research, Chang Gung University/Chang Gung Memorial Hospital, Linkou, Taoyuan, Taiwan

Corresponding author: clee@mail.cgu.edu.tw

The Particle Physics and Beam Delivery Core Laboratory (PBDL) at the Proton and Radiation Therapy Center of the Chang Gung Memorial Hospital in Linkou started trial operation in October 2019. Beam characteristics of this research beamlines such as intensity, energy spectra, and spatial/fluence distributions were determined for the broad beamline. This beamline used the double scattering technique for spreading out the beam laterally, and a rotating propeller for spreading out the Bragg peak. The beamline simulation was established based on the Monte Carlo based Particle Therapy Simulation Framework (PTSim) and was commissioned by comparing to measurements from beam stopper, transmission type parallel plate ionization chamber, poor man Faraday cup, Gafchromic EBT3 film, and Zebra (IBA). The geometric structure information of the secondary scatterer imported into simulation program was obtained by three dimensional scanning of the actual object. By feeding in those simulation results, we were able to determine beam characteristics. These results are essential for the PBDL and will support future researches and services in testing for radiation biology and radiation hardness of microelectronic components. Compared to the measurements, the difference of these simulations of optimized secondary scatterer were less than 0.2 mm and 0.02 mm in the range ( $R_{80}$ ) and distal dose fall-off ( $W_{80-20}$ ), respectively. To evaluate the consistency of simulation and measurement of proton lateral distribution, the difference of indicators used to describe the lateral distribution, such as FWHM,  $W_{8080}$  and  $W_{9090}$ , were within 9.24 mm, 13.41 mm and 16.29 mm, respectively. The efficiency of proton transmission in the simulation system was analysed and compared with the experimental irradiation system. These data can be applied in practical and clinical uses.



**A255 - Correlation between the different mammography dose quantities, breast thickness and scan parameters using regression models**

Salam Dhou<sup>1,3\*</sup>, Entesar Dalah<sup>2\*</sup>, Reda Al Ghafeer<sup>3</sup>, Aisha Hamidu<sup>3</sup>, Abdulmunhem Obaideen<sup>4</sup>

<sup>1</sup>Department of Computer Science and Engineering, American University of Sharjah, United Arab Emirates

<sup>2</sup>HQ Diagnostic Imaging Department, Dubai Health Authority, United Arab Emirates

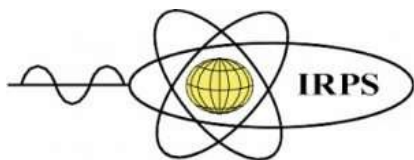
<sup>3</sup>Biomedical Engineering Graduate Program, American University of Sharjah, United Arab Emirates

<sup>4</sup>Diagnostic Imaging Department, University Hospital Sharjah, United Arab Emirates

\*These authors contributed equally to this work.

Corresponding author: sdhou@aus.edu

Genome profiling calls for accurate estimation and good understanding of parameters that could affect glandular absorbed dose. Herein, we estimate the mean glandular dose (MGD) per craniocaudal (CC) and mediolateral-oblique (MLO) views using skin entrance dose (SED), x-ray spectrum information, patient age, breast glandularity, and breast thickness. Further, a regression analysis was performed to correlate between the different mammography dose quantities including: machine provided organ dose (OD) and SED both measured in mGy and the estimated MGD measured in mGy. Further, a regression model was used to correlate between OD, SED, MGD and patient age, breast thickness, and the mammography scan parameters. Mammography scan data for a cohort of 486 subjects with an age range of (28-86 years) who underwent screening mammography examinations were collected and retrospectively analyzed. Mammography scan parameters from a total of 2035 mammograms were extracted from the DICOM headers. Linear regression metrics were calculated to evaluate the strength of the correlation. Our mean (and range) MGD per CC-view was 0.832 (0.110-3.491) mGy and per MLO-view was 0.995 (0.256-2.949) mGy. All mammography dose quantities strongly correlated with tube exposure (mAs), OD ( $R^2=0.969$  per CC-view and  $R^2=0.983$  per MLO-view), SED ( $R^2=0.938$  per CC-view and  $R^2=0.945$  per MLO-view) and MGD ( $R^2=0.980$  per CC-view and  $R^2=0.972$  per MLO-view). Patient age showed poor correlation with all mammography dose quantities OD ( $R^2=0.096$  per CC-view and  $R^2=0.066$  per MLO-view), SED ( $R^2=0.053$  per CC-view and  $R^2=0.0302$  per MLO-view) and MGD ( $R^2=0.054$  per CC-view and  $R^2=0.032$  per MLO-view). Breast thickness showed better correlation with all mammography dose quantities comparing to patient age. MGD estimation is a labor-intensive and time-consuming task. Both OD and SED do not reflect glandular tissue absorbed dose. MLO scan view yields slightly higher dose to the patient than the CC scan view. Glandular absorbed dose is glandularity-dependent more than size.



**ISRP 2021**  
**International Symposium on Radiation Physics**  
**Kuala Lumpur – Malaysia**  
**6 – 10 December 2021**

**A256 - Natural radioactivity and associated radiation hazard indicators from granite rocks in Gabal-Qash-Amir area, south Eastern Desert, Egypt**

Bahaa M Emad<sup>1</sup>, M. I. Sayyed<sup>2,3</sup>, Mayeen Uddin Khandaker<sup>4</sup>, D.A. Bradley<sup>4,5</sup>, M.Y. Hanfi<sup>1,6</sup>

<sup>1</sup>Nuclear Materials Authority, 530, Cairo, Egypt

<sup>2</sup>Department of physics, Faculty of Science, Isra University, Amman 11622, Jordan

<sup>3</sup>Department of Nuclear Medicine Research, Institute for Research and Medical Consultations, Imam Abdulrahman bin Faisal University, Dammam 31441, Saudi Arabia

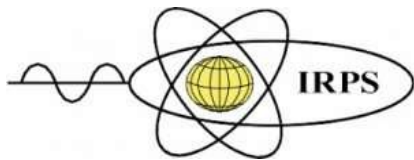
<sup>4</sup>Centre for Applied Physics and Radiation Technologies, School of Engineering, Sunway University, 47500 Bandar Sunway, Selangor, Malaysia

<sup>5</sup>Department of Physics, University of Surrey, Guildford, Surrey, GU2 7XH, UK

<sup>6</sup>Ural Federal University, Mira Street 19, 620002, Ekaterinburg, Russia

Corresponding author: M.Y. Hanfi: mokhamed.khanfi@urfu.ru

Because of their greater uses in construction industry, the granite rocks are found to play an important role in Egyptian economy as well as the world. The present study is aimed to determine the concentrations of radioactive materials in granite rocks to assess the potential radiological hazards to human beings. A total of 136 muscovite granite samples are analyzed by using HPGe gamma-ray spectrometry. Activity concentrations (Bq/kg  $\pm$  Std. Dev.) for <sup>238</sup>U, <sup>232</sup>Th and <sup>40</sup>K radionuclides were found to be  $193 \pm 268$ ,  $63 \pm 29$  and  $1034 \pm 382$ , respectively in the studied granite samples, all show higher values than the UNSCEAR reported worldwide average values. The associated radiological risk to the public were assessed via some well-defined hazard parameters like radium equivalent activity (Raeq), absorbed dose rate in air (Dair), outdoor and indoor annual effective dose (AEDout and AEDin), annual gonadal dose equivalent (AGDE), external and internal hazard indices (Hex and Hin), and excess lifetime cancer risk. Most of the parameters exceeded the recommended limits except the Raeq, which show a concern and indicates the requirement of guideline for use of the granites in dwelling purpose. The multivariate statistical analyses such as Pearson analysis, hierarchical cluster analysis (HCA) and principal component analysis (PCA) are utilized to obtain the correlation between radioactive materials variables. The reported data may serve as a reference and provide a preliminary information on the heavy mineral deposits in the study region.



**A257 - Evaluation Of Patient-Specific VMAT QA Dosimetry Systems for Linac Mechanical Errors and Investigation of Correlations with Dose Volume Histogram in SBRT Treatment**

Hande Ayata<sup>1,2</sup>, Eda Yirmibesoglu<sup>3</sup>, Gorkem Aksu<sup>3</sup>, Emrah Gokay Ozgur<sup>4</sup>, David Bradley<sup>5</sup>, Ozcan Gundogdu<sup>2</sup>

<sup>1</sup>Radiation Oncology, Göztepe Medicalpark Hastanesi, Turkey

<sup>2</sup>Biomedical Engineering, Kocaeli University, Turkey

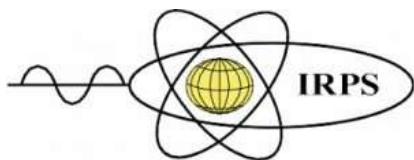
<sup>3</sup>Radiation Oncology, Kocaeli University, Turkey

<sup>4</sup>Biostatistics and Medical Informatics, Turkey

<sup>5</sup>Nuclear Physics, Sunway University, Malaysia

Corresponding author: ayata.hande@gmail.com

To investigate the sensitivity of various gamma criteria used in the gamma-index method according to the Linac-based errors for patient-specific volumetric modulated arc therapy (VMAT) quality assurance (QA) for stereotactic body radiation therapy (SBRT). Two types of intentional misalignments (collimator and MLC) were introduced to original high-definition multi-leaf collimator (HD-MLC) plans. Patient-specific QAs for the original and the modified plans were performed with iba COMPASS, EpiQA, ArcCHECK and PTW Octavius 4D. The sensitivity of both the global and local gamma analyses using criteria of 1%/1 mm, 1%/2 mm, 2%/1 mm, 2%/2 mm, 3%/2 and 3%/3 mm was investigated with absolute passing rates according to the magnitudes of MLCs misalignments. The Pearson correlation coefficients ( $r$ ) were calculated 1) between the global and the local gamma passing rates, 2) between gamma passing rates with the COMPASS, the EpiQA, the ArcCHECK and the Octavius 4D dosimeters, 3) and between gamma passing rates and the mechanical errors during the VMAT delivery. For the EpiQA, SNCpatient, 3DVH and Octavius 4D measurements, strong correlations between the global and local GPRs were observed with 2%/2 mm, 1%/2 mm and 1%/1 mm ( $r > 0.6$  with  $p < 0.001$ ), only with 2%/1 mm for EpiQA and Octavius 4D, while weak or no correlations were observed with 2%/1 mm for the SNCpatient and 3DVH measurement. Between the EpiQA-SNCpatient, EpiQA-3DVH, EpiQA-Octavius and EpiQA-Compass measurements, the global GPRs showed no correlations (all with  $p > 0.05$ ), while the local GPRs showed moderate correlations with 3%/2 mm, 2%/2 mm, 2%/1 mm, 1%/2 mm and 1%/1 mm for EpiQA and SNCpatient ( $r > 0.5$  with  $p < 0.001$ ). Gamma criterion of 2%/1 mm was found to be suitable as a tolerance level with passing rates of 90% and 80% for patient-specific VMAT QA for SBRT.



**ISRP 2021**  
**International Symposium on Radiation Physics**  
**Kuala Lumpur – Malaysia**  
**6 – 10 December 2021**

**A264 - Study on trace elements concentration and electron density variation in canine mammary tissues using a synchrotron-based micro X-ray fluorescence system**

Camila Salvego<sup>1</sup>, Marcelo Antoniassi<sup>1</sup>, Natália Oliveira, Felipe Burille<sup>1</sup>, Renato Sousa<sup>2</sup>, André Conceição<sup>3</sup>

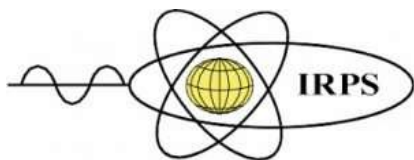
<sup>1</sup>Physics Department, Universidade Tecnológica Federal do Paraná (UTFPR), Brazil

<sup>2</sup>Veterinary Pathology Department, Universidade Federal do Paraná, Brazil

<sup>3</sup>Photon Science at DESY, Germany

Corresponding author: [antoniassi@utfpr.edu.br](mailto:antoniassi@utfpr.edu.br)

Mammary neoplasms are the most common in female dogs, with malignancy rates around 50%. Despite sharing many similarities with human breast tissues, the prevalence of cancer in dogs are nearly three times higher. This study aims to present results about chemical and structural changes occurring in canine mammary tissues, by combining micro X-ray fluorescence ( $\mu$ -XRF) and Compton Scattering technique to respectively map the spatial distribution of Fe, Cu and Zn and to determine the electron density of seven canine samples (two normal, two benign and three malignant). For the  $\mu$ -XRF experiments, the samples were scanned with a white beam collimated with 30  $\mu\text{m}$  of internal diameter, in 0.04 mm steps. For the Compton scattering measurements, the experimental arrangement was modified with the addition of a Si (111) double crystal monochromator, used to select an energy of 12 keV. Four to six points covering the transition region between healthy and neoplastic tissues were chosen for each sample. Results showed an accumulation of Fe in regions of blood vessels for all measured samples. Cu and Zn distributions were spatially correlated in normal tissues, with lower intensities in adipose regions and higher in the fibrous ones. Regarding the benign neoplasms, one sample exhibited a significant increase in Cu intensity in the tumor area, with a similar behavior in the second sample, albeit in smaller proportions. Zn intensity was increased in the tumor region for both samples. For the malignant ones, the presence of Fe was observed mostly in the tumor-adjacent regions. Cu and Zn showed similar distributions throughout the samples, with small variations, including an accumulation of Cu over the tumoral region of one of the measured samples. The electron density values obtained allowed differentiating tissue structures, with generally higher density in tumorous regions and lower in adipose tissues.



**ISRP 2021**  
**International Symposium on Radiation Physics**  
**Kuala Lumpur – Malaysia**  
**6 – 10 December 2021**

**A265 - Electrons and positrons collision cross sections with DNA and water in the low and intermediate energy regime**

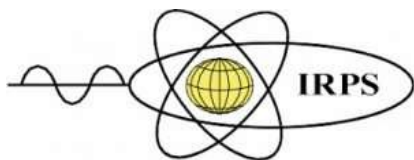
Aouina Nabila Yasmina<sup>1</sup> and Chaoui Zine El Abidine<sup>2</sup>

<sup>1</sup>Faculty of science; Department of Microbiology and Biochemistry. University of M'Sila

<sup>2</sup>Faculty of science; Department of Physics. Ferhat Abbas University, Setif1

Corresponding author: zchaoui@univ-setif.dz

The assessment of the damage created by radiation in the biological environment is based on knowledge of the cross sections of the collisions of electrons and positrons with the different constituents of DNA such as nucleotides (NT). In this perspective, to get closer to the real model, different water contents were used in this simulation from the point of view that the DNA molecule consists mainly of water; B-DNA needs about 30% by weight of water to maintain its native crystalline conformation. Our calculations relate to the study of the passage of charged particles in DNA and water, which presents a rapidly developing area of research. The elastic cross sections of the atoms constituting molecules of interest were evaluated using the relativistic (Dirac) partial wave analysis. We applied the screening corrected additivity rule for the differential and total molecular cross sections. The results obtained compared, when possible, with the experimental and theoretical results existing in the literature prove to be reasonable and acceptable. The current calculations of inelastic cross sections use the full Penn model; it is the Lindhard dielectric function weighted by the measured optical data. The passage to macromolecules such as NT and different contents of H<sub>2</sub>O / NT molecules is possible with the SCAR-macro method for. We are confident about their use as a database of the cross section of elastic and inelastic collisions of electrons and positrons in the energy range 10 eV -100 keV.



**ISRP 2021**  
**International Symposium on Radiation Physics**  
**Kuala Lumpur – Malaysia**  
**6 – 10 December 2021**

**A266 - Monte Carlo simulation of electron energy deposited and backscattered fractions in dry and hydrated DNA**

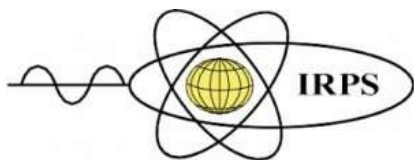
<sup>1</sup>Chaoui Zine El Abidine and <sup>2</sup>Aouina Nabila Yasmina

<sup>1</sup>Faculty of science; Department of Physics. Ferhat Abbas University, Setif1

<sup>2</sup>Faculty of science; Department of Microbiology and Biochemistry. University of M'Sila

Corresponding author: zchaoui@univ-setif.dz

In radiation physics, it is especially desirable to determine the energy of charged particles deposited in matter. In particular, this deposited energy is important in living matter. Detailed knowledge of the energy loss distributions of electrons in DNA is needed to explain the damage mechanisms of hydrated DNA, the so-called direct effects of radiation damage. We modeled the transport of electrons in a DNA segment of 2 nm and 4 nm for different levels of water molecules, taking into account the distribution of energy losses and the most probable energy loss of electrons. Therefore, there is a much higher probability of radiation interacting with the water. The influence of the water content is significant, an increase in energy deposited in the water molecules will lead to an increase in free radicals and therefore more damage in the nucleotides. The most probable energy is found to 22 eV for a DNA segment of 2m and 4 nm. The resulting distribution of energies deposited in a small target such as the DNA helix leads to a corresponding spectrum in the severity of damage produced. This damage can be interpreted as the probability of destroying cancer cells. Programs using the Monte Carlo statistical tool have been set up for a molecule of biological interest such as DNA.



**ISRP 2021**  
**International Symposium on Radiation Physics**  
**Kuala Lumpur – Malaysia**  
**6 – 10 December 2021**

**A267 - Study of contrast, SNR and CNR of digital images from biomaterial applied in odontology**

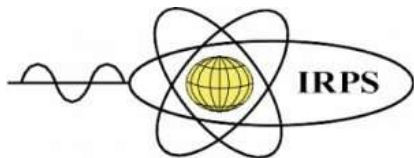
Fernando Nóbrega<sup>1</sup>, Kellen Daros<sup>1</sup>, Erica Policarpo<sup>1</sup>, Andrea Puchnick<sup>1</sup>, Claudio Costa<sup>2</sup>, Sergio Ajzen<sup>1</sup>

<sup>1</sup>Department of Diagnostic Imaging, Universidade Federal de São Paulo (UNIFESP), Brazil

<sup>2</sup>Department of Odontology, Universidade de São Paulo (USP), Brazil

Corresponding author: daros.kellen@unifesp.br

This study proposed to investigate the contrast, signal-to-noise (SNR) and contrast-to-noise (CNR) of the digital images from biomaterials applied in odontology. The images were acquired with a handheld portable X ray with a spectrum performed by 60 kV, 2 mA and 0.2s, and a computed radiography system. The parameters of digital images quality evaluated were low contrast (CNR and SNR) and spatial resolution. The biomaterials routinely used in clinical practice were: glass ionomer cement (GIC), glass ionomer cement photopolymerizable (GICP), dual adhesive resin cement (DARC), photopolymerizable restorative resin (PRR), lyophilized bone (LB), and zirconium (Zr). The CNR of different thickness of aluminium was performed using a step wedge phantom. The quantitative analysis of DICOM image (processed-pixels) and raw data (without processing) was performed with the RadiAnt® software. The qualitative visual analysis was performed in an environment with adequate illumination and in a high-resolution monitor and repeated in an environment equivalent to the clinical practice and conventional monitor. The relative contrast of the biomaterials was normalized by the higher contrast result, in this case Zr. The Zr image showed no noise because its  $\sigma_{bio}$  was zero. However, the relative SNR of biomaterials was normalized by the DARC, which had the highest SNR result. The relative CNR to the different thicknesses of Al were 0.11 to LB,  $0.3 \leq CNR \leq 0.35$  to PRR, GIC and GICP. The spatial resolution was the same to both monitors, however, with a clinical exposure of 0.2s, the resolution increased on the high-quality monitor. The contrast, SNR and CNR of the digital images shown that the biomaterials GIC, GICP, DARC and PRR are similar in processed images. This indicated that is difficult recognized the biomaterials when they are together in the clinical evaluation image. Reverse situation occurs when Zr and LB are in the images.



**ISRP 2021**  
**International Symposium on Radiation Physics**  
**Kuala Lumpur – Malaysia**  
**6 – 10 December 2021**

**A268 - The establishment of radioactive radon measurement technology in hot spring water**

Chun-Chih Lin<sup>1</sup>, Chien-Yi Ting<sup>2\*</sup>, Li, Yuan-Si<sup>3</sup>, Li, Jyun-Wei<sup>3</sup>

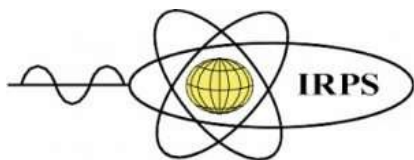
<sup>1</sup>Department, Institution, Country<sup>3</sup>Department of Natural Biotechnology/Graduate Institute of Natural Healing Sciences, Nanhua University, Taiwan, R.O.C.

<sup>2</sup>Department of Medical Imaging and Radiology, Shu-Zen Junior College of Medicine and Management, Taiwan, R.O.C.

<sup>3</sup>Department of Medical Imaging and Radiological Sciences, Kaohsiung Medical University, Taiwan, R.O.C.

\*Corresponding author: [chienyien@gmail.com](mailto:chienyien@gmail.com)

Hokutolite is the only one mineral named after a topom in Taiwan, which originates in the downstream (about 150-400 meters away from Geothermal Valley Hot spring) of Peitou Creek and is famous for its radioactivity from radium isotopes. The background radiation in the area of Geothermal Valley is relatively higher than elsewhere in Taiwan and is valuable for the research of natural radiation sources as well as human doses and biological effects in the environment of high background radiation. we aim to measure environmental radioactivity and dose in this area so that to enhance the management of radiation safety and public participation in Taiwan. In addition, the optimal condition for hokutolite formation was investigated in lab and hot spring water for restoration of hokutolite. The <sup>238</sup>U activity in soil revealed insignificant tendency along the area from Geothermal Valley toward downstream Beitou Creek, which was highest at Geothermal Valley. The <sup>232</sup>Th activity in soil decreased from Geothermal Valley toward downstream Beitou Creek, which was much higher than <sup>238</sup>U. The water temperature decreased from Geothermal Valley toward downstream Beitou Creek and the highest value (~73 °C) occurred at Geothermal Valley. The <sup>226</sup>Ra was found at a few sites, and <sup>228</sup>Ra was higher than <sup>226</sup>Ra. In soil, the <sup>238</sup>U activity was highest at Geothermal Valley (>31 Bq/kg) and revealed insignificant tendency along the area from Geothermal Valley toward downstream Beitou Creek. The <sup>232</sup>Th activity (>190 Bq/kg) decreased from Geothermal Valley toward downstream Beitou Creek and was much higher than <sup>238</sup>U. The test of hokutolite formation revealed that hokutolite was easier formed by generating deposited hull on the andesite rock and placed by exposing the upper part to the air where could be splashed by hot spring water.



**ISRP 2021**  
**International Symposium on Radiation Physics**  
**Kuala Lumpur – Malaysia**  
**6 – 10 December 2021**

**A273 - Correlation Between Radiation Damage And Electrical Characteristics Of The Proton-Irradiated Silicon PN Diode**

Minh-Phuoc Dang<sup>1,2</sup>, Sy Minh Tuan Hoang<sup>3\*</sup>

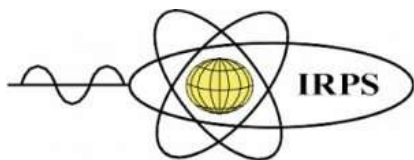
<sup>1</sup>Cho Ray Hospital, 210B, Nguyen Chi Thanh, District 5, Ho Chi Minh City, Vietnam, 700000

<sup>2</sup>Nuclear Training Center – VINATOM, 140, Nguyen Tuan, Thanh Xuan, Ha Noi City, Vietnam, 100000

<sup>3</sup>Institute of Applied Technology - Thu Dau Mot University, 6, Tran Van On, Phu Hoa Ward, Thu Dau Mot City, Binh Duong, Vietnam, 820000

Corresponding author: hoangsytuan@tdmu.edu.vn

The present study describes the correlation between radiation damage and electrical properties of the PN diode after irradiation of the energy proton. The PN diodes were irradiated at difference irradiation energies of 5.26, 7.2, and 8.67 MeV with the proton doses of  $1 \times 10^{10}$ ,  $1 \times 10^{11}$ , and  $1 \times 10^{12}$  cm<sup>-2</sup>. The final 3D distribution of the ions and all kinetic phenomena associated with the ion energy loss, such as vacancies, sputtering, ionization, and phonon production, can be estimated using the calculation packages (SDTrimSP and IM3D). The findings show that the penetration of protons into the PN diode leads to the production of lattice defects in the form of vacancies, defect clusters, and dislocations. As to the ionization effects in the PN diode, the total ionizing dose and single event effects were also calculated. In practical terms, the capacitance-voltage and current-voltage characteristics of the PN diode after irradiation have been measured to deduce the correlation between the damage creations and the electrical properties.



**ISRP 2021**  
**International Symposium on Radiation Physics**  
**Kuala Lumpur – Malaysia**  
**6 – 10 December 2021**

**A274 - Application Of Migrad Optimization Subroutine In Root Framework To Precisely Calculating U-235 And Ra-226 Photopeak Intensities In NORM**

Truong-Son Truong<sup>1,2</sup>, Sy Minh Tuan Hoang<sup>3\*</sup>

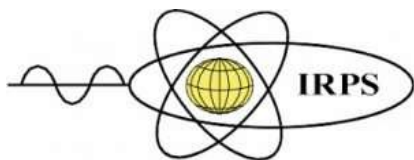
<sup>1</sup>HCMC University of Education, 280, An Duong Vuong, District 5, Ho Chi Minh City, Vietnam, 720000

<sup>2</sup>Nuclear Training Center – VINATOM, 140, Nguyen Tuan, Thanh Xuan, Ha Noi City, Vietnam, 100000

<sup>3</sup>Institute of Applied Technology - Thu Dau Mot University, 6, Tran Van On, Phu Hoa Ward, Thu Dau Mot City, Binh Duong, Vietnam, 820000

Corresponding author: hoangsyminhtuan@tdmu.edu.vn

The need for determining the U-235/U-238 isotopic ratio in a naturally occurring radioactive material (NORM) is increasing to warn against leakage of uranium into the environment. While seeking a non-destructive method of analysing natural matrices for uranium isotopes U-235 and U-238, a significant source of uncertainty was found to be the gamma-ray intensities. Ra-226 and U-235 are always found in the presence of each other in soil samples, and each has primary gammas whose energies differ by only  $0.496 \pm 0.014$  keV. The least-squares fitting method was implemented to obtain reliable values for the two photopeak intensities of Ra-226 and U-235 using the MIGRAD optimization subroutine in ROOT framework. This framework was developed to examine the effect of increasing or decreasing the number of degrees of freedom in the fit on the confidence intervals of the fitted intensity parameters (heights of the two Gaussians). An IAEA U1GX natural uranium reference material in secular equilibrium has been counted using an ORTEC HPGe detector with the sample in a Marinelli beaker geometry. It was found that the increased number of degrees of freedom approach (i.e., with a reduced number of free parameters) gives more accurate results for the photopeak intensities, with the determined ratio of U-235 to Ra-226 intensities having discrepancies in the range 0.27-2.8% from the expected ratio for natural uranium that is in secular equilibrium.



**ISRP 2021**  
**International Symposium on Radiation Physics**  
**Kuala Lumpur – Malaysia**  
**6 – 10 December 2021**

**A277 - A Study of Linear Attenuation Coefficients of Materials from X-ray Radiography Using Fluorescent Screen and Digital Camera**

Panapon Savitot<sup>1\*</sup>, Manasavee Lohvithee<sup>2</sup>, Yanisa Saenjaiwut<sup>1</sup>, Wanatchaphorn Phueaphae<sup>1</sup>,  
Suprawee Phaluek<sup>1</sup>, Nitchakan kudliang<sup>1</sup>, Tanyarat Hukkuntod<sup>1</sup>, Noppagate Sararut<sup>1</sup>,  
Punyisa Khruueakhun<sup>1</sup>, Nawabordin Daengnam<sup>1</sup>

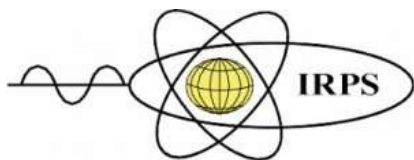
<sup>1</sup>Department of science, Ramkhamhaeng University, Thailand

<sup>2</sup>Department of engineering, Chulalongkorn University, Thailand

\*Corresponding author: panapon8961@gmail.com

**Abstract:**

X-ray radiography has played a vital role as a part of radiation technique in Non-Destructive Testing (NDT). This technique is utilized as a tool to measure a material's density and defect, which are invisible by a visual inspection. **Objectives:** This work aims to study linear attenuation coefficients of different materials' thicknesses and liquids using the X-ray image acquisition system of fluorescent screen and digital camera. **Methods:** The X-ray radiography acquisition and analysis system consists of 4 parts; an X-ray generator, a fluorescent screen, a digital camera, and ImageJ program. The materials being used as samples for this study are: rubber compound with Barium Sulfate (thickness of 3 mm, 6 mm, and 9 mm), aluminium sheets (each of 1 mm thickness) and different types of liquids (CaCl<sub>2</sub>, CaCO<sub>3</sub>, MgCl<sub>2</sub>, CaSO<sub>4</sub>, BaSO<sub>4</sub>). **Data analysis procedure:** The materials of interest are radiographed using X-ray radiation and the acquisition system. The current of the X-ray tube is fixed at 5 mA with varying kVp of 90,100,110,120, and 130 V. The X-ray images of materials (taken at varying settings of the image acquisition system) are analysed using ImageJ program to observe relationships between different intensities of image pixels in RGB as a result from varying settings of the image acquisition system. Linear attenuation coefficients are calculated for different liquid samples and different thicknesses of rubber compound with Barium Sulfate and aluminium sheets using the intensities of acquired X-ray images. **Result:** The potential result from this study is: the materials with higher image intensities and higher density are likely to have higher linear attenuation coefficients, i.e., the materials can attenuate higher amount of X-ray radiation. The knowledge of attenuation coefficients of different liquids and materials' thicknesses can be utilized for appropriate radiation protection and shielding, as well as material classification for certain energies of X-ray radiation.



**ISRP 2021**  
**International Symposium on Radiation Physics**  
**Kuala Lumpur – Malaysia**  
**6 – 10 December 2021**

**A280 - Measurement of Reactive Oxygen Species Generation By Iridium Nanoparticles in External Beam Radiotherapy**

Wan Nordiana Rahman<sup>1</sup>, Amirah Jamil<sup>1</sup>, Noor Nabilah Talik Sisin<sup>1</sup>, Reduan Abdullah<sup>2</sup>, Moshi Geso<sup>3</sup>

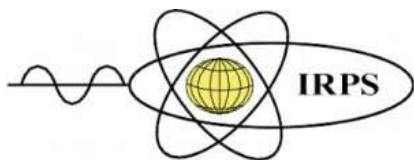
<sup>1</sup>School of Health Sciences, Universiti Sains Malaysia, Malaysia

<sup>2</sup>Hospital of Universiti Sains Malaysia, Kubang Kerian, Kelantan, Malaysia,

<sup>3</sup>School of Health and Biomedical Sciences, RMIT University, Victoria, Australia.

Corresponding author: wandiana@usm.my

The purpose of this study is to investigate the reactive oxygen species generation by iridium nanoparticles in external beam radiotherapy which includes photon and electron beam radiotherapy. In this study, HeLa cells were incubated with two different concentrations of Iridium NPs which are 0.1mMol/L and 0.5 mMol/L. Then, the samples were irradiated with photon beam of 6 MV and electron beam of 6 MeV with doses of 3 Gy and 6 Gy. As a results, for 6 MV photon beam, the highest reactive oxygen species (ROS) measured was demonstrated by cells irradiated with dose of 3 Gy with concentration of 0.1 mMol/L. Meanwhile electron beam show highest ROS measured for cells irradiated with dose of 3 Gy with concentration of 0.5 mMol/L. In conclusion, the study concluded that Iridium nanoparticles have the potential to become radiosensitisers in both photon and electron beam radiotherapy. Enhanced ROS generation is observed to be dependent on beam types, dose, and concentration of nanoparticles.



**ISRP 2021**  
**International Symposium on Radiation Physics**  
**Kuala Lumpur – Malaysia**  
**6 – 10 December 2021**

**A281 - Conceptual framework of effective dose evaluation in NORM-added products using Monte Carlo simulations and ICRP computational human phantom**

N. Z. H. Abu Hanifah<sup>1</sup>, S. Hashim<sup>1,2</sup>, Halmat J. Hassan<sup>1,3</sup>, N.A. Basri<sup>4</sup>, M.R. Fahmi<sup>5</sup>, M.S.M. Sanusi<sup>1</sup>

<sup>1</sup>Department of Physics Faculty of Science, Universiti Teknologi Malaysia, Malaysia

<sup>2</sup>Ibnu Sina Institute for Scientific and Industrial Research (ISISIR), Universiti Teknologi Malaysia, Malaysia

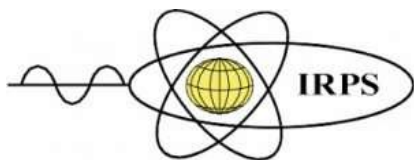
<sup>3</sup>Department of Physics, College of Education, University of Sulaimani, Kurdistan-Iraq

<sup>4</sup>Advanced Nuclear Engineering Research Group, School of Chemical & Energy Engineering, Universiti Teknologi Malaysia, Malaysia

<sup>5</sup>School of Physics, Universiti Sains Malaysia, Malaysia

Corresponding author: norafifah@utm.my

The human computational phantom for radiation dose assessment has been rapidly evolving from simple mathematical phantom model to a complex model of mesh-type phantom. One of the latest phantom developed is the International Commission on Radiological Protection ICRP-145 Adult Mesh-Type Reference Computational Phantoms, which is used to calculate dose coefficient factor (DCF) for internal and external exposure. Recently, consumer products containing naturally occurring radioactive material (NORM) can be easily accessible by the general public through online and offline markets in Malaysia. The products have various categories such as cosmetics, clothes, bath products, wall paint, and many others. The NORM-added products are continuously in contact with any part of human body, which may caused prolonged internal and external radiation exposure. To evaluate the effective dose from the NORM-added consumer product, direct measurement is obviously impossible. Hence, modelling by computational phantom can be used as an alternative. Because of the variety of consumer products categories, the modelling for each categories can be challenging for radiation safety control. This paper proposes a conceptual framework of effective dose evaluation for NORM-added products with consideration to the dose modelling for each categories. The framework highlights the important criteria for effective dose assessment such as phantom type specifications, type of source model, and the Monte Carlo transport code. This framework can be used to develop the effective dose calculation system by product categories to assist the safety control of NORM-added consumer products in Malaysia.



**A284 - Humidity dependence of radon equilibrium factor measurement using an alpha beta filter detector**

Javier Enrique Marínez<sup>1</sup>, Belén Juste<sup>1</sup>, Gumersindo Verdú<sup>1</sup>

<sup>1</sup> Instituto de Seguridad Industrial, Radiofísica y Medioambiental, Universitat Politècnica de València, Spain

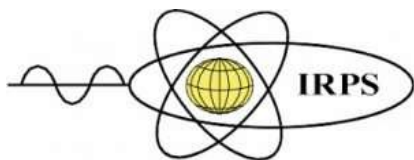
Corresponding author: gverdu@upv.es

A widely used method to measure radon progeny consist of employing detectors with a suction pump that trap the radon descendants in fixed-filters that are then analyzed by alpha or gamma spectrometry. The problem with these techniques is that they cannot offer long period continuous measurements since the dust and/or humidity clogs the filter and the measurement must stop to renew a clean new filter. To register radon progeny without interruptions during long time periods, the SmartCAM (*Ultraelectronics*) moving filter monitor has been used.

Measurements analyze radon progeny collected on the filter. To that, alpha and beta particles emitted from filter are recorded by two high resolution PIPS solid state alpha-beta detectors. Comparison experiments with other equilibrium factor estimation techniques were carried out in different places at the Universitat Politècnica de València (Spain) to measure radon equilibrium factor.

The different locations where the equilibrium factor study has been carried out, consist on an underground bunker and two indoors laboratories, one of them ventilated and the other one without ventilation. The equilibrium factor has also been measured in a Waste Water PreTreatment Plant (WWPTP) on the Mediterranean coast. The equilibrium factor values obtained in the ventilated and not ventilated laboratory present a slight difference, being 0.5 and 0.56 respectively. The equilibrium factor measured in the WWPTP has been 0.27 and results obtained at the underground bunker was 0.1. Each location present different ventilation characteristics and diverse presence of aerosols, which justifies this wide range of results obtained.

The relative humidity in the studied locations under normal conditions is around 50%. To study the influence of this variable on the equilibrium factor, a commercial humidifier has been used to increase the humidity percentage up to 90%, measuring a continuous increment of the equilibrium factor. It is proven how the number of aerosols present in the air, allows a greater proportion of radon descendants to be attached to them, thus increasing the equilibrium factor.



**ISRP 2021**  
**International Symposium on Radiation Physics**  
**Kuala Lumpur – Malaysia**  
**6 – 10 December 2021**

**A286 - Low-dose radiation effects on wound healing – a review**

Komathi Perumal<sup>1\*</sup>, Ming Tsuey Chew<sup>1\*</sup>, David A Bradley<sup>1,2</sup>, Ronald Sin Yeang Teow<sup>3</sup>, Suat Cheng Peh<sup>3</sup>

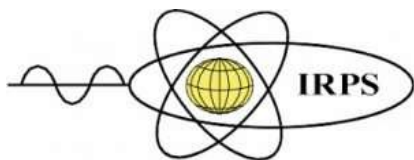
<sup>1</sup>Centre for Applied Physics and Radiation Technologies, Sunway University, Malaysia

<sup>2</sup>Department of Physics, University of Surrey, United Kingdom.

<sup>3</sup>Department of Medical Sciences, School of Medical and Life Sciences, Sunway University, Malaysia

Corresponding authors: pkomathi08@gmail.com and mtchew@sunway.edu.my

Radiation therapy is a vital integrated part of modern comprehensive cancer management. Aside from the more typical use of radiotherapy in treatment of cancer, low dose radiation (LDR), typically < 100 mGy, has also been used to treat inflammation, pneumonia, skin diseases, bacterial infections, and many other benign diseases. Moreover, animal studies have shown LDR attenuates systemic acute inflammatory response by regulating inflammatory cytokines, alleviates damage following burn injuries and promotes healing. Wounds are disruptions of the skin's structural and functional integrity which transit through four distinct phases, namely hemostasis, inflammation, cellular migration, and proliferation and remodeling. Common skin wounds include, open wounds caused by external factors such as trauma, accidents or infections, closed wounds due to internal factors, burn wounds and diabetic wounds. Photo-stimulation and photo-biomodulation using low intensity lasers have been used to promote wound healing. Recently, there has been seen to be of interest in using low doses for wound healing and burn wound healing. Normal wound healing (tissue repair) is well-orchestrated, with an overlapping sequence of cellular and biochemical events, and it involves three phases of repair processes. The first phase is characterized by the inflammatory response that results in inflammation; the second phase encompasses the proliferative phase, where cells proliferate for tissue formation; and finally, wound healing in the form of maturation and remodeling. Wound healing takes time and is dependent on many factors. Herein, the mechanisms of wound healing induced by LDR in each phase of tissue repair are of interest, being matters of present focus.



**ISRP 2021**  
**International Symposium on Radiation Physics**  
**Kuala Lumpur – Malaysia**  
**6 – 10 December 2021**

**A287 - Characterization of a cost-efficient OPT101 photodiode as relative dosimeter in low-energy radiation dosimetry: An IoT application**

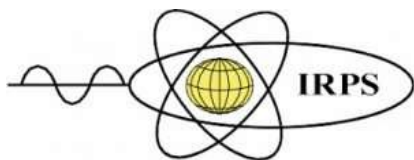
Yasmin Md Radzi<sup>1</sup>, Azhar Abdul Rahman<sup>1</sup>, Mirza Karmila Zainol<sup>1</sup>, Al Nagggar Azzam Salleh Abdullah<sup>1</sup>, Nor Zakiah Yahaya<sup>2</sup>

<sup>1</sup>School of Physics, Universiti Sains Malaysia, 11800, Penang, Malaysia

<sup>2</sup>School of Distance Education, Universiti Sains Malaysia, 11800, Penang, Malaysia

Corresponding author: yasminradzi@usm.my

Photodiode is increasingly become a detector of choice alternative to the silicon diode dosimeter because of its small size, real-time operation, low-cost, high accuracy also very precise in wide range of doses. In this work, the immediate read-out signals from the photodiode are facilitated by the used of an IoT system applications from Arduino IDE microcontroller and Blynk app are used in characterization of the photodiode to possess characteristics of an ideal dosimeter. The whole transducer system is irradiated using x-ray alongside PTW semiconductor detector (Freiburg, Germany). Photovoltaic signals were extracted under set of exposure settings, including tube voltage (kVp), current-time product (mAs) and source-to-detector distance (SDD). The performance was based on signal linearity to mAs and air kerma, and sensitivity dependence on absorbed dose and dose rates. The results highlighted two important aspects: (i) OPT101 photodiode has a potential to be optimized as a relative dosimeter in the future application of low-energy radiation with an excellent linearity against increasing kVp and mAs with  $R^2$  value of 0.964 and 0.999 respectively. However, low radiation-induced signal/sensitivity was detected possible due to the increasing energy irradiated to the active area. Secondly, (ii) the transducer system can be well-versed into a sophisticated IoT integration with less set-up required to extract real-time data coming from OPT101 sensor. OPT101 photodiode having advantages of high sensitivity with immediate readout, low cost, and portability also could replace passive dosimetry such as thermoluminescent dosimeter (TLD) for dose measurements in diagnostic radiology.



**ISRP 2021**  
**International Symposium on Radiation Physics**  
**Kuala Lumpur – Malaysia**  
**6 – 10 December 2021**

**A290 - Monte Carlo modelling of PMTs System for optical detection of alpha sources**

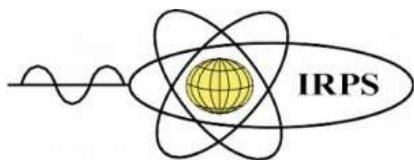
Ioana Lalau<sup>1,2</sup>, Mihaela Parvu<sup>2</sup>, Mastaneh Zaderafi<sup>1</sup>, Mihail-Razvan Ioan<sup>1</sup>, Andrei Antohe<sup>1</sup>, Ionel Lazanu<sup>2</sup>

<sup>1</sup>Radioisotopes and Radiation Metrology Department, Horia Hulubei National Institute for Research and Development in Physics and Nuclear Engineering, Romania

<sup>2</sup>Faculty of Physics, University of Bucharest, Romania

Corresponding author: ioana.lalau@nipne.ro

The radioluminescence process is an alternative method to detect alpha radiation at a much greater distance than the use of standard methods in which the signal is obtained from the energy deposition inside the detection system. In this method, when alpha particles interact with nitrogen molecules from air, photons in UV domain are emitted. The goal of this work is to simulate the Optical Chamber with the PMTs System which is used for radioluminescence detection. The design of a simple system that can be used for UV photon detection was targeted. Using FLUKA Monte Carlo code, the photon fluence generated by 5 MeV alpha particles and the number of counts as a function of energy were estimated. Also, the simulated results are compared with the obtained experimental data. In order to validate the results, the ranges of the alpha particles were calculated using FLUKA and SRIM codes and a good agreement was found with the experimental data. This paper evaluates the alpha induced air radioluminescence Optical Chamber with PMTs Detection System which can be used for different applications. In particular, if the system is sensitive, it could be used to monitor the concentration of radon and their progenitors in experiments with low radioactive background.



**ISRP 2021**  
**International Symposium on Radiation Physics**  
**Kuala Lumpur – Malaysia**  
**6 – 10 December 2021**

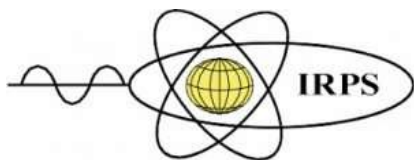
### **A291 - Ab Initio $K\alpha$ and $K\beta$ Energy Calculations in 3d Transition Metals**

Truong V. B. Nguyen, Jonathan W. Dean, Hamish A. Melia, Christopher T. Chantler

The University of Melbourne, Australia

chantler@unimelb.edu.au

Characteristic X-Ray energies are essential parameters for elemental and molecular analysis. Techniques from X-Ray fluorescence, wavelength dispersive, and energy dispersive spectroscopy all require well measured characteristic energies. The 3d transition metals (Z number 21 to 30) are particularly important due to their abundance in the Earth's core, alloying potential, and being common X-Ray sources. A substantial body of work exists on characterising the peak energies, energy centroids, and profiles of many characteristic X-Ray spectra. However, ab initio calculations do not exist in nearly the same quantity, nor quality, as the empirical works. Our group has completed theoretical calculations on copper and scandium  $K\alpha$  and  $K\beta$  using the relativistic multiconfiguration Dirac-Hartree-Fock method which agree very well with the empirical data representing an increased understanding of fundamental radiation processes. All other 3d transition metals have had successful, however inaccurate, ab initio calculations performed while scandium has not. Being able to arrive at a convergent Multi Configurational Dirac-Hartree-Fock calculation for one element does not immediately transfer to other systems, but it does provide useful insight that will help increase the accuracy, and likelihood of convergence, of all calculations.



**A292 - The use of fabricated optical fibres for dose mapping of Cs-137 gamma rays in blood irradiator machine**

Nur Syafinaz Sohini<sup>1</sup>, Mohd Amirul Azrie Mohd Roslee<sup>2</sup>, Nur Amalina Amu<sup>2</sup>, Mohammad Faizal Hassan<sup>3</sup>, Mohammad Azwin Abdul Karim<sup>4</sup>, David Andrew Bradley<sup>5,6</sup>, Noramaliza Mohd Noor<sup>2,3</sup>

<sup>1</sup>Department of Physics, Universiti Putra Malaysia, 43400 UPM Serdang, Selangor, Malaysia

<sup>2</sup>Medical Physics Unit, Teaching Hospital Universiti Putra Malaysia, 43400 UPM Serdang, Selangor, Malaysia

<sup>3</sup>Department of Radiology, Faculty of Medicine and Health Sciences, Universiti Putra Malaysia, 43400 UPM Serdang, Selangor, Malaysia

<sup>4</sup>Department of Radiology, Hospital Kuala Lumpur, 50586 Jalan Pahang, Kuala Lumpur, Malaysia

<sup>5</sup>Centre for Applied Physics and Radiation Technologies, School of Engineering and Technology, Sunway University, 47500 Bandar Sunway, Selangor, Malaysia

<sup>6</sup>Centre for Nuclear and Radiation Physics, Department of Physics, University of Surrey, Guildford, Surrey, GU2 7XH, United Kingdom

Corresponding author: [noramaliza@upm.edu.my](mailto:noramaliza@upm.edu.my)

Irradiation of the blood kills the proliferative ability of lymphocytes found in red blood cells, platelets, and freshly obtained plasma. The use of gamma rays to irradiate blood products has been shown to reduce the likelihood of post-transfusion graft versus host disease. The aim of this study was to determine the homogeneity of the dosage of radiation delivered to the blood and identify the lowest and highest levels of radiation exposure to the blood. A Gammacell 3000® Elan Blood Irradiator with Cesium-137 source was used. The absorbed doses distribution was measured using 2.3 mol % Ge-doped optical fibres of large core (in cylindrical and flat shapes), as well as Gafchromic EBT3 and EBT-XD films. All the dosimeters were placed at the centre of a blood-equivalent phantom. The calibration curves for all dosimeters were plotted first to study the linearity of the dose-response. Dose mapping with fabricated fibres yielded minimum and maximum doses of 17.4 and 31.0 Gy respectively for a gamma irradiation exposure of 8 minutes 51 seconds. The doses obtained from the mapping using both cylindrical and flat shape fibres were in agreement with that obtained from use of the EBT-XD and EBT3 film to within  $\pm 5\%$  and  $\pm 10\%$  respectively. In conclusion, the fabricated 2.3 % fibres have the potential to dose map the blood irradiator.